

# **Identification of novel genes involved in the commitment of endodermal cells to the thymic epithelial cell fate**

**Inauguraldissertation**

zur  
Erlangung der Würde eines Doktors der Philosophie  
vorgelegt der  
Philosophisch-Naturwissenschaftlichen Fakultät  
der Universität Basel

von

**Yves D. Mathieu**

aus Eschenbach, St Gallen

Basel, September 2006

Genehmigt von der Philosophisch-Naturwissenschaftlichen Fakultät

auf Antrag von

Fakultätsverantwortlicher:	Prof. Dr. Antonius Rolink
Dissertationsleiter:	Prof. Dr. Georg. A. Holländer
Korreferent:	Prof. Dr. Ed Palmer

Basel, den 19 September 2006

Dekan: Prof. Dr. Hans-Jakob Wirz

## **Dedication**

I would like to dedicate my thesis to Pascal, my twin brother, who died during his Ph.D. thesis early in 2001.

# Acknowledgments

The presented work was done in the laboratory of Pediatric Immunology at the Department of Research of the University Hospital Basel and later in the Center for Biomedicine of University of Basel under the supervision of Prof. Georg Holländer.

First I would like to thank Georg for giving me the opportunity to do the Ph.D thesis work in his laboratory. I am very grateful for his constant support, patience, helpful discussions and the freedom to improvise in his laboratory, where I have learned to handle and improve in almost all the abilities required for the presented work.

I would further like to express many thanks for support, helpful discussions and for good friendship to all member or ex-members of the lab: Marcel Keller, Jason Gill, Simona Rossi, Mathias Hauri, Lukas Jeker, Simona Frigerio, Luca Piali, Saulius Zuklys, Katrin Hafen, Noriko Shikama, Gina Balciunaite, Thomas Boulay, Peter Annick, Werner Krenger, Elli Christen, Isabelle Grass, Vreni Wyss, Kyung Na, Thomas Barthlott, Elena Litvinova, Emanuela Burchielli.

A special thanks to Marcel Keller for his general expert help in all experimental techniques, to Jason Gill for teaching me embryonal cryosectioning of the earliest thymus primordium and laser microscopy; also to Simona Frigerio and Vreni Wyss for their advices in laser microdissection preparation, Luca Piali for his special patience and assistance in immunohistochemistry as well as to Simona Rossi and Katrin Hafen for teaching me the extraction of mouse embryos, the fetal thymic organ culture and for making all different kind of cell sorting and flow cytometry analysis presented in this work for me. I thank also Annick Peter for her assistance in cell culturing, Isabelle Grass for teaching me in situ hybridization, Noriko Shikama and Lukas Jeker for LacZ staining advices, Thomas Boulay for advices in cloning of plasmids, Teo Soon Siong for his assistance in sequencing and Thomas Barthlott for the isolation of mouse adult primary thymic epithelial cells.

I would also like to thank Dr. Sinue Hahn for allowing me to use his Palm Robot-Microbeam system for laser microscopy and Dr. Ullrich Certa for allowing me to use the Genechip core

facility of Hoffman La Roche in Basel for the preparation, the scanning and the analysis of the different microarrays. In that regard I would like to give a special thank to Sandra Klur for her technical assistance in Genechip preparation and analysis. I would also like to give special thanks to Prof. Ed Palmer and Prof. Antonius Rolink for taking their time to be an expert on the thesis jury.

Finally I would to thank, where I lack the appropriate words to express myself, all my family and my girl-friend for all their inimaginable support, encouragement as for helping me to recover from the recent death of my twin brother.

## Summary

The thymus provides the microenvironment for the maturation and selection of the majority of peripheral T cells. Endodermal cells of the ventral aspect of the third pharyngeal pouch (3<sup>rd</sup>pp) at 10.5 days of mouse gestation (E10.5) adopt a thymic epithelial cell fate while cells of the dorsal part of the 3<sup>rd</sup>pp give rise to the parathyroid glands. To identify novel genes potentially involved in the commitment of endodermal cells to the thymic epithelial cell fate, the transcriptome of the 3<sup>rd</sup>pp was compared to that of the 2<sup>nd</sup>pp and to that of the 4<sup>th</sup>pp with the help of laser microdissection and gene expression profiling (microarrays). Similarly, the transcriptome of the ventral circumference of the 3<sup>rd</sup>pp was in addition compared to its dorsal counterpart. Taken together, fifty genes were identified by microarray and confirmed by quantitative RT-PCR as being differentially expressed between the ventral and the dorsal aspects of the 3<sup>rd</sup>pp while 12 genes were revealed as being upregulated if not exclusively expressed in the entire 3<sup>rd</sup>pp when compared to the 2<sup>nd</sup>pp. Among the genes revealed to be differentially expressed within the 3<sup>rd</sup>pp, two expressed sequence targets (ESTs) were found as being expressed in the ventral aspect of the 3<sup>rd</sup>pp but not in the dorsal side of the pharyngeal pouch while 5 genes (*Tbx1*, *FoxA1*, *FoxA2*, *Sfrp2* and *CXCL12*) demonstrated an upregulation in the dorsal aspect of the 3<sup>rd</sup>pp. Analysis of fetal thymic tissue at different stages of development (E10.5, E12.5, E16.5, E18.5) demonstrated that 8 of the candidate genes (*Nrxn1*, *WIF1*, *Bmp4*, *Fst*, *c-Myc*, *Phlda2* and *Flrt3*) further examined were expressed throughout development. Analysis of embryos at E10.5 by immunohistochemistry for the protein expression of CCL21, Meox2, CD44, WIF1, Fst, Phlda2 confirmed an upregulation if not an exclusive expression in the 3<sup>rd</sup>pp. Moreover, an analysis of the thymic expression revealed that two of the candidate genes examined (*WIF1* and *Flrt3*) are expressed in adult primary thymic epithelial cells but not in thymocytes in contrast to other candidate genes analysed (e.g. *Nrxn1*, *Bmp4*, *Fst*, *c-Myc* and *Phlda2*). Other candidate genes like Sp8 and Phlda2, for which deficient embryos were available to us, respectively, were analysed for their thymic architecture by immunohistochemistry for several markers (e.g. K5, K8 and CD45). However, any significant difference in comparison to wild type littermates could be noticed for these two genes. A functional analysis by Fetal thymic organ cultures (FTOCs) of E13.5s in the presence of human WIF1 recombinant proteins revealed that WIF1 can positively influence the overall cellularity of thymocytes if not expressed at too high levels. However, in

contrast to FTOCs in presence of Bmp4 proteins, the in vitro overexpression expression of WIF1 did not inhibit the normal development of thymocytes in these FTOCs.

In conclusion, this project allowed to identify several candidate genes using microdissected tissues to not only provide global information on gene expression during early development of the thymus but it also provides novel targets to study the inductive signalling pathways that direct the patterning and the differentiation of endodermal cells to the thymic epithelial cell fate. In that regard, several of the candidate genes are known to be involved in Wnt, Tgf $\beta$ 2 signaling pathways or other signaling pathways, predicting that several pathways seem to play a role in early thymus organogenesis.

# Table of contents

Acknowledgments.....	4
Summary.....	6
Table of contents.....	8
Abbreviations.....	12
<b>1. Introduction.....</b>	<b>14</b>
<b>1.1 An overview on thymic function and development.....</b>	<b>14</b>
<b>1.2 Thymus organogenesis.....</b>	<b>16</b>
1.2.1 Development of pharyngeal endoderm.....	17
1.2.1.1 Expansion of pharyngeal pouches.....	18
1.2.2 Interaction of the thymic epithelium with the perithymic mesenchyme.....	20
1.2.2.1 Neural crest cells as a source of mesenchyme.....	20
1.2.2.2 Interference with epithelial-mesenchymal interactions.....	20
<b>1.3 Defective thymic development.....</b>	<b>23</b>
<b>1.4 Origin of thymic epithelial cells.....</b>	<b>25</b>
1.4.1 The duel-origin model for thymus organogenesis.....	25
1.4.2 The simple-origin model for thymus organogenesis.....	26
1.4.3 Fate of the pharyngeal ectoderm.....	27
1.4.4 A putative common thymic epithelial progenitor cell.....	28
<b>1.5 The genetic control of early thymus development.....</b>	<b>32</b>
1.5.1 Transcription factors.....	33
1.5.2 Signalling molecules.....	37
1.5.3 Regulation of TEC differentiation.....	43
1.5.3.1 Lymphocyte-dependent and independent development.....	43
1.5.3.2 Molecular regulation of TEC differentiation.....	45
<b>1.6 T-cell development in the thymus.....</b>	<b>48</b>
1.6.1 Commitment of T cell development in the fetus.....	48
1.6.2 Thymocyte precursors seeding and migration to the developmental thymus murine fetus.....	48
1.6.3 T cell differentiation in fetal thymus.....	49
1.6.4 Positive and negative selection in the thymus.....	51
1.6.5 The final step: export from the thymus.....	53
<b>2. Materials and Methods.....</b>	<b>54</b>
<b>2.1 Material.....</b>	<b>54</b>
2.1.1 Mice.....	54
2.2.2 Tissues.....	54
2.2.3 Cell lines.....	54
2.1.4 Cell culture, plastic ware, and chemicals.....	55
2.1.4.1 Supplements for thymic epithelial cells.....	55
2.1.4.2 Supplements for HEK 293 cells.....	55



2.1.5 Antibodies.....	56
2.1.6 Standard buffers.....	57
2.2 Methods.....	57
2.2.1 Microarray analysis from microdissected tissues.....	58
2.2.1.1 Laser capture microdissection (LCM).....	58
2.2.1.2 Total RNA extraction for microdissected tissue.....	59
2.2.1.3 Random PCR-based amplification.....	60
2.2.1.4 In vitro transcription labelling (IVT).....	63
2.2.1.5 Hybridization and staining of Microarrays.....	64
2.2.1.6 Microarray analysis.....	66
2.2.2 Linear amplification.....	67
2.2.3 Quantitative PCR (real time PCR).....	70
2.2.4 Immunohistochemistry.....	73
2.2.5 In situ hybridization on cryosections.....	75
2.2.6 Total RNA extraction and RT-PCR.....	79
2.2.6.1 isolation of Total RNA.....	79
2.2.6.2 Reverse transcription.....	80
2.2.6.3 Conventional PCR amplification.....	81
2.2.6.4 Nested PCR (for microdissected tissue).....	82
2.2.7 Transfection and purification of hWIF-IgG.....	83
2.2.8 Western blot for hWIF1-IgG.....	86
2.2.9 Fetal thymic organ culture (FTOC).....	88
2.2.10 Staining Protocol for flow cytometry.....	89
2.2.11 Immunofluorescent analysis using confocal microscopy.....	89
2.2.12 Rapid amplification of cDNA ends (RACE).....	90
2.2.12.1 Smart RACE.....	90
2.2.12.2 Marathon RACE.....	92
2.2.13 Cloning & Sequencing of EST RACE products.....	95
2.2.13.1 Cloning.....	95
2.2.13.2 Sequencing of the pGEM insert.....	98
2.2.14 LacZ staining.....	99
2.2.15 Isolation of thymocytes and TECs.....	100
2.2.15.1 Isolation of entire pool of thymocytes from adult thymus.....	100
2.2.15.2 Isolation of single positive mature thymocytes from adult thymus.....	100
2.2.15.3 Isolation of MTS24+ and MTS24- thymic epithelial cells from adult thymus.....	101
3. Results.....	102
3.1 Overview.....	102
3.2 Laser microscopy, RNA isolation and faithful amplification.....	103
3.2.1 RNA isolation from embryonal sections prepared for LCM.....	103
3.2.2 FoxN1 expression in the 3 <sup>rd</sup> pharyngeal pouch.....	104
3.2.3 Amplification of RNA for microarray analysis.....	106

<b>3.3 Identification of candidate genes for thymic epithelial cell fate commitment and function.....</b>	<b>107</b>
<b>3.3.1 Differential expression analysis between the 2<sup>nd</sup> and 3<sup>rd</sup> pp.....</b>	<b>107</b>
<b>3.3.1.1 Comparison of expression analysis for FoxN1, Gcm2 and Pax1 using either qPCR or microarrays.....</b>	<b>108</b>
<b>3.3.1.2 Comparison of differential gene expression.....</b>	<b>110</b>
<b>3.3.1.3 Identification of genes that are upregulated in the 3<sup>rd</sup> pp.....</b>	<b>112</b>
<b>3.3.1.4 Independent confirmation of candidate genes.....</b>	<b>117</b>
<b>3.3.1.5 Immunohistochemical analysis for CCL21 and Meox2 expression in the 3<sup>rd</sup> pharyngeal pouch.....</b>	<b>119</b>
<b>3.3.2 Differential expression analysis between the dorsal and ventral aspect of the 3<sup>rd</sup> pp.....</b>	<b>121</b>
<b>3.3.2.1 Comparing the expression of FoxN1, Gcm2 and Ehox using either qRT-PCR or microarrays.....</b>	<b>121</b>
<b>3.3.2.2 Comparison of differential gene expression.....</b>	<b>124</b>
<b>3.3.2.3 Identification of genes specifically upregulated among epithelial cells on the ventral side of the third pharyngeal pouch.....</b>	<b>126</b>
<b>3.3.2.4 Independent verification by qRT-PCR of some candidate genes.....</b>	<b>136</b>
<b>3.3.2.5 Expression of candidate genes in the 2<sup>nd</sup>, 3<sup>rd</sup>, and the 4<sup>th</sup> pp.....</b>	<b>138</b>
<b>3.3.2.6 Verification by Immunohistochemistry (IHC) the upregulation of some confirmed candidate genes .....</b>	<b>139</b>
<b>3.3.2.7 Nrnx1 expression in the common thymus-parathyroid primordium at E10.5 and in E12.5 thymus.....</b>	<b>145</b>
<b>3.3.2.8 Expression of Nrnx1 isoforms in the ventral aspect of the 3<sup>rd</sup> pp.....</b>	<b>145</b>
<b>3.3.2.9 Expression of candidate genes during thymus development.....</b>	<b>147</b>
<b>3.3.2.10 Expression of candidate genes in adult thymocytes and thymic epithelial cells.....</b>	<b>148</b>
<b>3.3.2.11 Expression of candidates genes in thymic epithelial cell lines.....</b>	<b>149</b>
<b>3.3.2.12 Expression of candidate genes in embryonal and adult tissues.....</b>	<b>150</b>
<b>3.3.2.13 Extention of EST DNA sequences.....</b>	<b>151</b>
<b>3.3.2.14 Effect of WIF1 on thymopoiesis in FTOC.....</b>	<b>154</b>
<b>3.3.2.15 Confocal analysis of E13 thymus of Phlda2 deficient mice.....</b>	<b>160</b>
<b>3.3.2.16 Genes confirmed to be upregulated in the dorsal side of the 3<sup>rd</sup> pp..</b>	<b>161</b>
<b>3.3.2.17 Expression of candidates genes in the 4<sup>th</sup> pp.....</b>	<b>162</b>
<b>4 Discussion.....</b>	<b>164</b>
<b>4.1 Comparative analysis between data sets from microarrays and qRT-PCR.....</b>	<b>165</b>
<b>4.2 Genes that are involved in the chemotaxis and that are upregulated in the 3<sup>rd</sup> pp.....</b>	<b>166</b>
<b>4.3 Differential expression of transcriptional regulators within the 3<sup>rd</sup> pp.....</b>	<b>167</b>
<b>4.4 Differential expression of cell surface antigens in the ventral aspect of the 3<sup>rd</sup> pp.....</b>	<b>170</b>
<b>4.5 Differential expression of genes involved in growth factor signalling in the 3<sup>rd</sup> pp.....</b>	<b>172</b>
<b>4.6 Genes involved in Wnt-mediated signalling are differentially expressed in the 3<sup>rd</sup> pp ..</b>	<b>173</b>
<b>4.7 Differential expression within the 3<sup>rd</sup> pp of genes involved in the Tgfb signalling.....</b>	<b>176</b>
<b>4.8 Increased expression of c-Myc, a target gene of Wnt and Tgfb signalling in the ventral aspect of the 3<sup>rd</sup> pp.....</b>	<b>179</b>
<b>4.9 Increased expression of Tnfrsf19 in the ventral aspect of the 3<sup>rd</sup> pp.....</b>	<b>180</b>

<b>4.10 Increased expression of Delta-like homolog 1 in the ventral aspect of the 3<sup>rd</sup>pp.....</b>	<b>180</b>
<b>4.11 Increased expression of Nr xn1 in the 3<sup>rd</sup>pp, a gene involved in cell-cell interaction....</b>	<b>181</b>
<b>4.12 Genes upregulated in the ventral aspect of the 3<sup>rd</sup>pp involved in extracellular matrix interactions.....</b>	<b>182</b>
<b>4.13 Expressed sequence target genes upregulated in the 3<sup>rd</sup>pp.....</b>	<b>184</b>
<b>5 Conclusions.....</b>	<b>185</b>
<b>6 Perspectives and Outlook.....</b>	<b>186</b>
<b>7 Appendix.....</b>	<b>188</b>
<b>7.1 Annexes.....</b>	<b>188</b>
<b>8 References.....</b>	<b>192</b>
<b>9. Curriculum Vitae.....</b>	<b>227</b>
<b>9.1 Publications.....</b>	<b>228</b>

# Abbreviations

ATP	adenosine triphosphate
B cell	bone marrow-dependent lymphocyte
BM	bone marrow
bp	base pairs
BSA	bovine serum albumine
cDNA	complementary DNA
°C	degrees Celsius
CD	cluster of differentiation
c-kit	tyrosine kinase receptor for stem cell factor
cTEC	cortical thymic epithelial cell
CTP	cytosine triphosphate
DC	dendritic cells
DMEM	Dulbecco's modified Eagle's medium
DMSO	dimethylsulfoxide
DNA	deoxyribonucleic acid
DN	double negative T cells
dNTP	deoxyribonucleic acid
DP	double positive T cells
dsCDNA	double stranded DNA
DTT	dithiothreitol
E	embryonic day of gestation
EB	Elution buffer
ECM	extracellular matrix
EDTA	ethylenediaminetetraacetic acid
i.e	as for example
EtOH	ethanol
FACS	fluorescent-activated cell sorter
FCS	Fetal calf serum
FITC	Fluorescein isothiocyanate
FTOC	Fetal thymic organ culture
g	gram
G	gravity
GAPDH	glyceraldehyde-3-phosphate dehydrogenase
GTP	guanosine triphosphate
h	human
hr	hour
HEPES	N-2-Hydroxyethylpiperazine-N'-2-ethansulfonic acid
HSC	Hematopoietic stem cell
Ig	immunoglobulin
ISH	in situ hybridization
K	cytokeratin
Kb	kilo base
KDa	Kilo Dalton
L	liter
LB	lurea broth
LCM	Laser capture microdissection
LN	lymph node
m	mouse
M	molar
2-ME	2-Mercaptoethanol
MHC	major histocompatibility complex
min	minute
mol	mole
ml	milliliter

µl	microliter
mM	millimole
mRNA	messenger RNA
mTEC	medullary thymic epithelial cell
NK	natural killer cell
NTP	nucleotide triphosphate
O.D.	optical density
O.N.	over night
ORF	open reading frame
PBS	Phosphate-buffered saline
PCR	polymerise chain reaction
PE	phycoerythrin
pH	negative logarithm of the hydrogen ion concentration
qPCR	quantitative PCR (real time PCR)
Rag	recombination activating gene
RACE	rapid amplification of cDNA ends
RNA	Ribonucleic acid
rpm	revolutions per minute
RT	reverse transcription
RT-PCR	reverse transcriptase PCR
s	second
SCID	severe combined immunodeficient
SDS	sodium dodecyl sulfate
SH2	src-homology 2
SP	single positive T cells
ssDNA	single stranded DNA
SSC	standard saline citrate
TBS	Tris buffered saline
TE	Tris (10mM)/EDTA(1mM) buffer
TEC	thymic epithelial cell
TCR	T cell receptor
Tris	tris (hydroxymethyl) aminomethane
TTP	thymidine triphosphate
U	Unit
UTC	Uracyl triphosphate
UV	Ultraviolet
VDJ	variablility, diversity, and joining regions
wt	wild type

# **1.Introduction**

Little is known concerning the molecular mechanisms of early thymus development. Therefore the aim of this project will be to characterize further the genetic programs which determine thymic epithelial cell fate and differentiation by identifying new genes critically involved in this process. Since the thesis work will mainly focus on aspects of thymus development, a detailed description of the known cellular and molecular events related to the organogenesis of the thymic microenvironment will first be given.

## **1.1 An overview on thymic function and development**

The thymus is located in the mediastinum. The completion of its development has two major functions for the immune system. First, the thymus provides the correct microenvironment for haematopoietic progenitors to differentiate into functional T cells. Developing T cells in the cortex of the thymic microenvironment are designated thymocytes. Immediate extrathymic precursors to the T cell lineage are generated during embryogenesis in the fetal liver and usually in the bone marrow after birth. The CD4 and CD8 co-receptors are exclusively expressed by T cells (with some notable exceptions such as dendritic cells) and therefore serve as specific T cell markers.

The second and related function of the thymus concerns its role in central T cell self-tolerance. This event prevents the recognition of self-antigens and thus precludes the changes of T cells eliciting an autoimmune disease. The establishment of a functional T cell repertoire is achieved by a complex series of events referred to as positive and negative thymic selection. Positive selection occurs if the T cell receptor (TCR) of the thymocytes engages a peptide self MHC (major histocompatibility complex) ligand with low affinity, resulting in the transduction of a survival and differentiation signal. The thymocytes that fail to engage a peptide-MHC ligand and therefore do not undergo positive selection, die by neglect in a passive manner because they do not receive a survival signal. Negative selection occurs when the TCR of a thymocyte engages a peptide-MHC ligand with high affinity, leading to the apoptotic death of the cell. Negative

selection deletes potentially self-reactive thymocytes, thereby generating a repertoire of peripheral T cells that is largely self-tolerant. For these reasons fewer than 5% of the developing thymocytes survive and leave the thymus as mature T cells. For autoreactive T cells that escape regular negative selection there are additional regulatory mechanisms in place that function in the periphery and that control their functionality.

The maturation and selection processes during thymocyte development are effected by the thymic stroma which provides a unique microenvironment for T-cell development. The epithelial compartment of the thymic stroma center is subdivided based on phenotype and function into cortex and medulla. The cortical thymic stroma consists of epithelial cells that are closely associated with the early maturational stages of intrathymic development, and scattered macrophages, which are involved in clearing apoptotic thymocytes. The medullary thymic stroma consists of epithelial cells, together with haematopoietic macrophages and dendritic cells, that interact with mature thymocytes. The thymic stroma also comprises surrounding mesenchyme that consists of mesenchymal cells of ectodermal origin.

Thymus organogenesis commences in the mouse embryo at day 10.5 of gestation (E10.5) although an overt thymus primordium is only formed at around E11.5. At this time point during mouse development, the mouse thymus primordium emerges as an epithelial anlage budding from the ventral endodermal lining of the 3<sup>rd</sup> pharyngeal pouch (pp) while dorsal aspects of this invagination develop into the parathyroid glands (Rowen *et al.*, 2002). Each organ is surrounded by a condensing mesenchymal capsule that still contacts both the surface ectoderm and the pharyngeal endoderm. Seeding of lymphoid precursor cells into the epithelial primordium occurs at around E12.5. This immigration of haematopoietic precursors cells is paralleled by rapid epithelial cell proliferation and differentiation giving eventually rise to distinct stromal compartments. By E13.5, the parathyroid and thymus are separated into physically distinct organs and soon afterwards they reach their respective adult positions within the embryo. The thymus anlage separates from the pharynx and with the accompanying neural crest-derived mesenchyme descend to the mediastinum where it sits on top of the heart with the lobes touching each other at the midline while the parathyroid glands are positioned at the lateral margins of the thyroid gland. The different events that occur in early thymus organogenesis have been schematized in Fig.1.1.

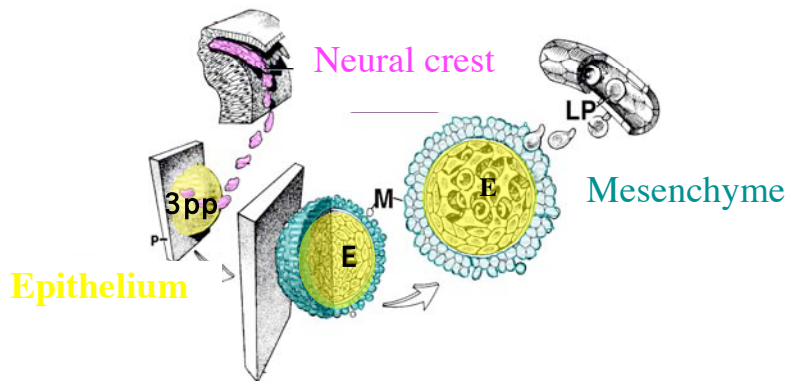


**Figure 1.1. Diagram of the early steps in the formation of the thymus anlage.** Neural crest (NC) cells migrate from rhombomere 6 to the region of the third pharyngeal pouch (3pp). Mesenchymal cells of ectodermal origin (M) surround the expanding epithelial mass (E). The developing epithelial primordium attracts lymphoid precursor cells (LP) from neighbouring blood vessels. The haematopoietic cells migrate into the epithelial anlage. The figure has been adopted from ( Bockman, 1997).

## 1.2 Thymus organogenesis

The 3<sup>rd</sup> pharyngeal pouch is lined by the endoderm. Adjacent to this tissue, the mesenchymal core with the contributions of neural crest cells that have migrated to the 3<sup>rd</sup> pharyngeal arches where they adopt a mesenchymal phenotype (Le Lievre and Le Douarin, 1975)(Gordon *et al.*, 2004). These ectomesenchymal cells surround the emerging thymus primordium and provide molecular cues necessary for the expansion of thymic epithelial cells (Sunjara *et al.*, 2000)(Jenkinson *et al.*, 2003; Revest *et al.*, 2001b). Whether the proximity of cleft ectoderm is important for and may thus contribute (directly or indirectly) to the thymus development is still controversial (Manley and Blackburn, 2003). However most recent studies would argue against such a contention (Gordon *et al.*, 2004).



Recent studies have further more shown that most of the mesenchymal cells surrounding the pharyngeal pouch is originating from neural crest cells and does not derive from the surrounding mesoderm (Jiang *et al.*, 2000). Moreover endothelial cells derived from the pharyngeal arches may also play a role in the patterning of the thymus primordium, albeit such a contribution to thymic epithelial cell differentiation has still to be unequivocally proven (Lammert *et al.*, 2001; Matsumoto *et al.*, 2001). Nevertheless, a recent study of the thymic vasculature provided cues that discrete segments of thymic vessels may act in concert with thymocyte-derived stimuli to effect normal development of the thymic environment (Anderson *et al.*, 2000). However, a study from Müller and colleagues who demonstrated that the inactivation of the vascular endothelial growth factor A (VEGF-A), a key vascular factor in thymic epithelial cells, results in a hypovascularization and disruption of the thymic typical network of vascular arcades but support normal thymopoiesis (Muller *et al.*, 2005). Thus, vascular growth factor production by thymic epithelial cells is rather required for normal thymus vascular architecture than conversely. Interfering with the mesenchymal derivatives from neural crest cells during the functional development of the epithelial primordium inhibits thymic development in a manner similar to that observed in congenital conditions such as the DiGeorge syndrome or the fetal alcohol syndrome (Ammann *et al.*, 1982; Bockman, 1997; Suniara *et al.*, 2000).

### **1.2.1 Development of pharyngeal endoderm**

In contrast to many other organs including the bone marrow and all secondary lymphoid organs, where the cellular framework is made of connective tissue, it is the epithelial cells in the thymus that form the scaffold for T cell development. The thymic epithelium is derived from the endodermal germ layer through a series of consecutive steps, each of which have to be completed in order to achieve the capacity to form the correct environment able to provide the primary function of the thymus i.e. the development and selection of T cells (Gill *et al.*, 2003). Early in development, the embryo assumes a roughly cylindrical form with the endoderm forming the inner lining. The epithelium of the roof of the endodermal yolk sac is folded into the expanding embryo and forms the lining of the primitive gut. A blind-ending sac of this epithelial lining extends forward in the embryo as the foregut. The foregut extends as the embryo expands, eventually forming both the anterior parts of the digestive tract and the respiratory tract. The development of the pharyngeal region occurs as part of foregut differentiation and is required for

the formation of the thymus anlage. The embryonic pharynx serves also as the anatomical origin for the thyroid, the parathyroid glands, the ultimobranchial body, the palatine tonsil, the auditory tube, the mastoid antrum as well as the tympanic cavity. In more detail, the first pharyngeal pouch (1<sup>st</sup>pp) elongates to form the tubotympanic recess, which will give rise to the lining of the tympanic cavity, auditory tube and mastoid antrum. The second pharyngeal pouch (2<sup>nd</sup>pp) forms the surface epithelium and lining of the crypts of the palatine tonsil. The third pharyngeal pouch (3<sup>rd</sup>pp) (as already mentioned above) differentiates into the thymus and the parathyroid glands while the fourth pharyngeal pouch (4<sup>th</sup>pp) gives rise to the ultimobranchial body that contributes to the development of the thyroid gland. This close proximity of these different tissues during early development does explain why some of the complex anatomical defects regularly observed can also be associated with a defective thymic development despite the fact that some of these organs in the adult mouse are not adjacent anymore (Cordier and Haumont, 1980).

#### **1.2.1.1 Expansion of pharyngeal pouches**

The walls of the developing pharyngeal region consist in mammals of a series of individual pairs of branchial (a.k.a. pharyngeal) arches, designated ba1 to ba6. As ba5 is not found in mammals but does exist in fish the annotation jumps in the former species from ba4 to ba6. Hence only 5 branchial arches are present in mammals. Primitive blood vessels, called aortic arches, run through the branchial arches. The vessels are surrounded by mesenchyme. The boundaries of each arch are demarcated on the embryo's surface by intervening grooves. The anterior region of the foregut, which forms the primitive pharynx, expands toward the surface within this framework and is directed along the intervals between the branchial arches. Consequently, blind-ending sacs extend from the foregut laterally in the direction of the embryo's body surface, producing a bilateral series of four different pharyngeal pouches (pp) that are lined by endodermal epithelium. These pouches designated 1<sup>st</sup>, 2<sup>nd</sup>, 3<sup>rd</sup> and 4<sup>th</sup>pp are located between the ba1 and ba2, ba2 and ba3, ba3 and ba4 and finally ba4 and ba6 respectively (Fig.1.2A). Since the thymus emerges from the 3<sup>rd</sup> pharyngeal pouch (3<sup>rd</sup>pp), its formation is juxtaposed to the third and fourth branchial arches (ba3 and ba4) (Fig.1.2B).

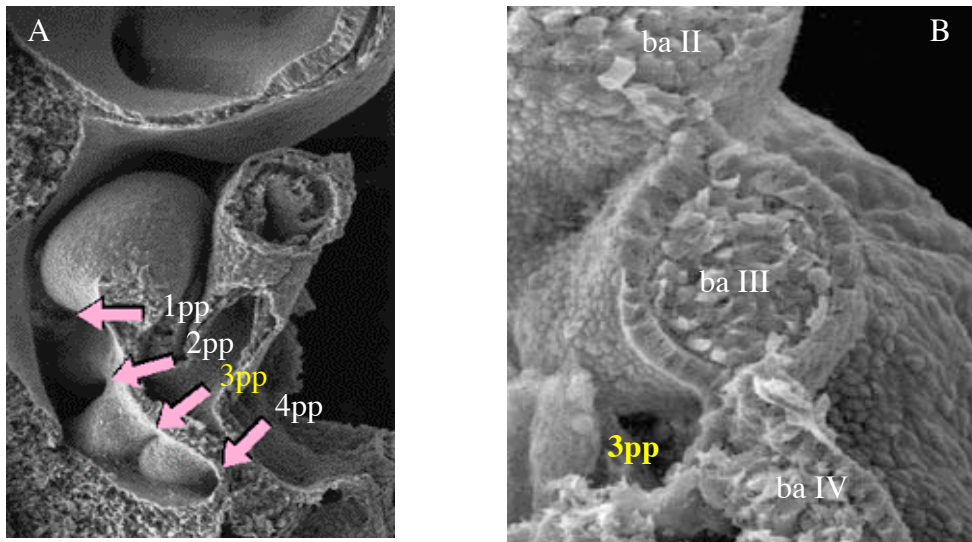


**Figure 1.2. Scanning electron microscopy of the mouse pharyngeal area at E10.5.** **A.** Pharyngeal area, pink arrows are pointing to the four distinct pharyngeal pouches (pp) each located between two branchial arches (ba). **B.** Close up view of the third pharyngeal pouch area located between the third branchial arch (ba III) and fourth branchial arch (ba IV). The pictures have been adopted from a public database.

The developing endodermal lining is in contact with the ectoderm, which covers the surface of the embryo, thereby temporarily producing thin, narrow diaphragms called pharyngeal membranes. These structures fill the interval between the arches. Evidence had previously been presented suggesting that ectodermal cells with endodermal cells in the area of the pharyngeal membranes results in ectoderm being incorporated into the thymus epithelial primordium (Cordier and Heremans, 1975). Although this understanding had been broadly accepted, recent studies in mice could not demonstrate any evidence supporting the fact that ectodermal cells play a direct role in the development of the thymic anlage (Cordier and Haumont, 1980)(Gordon *et al.*, 2004). Specifically, these studies show by ectopic transplantations of pharyngeal endoderm that a fully functional thymus could develop from endodermal epithelium alone. Importantly, this capacity was not enhanced by pharyngeal ectodermal cells.

Overtime, the proliferating epithelial cells from the third pharyngeal pouch form on each bilateral side of the embryo a cellular accumulation that extends into the surrounding mesenchyme. The continued cell proliferation and development of the thymic primordium lead to a separation of the cell mass that has formed in this area and eventually the attachment to the pharyngeal cavity is

lost. Thus a solid body of cells is formed that expands as it migrates ventrally and caudally. The mass of epithelial cells now constitutes the primordial thymus and is finally in the position to attract lymphoid precursor cells that colonizes the ba3 and ba4. These latter cells will then have to migrate to the perithymic mesenchyme before they can enter the epithelial compartment as long as the vascularization of the thymic rudiment is not established (Itoi *et al.*, 2001). This latter aspect of thymus development occurs at E14.5-E15.5.

## **1.2.2 Interaction of the thymic epithelium with the perithymic mesenchyme**

### **1.2.2.1 Neural crest cells as a source of mesenchyme**

Much of the mesenchyme that fills the pharyngeal arches is derived from descending neural crest cells. Neural crest cells are of ectodermal origin and originate at the dorsal most aspect of the neural tube. These cell's importance lies in their ability to migrate extensively and generate various differentiated cells types. Neural crest cells from the 2<sup>nd</sup> and 4<sup>th</sup> rhombomeres migrate to the 1<sup>st</sup> and 2<sup>nd</sup> pharyngeal arches respectively, while cells from the 6<sup>th</sup> rhombomere travel into the 3<sup>rd</sup> and 4<sup>th</sup> pharyngeal arch. Neural crest cells from the 3<sup>rd</sup> and 5<sup>th</sup> rhombomeres do not migrate through the mesoderm but instead enter the migrating streams of an adjacent rhombomere. During their ventrolateral migration, neural crest cells proliferate and some aggregate to produce neural components, such as the dorsal root ganglia and sympathetic ganglia, while others become ectomesenchymal cells (mesenchymal cells of ectodermal origin). Once migrated into their respective pharyngeal region and transformed to ectomesenchymal cells, these cells interact with the epithelial cells of the pharyngeal endoderm, inducing the proliferation, migration, and differentiation of these latter cells (Bockman, 1997).

### **1.2.2.2 Interference with epithelial-mesenchymal interactions**

The interaction required to occur between epithelium and the mesenchyme for a regular thymus development to take place was experimentally verified by (Auerbach, 1960) in mice. Explantation of the thymus (fetal thymic organ culture) at E12.5 produces robust epithelial proliferation. This does, however, not occur if the mesenchymal component of the developing thymus is removed at the beginning of the culture. Importantly, recombining the epithelial

component with mesenchyme from various sources reveals that both the origin of the mesenchyme and the timing appear to be significant factors in the development of the thymus. For example, delayed growth occurred when mesenchyme from lung or submandibular gland were used as an mesenchymal source to be allowed to interact with thymic epithelium and practically no induction of growth was observed when the mesenchyme was taken from fetal limb bud or from newborn mice. That is, the presence of mesenchyme from an appropriate source and at a proper stage of development permits the proliferation of previously committed epithelial cells along the regular course of thymic development.

Extending these observations to an *in vivo* experiment in chicks, the extirpation of the neural crest resulted in a severely compromised development of the thymus. This effect was explained by the lack of the ecto-mesenchymal contribution to the developing thymus anlage (Bockman and Kirby, 1984; Bockman and Kirby, 1989). Specifically the ablation of neural crest over the somites 1–5, reduced the ectomesenchyme and results in either a thymus that was completely missing or a thymus that was greatly reduced in size. In the latter instance, the lobes were irregularly shaped, remained of primitive pharyngeal lumen and inhibited lymphocyte proliferation occurred in these lobes.

A more direct assessment of the capacity of ectomesenchymal cells to participate in the development of thymic epithelium was carried out in more recent experiments where neural crest cells from selected axial levels were transplanted. Unilaterally grafted from quail donors to the corresponding region in chick hosts these neural crest cells migrate normally and interact with the primordial thymus (Kuratani and Bockman, 1991). Thus, these experiments revealed that neural crest from isotopic locations contributed most significantly to the developing thymus while this capacity obviously decreased when neural crest transplants were derived from more anterior or posterior anatomical locations. These observations were later confirmed and extended to the understanding, that the mesenchymal production of soluble growth factors, such as epidermal growth factor, might be needed for normal thymic epithelial development to occur (Shinohara and Honjo, 1996; Shinohara and Honjo, 1997). In addition, reaggregate thymus organ culture studies with individual or combinations of different precursor subsets of stromal cells showed that mesenchymal cells were required for the maturation of early thymocytes (Anderson *et al.*, 1997; Anderson *et al.*, 1993; Kawakami *et al.*, 1999). In these studies, treatment of mesenchymal

cells with hyaluronidase was found to abrogate the ability to support thymocyte development, indicating a direct role for mesenchymal-associated extracellular matrix in early T-cell development. Although the precise mechanism by which the mesenchymal cells contribute to the thymic development is still incompletely understood.

In the fetal thymus, neural crest derived mesenchymal cells contribute to the thymic capsule and septae, and can also be located within the thymic cortex where they interact with immature thymocytes as shown by immunohistochemistry analysis (Anderson *et al.*, 1997; Owen *et al.*, 2000; Suniara *et al.*, 2000). However, one cannot exclude the possibility that ectomesenchymal cells indirectly influence thymopoiesis by providing inductive signals to generate and maintain a correctly organized epithelial microenvironment. As thymus development proceeds, the mesenchyme of neural crest origin surrounding the pharyngeal organs is replaced by mesodermal mesenchyme (Yamazaki *et al.*, 2005). Thus, ecto-mesenchyme provides only a modest to marginal contribution to the thymus in late fetal and postnatal life (Jiang *et al.*, 2000). Indeed, the recent study of Yamazaki and colleagues demonstrated that large numbers of neural crest-derived cells are detected as part of the thymus between E11.5 to E16.5 but were rarely present at later stages and almost absent after birth (Yamazaki *et al.*, 2005). These data suggest that neural crest-derived cells may only play a role in thymic organogenesis at an early embryonic stage.

A two-stage mechanism for the involvement of the mesenchyme in thymopoiesis has been proposed on the basis of current experimental data (Anderson and Jenkinson, 2001). One requirement for mesenchyme in thymus development might be in the initial stages of thymic formation, when neural crest-derived mesenchymal cells surround the thymus anlage and eventually migrate into the thymic epithelial rudiment. Distinct epithelial–mesenchymal interactions, possibly involving the production of fibroblast growth factors (Fgfs) by mesenchyme (Xu *et al.*, 1999), might then directly regulate the differentiation and/or proliferation of the thymic epithelial cells. These kind of interactions have been shown to have an important role in the formation of many organs shaped by epithelial–mesenchymal interactions. A typical example is the limb bud, where the mesenchymal production of fibroblast growth factors stimulates the growth and differentiation of Fgf-receptor-bearing epithelial cells (Xu *et al.*, 1999). Indeed, mice lacking either Fgf10 (Ohuchi *et al.*, 2000) or its receptor FgfR2-IIIb (Revest *et al.*, 2001a) display a thymus that is largely reduced in size (Revest *et al.*, 2001b). This result indicates

a role for specific Fgfs for epithelial–mesenchymal interactions during thymus development. However, signals of Fgf10 via its receptor, Fgfr2-IIIb, seem not to be essential for the commitment to a thymic epithelial cell fate and the ability to support thymocyte development, as mice deficient for Fgf10 or its receptor display a phenotypically regular maturation of the few thymocytes that are present in their thymus. Fgfr2-IIIb deficient mice die at birth because those mutant mice fail to develop lungs. Consequently, any conclusion as to the competence of the thymus in these mutant mice to generate a regular repertoire of T cells is not known. A time-constrained role of the mesenchyme for thymic epithelial cell development was described by Jenkinson and colleagues who provided evidence that after E12, the differentiation of immature thymic epithelial cells into cortical and medullary phenotypes is independent of sustained interactions with mesenchyme (Jenkinson *et al.*, 2003). However, the continued presence of Fgf7 and Fgf10 is necessary to support the proliferation of thymic epithelial cells leading to thymus growth. These experiments have therefore defined a key role for Fgfs in the regulation of thymic organogenesis.

A role for mesenchymal cells in thymus development has also been shown in experiments involving the generation of reaggregate thymus organ cultures (RTOC) (Anderson *et al.*, 1997; Anderson *et al.*, 1993). In addition to mature thymic epithelial cells from 2-deoxyguanosine-treated thymus lobes, mesenchymal fibroblasts were found to be necessary for the maturation of thymocyte precursors beyond the most immature, intrathymic stage ( i.e. DN1 stage, see below)(Anderson *et al.*, 1993). However it remains uncertain just how mesenchymal cells influence thymocyte development. Possible mechanisms include the generation of specific components of the extracellular matrix (ECM) and soluble growth factors such as cytokines that effect the development of the immature T-cell precursors (Banwell *et al.*, 2000).

### **1.3 Defective thymic development**

The thymic stromal development (and there in particular that of thymic epithelial cells) and the maturation of thymocytes influence each other, a phenomenon referred as "crosstalk". It has been postulated that in the absence of crosstalk development of both T-cells and thymic epithelium are

impaired, thus affecting the functions of each of the participating cell types (Hollander *et al.*, 1995; van Ewijk *et al.*, 2000b; van Ewijk *et al.*, 1994; van Ewijk *et al.*, 1999).

One of the first studies to reveal the importance of the thymic stromal components for normal thymopoiesis were drawn from mice with a spontaneous deficiency in the transcription factor FoxN1, resulting in an abortive thymic development (Kingston *et al.*, 1984). These mice are also known as nude mice due their inability to form a normal coat. In that study from Kingston and colleagues, the stromal composition of a developing thymus from a normal mouse was compared to that of a nude mouse (Kingston *et al.*, 1984). This analysis revealed that class II major histocompatibility complex (MHC) antigens were missing on the epithelial cells of the nude mice in contrast to normal mice. As the class II MHC antigens enables functional cell-cell interaction with lymphoid cells, it was concluded that the epithelial cells of the thymus are the components of the thymus that are essential for a normal thymic function.

The so called complete DiGeorge syndrome is an other example of a congenital condition in which defective development of the thymus stroma is accompanied by an impairment of the T cell development and thus a deficiency in the adaptive immune system. This condition also comprises the clinical findings of parathyroid hypoplasia or aplasia, a submucous cleft palate, velopharyngeal insufficiency, an aberrant function of the cardiac outflow tract, and typical facial features such as a short philtrum and a small mouth. The DiGeorge syndrome is caused in the majority of patients by a heterozygous deletion within the chromosomal band of 22q11 (del22q11). Recent studies have shown that a mutation in *Tbx1* (T-box transcription factor 1), a gene situated in this region of chromosomal 22 may suffice to explain most of the features of the DiGeorge syndrome (Brown *et al.*, 2004; Lindsay *et al.*, 1999; Lindsay *et al.*, 2001; Merscher *et al.*, 2001). It has been suggested that the DiGeorge syndrome is caused by a failure of neural crest cells to contribute appropriately to the development of great vessels, which then serve the thymus and other organs (Couly *et al.*, 1983; Kirby and Bockman, 1984). In agreement with this suggestion is a study from Vitelli and colleagues, in which they compared the phenotype and the gene expression of mice homozygously deficient for *Tbx1* using a *Tbx1-lacZ* reporter allele construct. Although their data do not support a direct role of neural crest cells in the pathogenesis of the *Tbx* mutant phenotype, the authors hypothesise that the misdirection of neural crest cells in these *Tbx1* deficient mice is due to the lack of a guidance role from the pouch endoderm.



The fact that during development several closely associated anatomical structures appear to be affected is referred to as a "field defect". Offspring of women who had been exposed during pregnancy to the vitamin A analogue 13-cis retinoic acid (a.k.a. isotretinoin or Accutane) displayed a combination of structural defects clinically reminiscent of the DiGeorge syndrome (Lammer *et al.*, 1985). Similarly, the fetal alcohol syndrome which results from excessive alcohol intake during early pregnancy provokes a similar clinical presentation (Ammann *et al.*, 1982). Thus, several environmental substances can cause "field defects" that are alike to the by now rather well characterized DiGeorge syndrome. Moreover, it is likely that surgical ablation of neural crest cells, and administration of certain substances such as excess alcohol, or 13-cis retinoic acid causes diminished ectomesenchyme as it is a lack of regular development, which in turn inhibits proper development of the thymic epithelium and the capacity of the microenvironment to support thymocyte maturation.

Other defects have been observed in the spontaneous mutant mouse strain "splotch", which is deficient for the transcription factor Pax3 or in mice that have a homozygous mutation for the platelet-derived growth factor receptor alpha subunit, PDGFR $\alpha$ , which are designated Patch. In both of these strains the formation of neural crest is altered resulting in a loss of normal organogenesis for the thymus and the parathyroid glands (Franz, 1989; Morrison-Graham *et al.*, 1992). Mice rendered deficient for the homeobox gene hox-1.5 (a.k.a. Hoxa3) present a lack of both thymus and parathyroids and have also a reduced size of their thyroid in addition to other anatomical defects (e.g. heart and arteries) (Chisaka and Capecchi, 1991).

## **1.4 Origin of thymic epithelial cells**

### **1.4.1 The dual-origin model for thymus organogenesis**

Until a couple of years ago, the most widely favoured model of thymus organogenesis suggested that both the third pharyngeal cleft ectoderm and the third pharyngeal pouch endoderm contribute physically to the thymus anlage, such that the epithelial component of the cortical compartment is generated from ectodermally derived cells, whereas cells of the medullary epithelium are of endodermal origin. Support for this model was drawn from several morphological studies. The

most convincing of these investigations used a histological sectioning and reconstruction approach to compare thymus organogenesis between nude mutant and wild-type embryos (Cordier and Haumont, 1980; Cordier and Heremans, 1975). This study reported that the endodermal and ectodermal germ layers made physical contact at E9.5, after which a strong proliferation of the third pharyngeal clefts occurred, such that ectodermal cells covered the third pouch endoderm between E10.5 and E11.5. The resulting compound structure would detach from both the ectoderm and endoderm by E12.5, giving rise to the thymus primordium. As a markedly diminished proliferation of the ectoderm was reported in nude embryos, it was concluded that the primary nude defect affects ectodermal cells (Cordier and Haumont, 1980; Cordier and Heremans, 1975). As the essential embryological anomaly of nude mice noticeable at E11 consists of a failure of the ectoderm from the 3<sup>rd</sup> branchial cleft to proliferate and differentiate into a cervical vesicle, this analysis concluded that in consequence of an ectodermal defect the 3<sup>rd</sup>pp endoderm degenerates and forms cysts. Based on these conclusions, the so called “dual-origin” model of thymus development was proposed that postulates that the cortical epithelium derives from the ectoderm while the endoderm gives rise to medullary epithelium. Experimental-support for this model was provided by several independent studies (Van Vliet *et al.*, 1985) (Kingston *et al.*, 1984; Owen and Jenkinson, 1984) that all concluded that a dichotomy in cellular origin reflects the anatomically separate compartments of cortex and medulla.

#### **1.4.2 The single-origin model for thymus organogenesis**

Morphological studies in mice and other mammals could have also been interpreted in an alternative fashion and thus concluded that the thymic epithelium is solely derived from the third pouch endoderm (Gordon *et al.*, 2004; Smith, 1965). Strong functional evidence supporting the "single-origin" model has existed since 1975, when Le Douarin and Jotereau generated chimaeras by transplantation of quail pharyngeal endoderm to the somatopleura of a 3 day old chick (Le Douarin and Jotereau, 1975). Importantly, the graft had been taken at the 15-somite stage, a time when neither the development of the third pharyngeal pouch had yet occurred nor pro-thymocytes had homed to the anatomical area from which the tissue for transplantation was taken. Upon engraftment, the donor endoderm developed into a thymus anlage able to support T cells of chick origin. Importantly, the epithelial cells in both the cortical and medullary compartments were exclusively of quail origin. These experiments did thus provide evidence that purified pharyngeal

endoderm is sufficient to generate the epithelial component of both the cortical and medullary compartments. Finally these data also conveyed that, at least in birds, cells in the developing endoderm have adopted a fate for thymic epithelial cells well before the formation of the third pharyngeal pouch. Although these experiments did neither test the commitment to a single cell lineage directly, nor utilize a single cell approach, their data provide a stringent assessment of the developmental potential of the pharyngeal endoderm. Since the publication of this study the single-origin model has received further support from additional experimental evidence.

### **1.4.3 Fate of the pharyngeal ectoderm**

The controversy whether the dual-origin or the single-origin model, respectively, is correct had however, persisted due to several methodological constraints. In 2004, the issue whether the ectoderm contributes at all to the organogenesis of the thymus epithelial stroma, was elegantly readdressed by Gordon and colleagues (Gordon *et al.*, 2004). To investigate the fate of the pharyngeal ectoderm in the developing mouse embryo a lineage-tracing analysis was developed using a whole embryo culture system (Moore-Scott *et al.*, 2003). To this end, the pharyngeal ectoderm of E10.5 mouse embryos was labelled specifically by dropping a cell tracker dye (5-chloromethylfluorescein diacetate) onto each of the pharyngeal region of an E10.5 embryo. The embryos were then cultured for a further 30 hours. Importantly, thymus development proceeded normally during this time, as assessed by morphological criteria and marker analysis (*Hoxa3*, *Pax1*, *Shh*, *Gcm2* and *FoxN1*). The fate of the labelled pharyngeal ectoderm was subsequently analysed by histological and fluorescence analysis of sectioned embryos. The developmental period covered in this experiment spanned the stages at which the ectodermal contribution to the thymus occurs, i.e. E10.5 to E11.5 (Moore-Scott *et al.*, 2003). The analysis of labelled and cultured embryos revealed that none of the labelled cells contributed to the thymic primordium. Therefore, a physical contribution by pharyngeal cleft ectoderm to the developing thymus anlage does not occur, despite the physical contact between the 3<sup>rd</sup>pp endoderm and 3<sup>rd</sup>cleft ectoderm between E10.5 and E11.5. Taken together, these data fail to support the dual-origin model of thymus organogenesis (Cordier and Haumont, 1980).

The developmental potential of mouse third pharyngeal pouch endoderm was also directly assessed in mice using an ectopic transplantation model (Gordon *et al.*, 2004). In these

experiments, the 3<sup>rd</sup>pp and 4<sup>th</sup>pp endoderm of E8.5 to E9.0 mouse embryos was isolated from surrounding mesenchyme and cleft ectoderm by enzymatic and manual dissection, and transplanted under the kidney capsule of nude mice, which provides a permissive environment for thymus organogenesis (Bennett *et al.*, 2002; Bogden *et al.*, 1979; Zinkernagel *et al.*, 1980). Under the given experimental condition, the extracted endodermal tissue was isolated before its contact with the pharyngeal cleft ectoderm. Again, purified endoderm was sufficient to generate a functional thymus regularly organized into a distinct cortical and medullary compartment, respectively. When compared to stage-matched endoderm, E9.0 tissue from the entire third and fourth pharyngeal arch grafted under the kidney capsule and analysed, for the capacity to confer thymus function to recipients, was less efficient. These data revealed that pharyngeal cleft ectoderm provides no advantage for thymus development in these grafts. As a variety of other tissues than thymus including skin, hair follicles, cartilage, ossified bone, muscle and adipose tissue developed in some of these grafts in contrast to purified pharyngeal endodermal grafts, the authors suggested that cleft ectoderm does even inhibit thymus formation in favour of other differentiated cell types. This study therefore confirmed and expanded in mice the results of the classic chick–quail chimera experiments, indicating that purified pharyngeal endoderm can generate both cortical and medullary thymic epithelial cell (TEC) compartments, while the cleft ectoderm fails to contribute to the formation of a normal thymus. These experiments also indicated that some cells in the pharyngeal endoderm are specified to enter the TEC lineage before overt signs of organogenesis, as previously reported in birds (Le Douarin and Jotereau, 1975).

#### **1.4.4 A putative common thymic epithelial progenitor cell**

The existence of a common thymic epithelial stem cell has previously been suggested by several authors, based on evidence from marker studies of normal thymus and the observation that some thymomas can give rise to both cortical and medullary TEC types (Ropke *et al.*, 1995; Schluep *et al.*, 1988; Von Gaudecker *et al.*, 1997). An indication of the probable phenotype of thymic epithelial progenitor cells (TEPCs) was provided by analyses of thymi in nude–wild-type aggregation and transplantation chimaeras (Blackburn *et al.*, 1996; Klug *et al.*, 1998). These studies investigated whether all or part of the nude thymic epithelium could be rescued by the presence of wild type cells in nude-wild type chimeric mice. Detailed immunohistochemical

analyses indicated for the development of all major subpopulations of mature thymic epithelium a cell autonomous requirement for the nude gene product, forkhead box N1 (FoxN1) (Blackburn *et al.*, 1996). This study also showed that nude cells apparently committed to TEC lineages were phenotypically similar in nude–wild-type chimaeras and in the thymic remnants of nude mice. However these nude cells lacked markers associated with mature TEC subtypes, including MHC class II molecules, but expressed the determinants recognized by monoclonal antibodies MTS20 and MTS24. The use of these antibodies defines in the adult mouse thymus a rare subpopulation of cells with thymic epithelial cell precursor potential (Bennett *et al.*, 2002; Blackburn *et al.*, 1996; Gill *et al.*, 2002; Godfrey *et al.*, 1990). When purified and grafted ectopically into mice, these cells can differentiate into all known thymic epithelial cell types, attract lymphoid progenitors, and support normal thymopoiesis (Bennett *et al.*, 2002; Gill *et al.*, 2002). Collectively, these data indicated that in the absence of functional FoxN1, TECs are arrested at an immature progenitor stage that is characterized phenotypically by expression of the MTS20 and MTS24 determinants (Blackburn *et al.*, 1996).

The differential expression of cytokeratin 5 (K5) and 8 (K8) further distinguish several mouse TEC subpopulations (Klug *et al.*, 1998). The main cortical and medullary subsets are  $K8^+K5^-$  and  $K8^-K5^+$ , respectively, with a minor subpopulation of K5 and K8 double positive cells found typically at the cortico–medullary junction. An aberrant, mainly  $K5^+K8^+$  epithelial-cell phenotype was observed in the thymi of transgenic mice that express human CD3epsilon under the control of its endogenous promoter (designated CD3epsilon line 26, CD3ε26) which was found to correlate with a block in TEC differentiation due to an absence of cross-talk between early prothymocytes and thymic epithelial and an early block in thymopoiesis at the transition from DN1 ( $CD44^+CD25^-$ ) to DN2 thymocytes ( $CD44^+CD25^+$ ) (Wang *et al.*, 1994) (Hollander *et al.*, 1995). This abnormality can be corrected in fetal but not adult animals by transplantation of either fetal or adult wild-type haematopoietic stem cells (Hollander *et al.*, 1995). Furthermore transplantation of newborn CD3ε26 transgenic thymi under the kidney capsule of recombination-activating gene 1 (Rag1) deficient mice resulted in a partial correction of the observed defect, as indicated by the development of a substantial  $K5^+K8^+$  TEC population (Klug *et al.*, 1998). These data indicate a precursor–progeny relationship, in which  $K5^+K8^+$  progenitors give rise to  $K5^-K8^+$  cortical epithelial cells (Klug *et al.*, 1998). Moreover, these results are also consistent with subsequent ontological studies that show the presence of  $K5^+K8^+$  TECs in the earliest thymic

rudiments, including stages before the appearance of cortex or medulla-specific markers (Bennett *et al.*, 2002; Klug *et al.*, 2002). A subsequent study has shown that the T-cell development blockade in CD3ε26 transgenic mice results from an insertion effect that affects the T/B-cell fate choice by reporting that an abnormal accumulation of mature B cells was found in the thymi of these mice (Tokoro *et al.*, 1998). As this accumulation of B cells could not be observed in other human CD3ε26 transgenic mouse lines, ruling out the possibility that the aberrant mainly K5<sup>+</sup>K8<sup>+</sup> TEC phenotype which predominates in any CD3ε26 transgenic mouse line results as a direct consequence of increased intrathymic B-cell development in CD3ε26 transgenic mice (Tokoro *et al.*, 1998). Taken together these results suggest (but do not prove) that a common progenitor cell might exist, bearing the phenotype of MTS20<sup>+</sup>MTS24<sup>+</sup>K5<sup>+</sup>K8<sup>+</sup>.

To test the contention that MTS24<sup>+</sup> cells serve as a pool of thymic epithelial precursor cells, TECs with this phenotype were isolated from mouse thymic tissue at distinct developmental stages. Using immunohistochemistry, the population of MTS24<sup>+</sup> cells constitute half of all thymic epithelial cells at E12.5 but only a very small population at developmental stages beyond E15.5 (Bennett *et al.*, 2002; Gill *et al.*, 2002). Intriguingly, the MTS24<sup>-</sup> population could not reconstitute thymic function as assessed by any of the parameters mentioned earlier. Thus, all thymic epithelial precursor cell activity is contained in the MTS24<sup>+</sup> fraction, which is, however, still rather heterogeneous when analysed for other cell surface markers.

Phenotypic analysis of MTS24<sup>+</sup> thymic epithelial cells from both E11.5 and E12.5 tissue displayed homogeneously the co-expression of K5 and K8 (Bennett *et al.*, 2002). At E12.5, this population also stains either weakly or is completely negative for other differentiation markers that are indicative of mature cortical and/or medullary epithelial-cell types including 4F1, MTS10, MHC class II molecules (Bennett *et al.*, 2002). At E15.5, 96% of MTS24<sup>+</sup> cells express MHC class II molecules and the population can be further divided on the basis of UEA-1 reactivity, which identifies a subpopulation of medullary TECs in the postnatal thymus (Gill *et al.*, 2002). Based on these data, it has been proposed that MTS24<sup>+</sup>K5<sup>+</sup>K8<sup>+</sup> cells comprise the multipotent TEC precursor, which via intermediate TEC populations gives rise to fully differentiated (MTS24<sup>-</sup>) cortical and medullary epithelial cells (Gill *et al.*, 2003). The regenerative capacity of the thymus and turn over studies focusing on thymic epithelial cells, suggest that tissue-resident multipotent precursor cells could persist in the post-natal thymus.

However, whether this population still contains in the adult mouse true precursor stem cells with or without self-renewing potential is unclear. In the absence of clonal analysis for the demonstration of a single thymic epithelial cell progenitor, the possibility has to be entertained that the population of MTS20<sup>+</sup>MTS24<sup>+</sup> cells harbours distinct cortical and medullary progenitors. However, new unpublished data has revealed that a single MTS24<sup>+</sup> thymic epithelial cell is able to reconstitute both cortical and medullary thymic epithelial cells (S.Rossi, in press).

The medullary compartment appears to arise as a series of clonal islets, each arising from a single progenitor rather than from an epithelial cell layer, which coalesce as the thymus matures (Rodewald *et al.*, 2001). This has been revealed by non-parental balanced chimeric mice, whereby injection of embryonic stem (ES) cells into blastocysts using ES cells and blastocysts that differ in their major histocompatibility complex (MHC) type revealed that the medullary epithelium in these chimaeras is composed of discrete cell clusters derived from either the embryonic stem cell or from the blastocyst, but never of mixed origin. Notably, no correlation was found between the haplotype of a given medullary islet and that of the surrounding cortical epithelium, suggesting the existence of medullary thymic epithelial precursor cells. This finding is however in contradiction to more recent work mentioned above. The mechanism of the thymic epithelial architecture formation from such progenitor cells might not only occur during organogenesis, but might also be involved in tissue maintenance or self-reorganization. To test this, Rodewald and colleagues investigated whether the compartmentalization between the cortex and the medulla can occur from isolated and purified thymic epithelial cells. These thymic epithelial cells were taken at E16.5 (a stage at which the medulla is already partly developed) and were then re-assembled to form epithelial reaggregate fetal thymic organ cultures (RFTOC) *in vitro* before they were grafted under the kidney capsule of recipient mice (Rodewald *et al.*, 2001). These RFTOC grafts restored a normal cortex-medulla organization and thymopoiesis, thereby showing that purified thymic epithelium has the capacity to self-reorganize into a structurally and functionally competent microenvironment. To reveal in these RFTOC grafts whether the medulla formation has occurred by the segregation and the clustering of pre-existing medullary epithelial cells, or, alternatively, from single progenitors, the reaggregates were assembled from an equal mixture of thymic epithelial cells isolated from two different mouse strains characterized by separate MHC class II molecules. To avoid any ambiguity caused by the colonization of the graft by bone marrow-derived MHC class II positive host cells such as the dendritic cells, the mixed-

MHC reaggregates were implanted into MHC class II deficient mice. These experiments showed the persistence of a putative medullary epithelial progenitor cell until at least E16.5 (Rodewald *et al.*, 2001). These results can be interpreted by one of two ways. First, a common endoderm-derived thymic epithelial precursor cell might give rise directly to all TEC populations, or second, separate progenitors exist for the cortical and the medullary epithelial compartment. Although at the time of writing this thesis, single cell analysis have not been reported that can discriminate between these two distinct models, Rodewald's data on the clonal origin of medullary islets seem to favour a model in which intermediate progenitor cells exist for the cortical and medullary epithelial-cell compartments. Observations on the early patterning of the thymic primordium into cortical and medullary compartments would, however, be consistent with either model (Bennett *et al.*, 2002; Klug *et al.*, 2002).

## **1.5 The genetic control of early thymus development**

The existing data on the development of thymic epithelial cells suggests that endodermal cells of the 3<sup>rd</sup>pp acquire a thymic epithelial cell fate and form a population of progenitor cells that subsequently differentiate phenotypically into diverse thymic epithelial cells. Some of the important molecular mechanisms that control the individual steps in this thymic differentiation have been identified from genetic studies.

### **1.5.1 Transcription factors**

Analyses of gene-expression and mutant phenotype patterns have identified a network of transcription-factors that is required for the initial formation and early patterning of the thymus/parathyroid rudiment. At present, this network is composed of six factors: homeobox A3 (Hoxa3), pre-B-cell leukaemia transcription factor 1 (Pbx1), paired box gene 1 (Pax1), Pax9, eyes absent 1 homologue (Eya1) and sine oculis-related homeobox 1 homologue (Six1). In mice, these 6 transcription factors are co-expressed in the pharyngeal endoderm. In addition, Pax1 and Pax9 are also expressed in the neural crest-derived mesenchyme. The direct importance of these factors for thymus organogenesis have been demonstrated in spontaneous and gene targeted mutant mice (Chisaka and Capecchi, 1991; Hetzer-Egger *et al.*, 2002; Laclef *et al.*, 2003; Manley and



Capecchi, 1995; Manley *et al.*, 2004; Peters *et al.*, 1998; Wallin *et al.*, 1996; Xu *et al.*, 2002). Interestingly, some of these factors have been identified to be important for the eye development in *Drosophila* where the Pax–Eya–Six axis operates cell-autonomously to regulate common steps in eye development including cell proliferation, patterning, and neuronal development (Pignoni *et al.*, 1997). Taken together, these data have suggested that the Pax-Eya-Six regulatory network, if indeed conserved in the vertebrate organogenesis, must act specifically during the development of some of the endodermal derivatives, as the thymus, parathyroid glands and thyroid are all dependent on this network (Laclef *et al.*, 2003).

Based on the understanding that Hox genes control the axial position identity during embryogenesis and in view of the observation that the anterior boundary of *Hoxa3* expression is along the third pharyngeal pouch, it has been hypothesized that the expression of *Hoxa3* determines the positioning and identity of the thymus/parathyroid rudiment (Krumlauf, 1994). Moreover, the Pax–Eya–Six pathway together with *Hoxa3* might also control the separation of the thymus/parathyroid primordium from the pharynx and its subsequent migration. Indeed, thymic rudiments do not detach from the pharynx of Pax9 mutant mice and the normal separation is delayed in *Hoxa3*<sup>+/-</sup>*Pax1*<sup>-/-</sup> deficient animals (Hetzer-Egger *et al.*, 2002; Su *et al.*, 2001). The intrinsic ability of the thymus primordium to migrate caudally is also disturbed in *Hoxa3*<sup>+/-</sup>*Pax1*<sup>-/-</sup> mutant mice (Manley *et al.*, 2004).

Following initiation of organogenesis, two additional processes must occur for the development of the thymus to be eventually successful: (i) a patterning of the rudiment into thymus and parathyroid-specific domains needs to take place; and (ii) TEC differentiation has to be initiated. Insights into these processes have come from analysis of two transcription factors, forkhead box N1 (FoxN1) and glial cells missing homologue 2 (Gcm2). FoxN1 and Gcm2 are expressed in complementary domains by the developing thymus/parathyroid primordium at E11.5, indicating at this point in development the existence of distinct, prospective thymus and parathyroid regions (Gordon *et al.*, 2001). Gcm2 was identified as a homologue of the *Drosophila* gene Gcm that acts as a binary switch between neuronal and glial cell determination (Kim *et al.*, 1998). A loss of function of the mammalian homologue results in a failure to form the parathyroid glands (Gunther *et al.*, 2000). Gcm2 is already expressed in a discrete domain of the third pharyngeal pouch as early as E9.5, while FoxN1 expression is only detectable by PCR at E10.5 (Balciunaite

*et al.*, 2002) and by in situ hybridization by E11.25 (Gordon *et al.*, 2001). Thus, establishment of the Gcm2-expression domain may in fact define the future thymus–parathyroid boundary. Gcm2 expression seems to be controlled in the endoderm by the Pax–Eya–Six pathway together with Hoxa3 and Sonic hedgehog (Shh), as it is not initiated in either Hoxa3, Shh or Eya1 deficient mice and downregulated in Hoxa3<sup>+/-</sup>-Pax1<sup>-/-</sup> compound mutants (Blackburn and Manley, 2004; Moore-Scott and Manley, 2005; Su *et al.*, 2001; Xu *et al.*, 2002).

The FoxN1 transcription factor (Nehls *et al.*, 1994), encoded by the gene that is mutated in nude mice, is crucial for the development of a mature thymus (Flanagan, 1966; Nehls *et al.*, 1996; Pantelouris, 1968). Although often referred to as athymic, FoxN1-deficient mice undertake the initial stages of thymus organogenesis. Although a primordium is formed, this anlage fails to differentiate further and is not colonized by lymphocyte progenitors (Nehls *et al.*, 1996). This observation fits a "two-step model", in which expression of FoxN1 divides thymus development into a FoxN1-independent, early phase in organogenesis culminating in thymic epithelial precursor cell formation, and a FoxN1-dependent late phase that includes thymic epithelial precursor cell differentiation. FoxN1 expression was not detected by in situ hybridization in the Hoxa3, Eya1 or Six1 mutants. At present, the only factors known to regulate the expression of FoxN1 in the thymus are specific Wnt glycoproteins and Bmp4 (Balciunaite *et al.*, 2002; Tsai *et al.*, 2003). FoxN1 expression was not detected by in situ hybridization in the Hoxa3, Eya1 or Six1 mutants at E11.5. Since high-level of FoxN1 expression is detected (as already mentioned) at E11.25, the lack of these transcription factors reveal a block in thymus organogenesis that occurs before FoxN1 expression (Gordon *et al.*, 2001).

It is unlikely that FoxN1 is responsible for specifying thymic identity during the initial steps of organogenesis because there is no specific phenotype in FoxN1-deficient mice before E11.25. Moreover, cells with an apparent phenotype typical for thymic epithelial precursor cells are generated despite the absence of FoxN1 function (Blackburn *et al.*, 1996). The transplantation experiments of quail tissues to chicks provide functional evidence for these species that the endoderm is specified to a thymus fate well before an obvious organ formation has taken place (Le Douarin and Jotereau, 1975). A possible explanation for this observation is that the thymus fate constitutes a "default" identity for tissue of the third pharyngeal pouch that does not receive the normal set of molecular cues. Such a program could be either established by the Pax–Eya–Six

axis in conjunction with the function of *Hoxa3* and *Pbx1* or alternatively, the expression of *Gcm2* in the third pharyngeal pouch may suppress the acquisition of a thymus identity and replaces it with a parathyroid fate. In that regard a very recent study provides support for this explanation since *Shh* acts in unison with *Gcm2* as a factor required for the development of the parathyroids but not the thymus (Moore-Scott and Manley, 2005). Moreover, an abnormal expansion of the thymus within the third pharyngeal pouch has been observed in *Shh* deficient mice as the expression of *Gcm2* was absent. Concomitantly, the expression of *FoxN1* and *BMP4* was expanded in these animals throughout the entire primordium. Taken together, these data suggest that *Shh* expression in the thymus/parathyroid primordium is required for its dorsal-ventral patterning and for parathyroid specification and organogenesis by acting as a positive regulator of *Gcm2* and a negative regulator of *BMP4* in the 3<sup>rd</sup>pp. However *BMP4* expression in the entire 3<sup>rd</sup>pp alone does not explain *FoxN1* expanded expression within the primordium in *Shh* deficient mice because *BMP4* has been recently shown to be not immediately required for *FoxN1* expression, as transgenic mice for xenopus *noggin* (a direct inhibitor of *BMP4*) under the control of the *FoxN1* promoter did not affected *FoxN1* expression at E11.5 and E12.5 (Bleul and Boehm, 2005).

Factors other than *Gcm2* may also specify parathyroid fate within the third pharyngeal pouch. A possible candidate for such a function is *Ehox*, a distant member of the paired-box family of homeodomain transcription factors (Jackson *et al.*, 2002). *Ehox* displays a markedly restricted expression pattern that would be consistent with a role in early thymus organogenesis and/or specification of the thymic epithelial lineage. *Ehox* is expressed throughout the foregut endoderm at E8.5, but by E9.5, its expression is limited to a ventral domain in the second and third pharyngeal pouches (Jackson *et al.*, 2003). At E10.5, *Ehox* is largely restricted to a domain complementary to that of *Gcm2*. A day later, *Ehox* cannot be detected anymore by in situ hybridization within the pharyngeal pouches but the domain previously marked by its expression is now strongly positive for *FoxN1* transcripts (Blackburn and Manley, 2004). Therefore, the expression of *Ehox* defines a region that will eventually give rise to the thymus.

The T-box transcription factor *Tbx1* is normally expressed in the endodermal lining of the third pharyngeal pouch and the mesodermal core of the third pharyngeal arch (Garg *et al.*, 2001). *Tbx1*, which is also detected in the thymus at later stages of development is regulated by Sonic

hedgehog signalling. Tbx1 has been implicated in the complex phenotype of the DiGeorge syndrome (Abu-Issa *et al.*, 2002; Frank *et al.*, 2002b; Jerome and Papaioannou, 2001; Lindsay *et al.*, 2001; Merscher *et al.*, 2001; Yagi *et al.*, 2003). In the mouse, overexpression of Tbx1 resulted in a small thymus that was abnormally positioned in the mediastinum (Merscher *et al.*, 2001). It was concluded from these experiments that the overexpression of Tbx1 may in turn effect the coordinated expression of several factors required for the descent of the thymus into the thoracic cavity. The DiGeorge syndrome is likely caused by haploinsufficiency of Tbx1, but its variable phenotype indicates the involvement of additional genetic modifiers. For example, absence of the Vegf(164) isoform causes birth defects in mice, that are reminiscent of those found in the DiGeorge patients (Stalmans *et al.*, 2003). Indeed, Tbx1 expression was reduced in Vegf(164)-deficient mice and a knock-down of Vegf in zebrafish enhanced pharyngeal arch artery defects induced by Tbx1 deficiency (Stalmans *et al.*, 2003). Moreover, five of 12 Vegf (120) isoform deficient mice had either a hypoplastic, an absent, or an ectopically located thymus and the parathyroid glands were absent in four of 12 of these mutants, whereas all of these animals had cardiac outflow tract anomalies, characteristically observed in DiGeorge patients (Stalmans *et al.*, 2003). In keeping with this experimental evidence is the observation in DiGeorge patients that a specific Vegf promoter haplotype, documented to reduce Vegf expression, was associated with an increased risk for cardiovascular defects (Stalmans *et al.*, 2003). Taken together these data suggest that Vegf is involved in the DiGeorge syndrome by regulating Tbx1.

Although marked progress has been made in identifying the transcription factors that act in the endoderm during early thymus organogenesis, the molecular events that occur concurrently in the mesenchyme are less well established. Hoxa3, Eya1 and Six1 are also expressed in the mesenchyme, and a role for neural crest cells during thymus organogenesis has been suggested by Kuratani and colleagues (Kuratani and Bockman, 1990a; Kuratani and Bockman, 1990b; Kuratani and Bockman, 1991). Hence the expression of Hoxa3, Eya1 and Six in neural crest cells might also be required for a proper development of the thymus. In fact an analysis of mutants of Hoxa3 and its paralogues, Hoxb3 and Hoxd3, indicate that these gene products have a redundant function in promoting migration of the primordium after it separates from the pharynx. The removal of one functional copy of Hoxa3 from the Hoxb3, Hoxd3 double mutants (Hoxa3<sup>+/-</sup>, Hoxb3<sup>-/-</sup>, Hoxd3<sup>-/-</sup>) results in the failure of the thymus and parathyroid glands to migrate to their

normal positions in the throat (Manley and Capecchi, 1998). Defining specific functional roles for *Hoxa3*, *Eya1* and *Six1* in neural crest cell and in endodermal cell differentiation and function, respectively, during thymus organogenesis will require tissue-specific genetic approaches that separate their role for endoderm development from that of other functions in the mesenchyme. So far, *Pax3* is the only transcription factor known to affect thymus development and to be expressed by neural crest cells. Mutations in *Pax3* cause the splotch phenotype in mice (Franz, 1989). However, the thymus hypoplasia/aplasia observed in *Pax3* mutants appears to be secondary to the death or failure in migration of neural crest cells (Conway *et al.*, 1997; Epstein *et al.*, 2000).

### **1.5.2 Signalling molecules**

The evidence presented so far indicates that at least some molecular mechanisms operational in the patterning of the thymus/parathyroid primordium may be intrinsic to the endoderm. But, many of the initial steps in the formation of different organs are known or thought to involve cell–cell interactions including those between mesenchymal and epithelial cells. In fact, signals from cell types, such as the surrounding neural crest-derived mesenchymal cells have been shown to be required for thymus organogenesis (Anderson *et al.*, 1993; Jenkinson *et al.*, 2003; Kuratani and Bockman, 1990b). Such an interaction is in keeping with additional observations detailing neural crest cells to contribute to the formation of the fetal thymus (Sunjara *et al.*, 2000).

As discussed previously, ablation studies in chicks, and the phenotypes of mutant and transgenic mice with specific defects in neural crest cell formation, migration or survival, have indicated that the loss of these cells correlated with an absence or a variable reduction in thymic size (Bockman and Kirby, 1984; Bockman and Kirby, 1989; Conway *et al.*, 1997; Ohnemus *et al.*, 2002; Soriano, 1997). Furthermore, thymic aplasia or hypoplasia secondary to a compromised function of neural crest cells did occur despite a normal expression pattern of *Tbx1*, *Pax1*, *Pax9* and *Hoxa3* in the pharyngeal endoderm and were concurrent with a regular thymopoiesis (Ohnemus *et al.*, 2002). The different thymic phenotypes produced by neural crest deficiencies may thus be the consequence of an aberrant formation of the pharyngeal pouches and the impaired migration of thymic primordia caused by alterations of the mesenchymal content of the branchial arches.

Similarities with the development of other endodermal organs would predict that a cascade of reciprocal signals between the endoderm and mesenchyme control positioning and outgrowth of the thymic rudiment. Although all of the main developmental signalling pathways including the fibroblast growth factors (Fgfs), Wnts, bone morphogenetic proteins (Bmps) and Shh have been implicated in thymus development, unequivocal genetic evidence for their involvement in the very early stages of development is however scarced and at present only available for Fgfs.

Two recent genetic studies have shown that decreasing Fgf signalling between the endoderm and mesenchyme results in thymus hypoplasia, but does not markedly affect thymocyte differentiation. Fgf8 is expressed at E10.5 in the pharyngeal pouch endoderm, where it presumably signals to the surrounding neural crest-derived mesenchyme (Abu-Issa *et al.*, 2002; Brown *et al.*, 2004). Reduction of Fgf8-signaling using a hypomorphic Fgf8 allele resulted in two separate phenotypes: (i) some embryos were athymic, possibly due to a secondary effect of severe defects in the formation of the third and fourth pharyngeal arch and pouch, and (ii) some embryos displayed a hypoplastic, sometimes ectopic thymus which supported a phenotypically normal thymopoiesis (Frank *et al.*, 2002b). This second phenotype is reminiscent of the one reported for a knockout of the isoform IIIb of Fgf receptor 2 (FgfR2IIIb); This receptor is expressed by TECs as early as E13, where it is thought to receive signals from its ligands Fgf7 and Fgf10, which are apparently secreted by the surrounding mesenchyme (Jenkinson *et al.*, 2003; Revest *et al.*, 2001b). In FgfR2IIIb deficient mice, thymus organogenesis proceeds normally until about E12.5, after which the organ fails to increase in size (Revest *et al.*, 2001b). However, sufficient TEC differentiation occurs in the hypoplastic thymus of these animals to support a phenotypically normal T-cell differentiation. The few T cells generated in FgfR2IIIb-deficient thymi have never been tested functionally (Revest *et al.*, 2001b). There may be a genetic link between the phenotype observed in Fgf8 and FgfR2IIIb mutant mice as the expression of Fgf10 is reduced in mice homozygous for an hypomorphic Fgf8 allele (Frank *et al.*, 2002b). Thus, it is thought that reciprocal Fgf signalling may be required between the endoderm and the mesenchyme at an early stage of thymus formation. This interdependence is reminiscent of reciprocal Fgf signalling that is required both for initial placement and induction of limb-bud formation and for the initial lung organogenesis (Hogan and Yingling, 1998; Martin, 1998). In view of a role for Fgf8 in pouch formation, mice homozygous for a hypomorphic allele of Fgf8 containing loxP sites have been converted to a null allele by being mated to cre transgenic

animals (Meyers *et al.*, 1998). However, from the analysis of these mutants it could still not be established whether Fgf signalling is directly required for the initial development of the thymus primordium.

Fetal thymic organ-culture (FTOC) experiments have recently provided evidence that at least some of the observed effects by Fgfs may be related to Bmp4 signalling. The addition of Bmp4 to FTOCs affected the differentiation of double negative (DN1) thymocytes along the  $\alpha\beta$ -lineage T cell development as this treatment led to an abnormal accumulation of these immature cells (Hager-Theodorides *et al.*, 2002). This effect of Bmp4 was suppressed by inhibition of Fgf signalling (Tsai *et al.*, 2003). Moreover, stimulation via Bmp4 also upregulated the expression of FoxN1 and FgfR2IIIb. Taken together, this study suggested that Bmp4 upregulates FoxN1, which in turn upregulates FgfR2IIIb expression, rendering TECs susceptible to Fgf7 and Fgf10 signals provided by different cells including cells of the mesenchyme as well as double or single positive thymocytes (Erickson *et al.*, 2002).

Alterations in the formation of the third pharyngeal pouch and endodermal expression of Fgf8, Tbx1, Pax1 and Pax9 have been noted in the absence of signals mediated by retinoic acid (Niederreither *et al.*, 2003; Roberts *et al.*, 2005; Wendling *et al.*, 2000). It has therefore been concluded that the retinoic acid (RA) receptor constitutes an indispensable component for the specification of the pharyngeal endoderm (Dupe *et al.*, 1999; Wendling *et al.*, 2000). To further investigate its role, targeted inactivation of the mouse retinaldehyde dehydrogenase 2 (Raldh2/Aldh1a2), the enzyme responsible for early embryonic retinoic acid synthesis, has been investigated (Niederreither *et al.*, 2003). Because these mutant mice die between E9.5 and E10.5 from severe defects in early heart morphogenesis, maternal RA was supplemented transplacentally to Raldh2(-/-) embryos to prevent heart defects and other anomalies (e.g. the formation of organs from the 2<sup>nd</sup> branchial arch, hindbrain patterning early in development) (Niederreither *et al.*, 1999). However, despite the rescue of several of the aforementioned defects, these RA-supplemented mutant embryos still exhibit impaired development of their posterior (3<sup>rd</sup>-6<sup>th</sup>) branchial arch region (Mark *et al.*, 2004; Niederreither *et al.*, 2003; Vermot *et al.*, 2003). While in the RA-supplemented mutant embryos, the development of the first and second arches and their derivatives, as well as the formation of the first pharyngeal pouch, appear to proceed normally, more posterior pharyngeal pouches and the cardiac outflow tract septation fail

to form (i.e. 3<sup>rd</sup>pp and 4<sup>th</sup>pp). Hence, all derivatives of the posterior branchial arches are affected in these embryos, including the aortic arches, pouch-derived organs (thymus, parathyroid gland) and the postotic neural crest cells, which normally establish regular segmental migratory pathways (Niederreither *et al.*, 2003). Raldh2 is responsible for producing RA which in turn is required for the proper development of the posterior branchial arches and its endodermal derivatives. During the development of the posterior branchial arches, the mesoderm-specific Raldh2 expression is restricted to the posterior most pharyngeal region (Niederreither *et al.*, 1999). Thus, Raldh2 appears to play a crucial role in producing high levels of RA required for the pharyngeal development of the branchial arches 3 to 6. Consequently, RA is one of the diffusible mesodermal signals that pattern the pharyngeal endoderm of the 3<sup>rd</sup>pp and 4<sup>th</sup>pp. The defects in RA-supplemented Raldh2 deficient mice are similar to those observed in mice deficient for Tbx1 expression which are providing defect similar to the clinical presentation of the DiGeorge syndrome (DGS) and the velocardiofacial syndrome (VCFS). These related syndromes are characterized by numerous but largely overlapping defects including thymic aplasia, or hypoplasia, hypoparathyroidism, cardiovascular pathologies, and craniofacial anomalies. In fact, both syndromes are resulting from a heterozygous deletion of contiguous genes and are therefore commonly referred to as a single disease entity, designated DGS/VCFS or, alternatively, the 22q11.2 deletion syndrome. Moreover, a hypomorphic Raldh2 mutation in mice was found to selectively lead to DGS/VCFS-like defects, albeit less severe than in the Raldh2-null mutants (Vermot *et al.*, 2003). Thus, decreased levels of embryonic RA (through genetic mutations and/or nutritional deprivation during embryogenesis) may act as a major modifier for the clinical presentation of human 22q11del-associated DGS/VCFS syndrome. Sufficiently severe, a decrease in RA may also on its own lead to some of the clinical features typical for the DiGeorge syndrome. As Tbx1 expression is only mildly affected in both the null and hypomorphic Raldh2 mutants this transcription factor cannot be considered as a critical determinant of the Raldh2 phenotype (Niederreither *et al.*, 2003; Vermot *et al.*, 2003). Although overexpressing RA has shown to down-regulate Tbx1 expression in avian embryos and quail lacking endogenous RA in early development results in a subsequent loss of Tbx1 expression in all tissues, it has been suggested by Roberts and colleagues that RA acts downstream of Tbx1 to regulate expression signalling of molecules required for proper pharyngeal development (Roberts *et al.*, 2005). Fgf8 could represent such a critical downstream signal, as (i) Fgf8 expression is altered in Tbx1<sup>-/-</sup> and Raldh2<sup>-/-</sup> mutants, and as (ii) the Fgf8 hypomorphic mutation also leads to



DGS/VCFS-like phenotype (Abu-Issa *et al.*, 2002; Frank *et al.*, 2002b; Niederreither *et al.*, 2003; Vermot *et al.*, 2003).

Signalling via members of the Wnt family of glycoproteins has also been implicated in the promotion of TEC differentiation and thymocyte development, respectively (Balciunaite *et al.*, 2002; Mulroy *et al.*, 2002; Mulroy *et al.*, 2003; Pongracz *et al.*, 2003; Staal *et al.*, 2001; Staal *et al.*, 2004). Wnts which are differentially expressed by both TECs and developing thymocytes as secreted proteins act in a cell non-autonomous fashion. Wnts bind to glycosaminoglycans in the extracellular matrix and to two distinct families of cell-surface receptors, the frizzled (Fz) and low-density lipoprotein receptor-related proteins 5 and 6 (LRP5/6). With the latter two molecules, Wnts form a complex that promotes the activation of  $\beta$ -catenin, a cytoplasmically located second messenger. The subsequent nuclear translocation of  $\beta$ -catenin allows for its association with T cell factor 1 (Tcf-1) and Lymphoid enhancer factor 1 (Lef-1) transcription factors which on their own act as transcriptional repressors (Balciunaite *et al.*, 2002; Pinson *et al.*, 2000; Pongracz *et al.*, 2003). In vitro culture studies using thymic epithelial cell lines demonstrated that some (e.g. Wnt4, Wnt5b) but not all Wnts induce FoxN1 expression in TECs (Balciunaite *et al.*, 2002). These studies indicated that Wnts might maintain/modulate FoxN1 expression by TECs in both an autocrine and paracrine fashion.

Signalling via the bone morphogenetic proteins (BMP) has been implicated in thymus organogenesis (Bachiller *et al.*, 2003; Bleul and Boehm, 2005; Ohnemus *et al.*, 2002). This has been revealed from a study of mice transgenic for noggin which displayed thyroid hypoplasia, ectopic thymic, parathyroid hypoplasia or aplasia, and cardiac outflow tract defects (Kanzler *et al.*, 2000; Ohnemus *et al.*, 2002). Noggin as a transgene in these mice was under the control of an genomic fragment and enhancer of Hoxa2 to drive its expression in the second and more caudal branchial arches as well as in rhombomere 4 and more caudal rhombencephalic areas. When evaluating the role of BMP-dependent neural-crest cells in these mice, it could be observed that these cells failed to migrate (Ohnemus *et al.*, 2002). Taken together, these findings demonstrated that BMP-dependent neural-crest cells play a role in the development of the thymus, parathyroid and thyroid glands, and aortic arches (i.e. carotid and subclavian arteries). Hence, interfering with BMP signalling in the premigratory neural crest cells produces a phenotype closely resembling that of the DiGeorge syndrome. The expression of Tbx1, Pax9 and Hoxa3 endodermal markers

was not affected in these transgenic mice but Pax1 was reduced in the 3<sup>rd</sup>pp and Hoxa3 expression was found to be absent in the neural crest cells of these mice. Thus, suggesting that Pax1 expression in the 3<sup>rd</sup>pp endoderm is at least partially controlled by Hoxa3-expressing and BMP-dependent neural crest cells (Ohnemus *et al.*, 2002). Moreover, mice deficient for Chordin, a Bmp signalling antagonist, displayed an extensive array of malformations that encompass most features of the DGS/VCFS syndrome. For instance, these mice lack a thymus and parathyroid glands, and display hypoplastic thyroid gland as a consequence of a malformation of the pharyngeal arches 2 to 6. In addition, these mice also have a cardiac outflow tract defect possibly resulting from the failure of cardiac neural crest cells to reach the heart (Bachiller *et al.*, 2003). Concurrently, there is a major reduction of Tbx1, Pax9 and Fgf8 expression in the pharyngeal endoderm. Taken together, these data suggest that Chordin acts upstream of Tbx1 and Fgf8. In turn, Tbx1 relays the autocrine effect of Chordin in the pharyngeal endoderm necessary for a proper development of the thymus, parathyroid and thyroid glands. Given these results it is conceivable that an allelic variant of components of the Bmp signal transduction pathway could cause a DiGeorge-like phenotype. In fact, a recent study demonstrated a direct role of Bmp signalling in thymus development. Transgenic overexpression in thymic epithelial cells patterned for a thymus cell fate caused a hypoplastic and ectopically positioned but functional thymus (Bleul and Boehm, 2005). Bmp4 is normally strongly expressed at E10.75 in epithelial cells in the ventral aspect of the 3<sup>rd</sup>pp and in the neural crest-derived mesenchymal cells that surround the thymus anlage. By E12.5, Bmp4 expression is restricted to thymic cells of mesenchymal phenotype. In contrast, Bmp2 remains undetectable at this site until at least E12.5 and the expression of the Bmp target gene Msx1 is identical to that of Bmp4 but transcripts are more abundant in the peri-thymic mesenchymal cells when compared to the thymic epithelial cells (Bleul and Boehm, 2005). In the noggin transgenic mice, Bmp4 expression is aberrantly maintained in thymic epithelial cells and absent in thymic mesenchymal cells at E12.5. Bmp2 expression which was undetectable at any time point in wild type mice, was aberrantly up-regulated in thymic epithelial cells and Msx1 expression could not be detected in the thymic capsule at E12.5 (Bleul and Boehm, 2005). The expression of FoxN1 is unchanged in these mice suggesting that the transcription of the FoxN1 gene does not depend directly on Bmp signalling. The change in Bmp4 and Msx1 expression in the noggin transgenic mice suggest, however, a role for Bmp signalling in shaping the thymic stroma (Bockman and Kirby, 1984; Ohnemus *et al.*, 2002; Suniara *et al.*, 2000). In keeping with a role for Msx in thymic development is the

observation that mice deficient for *Msx1* and *Msx2* have an impaired patterning and survival of their neural crest cells, and display an abnormal location of the thymus (Ishii *et al.*, 2005). Furthermore *Bmp4* expression was found to be increased in the cranial neural crest and pharyngeal arches of these mutant embryos, suggesting that *Msx* genes may negatively control *Bmp* signals in these tissues (Ishii *et al.*, 2005). In *Shh* deficient mice, the expression of *Bmp4* in the ventral endoderm of the 3<sup>rd</sup>pp is expanded through the entire pharyngeal pouch. It is thus possible that *Shh* and *Bmp4* have opposing roles to establish the dorsal/ventral polarity of the third pouch. During later stages of development, *Shh* is also required for normal thymopoiesis to occur. Thymocyte differentiation is partially blocked in the transition from the earliest CD44<sup>+</sup>CD25<sup>-</sup> DN1 population to the subsequent CD44<sup>+</sup>CD25<sup>-</sup> DN2 population and from double negative to double positive thymocytes (DN to DP) in *Shh* deficient mice. Consequently, thymocyte cellular is greatly reduced in *Shh* deficient embryos (Shah *et al.*, 2004).

### **1.5.3 Regulation of TEC differentiation**

#### **1.5.3.1 Lymphocyte-dependent and independent development**

The establishment of distinct cortical and medullary compartments within the thymus is dependent on a mechanism termed cross-talk, a notion which refers to the direct interaction between TECs and developing thymocytes (Hollander *et al.*, 1995; Ritter and Boyd, 1993; Shores *et al.*, 1994; van Ewijk *et al.*, 2000a; van Ewijk *et al.*, 1994). The concept of "cross-talk" relates to a stepwise and interdependent development of the thymic stroma and thymocytes. Initial data pointing to the phenomenon of "cross-talk" was derived from the analysis of the *tgε26* mice. These mutant mice overexpress the human CD3 epsilon component of the T-cell receptor (TCR) as a transgene. This alteration has been believed to cause excessive signal transduction resulting in an observed arrest at the DN1 stage (CD44<sup>+</sup>CD25<sup>-</sup>) and lack functional thymic epithelium (Hollander *et al.*, 1995; Wang *et al.*, 1994; Wang *et al.*, 1995). A characteristic feature of the *tgε26* mice is the presence of several thymic cysts, and the lack of a regular organisation of a cortical and medullary microenvironments. In particular, a distinct border between cortex and medulla is lacking and many thymic epithelial cells are organized in a typical two-dimensional (2-D) fashion instead of an 3-D manner (Hollander *et al.*, 1995). These abnormalities could be corrected in fetal but not in adult transgenic animals by transplantation of either fetal or adult

wild-type haematopoietic stem cells (Hollander *et al.*, 1995). This observation concluded that the interaction of fetal stromal cells with early prothymocytes is required for the induction of a cortical microenvironment and that such a interaction is restricted to a particular window of time. Compared to  $\text{tg}\epsilon 26$  mice, T-cell development in recombination-activating gene (Rag) deficient mice progresses to a slightly later stage of T-cell development, namely to the double negative DN3 stage ( $\text{CD44}^+\text{CD25}^+$ ) (van Ewijk *et al.*, 2000a). Rag-mutant mice have a thymus with an increased cellularity and a well-developed thymic cortex, but their medulla is still absent when compared to  $\text{tg}\epsilon 26$  mice (van Ewijk *et al.*, 2000a). By transplanting  $\text{tg}\epsilon 26$  mice with Rag2-deficient bone marrow, thymopoiesis in these mice progressed from the DN1 towards the DN3 T-cell developmental stage, which stimulated the conversion of 2-D organized thymic epithelial cell sheets into a 3-D organized thymic epithelial network (van Ewijk *et al.*, 2000a). Subsequent transplantation with wild-type bone marrow cells in these  $\text{tg}\epsilon 26$  mice enables normal thymopoiesis and is paralleled by a correct organization of the medullary microenvironments (van Ewijk *et al.*, 2000a). Similarly, the disorganized and immature thymic medullary epithelial islands of mice defective for the  $\beta$  chain of the T cell receptor (SCID mice) could be restored by the introduction of wild-type bone marrow cells (Shores *et al.*, 1991). Taken together, these data suggest that maturing thymocytes control the development of thymic stroma in a stepwise fashion, resulting first in the induction of a correct cortical structure which is then followed by the establishment of the medullary compartment. In that regard, thymic medullary organization was shown to be abnormal in mice deficient for the  $\alpha$  chain of the TCR, which suggests that the development of medullary thymic epithelial cells is regulated by  $\alpha\beta\text{TCR}^+$  thymocytes at the single positive stage of development (Palmer *et al.*, 1993). Interestingly, the ability of  $\alpha\beta\text{TCR}^+$  thymocytes to induce maturation of medullary TEC appeared not to be related to the antigen specificity of the TCR as thymi from positively selecting, negatively selecting and non-selecting  $\alpha\beta\text{TCR}$  transgenic SCID mice all have a medullary thymic compartment, although its size varies considerably (Shores *et al.*, 1994).

In contrast, studies in mice deficient for FoxN1 have shown that the initial stages of thymus development occur independently of interaction with cells of haematopoietic origin (Nehls *et al.*, 1996). Further evidence that the initial stages of TEC differentiation, does occur in the absence of thymocytes was recently provided by a comparative analysis of the stromal development of wild-type mice, Rag2/ $\gamma\text{c}$  mutant mice and Ikaros deficient animals (Klug *et al.*, 2002). The absence of

a functional  $\gamma c$  chain in Rag2 deficient mice (designated Rag/ $\gamma c^{-/-}$ ) precludes IL-7/IL-7R interactions and consequently reduces thymocyte cellularity drastically (Colucci *et al.*, 1999; Klug *et al.*, 2002). The Ikaros transcription factor is indispensable for the commitment of haematopoietic stem cells to the lymphoid lineage and mice deficient for this molecule are characterized by an absence of T cell precursors during the fetal period (Georgopoulos *et al.*, 1994). Despite an early T cell developmental block in either of these mutant mice, the thymic epithelial cell compartment was found to be organized into a 3-D structure (Klug *et al.*, 2002). However, the development into well-organized medullary region containing K8<sup>+</sup>K5<sup>+</sup> TECs and the patterning of separate medullary and cortical compartments in the neonate and adult mouse require the continued presence of thymocytes. In fact, a recent study of fetal tge26 thymi confirmed that thymocyte-derived signals are not required for the initial maturation of TECs. This conclusion was corroborated in FTOC experiments where TEC proliferation leading to the formation of a normal thymic epithelial microenvironment, the differentiation into cortical (K5<sup>+</sup>K8<sup>+</sup>) and medullary (K5<sup>+</sup>K8<sup>-</sup>) epithelial cells, and the acquisition of a functional competence were independent of developing thymocytes (Jenkinson *et al.*, 2005). On the contrary, the proliferation of fetal thymic epithelial cells appears to be regulated by thymic mesenchyme (Jenkinson *et al.*, 2003). Collectively, these findings are arguing against an essential early role for thymocyte-derived signals during the development of the thymic epithelium. However, these results do not contest or rule out a role for such signals in the maintenance of the thymic epithelial microenvironment once such a compartment has been established. Although these studies demonstrate a link between T-cell development and the formation of a normal thymic architecture, it still remains elusive how T-cell precursors influence the differentiation and function of thymic stromal cells.

### **1.5.3.2 Molecular regulation of TEC differentiation**

FoxN1 is expressed by all TECs throughout life, albeit lower amounts of transcripts have been observed in older mice (Nehls *et al.*, 1996) and unpublished data of the Holländer Lab. The phenotype of TECs present in nude mice would suggest that these cells are arrested at an early progenitor stage with a limited capacity to proliferate and to induce the entrance of haematopoietic progenitor cells into the epithelial primordium (Itoi *et al.*, 2001; Nehls *et al.*, 1996). It has therefore been concluded that FoxN1 promotes both the initial differentiation as

well as the proliferation of TECs. Such a role is not different to the one FoxN1 has been assigned to in skin and hair, where FoxN1 is believed to promote the proliferation of progenitor cells of the hair shaft and the inner root sheath (Lee *et al.*, 1999).

The domains of FoxN1 necessary for TEC differentiation have recently been identified in mice expressing a hypomorphic allele for FoxN1 (Su *et al.*, 2003). This allele (designated FoxN1- $\Delta$ ) has the sequences deleted encoding for the FoxN1 most of amino-terminal domain deleted but still encodes for the DNA-binding, nuclear-localization and the C-terminal domains, respectively. The truncated protein causes a thymic phenotype which is milder in extent when compared to the FoxN1 null allele, but displays no effect on hair development. The use of this mutant molecule highlighted a thymus-specific role for the amino-terminal domain and uncoupled the function of FoxN1 in the thymus from that in the skin. A detailed analysis of TECs in mice homozygous for this hypomorphic allele indicated that the initial development of TECs was phenotypically normal albeit delayed, however, the TECs subsequent differentiation into medullary and cortical compartments was blocked (Su *et al.*, 2003). As this phenotype is similar to that reported for human CD3 $\epsilon$  transgenic mice, which have an early block in thymocyte development and lack a functional thymic cortex, it may be concluded that FoxN1- $\Delta$  fails to confer thymocyte-mediated signals into normal TEC differentiation (Hollander *et al.*, 1995; Klug *et al.*, 1998; Klug *et al.*, 2002). In contrast to FoxN1-deficient TECs, cells expressing the hypomorphic FoxN1- $\Delta$  mutant support to a limited extent thymopoiesis because the number of double positive and single positive thymocytes observed in these mutants was decreased by 97% when compared to wild type mice (Su *et al.*, 2003). In conclusion, a partial block at both DN1 (CD44<sup>+</sup>CD25<sup>-</sup>) and DP (CD4<sup>+</sup>CD8<sup>+</sup>) stages of thymocyte differentiation was observed. However, SP CD4<sup>+</sup> or SP CD8<sup>+</sup> cells were generated in FoxN1- $\Delta$  homozygous mice and these cells were exported to the periphery, although in reduced numbers. The mechanism by which the FoxN1 amino-terminal domain regulates TEC differentiation remains to be determined, as does the basis for its tissue-specific activity.

For its architectural organization, the medulla is dependent on distinct signals provided by thymocytes that have been successfully selected in a positive fashion (Shores *et al.*, 1991). These signals may likely be mediated by the transcription factor RelB (component of the NF $\kappa$ B signalling pathway), as mice deficient for RelB display a medullary thymic atrophy and aberrant

clonal deletion of autoreactive thymocytes (Burkly *et al.*, 1995; Laufer *et al.*, 1996; Naspetti *et al.*, 1997; Weih *et al.*, 1995). After E14.5, the autoimmune regulator gene, designated Aire, is expressed in TECs and to a much lower degree in dendritic cells. Aire transcription in TECs is critically dependent on the presence of RelB (Heino *et al.*, 2000; Zuklys *et al.*, 2000). Homozygous mutations of the Aire locus causes in humans the monogenic autoimmune syndrome APECED (autoimmune-polyendocrinopathy-candidiasis-ectodermal dystrophy). This disorder is characterized by the loss of self-tolerance to multiple organ-specific antigens secondary to the specific reduction in ectopic expression for genes encoding peripheral antigens (Anderson *et al.*, 2002) (Liston *et al.*, 2004; Liston *et al.*, 2003).

While the mechanisms that regulate the initial and late-stage differentiation of medullary and cortical TECs remain largely undetermined, a recent study has shown that lymphocyte-dependent development of medullary TECs is controlled by signalling through the lymphotoxin beta receptor (LTbetaR), as mice deficient for LTbetaR display an aberrant differentiation and reduced numbers of thymic medullary TECs (Boehm *et al.*, 2003). Furthermore these deficient mice revealed an abnormal retention of mature T lymphocytes. This aberrant export of mature thymocytes has been suggested to result from an absence of normal medullary lympho-epithelial interaction, which in consequence may lead to autoimmunity.

The TNF receptor-associated factor 6 (Traf6), has also been recently identified to be required for the differentiation of medullary TECs (Akiyama *et al.*, 2005). The deficiency of Traf6 in mice results in a disorganized distribution of medullary TECs and a lack of mature TECs. Interestingly, Traf6 deficient mice also developed spontaneous autoimmunity underscoring the central importance for a regularly structured and normally differentiated thymic medulla for the process of a correct T cell repertoire selection. In this context, it was suggested that Traf6-dependent and independent NFκB signalling were both involved in the initial stages of mTEC differentiation (Akiyama *et al.*, 2005; Ishikawa *et al.*, 1997). In further support of this conclusion, mice spontaneously deficient for the NFκB-inducing kinase (NIK) also displayed a disorganized thymic microarchitecture with no clear cortical-medullary distinction (Miyawaki *et al.*, 1994; Shinkura *et al.*, 1999). Taken together, these results reveal a critical role for NFκB signalling in mTEC differentiation and reveal the importance of the thymic medulla in the induction of self-tolerance (Kurobe *et al.*, 2006).

## **1.6 T-cell development in the thymus**

### **1.6.1 Commitment of T cell development in the fetus**

The thymus is the main site where T cells are generated. T cell commitment occurs in the thymus by the activation of Notch 1, a member of a highly conserved family of transmembrane receptors that are involved in many cell lineages in the regulation of cell-fate choices (Allman *et al.*, 2002; Pui *et al.*, 1999). (Radtke *et al.*, 1999). In the post natal mouse thymus, Delta1, a specific ligand for Notch1 is expressed at the cortico-medullary junction on thymic stromal cells. At this site blood-borne haematopoietic precursors enter the thymus and upon Notch-signalling are instructed to differentiate along the T-cell/NK-cell lineage (Han *et al.*, 2000; Jaleco *et al.*, 2001; Lind *et al.*, 2001). In contrast to the seeding of the vascularised thymus, the entry of precursor to the thymus primordium occurs through the organ's capsule. Here, several lines of evidence suggest that T/NK cell commitment can occur prior to thymic immigration, as such a developmental restriction had been observed in the thymus, blood, and spleen of E15 embryos (Carlyle *et al.*, 1997; Carlyle and Zuniga-Pflucker, 1998; Rodewald *et al.*, 1994).

### **1.6.2 Thymocyte precursors seeding and migration to the developmental thymus murine fetus**

A major focus of research into the function of the thymus has been dedicated to delineate the precise pathways by which haematopoietic precursor cells develop into mature T cells of the  $\alpha/\beta$  T cell lineage. These precursor cells originate from haematopoietic stem cells (HSCs), which at the time of their seeding to the thymus are still located in the aorta-gonad-mesonephros (AGM) region or in the placenta (Gekas *et al.*, 2005; Godin and Cumano, 2002). The HSC pool in the placenta occurs prior to and during the initial expansion of HSCs in the fetal liver (Gekas *et al.*, 2005).



### 1.6.3 T cell differentiation in fetal thymus

The events that eventually lead to the generation of a mature T cell population with a diverse T-cell receptor (TCR) repertoire are divided into two separate but sequential phases: (i) the early development of thymocytes proceeds in the absence of a rearranged  $\alpha/\beta$  TCR locus, and (ii) the subsequent differentiation depends on the successful cell surface expression of an  $\alpha\beta$  TCR from a productively rearranged locus. The earliest intrathymic precursors approximately of all thymocytes in the post-natal thymus belong to a subpopulation of cells expressing neither CD4 nor CD8. This population of cells has been referred to as the double negative (DN) thymocyte cells. Using additional cell surface markers, the population of DN cells can be further subdivided in the mouse into four distinct populations, which reflect distinct and sequential stages in the maturation. The most immature population of T-cells (known as DN1) is defined by the concomitant cell surface expression of CD44 (phagocyte glycoprotein-1/Pgp-1), CD117 (c-kit, tyrosine kinase receptor for stem cell factor), CD127 (IL-7R $\alpha$ ), and CD90 (Thy-1) but with the notable absence of CD25 (IL-2 receptor  $\alpha$  chain) (Wu *et al.*, 1991) (Godfrey *et al.*, 1993). The term “DN“ is, however, a misnomer for this subpopulation as these cells express low levels of CD4. It appears that CD4 molecules are taken up by DN1 cells from cells that express this T-cell coreceptor. Moreover, these CD4 molecules do not seem to be functionally important for DN1 cells as their loss of CD4 does not affect their capacity to contribute to early T cell development (Rahemtulla *et al.*, 1991). In this context it is important to point out that a CD44<sup>+</sup>CD25<sup>-</sup> subpopulation of CD4<sup>+</sup>CD8<sup>-</sup> thymocytes has been identified that fails to express CD117 but that is positive for the expression of an  $\alpha\beta$  TCR (Godfrey *et al.*, 1994). However, these cells do not contribute to early thymopoiesis. The expression of CD25 marks the progression from a DN1 to a DN2 (CD44<sup>+</sup>CD25<sup>+</sup>) stage in thymocyte development (Godfrey *et al.*, 1994). This developmental stage is characterized by the start of the rearrangement of  $\beta$ ,  $\gamma$ , and  $\delta$  loci of the T cell receptor (TCR) (von Boehmer and Fehling, 1997). The subsequent loss of CD44 expression defines the DN3 (CD44<sup>-</sup>CD25<sup>+</sup>) stage of early T cell development. DN3 is also a population of cells, which are now also devoid of a CD117 expression and have completed their rearrangement of the  $\beta$ ,  $\gamma$ , and  $\delta$  chains locus. These cells are now in the position to either express a pre-TCR consisting of a productively rearranged  $\beta$  chain plus a surrogate and invariant TCR  $\alpha$  chain (known as pT $\alpha$ , as gp33) or, alternatively, to express a complete  $\gamma\delta$  TCR. Thymocytes

that fail to express any of these two receptors fail to receive survival signals and thus undergo apoptosis before they gain the ability to transit to the DN4 (CD44<sup>+</sup>CD25<sup>-</sup>) cell stage. In contrast, the cells that have successfully rearranged the TCR  $\beta$  loci and thus bear a pre-TCR on their cell surface begin to proliferate. Not all cells with a DN phenotype are yet committed to the  $\alpha/\beta$  T cell lineage as (i) DN1 and DN2 thymocytes retain the capacity to differentiate to NK (Nature Killer) and thymic DC (Dendritic cell) and (ii) harbour the potential to develop (given specific conditions) into B cells and myeloid cells (Ardavin *et al.*, 1993; Carlyle *et al.*, 1997; Wu *et al.*, 1996). The "Katsura/Kawamoto model" of haematopoiesis predicts that myeloid potential is a typical feature of early T and B cell development with T-cells and B-cells derived from a common myelo-lymphoid progenitor (CMLP) through bi-potent intermediates of myeloid-T-cell (MT) and myeloid-B-cell (MB) precursors, respectively (Akashi *et al.*, 2000; Katsura, 2002; Kawamoto *et al.*, 1999; Traver *et al.*, 2001). At E12, all cells of the T cell lineage correspond to DN1 cells and their absolute numbers have been estimated to be 80 (Douagi *et al.*, 2000). By E13 DN2 cells are also present and DN3 and DN4 develop over the course of the next 2 days. At E15, the number of T cell precursors has increased to more than 10,000. Although most thymocytes at this developmental stage divide every 10 hours, the observed increase in lymphoid cellularity cannot be only explained by in situ expansion of the originally seeding 80 haematopoietic cells. It has been calculated that approximately 20 T cell precursors enter the thymus between E11.5 and E12.5, 300 between E12 and E13, and 3000 between E13 and E14 (Douagi *et al.*, 2000). Multipotent haematopoietic cells have not been detected in the fetal thymus at any stage of gestation. This finding indicates that the differentiation potential of thymic immigrants is restricted to the lymphoid lineage and that commitment to the T cell lineage must occur prior to thymus colonization (Kawamoto *et al.*, 1998; Rodewald *et al.*, 1994). The majority of developing thymocytes are characterized by the concomitant expression of CD4 and CD8, a phenotype referred to as double positive (DP). DP thymocytes that have successfully rearranged their  $\beta$  locus for the TCR attain this developmental stage (so called  $\beta$ -selection). The stage of DP thymocytes follows that of DN cells and is attained via a transitional intermediary phenotype referred to as immature single positive (ISP) cells. These ISP express either CD4 or CD8 but not both co-receptors at the same time, and can be distinguished from more mature single positive thymocytes by a lower cell surface expression of their TCR  $\beta$  chain (Paterson and Williams, 1987; Yu *et al.*, 2004). The ISP to DP transition is an actively regulated differentiation step that leads to the generation of a large pool of DP thymocytes (Yu *et al.*, 2004). At the ISP stage of

maturation, the rearrangement of the TCR $\alpha$  locus is initiated which still coincides with cell's active phase of proliferation. Hence no rearrangement of the  $\alpha$  loci occurs until the proliferative phase has ended. This sequence of events ensures that each successful rearrangement of the TCR  $\beta$ -chain gives rise to many DP thymocytes. Each of these can independently rearrange their  $\alpha$ -chain genes once the cells stop dividing, so that a single functional  $\beta$  chain can be associated in the progeny of these cells with many different  $\alpha$  chains. Following the period of  $\alpha$  chain gene rearrangement, a complete  $\alpha/\beta$  TCR is expressed, which now allows for the process of positive thymic selection by peptide/MHC complexes.

#### **1.6.4 Positive and negative selection in the thymus**

Following their transition to a DP cell stage, developing thymocytes undergo extensive selection to ensure that the mature T cells to be exported from the thymus are functional and self-tolerant. In this context of testing the functional usefulness of specific thymocyte antigen specification, the terms positive and negative thymic selection denote two separate but interconnected and essential processes, designated positive and negative thymic selection. Positive and negative thymic selection are both dependent on lymphostromal interactions within the thymus (Anderson *et al.*, 1999; Chidgey and Boyd, 2001; Jameson and Bevan, 1998; Klein and Kyewski, 2000; Sebzda *et al.*, 1999). Positive selection occurs if the TCR of the thymocytes engages a self peptide-MHC ligand on cortical TECs with a sufficiently low affinity, resulting in the transduction of a survival and differentiation signal (Bevan, 1997; Palmer, 2003; von Boehmer, 1994). Thymocytes unable to recognize any peptide-MHC-ligand with a sufficiently high affinity that allows for positive selection will die by neglect. In other words developing T cells are destined to die by default unless they are rescued by life-sustaining signals from other cells or their products (Boursalian and Bottomly, 1999; Raff, 1992; Sprent and Kishimoto, 2001). In contrast, thymocytes bearing a TCR with an affinity which is high for the self peptide-MHC-ligand (i.e. higher than necessary for positive selection) are deleted by the process coined as negative selection, an event effected by apoptosis and resulting in the removal of thymocytes with a self-reactive TCR specificity (Nossal, 1994; Smith *et al.*, 1989; Sprent and Kishimoto, 2002) (Palmer, 2003; Starr *et al.*, 2003). The remaining thymocytes that express a low affinity TCR mature further and begin to express high levels of this  $\alpha\beta$  TCR on their cell surface and subsequently cease to express one or the

other of the two co-receptor molecules, becoming either CD4<sup>+</sup>CD8<sup>-</sup> or CD4<sup>-</sup>CD8<sup>+</sup> single-positive (SP) thymocytes (Kaye *et al.*, 1989; Merckenschlager *et al.*, 1997). Positive selection and the subsequent development into CD4<sup>+</sup> T-helper cells requires the interaction of their TCR with their cognate peptide-MHC class II complex presented by thymic stromal cells, while the corresponding selection and development into CD8<sup>+</sup> cytotoxic T lymphocytes (CTLs) requires the interaction of the cells TCR with a peptide-MHC class I complex on thymic stromal cells that serves as the cognate ligand for this receptor (Kaye *et al.*, 1989; Teh *et al.*, 1988). The different developmental stages of T-cell differentiation in the thymus have been summarized in Fig.1.3.

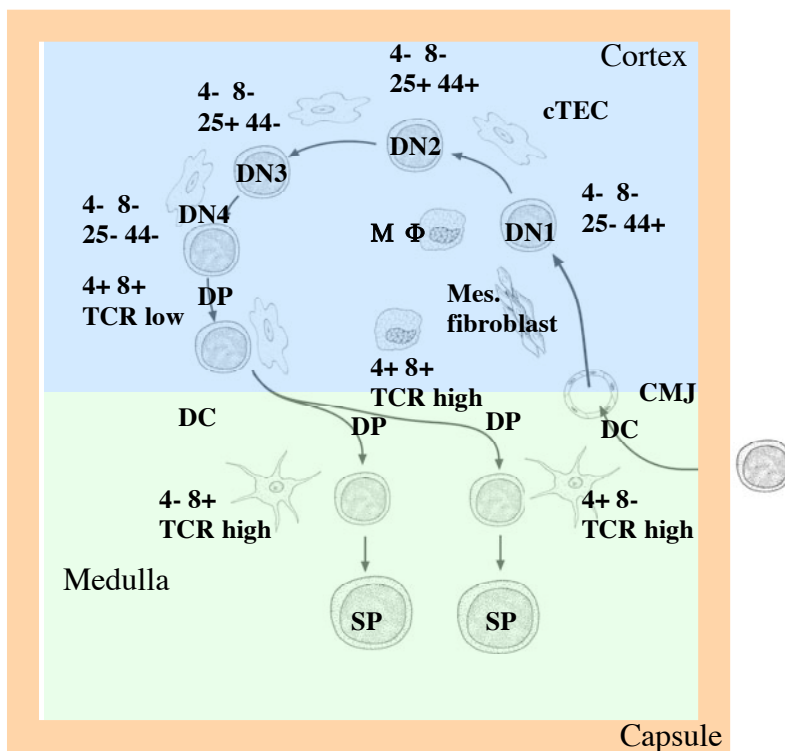


**Figure 1.3. Anatomical microenvironments in the adult thymus.** The thymus of mice is a bilobed organ divided by mesenchymal septae and surrounded by a capsule. Lobes are organized into discrete cortical and medullary areas, each of which is characterized by the presence of particular stromal cell types, as well as thymocyte precursors at defined maturational stages. Thymocyte differentiation can be followed phenotypically by the expression of cell-surface markers, CD4, CD8, CD44, CD25 as well as the T-cell receptor (TCR). Interactions between thymocytes and thymic stromal cells are known to be crucial in driving a complex thymic programme of T-cell maturation, which results in the generation of self-tolerant CD4<sup>+</sup> (helper) and CD8<sup>+</sup> (cytotoxic) T cells, which emigrate from the thymus to establish the peripheral T-cell pool. (4, CD4; 8, CD8; 44, CD44; 25, CD25; TCR<sub>low</sub>, expressing the TCR at low levels; TCR<sub>high</sub>, expressing the TCR at high levels; CMJ, Cortico-Medullary Junction; HP, Haematopoietic precursor; MΦ, Macrophage; Mes. fibroblast, Mesenchymal fibroblast); DN1-4, Double negative (CD4<sup>-</sup>CD8<sup>-</sup>) 1-4 stage; DP, Double positive (CD4<sup>+</sup>CD8<sup>+</sup>); SP Single positive (CD4<sup>+</sup> or CD8<sup>+</sup>).

Positive thymic selection is effected by cortical thymic epithelial cells (cTECs). Using reaggregate thymic organ culture (RTOC), it has been well established that MHC class II positive

cTECs are both necessary and sufficient for positive selection of DP of the  $\alpha/\beta$  TCR lineage to CD4<sup>+</sup> SP cells (Anderson and Jenkinson, 1997; Anderson *et al.*, 1996). In contrast, medullary epithelium and antigen-presenting cells (APCs) of haematopoietic origin have been reported to be either unable to positively select or display very inefficient selection of DP thymocytes (Bix and Raullet, 1992; Capone *et al.*, 2001; Chidgey and Boyd, 2001; Cosgrove *et al.*, 1992; Laufer *et al.*, 1996; Markowitz *et al.*, 1993; Zerrahn *et al.*, 1999). In contrast to positive selection, negative selection is believed to occur either in the cortex at the cortico-medullary-junction or in the medulla itself (Baldwin *et al.*, 1999; Murphy *et al.*, 1990; Surh and Sprent, 1994). The cells responsible for negative selection are mainly bone marrow-derived thymic stromal cells; although thymic medullary epithelial cells have also been implicated to effect negative selection for some self-antigens (Hoffmann *et al.*, 1992; Hoffmann *et al.*, 1995; Lo and Sprent, 1986; Murrack *et al.*, 1989; Throsby *et al.*, 2000). In fact, recent studies have demonstrated that medullary TECs are sites of promiscuous gene expression under the control of the autoimmune regulator gene (Aire), a phenomenon that is marked by the transcription of genes normally expressed in peripheral tissues (outside of the thymus) (Anderson *et al.*, 2002; Derbinski *et al.*, 2001; Heath *et al.*, 1998; Klein *et al.*, 1998; Klein *et al.*, 2000; Liston *et al.*, 2004; Liston *et al.*, 2003; Werdelin *et al.*, 1998). This finding suggests that medullary TECs might be able to express the entire peptide repertoire of a given individual, making the medulla the ideal site for negative selection (Palmer, 2003).

### **1.6.5 The final step: export from the thymus**

After positive and negative selection is completed, the correctly selected T-cells remain in the medulla for up to 14 days (Gabor *et al.*, 1997). Maintenance of the peripheral T cell pool with naive cells requires the controlled release of the newly generated T cells from the thymus into the peripheral circulation. It is presently perceived that mature T cells are exported via blood and lymphatic vessels (Bhalla and Karnovsky, 1978; Miyasaka *et al.*, 1990; Sainte-Marie and Leblond, 1965; Toro and Olah, 1967). In the mouse, approximately one million naive T cells are exported every day from the thymus to the periphery. In this regard, two predictions have been made concerning the exit of T cells from the thymus: (i) exit should only be possible for T cells that have achieved post selection maturity in the medulla, and (ii) in order to be able to exit the thymus, T cells change either the expression or activation of integrins, alter their requirements for adhesion and change their responsiveness to positional cues.

## 2. Materials and Methods

### 2.1 Materials

#### 2.1.1 Mice

Mice (C57BL6/J) were housed at the Animal Facility of the Kantonsspital Basel and at the Institute of Biomedicine of the University of Basel, according to Governmental regulations.

#### 2.1.2 Tissues

Tissues were obtained from adult mice and embryos of distinct developmental stages following timed pregnancies (Detection of the vaginal plug was considered as day 0.5 of gestation (designated E0.5). Embryos homozygously deficient for the transcription factor Sp8 and for the pleckstrin homology-like domain family A2 (Phlda2, a.k.a IPL) were kindly provided by Dr.A.Mansouri (Göttingen, Germany) and by Dr.B.Tycko (New York, USA), respectively. Embryos of different gestational age were embedded in O.C.T (Tissue-Tec, Miles, Elhart, IN) for immunohistological analysis. Some transgenic tissue (Dr.S.Bell, Cincinnati, OH, USA) was also examined by  $\beta$ -galactosidase-based histochemistry.

#### 2.1.3 Cell lines

The following cell lines were experimentally used as part of this thesis work:

Cell line	Origin	Reference
cTEC 1.2	Mouse thymic cortical epithelium	(Kasai <i>et al.</i> , 1996)
cTEC 1.4	Mouse thymic cortical epithelium	(Kasai <i>et al.</i> , 1996)
cTEC C9	Mouse thymic cortical epithelium	(Kasai <i>et al.</i> , 1996)
mTEC 2.3	Mouse thymic medullary epithelium	(Kasai <i>et al.</i> , 1996)
mTEC 3.10	Mouse thymic medullary epithelium	(Kasai <i>et al.</i> , 1996)
mTEC C6	Mouse thymic medullary epithelium	(Kasai <i>et al.</i> , 1996)
HEK 293	Human Kidney	(Kasai <i>et al.</i> , 1996)

Cells were grown at 37°C and in 5% CO<sub>2</sub> in Iscove's Mod. dulbecco's medium (IMDM) containing 5% of fetal calf serum (FCS). To detach cells from vessels, cells were incubated for 2-3 minutes in undiluted Trypsin solution (Invitrogen Corporation, Basel, CH).

## **2.1.4 Cell culture, plastic ware, and chemicals**

Media Iscove's Mod. Dulbecco's medium (IMDM) supplemented with  $\text{NaHCO}_3$  and L-Glutamine were purchased from (Invitrogen Corporation, Basel, CH). Additional supplements were employed according to the specific requirements (see 2.1.4.1 and 2.1.4.2). Sterile disposable plastic ware for tissue culture was purchased from Falcon Labware (Oxnard, CA, USA). Chemicals were purchased from Fluka (Buchs, Switzerland), Sigma (St. Louis, MO, USA) and other commercial vendors as indicated.

### **2.1.4.1 Supplements for thymic epithelial cells**

For 1L of media for thymic epithelial cells, 10 ml of 1M HEPES, 1ml of Gentamycin (50mg/ml) and 100ml of FCS (Fetal Calf Serum) were added.

### **2.1.4.2 Supplements for HEK 293 cells**

For 1L of media for HEK 293 cells, 20ml of FCS were added and 100 $\mu\text{l}$  of  $\beta$ -mercaptoethanol (1M) were added.

## 2.1.5 Antibodies

Antibody	Clone	Source
<b>Used in immunohistology</b>		
anti-CCL21, rabbit		
anti-Meox2, rabbit		Kindly provided Dr.K.Mankoo
anti CD44, rat	IM7	Pharmingen
anti CD44v6, rabbit		Kindly provided by Dr.U.Gunthert
anti CD44 v10, rabbit		Kindly provided by Dr.U.Gunthert
anti-mWIF1, goat		R & D systems
anti-hWIF1, rabbit		Kindly provided by Dr.J.Hsieh
anti-Fst, rabbit		Kindly provided by Dr.S.Werner
anti-Phlda2 (IPL, Tssc3), rabbit		Kindly provided by Dr.B.Tycko
anti-β gal (E.coli), monoclonal		Promega
anti-k5, rabbit		
anti-k8, goat		
anti-CD45, rat	30-F11	Pharmingen
anti-rabbit IgG, goat Biot conjugated		Southern Biotechnology
anti-rabbit IgG, goat HRP conjugated		Southern Biotechnology
anti-goat IgG, rabbit Biot conjugated		Southern Biotechnology
anti-goat IgG, rabbit HRP conjugated		Southern Biotechnology
anti-rat IgG, goat HRP conjugated		Southern Biotechnology
anti-mouse IgG, goat FITC conjugated		Southern Biotechnology
anti-human IgG, goat HRP conjugated		Sigma
<b>Used in flow cytometry</b>		
anti-CD3ε Biotin	145-2C11	Pharmingen
anti-CD4 (L3T4) PE	RM4-5	Pharmingen
anti-CD4 Biotin	RM4-5	Pharmingen
anti-CD8 FITC	53-6.7	Pharmingen
anti-CD8 Biotin	53-6.7	Pharmingen
anti-CD25 FITC	PC61	Pharmingen
anti-CD44 PE	IM7	Pharmingen



## 2.1.6 Standard buffers

Name	Composition
FACS-buffer	1% BSA, 0.1% NaN <sub>3</sub> in PBS
Formaldehyde gel-running buffer (5x)	0.1 M MOPS, ph 7.0, 40mM NA Acetate, 5mM EDTA, pH 8.0
SSC	150mM NaCl, 15 mM Na-citrate
TAE	40mM Tris/acetate, ph 8.0, 1mM EDTA
TBE	89 mM Tris, 89 mM boric acid, 2mM EDTA pH 8.3
PBS (1x)	0.14M NaCl, 2.7mM KCl, 6.5mM Na <sub>2</sub> HPO <sub>4</sub> , 1.5mM KH <sub>2</sub> PO <sub>4</sub> , pH 7.3, autoclave
TE	10mM Tris/Cl, 1mM EDTA, pH8.0
MES (12x)	70.4g MES (free acid monohydrate), 193.3g MES sodium salt complete to 1L with H <sub>2</sub> O-tridest pH 6.5-6.7 filter, do not autoclave
MES-Hyb (2x)	8.3ml of 12x MES, 17.7ml 5M NaCl, 4ml 0.5M EDTA, 0.1ml 10% Tween 20, 19.9ml H <sub>2</sub> O-tridest filter sterilize
MES-Wash	83.3ml 12x MES, 5.2ml 5M NaCl, 1ml 10%, complete to 1L with H <sub>2</sub> O-tridest, filter sterilize
SSPE-Tw (6x)	300ml 20x SSPE, 1ml 10% Tween 20, complete to 1L with H <sub>2</sub> O-tridest, pH 7.6, filter sterilize
Stain buffer (2x)	41.7ml 12x MES, 92.5ml 5M NaCl, 2.5ml 10% Tween 20, 113.3ml H <sub>2</sub> O-tridest, filter sterilize

## 2.2 Methods

### 2.2.1 Microarray analysis from microdissected tissues

Details to the method of preparation for total RNA extraction from laser microdissected tissue have been published elsewhere (Klur *et al.*, 2004). This report is based on procedures established part of this PhD work.

#### 2.2.1.1 Laser capture microdissection (LCM)

The preparation of the tissue for Laser capture microdissection (LCM) was carried out as follows:

- Embryos were immediately removed from euthanized pregnant mice of E10.5 days of gestation and rapidly frozen in a drop of O.C.T (Tissue-Tec, Miles, Elhart, IN) using a plastic support submerged in a mixture of dry ice (stored at -80°C until use) and a few ml of isopentyl (Flucka, Buchs, CH).
- For sectioning by the cyrotome (Roche, Basel, CH) the embedded tissue was placed onto the support block at -20°C with some O.C.T. Once O.C.T has solidified, each edge of the block is cut with a razor blade so that a small rectangular strip is formed.
- The sections were mounted on glass slides covered with a 1.35µm thin polyethylene foil (PALM Microlaser Technologies, Germany).
- Sections were fixed for 10s in 75% of ethanol (Flucka, Buchs, CH), followed by a short rinse in DEPC-treated water (Sigma, Buchs, CH).
- The sections were subsequently stained in 0.5% toluidine blue for 10s and rinsed twice in DEPC-treated water.
- Sections were dehydrated in 50, 75, 95 and 100% of ethanol for 10s each.
- Sections were then left at room temperature (RT) under a hood for 90min and subsequently used for LCM.

Importantly, only DEPC-treated water was used to dilute the ethanol and the Toluidine Blue solutions.

- For preparing the support in which the laser microdissected tissue was to be catapulted, the cap of an 0.5ml RNase free tube (Vaudaux-Eppendorf AG, Schonenbuch, CH) was detached with the help of cisors. Subsequently, 5µl of Trizol (Invitrogen corporation, Basel, CH) was pipetted and has been dropped into the inside of the separated cap before being placed on top of the specially designed cap-support of the LCM Robot-Microbeam microscope (PALM Microlaser Technologies, Germany).
- The tissue of interest were microdissected using the laser of the microscope according to the manufacturer's recommendations.
- The microdissected tissue was catapulted by slightly increasing the energy of the Laser. Importantly, the cap has to be as close as possible to the top of the section when catapulting the microdissected tissue into the 5µl of Trizol.
- At the end of each LCM session, the cap was put back on top of the 0.5ml tube and closed before being spined at 14,000g for 1min and stored at -80°C until further processing. The different steps above were repeated until at least 1000 cells of the region of interest were collected.

### **2.2.1.2 Total RNA extraction for microdissected tissue**

To extract total RNA from microdissected tissues, the standard protocol for the use of the Trizol reagent (Invitrogen Corporation, Basel, CH) has been modified. In short,

- Individual drops from a single LCM dissection were pooled for the same tissue so that the combined lysate would represent approx 1000 cells. The volume was then completed to 1ml with Trizol reagent and the tube was subsequently mixed gently. For the RNA analysis of complete cross-sectioning of embryos, the tissue was removed from the foil by use of a sterile razor blade, The recovered tissue was solved in 1ml of Trizol.
- After addition of 0.1ml of bromochloropropane (Flucka, Buchs, CH), the tube was vigorously shaken for 20 to 30s with the help and were left for 15min at room temperature before being centrifuged at 12,000 g for 15 min at 4°C.
- The aqueous phase (~450µl) was transferred into a new 1ml tube (Vaudaux-Eppendorf AG, Schonenbuch, CH), mixed with 1µl of Linear polyacrylamide LPA (Sigma, 5µg/µl) and 500µl of isopropanol to precipitate the RNA.

- The precipitated mix was stored for 1 hour at room temperature and centrifuged for 2 hours at 20,000g at 4°C.
- The RNA pellet was washed twice with 1ml of cold 75% ethanol and shortly spined in order to remove the remaining ethanol before being air-dried for 3min under a hood. The pellet was then stored at -80°C until further used.

### **2.2.1.3 Random PCR-based amplification**

cDNA synthesis and amplification were performed using the Microarray Target Amplification Kit (Roche Diagnostics, Germany) according to the manufacturer's recommendations.

#### First strand cDNA synthesis:

- The total RNA pellet was resuspended in 8.5µl of double-distilled water and transferred to a new 0.5ml tube and the subsequent components were added to the solved pellet: 2µl of TAS-T7 Oligo (dT)<sub>24</sub> (25µM), 4µl of 5x reverse transcriptase buffer, 2µl of DTT (100mM), 2µl of dNTP Mix (10mM each) and 1.5µl of the Reverse transcriptase Enzyme mix (17U/µl )
- The mixture was well mixed by vortexing before being shortly spined in a microcentrifuge. The reaction was then incubated in a thermal cycler at 42°C for 60 min.

#### Second strand cDNA synthesis:

- The reverse transcribed RNA was incubated at 95°C in a thermal cycler for 5 min to achieve the denaturation of the RNA/DNA hybrid, placed immediately on ice and left for 5 min. The following components were then added to the mixture: 2.5µl of dNTP mix (10mM each), 5µl of TAS-(dN)<sub>10</sub> (100µM), 5µl of 10x Klenow reaction buffer, 13.5µl of double-dist water and 4µl of Klenow Enzyme (2U/µl).
- The mixture has been mixed by vortexing before being briefly spined in a microcentrifuge. The reaction was then incubated in a thermal cycler at 37°C for 30min.

#### Purification of the double stranded cDNA:

The double stranded cDNA were purified using the Microarray Target Purification Kit (Roche Diagnostics, Germany) according to the instructions of the manufacturer. Importantly, 1.25µl of carrier RNA and 50µl of double-distilled water were added to each sample.

### First PCR:

A first PCR was required to determine the optimal cycle number so as to ascertain that the amplification of the cDNA was still exponential as "overcycling" may result in lower yields of cRNA which in turn could influence the subsequent quality of the microarray analysis. The correct cycle number for each sample is dependent on the initial amount and quality of the RNA recovered. In that regard, 50ng of intact total RNA from the K562 cell line (included in the microarray target amplification Kit) was amplified in parallel and served as positive control for the estimation of the RNA amount present in the microdissected tissue samples.

- The purified double stranded cDNA was pipetted into a new 0.2ml microtube and the subsequent components were added to the reaction: 1µl of TAS Primer (50µM), 2µl dNTP Mix (10mM each), 73µl of double-distilled water, 10µl of 10x Expand PCR buffer and 1.5µl of the Expand Enzyme Mix (3.5U/µl).
- The mixture has been mixed, briefly spined in a microcentrifuge before being placed in a PCR cycler. The PCR was effectuated as described here below (see PCR conditions).
- In the last minute of cycle 18 at the elongation step, 10µl were removed from each tube for an gel electrophoresis analysis. This procedure has been repeated in cycle 21/24/27/30.
- The aliquots of 10µl were analysed on a 1.2% agarose/ethidium bromide 0.25µg/ml gel for the determination of the optimal cycle number, which was considered when the observed smear of the PCR amplicons (ranging from 0.7 to 2.2kb) started to be clearly detected (see Fig.2.1 for example on next page).

PCR conditions: the reactions were incubated for 2min at 95°C and subsequently for 30s at 95°C, 30s at 55°C and for 3min at 72°C, respectively for the denaturation, the annealing and the elongation of the amplicons. These subsequent steps were repeated 29 times.

### Second PCR:

The second PCR, a PCR identical to the first PCR was performed, with the previously determined optimal cycling number (see First PCR section). The amplicons of this PCR were then analysed

by electrophoresis on a 1.2% agarose/ethidium bromide 0.25µg/ml gel for a quality verification of the amplified cDNA. The amplicons systematically presented an expected smear between 0.7 and 2.2kb.

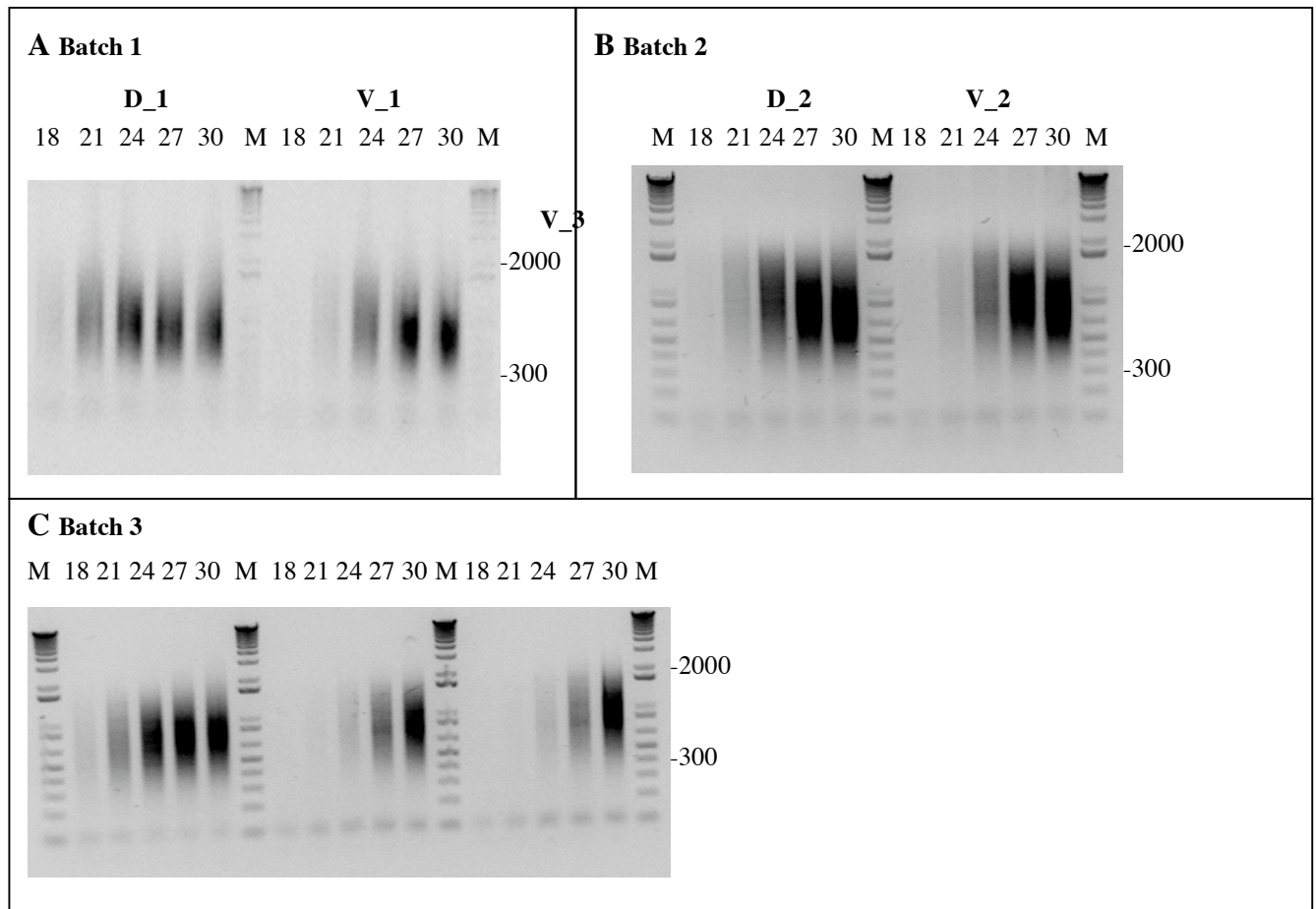


**Figure 2.1. Gel electrophoresis analysis of the semi-quantitative PCR-based amplified cDNA (First PCR step) for the different samples of the dorsal and ventral aspects of the 3<sup>rd</sup>pp.** Three different batches, Batch 1 (A), Batch 2 (B) and Batch3 (C) of the dorsal (D) and the ventral aspect (V) of the 3<sup>rd</sup>pp have been independently generated. Batch 1 and 2 were used for microarray and qRT-PCR analysis while Batch 3 was only used for the independent verification of candidate genes by qRT-PCR. Control sample for random PCR-based amplification (50ng of intact total RNA provided with the kit of amplification was used for the reverse transcription in parallel for the generation of Batch3 samples. The number above the lanes indicate at which PCR cycle 10µl have been subsequently deducted for the analysis. M, stands for the DNA molecular ladder and the number represented on the left or the right from it indicate the length in base pairs for two of its DNA products. From these data, the following PCR cycle for the second PCR step (see previous page) were decided: D\_1 (21 cycles), V\_1 (21 cycles), D\_2 (20 cycles), V\_2 (21 cycles), D\_3 (22 cycles), V\_3 (22 cycles).

### Purification of the PCR product:

The amplicons were purified using the Microarray Target Purification Kit (Roche Diagnostics, Germany) according to the instructions of the manufacturer. Importantly, the purified amplicons were eluted in 50 $\mu$ l of Elution Buffer B (included in the kit). For an OD (optical density) measurement, 5 $\mu$ l of the purified PCR reaction was deducted and was placed in a new 1.5ml tube containing 5 $\mu$ l of water before being centrifuged at 14,000rpm for 2min to spin down remaining purification column beads, as they can disturb OD measurement. The concentration of DNA in each sample was determined using the following formula: concentration ( $\mu$ g/ml) = 50 x OD260 x dilution. Importantly, DNA is considered to be pure when the ratio OD260/OD280 is more than 1.8.

#### **2.2.1.4 In vitro transcription labelling (IVT)**

- Two hundred and fifty nanogram of purified amplicons were deducted and desiccated using a Speedvact (BioRad, Reinach, CH). Fourteen and a half microliter of a prepared biotinylated-NTP mix sufficient for 4 reactions containing 8 $\mu$ l of Ambion's T7 10x ATP (75mM), 8 $\mu$ l Ambion's T7 10x GTP (75mM), 6 $\mu$ l of Ambion's T7 10x CTP (75mM), 6 $\mu$ l of Ambion's T7 10x UTP (75mM), 15 $\mu$ l of Biotinylated-11-CTP (10mM) and 15 $\mu$ l of Biotinylated-16-UTP (10mM) were added to the lyophilized sample. All ambion NTPs were ordered from Ambion (Huntingdon, UK).
- The volume of the mixture was adjusted to 16 $\mu$ l with DEPC-treated water and 2 $\mu$ l of the 10x T7 transcription buffer (Ambion, Huntingdon, UK), as well as 2 $\mu$ l of the 10x T7 enzyme mix (Ambion, Huntingdon, UK) were added to the mixture. The reaction was then incubated for 4 hours at 37°C for the synthesis of labeled cRNA.
- For an quality verification of the amplified cRNA, 3 $\mu$ l of the reaction was deducted for an gel electrophoresis analysis (gel composition: 1.2% agarose formaldehyde-treated/ethidium bromide (0.25 $\mu$ g/ml). The distribution of the cRNA was systematically found to be as expected between 0.24 to 4.4kb.

### Purification of the PCR product:

The labeled cRNA was purified using the Microarray Target Purification Kit (Roche Diagnostics, Germany) according to the instructions of the manufacturer. Importantly, the purified cRNA was eluted in 50µl of Elution Buffer A (included in the kit). For an OD (optical density) measurement, 3µl of the purified IVT reaction were deducted and placed in a new 1.5ml tube containing 19µl of water before being centrifuged at 14,000rpm for 2min to spin down remaining purification column beads, as they can disturb OD measurement. The concentration of DNA in each sample was determined using the following formula: concentration (µg/ml) = 40 x OD<sub>260</sub> x dilution. Importantly, RNA is considered to be pure when the ratio OD<sub>260</sub>/OD<sub>280</sub> is more than 1.8.

### **2.2.1.5 Hybridization and stainings of Microarrays**

The protocols as well as the reagents for microarray hybridization were kindly provided by Dr. Ullrich Certa and Sandra Klur (Hoffman La Roche, Basel, CH). Microarrays processing, reading/scanning were carried out at the Roche center for medical genetics (Basel, CH).

### Fragmentation of the IVT products:

- Twenty microgramm of the purified cRNA was deducted, placed in a new Rnase-free 1.5ml tube and dessicated in a Speedvac before adding 20µl of a fragmentation buffer to the lyophilized cRNA.
- The reaction was then incubated at 95°C for 35min in a thermal cycler and placed on ice after the incubation

### Genechip Hybridization:

- For the pre-hybridization of the microarrays of the MGU74v2 Genechip set (Affymetrix, Santa Clara, USA), a pre-treatment solution sufficient for 4 microarrays was prepared containing the following reagents: 25µl of acetylated BSA (20µg/µl), 50µl of Herring Sperm (HS) DNA (10µg/µl), 500µl of 2x MES-hybridization-Buffer (see section 2.1.6) and 425µl of DEPC-H<sub>2</sub>O). Two hundred and twenty microliter of the pre-treatment solution was loaded



into each microarray. Each microarray was then incubated in a hybridization chamber for rotation at 40°C at 60rpm for 15min.

- For the preparation of the sample to be loaded on the microarray, 2.5µl of a control stock mix (100x) (Roche, Basel, CH) was added to the fragmented cRNA, as well as 2.5µl of Biotinylated Oligo 948, 2.5µl of HS DNA (10µg/µl), 6.25µl of acetylated BSA (20µg/µl), 125µl of 2x MES-hybridization-buffer, 91.25µl of DEPC-H<sub>2</sub>O.
- The mixture was then incubated at 95°C for 5min in a thermal cycler and then in a 45°C waterbath until 220µl of it was loaded into the microarray. The microarray was then incubated in a hybridization chamber for rotation at 45°C, 60rpm O.N for microarray hybridization.

#### Washing and Staining:

- The remaining solution in the hybridized microarray was then removed and stored at -20°C until loaded on a subsequent microarray of the MGU74v2 Genechip set, as this set is composed of 3 different microarrays (A, B and C) that were subsequently hybridized with the same sample. The hybridized microarray was then rinsed with 6x SSPE-Tw solution (see section 2.1.6), washed on Basel Fluidics (BSFs) with 6x SSPE-Tw for 5min, before being rinsed with MES-wash-buffer (see section 2.1.6).
- Two hundred and thirty microliter of fresh MES-wash-buffer was loaded into the microarray, which was then placed in a hybridization chamber for rotation at 45°C for 30min to wash it. The MES-wash-buffer was then removed from the microarray.
- The microarray was stained with 250µl of a freshly prepared streptavidin-staining solution (125µl 2x Stain buffer, 91.25µl of DEPC-H<sub>2</sub>O, 31.25µl of acetylated BSA (20µg/µl) and 2.5µl of recombinant Streptavidin (1mg/ml)). The microarray was then incubated in a hybridization chamber for rotation at 40°C, 60rpm for 15min, before being rinsed with 6x SSPE-Tw and washed on BSFs with 6x SSPE-Tw for 5 min.

#### Amplification of staining:

- The SSPE-Tw solution was removed from the stained microarray and 230µl of a freshly made antibody solution (99µl DEPC-H<sub>2</sub>O, 125µl of 2x Stain Buffer (see section 2.1.6) , 25µl of

acetylated BSA (20µg/µl) and of 1µl biotinylated-anti-Streptavidin (500µg/µl)) was loaded into the microarray. The microarray was then incubated in a hybridization chamber for rotation at 40°C 60rpm for 30 min before being rinsed with 6x SSPE-Tw and washed on the BSFs for 5min with 6x SSPE-Tw.

- For amplifying the staining of the microarray, 250µl of a freshly made SAPE solution (125µl 2x Stain buffer, 91.25µl DEPC-H<sub>2</sub>O, 31.25µl of acetylated BSA (20µg/µl) and 2.5µl of Phycoerythrin (1mg/ml) was loaded into the microarray. The microarray was then incubated in a hybridization chamber for rotation at 40°C, 60rpm for 15min before being rinsed with 6x SSPE-Tw and washed on the BSFs for 5min.
- For scanning the microarray was completely filled with 6x SSPE-Tw so that there was no bubbles left!

### 2.2.1.6 Microarray analysis

All microarrays were analysed with the Affymetrix suite 5.0 software (Affymetrix, Santa Clara, USA) to determine the quality of the hybridization (see Table 2.1). All data reported in this thesis have been generated with a hybridization quality determined to be "good".

Table 2.1. Quality assessment for hybridization using the MGU74Av2 gene microarrays (adapted from Dr.C.Barlow, Salk institute for Biological Studies, Laboratory of Genetics, La Jolla, CA).

Quality measurements	Good	Questionable	Bad
Outliers	0-100	400-600	>600
Background	50-100	100-300	>300
Standard Deviation of Background	<7	7-10	>10
Raw Q	<3.4	3.6-8	>8
Scaling factor	<3.4	3.4-5	>5
Percent Present calls	>45%*	40-48%*	<40%
3'/5' Actin ratio	<2	2.0-2.5	>2.5
3'/5' GAPDH ratio	<2	2.0-2.5	>2.5

\* depends on tissue!

The Affymetrix suite 5.0 software was also used with its default settings for the determination of the normalized fluorescent intensity values as well as for the Present, Marginal and Absent calls. Whereas the dChip software (adapted from Dr. Cheng Li, Dana-Farber Cancer institute, Boston, USA) was used for analysing the representation of the Perfect Match vs the Mismatch of a given

probe set. The Mismatch is defined by being identical to the Perfect Match DNA sequence except for a single incorrect nucleotide in the middle of the oligomer. Hybridization conditions and probe compositions are such that the target sequence should hybridize to the Perfect Match but not to the Mismatch probe. Signals from the Mismatch features are subtracted from the perfect matches as background or non-specific binding. In cases of excessive background the gene is labeled as undetected and gets an absent call and vice versa. All these data can be exported to microsoft excel software and be analysed for differential gene expression (i.e Fold change).

### **2.2.2 Linear amplification**

The protocol for linear amplification has been published previously by (Baugh *et al.*, 2001) using the following (dT)-T7 primer sequence:

5'GCATTAGCGGCCGCGAAATTAATACGACTCACTATAGGGAGA(T)21V 3' (V = A, C, or G)

#### First strand synthesis: round 1

- Twenty nanogram of the (dT)-T7 primer was combined with 10ng of total RNA in a 0.5 ml tube. The mixture was then dessicated in a SpeedVac (BioRad, Reinach, CH) down to 1ml. Importantly, in case of overshooting the 1ml, milliQ 18.2 water was used to bring the volume back up.
- For denaturing the RNA and the (dT)-T7-primer in the reaction, the mixture was incubated at 70°C for 4 minutes in a thermal cycler with a heated lid and subsequently snap cooled on ice. Importantly, as the volume may drop after denaturation due to evaporation, the amount of water evaporated has to be determined and adjusted accordingly in a way that the volume of the mixture contains 1ml after the incubation.
- One microliter of the following prepared RT solution (per 5ml: 2.0 ml 5x 1st Strand Buffer (Invitrogen corporation, Basel, CH), 1ml of 100 mM DTT, 0.5 ml 10 mM dNTP, 0.5 ml T4gp32 (8.0 mg/ml) (BD Biosciences, Allschwil, CH), 0.5 ml Rnase Inhibitor (~20 U) (Ambion, Huntingdon, UK) and 0.5 ml of SuperScript II (100U) (Invitrogen corporation, Basel, CH) was added to the dessicated sample and mixed by pipetting. The mixture was then incubated for 1 hr at 42°C in either a thermal cycler with a heated lid. Subsequently, the reaction was inactivated at 65°C for 15 min before being chilled on ice.

## Second strand synthesis: round 1

- Thirteen microliter of a ice-cold second strand synthesis (SSS) premix (per 65ul: 15 ml of 5x Second-Strand Buffer (Invitrogen corporation, Basel, CH), 1.5 ml of 10 mM dNTP, 20U of DNA Polymerase I (Roche, Basel, CH), 1U of E. coli Rnase H (BD Biosciences, Allschwil, CH), 5U of E. coli DNA Ligase (Roche, Basel, CH), and completed with H<sub>2</sub>O), were added to the reverse transcribed RNA and mixed by pipetting.
- The mixture was then incubated at 16°C for 2 hours. For generating blunt ends of double stranded DNA, 2 units of T4 DNA Polymerase (Bioconcept, Allschwil, CH) were added to the reaction, mixed by gentle flicking the microtube and was incubated at 16°C for an other 15min.
- For the inactivation of the reaction, the mixture was incubated at 70°C for 10 min. Once inactivated the reaction was adjusted to 75 ml by adding 60 ml TE (see section 2.1.6).
- For purifying the double stranded DNA 75ml of a phenol:chloroform solution (1:1) was added to the reaction and mixed by pipetting vigorously before being loaded on a prespuned Phase Lock Gel Heavy 0.5 ml tubes (Vaudaux-Eppendorf, Schönenbuch, CH) and centrifuged at 13K rpm for 5min.
- The aqueous phase of the mixture was then further purified by being loaded on a BioGel P-6 MicroSpin Column (BioRad, Reinach, CH) and spined at 1000g for 4min in a microcentrifuge. Importantly the column has to be spined for 2 min at 1000 g before loading the aqueous phase. The flow through (approx. 80ml) was transferred into a new 1.5ml tube. For precipitating the RNA, 5mg of Linear polyacrylamide (LPA) (Sigma, Buchs, CH) carrier was added to the mixture and precipitated by adding 3.5ml (approx. 1/25th volume) of 5M NaCl, as well as 220ml (approx. 2.5 volumes of the mixture) of 95% ethanol (Fluka, Buchs, CH). The mixture was then allowed to precipitate at -20°C O.N.
- The precipitated DNA was then spined at 13K rpm for 20 min. The supernatant of the mixture was then carefully removed and the DNA pellet was washed with 500 ml of 70% ethanol, and spined for 5 min at 13K rpm. The 70% ethanol was then removed to the last drop. Importantly, all residual ethanol has to be removed. The DNA pellet was then dessicated by leaving it at 2-3 min under a hood.

### In vitro transcription (IVT): round1

- Twenty microliter of a IVT prepared premix (per 40ml: 16.5ml DEPC ddH<sub>2</sub>O, 4.0ml 10x of Ampliscribe Buffer (Epicentre, Madison, USA), 3.0ml 100 mM ATP, 3.0ml 100 mM CTP, 3.0ml 100 mM GTP, 3.0ml 100 mM UTP (Epicentre, Madison, USA), 4.0ml of 100 mM DTT, 1.5ml Rnase Inhibitor (~60U) (Ambion, Huntingdon, UK), 2.0ml of a highly concentrated T7 RNA Polymerase (80U/ml) (Catalys AG, Wallisellen, CH)) was added to the lyophilized pellet at room temperature.
- The reaction was then mixed by gently flicking and incubated at 42°C for 9 hours. The product can be stored at -20°C.
- For the purification of cRNA, 480ml of Rnase-free TE (10 mM of Tris, 1 mM of EDTA at pH 8.0) were added to the reaction and loaded on YM-50 Microcon columns (Millipore AG, Volketswil, CH). The columns were then spined for 20min at 12000g and have subsequently been washed with 500ml of Rnase-free TE.
- The cRNA was then recovered from the columns by inverting those, adding 10ml of milli-Q 18.2 water and by spinning the columns for 5min at 500g according to the manufacturer's instruction.

### First strand synthesis: round 2

- For reverse transcribing the cRNA, 5ml of random primers (0.5mg) (Invitrogen, Basel, CH) was added and desiccated in a Speedvac (BioRad, Reinach, CH). The mixture was then incubated at 70°C for 5 minutes in a thermal cycler with a heated lid before being snaped cooled on ice.
- Five microliter of the RT premix (same as an round1) were added to the purified cRNA. The reaction was then incubated using the following temperature protocol in a thermal cycler: RT incubation (round 2): 20 min at 37°C, 20 min at 42°C, 10 min at 50°C, 10 min at 55°C, 15 min at 65°C. The reaction was then maintained at 37°C in the thymal cycler until 1U of Rnase H was added to the mixture.
- The reaction was then incubated at 37°C for 30min and at 95°C for 2 min. For the collection of the condensation, the reaction was chilled on ice, briefly spined and returned on ice. One

microliter of the (dT)-T7 primer (100ng) was added to the mixture. The reaction was then incubated at 42°C for 10min to anneal the primer.

#### Second strand synthesis: round2

- Sixty five microliter of a prepared SSS premix (same as in round1 but without the adjonction of the ligase). The reaction was then incubated at 16°C for 2 hours before 10U of T4 DNA Polymerase were added to it in order to generate blunt ends. For inactivating the reaction, the mixture was incubated at 70°C for 10 min. The purification and the precipitation of the double stranded DNA has been carried as in round1.

#### In vitro transcription: round2:

Forty microliters of a prepared IVT premix. (same as in round1) was added to the purified cRNA pellet. The mixture was then incubated at 42°C for 9 hours. The reaction was then washed and purified as in round1.

### **2.2.3 Quantitative PCR (real time PCR)**

The primers for qRT-PCR were designed so that the amplicons were relatively short in size (< 200bp) so as to ensure a maximum for quantitative PCR (qPCR) amplification. Most primers of the 186 primer pairs ordered (Invitrogen, Microsynth or Sigma by Internet) were designed with the software Primerexpress 1.0. All primers (Table 2.2) were first verified using the conventional PCR as described in section of 2.2.5 using cDNA from unseparated E10.5 embryos. The amplification product was loaded on a 1% agarose/ethidium bromide gel for verification of the amplicon size. In case of a qPCR verification of the microarray differential gene expression the remaining purified dsDNA of the second PCR in section 2.2.1.3 was diluted 15 times (i.e 10ml + 140ml of milli-Q 18.2 water).

- Forteen microliter of a prepared master mixture of primers (per 14µl: 12.5µl of 2x SybrGreen Master Mix (Applied Biosystems, Rotkreuz. CH), 0.75µl of forward primer (10µM) and 0.75µl of reverse primer (10µM)) was pipetted into a well of a 96 well plate (Applied

Biosystems, Rotkreuz, CH). The sequence of the respective used primers can be found in Table2.

- Eleven microliter of a prepared mixture of template (per 11 $\mu$ l: 1 $\mu$ l of purified dsDNA or cDNA 2-10ng/ $\mu$ l) was then added to each well. The 96 well plate was sealed with a special adapted plastic foam for qPCR (Applied Biosystems, Rotkreuz, CH) according the manufacturer's instructions. The plate was briefly spined in a special adapted centrifuge (Vaudaux-Eppendorf, Schonenbuch, CH) and was placed in a Real time PCR ABI5700 instrument (Applied Biosystems, Rotkreuz, CH). The PCR was then effectuated as described here below (see PCR conditions).

PCR conditions: the reactions were incubated for 10min at 95°C and subsequently for 15s at 95°C and 1min at 60°C , respectively, for the denaturation, the annealing and the elongation of the amplicons. These subsequent steps were repeated 39 times. The software of the instrument was programmed as such as at the end of the PCR, an dissociation protocol from 60°C to 93°C was effectuated for the verification of the specificity of the amplicons.

#### Analysis:

The baseline of the amplification plot was selected from cycle 6 to cycle 15 (default settings). In case the measured fluorescence started to be detected earlier than cycle 15, then the baseline was adjusted appropriately according the manufacturer's instructions. The threshold of the fluorescence for determining the Ct value was systematically selected to 0.2. It was observed that when using this threshold the measured Ct values were always in the exponential phase of the reaction. The specificity of the amplicons was verified by comparing the theoretical melting value calculated by the Primerexpress 1.0 software with that measured by the qPCR instrument. Only samples that gave expected melting values within a range of 1 to 2°C of a difference with the theoretical value were considered for the calculations of the Ct values. The qPCR ratio is defined as being the difference in signal intensity between the 2<sup>nd</sup>pp and 3<sup>rd</sup>pp or the dorsal and ventral domains of the 3<sup>rd</sup>pp, respectively. It was calculated using the following formula:

$\Delta\Delta Ct = \Delta Ct \text{ (dorsal or 2}^{nd}\text{pp)} - \Delta Ct \text{ (ventral or 3}^{rd}\text{pp)}$  where  $\Delta Ct = Ct \text{ gene of interest} - Ct \text{ (housekeeping gene GAPDH or HPRT)}$ .

Table 2.2. Sequences of primers used for quantitative and conventional PCR

Gene symbol	Forward primer	Reverse primer
GAPDH	ACCATGTAGTTGAGGTCAATGAAGG	GGTGAAGGTCCGGTGTGAACG
HPRT	AGTCTGAAGCTCTCGATTTCTATCA	TGAAAGTGGGAAAATACAGCCAA
CXCR4	TGTAGAGGAAGAACTGAACATTCCA	CCTCGGAATGAAGAGATTATGCA
Wnt4	AGGTGGTGGGAGACTGTTTAAGTTA	GGCTCGTGGAGATGCACAC
FoxN1	TTGTGGAAGTGGAGTCCACG	TGTTGGGCATAGCTCAAGCC
Hoxa3	TTCCCTTTCTCCTCTGCACC	GACAGCCTTTCCAGCAACCA
Pax1	GGTGGTGAAGTTCATTTTGGTT	AATAGCCCTCTTGCCTAGCTCC
Pax9	CCTCAAAGGGCTTATGGAACAT	TCAACAATTGCACGTTTCGAA
Gcm2	ATCCCAGCACTCTGAGGGC	TGAAACACAGAACTGTCTGGTAGAA
115106_at	GGGTTATTTGTCAACTGAGTCTGAAA	ACCCAGCCTGTGTTTGTGAG
CCL21	GGCTGCAAGAGAAGTGAACAGA	CCACCCAGCTTGAAGTTCGT
168542_f_at	TTCTTTTGCTGAGGGCTGGA	CCAGTCTAAACACAGGTTGTACACA
Angpt2	TTCTGGGAAGGTTGTGGCTGAG	CGTGCTTAGAGGAATGTGGTCC
Apba2	GAGTGTGGTAGCCACAGCCC	GGAGCCTAAACATGGCTGCA
Ypel1	TGGTCCATTTCTTTGCC	CTTTGCTTTGCCAGCCTAGTC
Gphn	ATGTGCACCATGCCAAAAGA	CTGCTAGGGTGTGCTCCTTCCC
Lmna	TGAAGAGGGAAAGTTCGTGCG	GGGAAGCGATAGGTCATCAAAGG
163492_at	GTGAAAGATGAGAGACAAGCAAAGG	TGTCCCCTCAGCAGCCC
Prkag2	TTTGGATCTGGAAAGGCTATGC	TCCGTTACTTCTTCCCTGCG
Dmrt2	TGTAGCCAAACAAGTTGGAACG	TGAGTGACGGCAGATGAAGG
Meox2	CGGTCTGTGTTCCAACCTCATC	TGCTGCCACTTCTTCTCTACG
Klf16	AAGCCTACCCACTCCTTGTCTTC	TTCCCTGAACTTCCGCCAATGG
98890_at	CATGCACAGTAACAGCCCAACT	AGCAGCATGGTGTGGGAG
Keo4	TTTGTGTTCTTTGGCCCTTCA	AAGCACAGAGCTCAGTGATCCA
Pim3	GCTTAGTCACACAGGGTACACA	CAGTCTGCTTGGCTGGCTG
Zfp297	GATCCCCATGGCAAGGGT	TGTGTTGTGGACAAGGCCT
Fgf12	TGGAGAAAAGCAAGGACGCTC	AAAGGGAGGGAGAAGAAGGGACAG
Kif3c	TCCTTTGCTTTGTGCCTCCAG	CCTCCCCAAGATGTAACATAAGAAG
Map3k	CATGATTGTGCATCGGGACA	TGGTCTGTAGGCGTTTGTCTG
103405_at	TCACATCTCTTCCCAACACTTG	TTGTCCCCTTTCAGCCCTTC
160815_at	CTGCTCCACTCACCACCTCC	CAAGTGAAGTTGCCCAGCAGT
Pxk	AGCTCATTCTCTGCAGCATC	CCGCTGTTTCTCCCTCAGC
97355_at	CATTTGACCATCTTGGGCT	CAGGTCTGACTTCTGGCCTTG
Clock	GATGGCCAGAAAGAATCGCTC	CTTCCCTACCGTCTCATCAAGG
Meox1	ATCTTCTCCATGGGATGCATT	TCTTCCAAGGAGACTGTTGCC
Ehox	GAGTGTACTGGGCCAGTCCG	CCATGAGGTCTGCATCACA
CD44	GTTCCCAGCACTGTGACTCAT	TGTCCCATTGCCACCGTTGAT
Grial	GTCCGCCCTGAGAGGTCC	ATTCCCCTTATCGTACCACCA
Colla1	GGACGCCATCAAGGTCTACTG	GGTTCGGGCTGATGTACCAG
Nrxn1	TGAGCTGCAAGTGACACACG	GGCAAAGAGAGGATGCTGATG
CD200	GGATTTTGGTTTTTCAGTTCCACTG	TGATTTTCGGTGACGTTTCCA
Ebfl	GTCCATGCAGGGATGATGG	GAGTTGCGGGTGAAACCTTG
CD6	CACCTTTGATCCTAAGCCTTAGGAA	TCCTGGGTGATAATGGCAGC
137059_at (EST1)	TGTATGTGCCAGTGTCTCTGAA	CACAACCATCCATAACGCCA
101154_at (EST2)	TTCTAAACTGGTCTCCAAATTC	AGCAGCAAACACATTGAGGGT
WIF1	TGTAATTTATGCATCTCTGCCCA	CAGTGTGTAGTTGACAGATACTTGCAA
CXCL13	CCACCTCCAGGCAGAATGATG	TTTGTGTAATGGGCTTCCAGAA
Lmcd1	TTGGATCCCTCAGAAATGCAT	TGGATTTATTGTTCTTAGCTGCAA
Bmp4	GGACTTCGAGGCGACACTTC	GCCGGTAAAGATCCCTCATG
Fst	TCTGTGCCCCAGACTGTTCC	GCATCTGGCCTTGAGGAGTG
130608_at	ACACAGTGCCAGGCATACAATC	ACTCCTTTAAATCCCTGGCAGAG
c-myc	CACAGCAAACCTCCGCACAG	TGTGTGTCCGCCTCTTGTCTG
107112_at	GTGCAAACCTTGAAGCCTG	CCAAGCCGAAGAAGGCAAT
Khdrbs3	CCTCTCGCTCTGGGAGTGAG	GAAGTGGCGGTACCACGTG
104066_at	CCCTGGCTTTCACTGAAAAGC	GCCAAGACTAGAGTGGAGGAGC
Flrt3	AGATGACTTGTGACTCTGAAAAGTGAA	TGAAAACGGGCTGTGCTTA



Bambi	TCACCTGCAGCTCCCTAAGAC	CACAGTCAAATGGATTAAGGTGCT
135615_at	CCTCCCCTTATAGACCACACCA	TTCATTATTGTCCCCCTTCAGA
134352_at	CATGTGGGTATGTGCAGGTGA	CAGGTAGCGTAAAAATCATCTCCAG
Tec	GGTTTGAGTGCCAGCCATG	ACAACCACCCTGGCTTTCTG
168351_at	TCAGTGGGAGAAAAGTGCTTGC	TGAGGACATCTTTCAGCAGTCAG
116782_at	TCTACCTCCCCAGGATAGGCA	TGTTGGTAGAGCAATGGCTTAGC
Msx2	GACATATGAGCCCCACCACCT	CTTGCGCTCCAAGGCTAGAA
117279_at	ATGCTTGTTTCGTGCACCAAAG	TGGTAGCTCACAAACGTCCATAAC
Pr1	CGTCGTACAGAGGCACCCTT	TGACCTTGACACTGCCTCTTAGG
Lnpep	GGTTCAAAAATGAGTGATTCCTTT	CTTTGAATCCTTAGGAGAGAAGCTTTCTT
136661_at	AGCACCTGGCTACTTTTGC	TGTGAATTCTCTGACGTTGAATGA
Rbm9	TTTTGGAGCCTCTGTGGGAC	ATGGCAGTGAAACCTGGCTT
Sh3glb1	GAGCAGGCCTAAAGATTACGTTG	ACACAAGAGGACCCACCCAG
Srpk2	GCCTACTAATGGTTTGTATCCTGGA	CCCATGAATGAGAAGGCCA
Csnk1d	TTGTCTGCCCTTCACAGCAA	CGCATGTCCACCTCACAGAT
Phlda2	TCACCGAAGATATTCCCGTTG	TGGTGGGTTGGAAGCAGGTA
Spock2	ACAGACGGAACCCAAGCACT	AGCTACCCGCTTCTCAGCC
Nkd1	TGAAGGCTGGCTAAATATTAGTGGA	GCCCACACCCTAAGGCATTAT
Slc19a1	GGGCCACCTGTTAGCTTATCC	AGGGAGCTGCCCTTGAGTG
Syt4	ATCCACAAGGTCCAAGTGACT	TAAGGATATCTCTGTCCAACAAGTGC
Tnfrsf19	AAAGGTTTGTATTGGAAAGCGATAAC	AAGGAAAGAGACACAATCATGGCT
Galnt3	AGATATGGGAGATTCCGGAAGGAC	TGCGTCACATGGCACTAAGTTT
Hs2st1	ATACTTGTTCTTCATGGCGTATCT	GCAAATCCTACCCACATCACAG
Tbx3	GTTTTGTCTGGGAGGGAGCA	TTCAAAGCAACAGCAGCCTG
Sp8	ACCATTAGATTTAGCTCAGCACCA	CTGAGAAGGAAGCAGCAACATG
Fgf8	GGAAGCTAATTGCCAAGAGCA	CTCGTACTTGGCGTTCTGCA
Fgf10	AAGCTTGCAGAGTCCAAAAATAGAA	CCGAATTCATTTTGTATTATCTCTGT
Tbx1	TGCAGTGTAGACGACCGAGAGA	AACCGTTTATGAAATCGGCG
Foxa1	TGCCCAGATATGAAGACCTCG	CCTTGTAACCTGGCCAGTCAGG
Foxa2	GGTTGTAAGTATGTTGAAAAGAGGAA	TCACCATGTCCAGAATGGGAT
Sfrp2	GGCCTGAGAATCGGCATCTA	AGTTCTGTAGCTGGGATGGGAA
CXCL12	CCTCGACGGGCTAGCAGTAT	CGTTTTCAAATTATCTGGGAGAAAGA

## 2.2.4 Immunohistochemistry

As negative controls, test reactions were included whereby the primary antibody was either replaced with normal (non-immune) rabbit Ig, goat anti-CXCR3 antibody (demonstrated to not work under the used conditions) or mouse IgG according the animal specie that served for the generation of the tested antibody or instead omitted on purpose. In addition, for  $\beta$ -galactosidase immunoreactivity, non-transgenic embryos were examined in parrallel as controls. All control reactions were revealed to be negative.

- Seven micrometers of Cyrosections of frozen tissue mounted on SuperFrost plus slides (Menzel-Gläser, Braunschweig, Germany) were allowed to dry completely over night.
- One liter of the following saponin/PBS solution was prepared (per 1L: 0.1% of saponin (Sigma, Buchs,CH), 1% of filtered Fetal calf serum (Invitrogen, Basel, CH) completed with

PBC (see section 2.1.6) to 1L). Importantly the saponin reagent was pre-prepared by diluting 1g of saponin into a final volume of 10ml of PBS and filtered (20-40 $\mu$ m) through a syringe before being added to the saponin/PBS solution. In addition, the well mixed saponin/PBS solution was systematically verified to have a pH between 7.2 and 7.4.

- The sections were fixed in a Kopplin Jar filled with approx. 70ml of ice cold (-20°C) acetone (Merck, Dietikon, CH) by being incubated for 5min at -20°C. Once the sections were fixed, the slides were allowed to dry at room temperature for 10min to evaporate the remaining acetone. Alternatively, the sections were fixed in a Kopplin jar filled with approx. 70ml of an pre-prepared 4% paraformaldehyde (Sigma, Buchs, CH), diluted in water by being incubated for 15min at RT. Importantly, in case of the use of the 4% paraformaldehyde solution, this solution was incubated at 60°C in a waterbath for dissolving the paraformaldehyde, filtered and was cooled down to room temperature before the sections were fixed.
- The sections were then incubated in freshly prepared solution of 70ml Na/Az/peroxide solution (0.1 % NaAz (Sigma, Buchs, CH), 0.3% Peroxide (Sigma, Buchs, CH) completed with Saponin/PBS solution) for 10min in order to inactivate endogenous peroxidase activity of the fixed tissue. The sections were then rinsed once with approx. 70ml of Saponin/PBS solution. When using biotinylated antibodies, the Activin/Biotin blocking kit (Vector Laboratories, Peterborough, UK) was employed according the manufacturer's instructions to block all unspecific Activin binding.
- Heightly microliter of primary antibody solutions (primary antibody diluted at the appropriated final concentration (i.e 1-5 $\mu$ g/ml) with the saponin/PBS solution) were added to each section. Importantly, before adding the primary solution, the surface surrounding the sections was carefully wiped with a tissue wipe to remove all remaining liquid. The slides were then incubated in a closed humid chamber box with a paper sponged with water and left for 2 hours at room temperature.
- The sections were washed 3 times with Saponin/PBS solution for 5min each. All remaining liquid around the sections was removed using a tissue wipe, before the 80 $\mu$ l of the secondary antibody solution (secondary antibody diluted at the appropriated final concentration (i.e 5 $\mu$ g/ml for horadish peroxidase conjugated antibodies and 1 $\mu$ g/ $\mu$ l for biotinylated antibodies)) were added to the sections. The slides were then incubated in the humid chamber box for 30min at room temperature.

- The sections were then washed 3 times with the Saponin/PBS solution for 5min each. When using a biotinylated antibody, all surrounding liquid around the sections was removed and subsequently 80µl of Streptavidin-horadish peroxidase conjugated at the concentration of 1µg/ml (Sigma, Buchs, CH) was added to the sections. In such case, the sections were then incubated for an other 20min in the humid chamber box and subsequently washed 3 times with the Saponin/PBS solution for 5min each.
- Next, the sections were stained for 1-20min in a Kopplin Jarr filled with AEC (3-amino-9-ethylcarbazole) solution. The duration of time for staining depends on the intensity of the specific signal to be expected. The AEC solution was always freshly prepared by dissolving 1 AEC tablet (Sigma, Buchs, CH) in 2.5ml of DMF (dimethylformamide) (Fluka, Buchs, CH) in an erlenmeyer and by adding 70ml of an acetate buffer (50mM, pH 5.0) as well as of 30µl of an 30% peroxide solution (Sigma, Buchs, CH). The acetate buffer contained per 1L, 74ml of 0.2N acetic acid (Merck, Dietikon, CH), 176ml of sodium acetate 0.2M (Sigma, Buchs, CH) and 750ml of water. Importantly, the AEC solution was always filtered (i.e through blotting) to remove precipitates.
- The slides were then rinsed in water and counterstained with filtered Mayer's Hemalaun solution (Merck, Dietikon, CH) for 5-10s before being rinsed extensively with water.
- The slides were mounted with Crystal/Mount (Biomeda, Foster City, CA) under a coverslip (Menzel-Gläser, Braunschweig, Germany) and were left at room temperature in a box. Importantly, all remaining bubbles were removed before the slides were allowed to dry in the box. The sections were then analysed under a microscope and pictures of the sections were taken with the help of an CCD camera mounted on top of the microscope (Nikon AG, Egg, CH).

### **2.2.5 In situ hybridization on crysections (ISH)**

The protocol was essentially adapted from (Schaeren-Wiemers and Gerfin-Moser, 1993). As positive control an antisense probe of the recombination activating gene 1 (RAG1) was examined on a section from an E15.5 embryo whereas the negative control was a sense probe of the examined gene.

### Probe preparation:

The sense and antisense dioxigenin (DIG, Roche Molecular Biochemicals, Basel, CH) labeled cRNA probes were generated by standard in vitro transcription (IVT). Nrnx1 antisense and sense template for IVT was generated by inserting a purified PCR product into the pGEM-T easy vector (Bioconcept, Allschwil, CH) using the following PCR primers:

Nrnx1 forward primer: 5'-ACGAAGTTAAAATTCAGTACCCATTTTC-3'

Nrnx1 reverse primer: 5' GATGTAGTCAGTTTATGCCAGGTAGTG-3'

The DNA sequence of that amplicon is located within the affymetrix probe source sequence for the Nrnx1 probe set (114766\_at) of the MGU74Bv2 microarray (see section 2.2.10 for cloning, purification, and OD measurement). The orientation of the insert was verified using appropriate restriction enzymes as described in section 2.2.10.

- For producing the labeled cRNA of the probe, 1µg of the purified plasmid containing the PCR insert (i.e Nrnx1 amplicon) was used as template, to which were added the following reagents: 2µl of an 10x IVT buffer, 2µl of DTT (0.1M), 2µl of DIG-NTP mixture (10mM mixture: UTP-DIG (3.33mM), UTP (6.66mM), ATP (10mM), GTP (10mM), CTP (10mM)) (Roche, Basel, CH), 1µl of SuperaseIn (Ambion, Huntingdon, UK), 1µl of T7 RNA polymerase (20U/µl) (Roche, Basel, CH). The mixture was completed to 20µl with milli-Q 18.2 water.
- The reaction was briefly spined and incubated for 3 hours at 37°C in a thermal cycler. For the digestion of the DNA template, 2µl of DNase I (10U/µl.) (Roche, Basel, CH) was added to the reaction and was then incubated for an other 1 hour at 37°C.
- The labeled cRNA probe was then purified using Rneasy mini columns (Qiagen, Hombrechtikon, CH) according to the manufacturer's instructions. One microgramm of the purified cRNA probe was then analysed by gel electrophoresis (using a 1% agarose/ethidium bromide (0.25µg/ml) gel) for the verification of the expected size in bp of the probe.

### Sections:

- For the ISH, 15µm sections were cut using a cryotome (Leica, Glattbrugg, CH) and was mounted onto a SuperFrost Plus slide (Menzel-Gläser, Braunschweig, Germany). The sections were then allowed to dry for 20min at room temperature.
- The sections were then fixed in a freshly made 4% formaldehyde PBS solution for 10min. The sections were then subsequently washed 3 times in PBS for 5min each.
- The sections were then acetylated for 10min in a triethanolamine solution (3.5ml of triethanolamine (Sigma, Buchs, CH) and 296.5ml of DEPC-treated H<sub>2</sub>O). Seven hundred and fifty microliters of acetic anhydride (Sigma, Buchs, CH) was then added dropwise over the sections using a stirrer. The sections were then washed 3 times in PBS for 5min each using a shaker.

### Prehybridization:

For the prehybridization, the sections were prehybridized in a humid chamber with 1ml of the hybridization buffer over night (O.N.). The hybridization buffer was prepared in advance, stored at -20°C and contained 50% formamid (deionized), 5x SSC, 1x Denhards, 100µg/ml salmon sperm DNA, 100µg/µl tRNA and DEPC-treated H<sub>2</sub>O (Invitrogen, Basel, CH).

- ### Hybridization:
- For the hybridization the dioxigenin labeled RNA probe was added to the hybridization buffer as such as to have a final concentration of 200-400ng/ml. The mixture containing the probe was then incubated at 85°C for 5min before being chilled on ice.
  - Eighty microliters of the mixture were added to the sections, which were mounted under a coverslip (Menzel-Gläser, Braunschweig, Germany) and sealed with Rubber Cement Fixogum (Marabu, Milton Keynes, UK) for avoiding evaporation of the hybridization solution. The slides were then transferred into a Quadriperm dish (Heraeus, Frankfurt, Germany) and placed into a humid chamber box containing a tissue wipe soaked with 5xSSC (see section 2.1.6). Next, the sections were allowed to hybridize over night at 68°C.

### Post hybridization:

For the post-hybridization, 2L of a Maleic acid autoclaved solution (100mM maleic acid, 150mM, NaCl, pH 7.5, only sterile) were prepared in advance, as well as the B3 buffer (per 500ml: 50ml 1M Tris HCl pH 9.5, 5ml 0.5M MgCl<sub>2</sub>, 10ml 5M NaCl) which was filtered through a 0.45µm filter.

- The coverslips of the slides incubated over night at 68°C O.N have been carefully removed with forceps and with the help of some 5x SSC buffer. The sections were then subsequently washed with 0.2x SSC at 70°C for 60min, 0.2x SSC at room temperature for 5min and in maleic acid solution for 5min.
- The sections were incubated for 60min into a blocking solution (1% blocking reagent from Roche Molecular Biochemicals, Basel, CH) in maleic acid solution).
- For the detection of the hybridized labeled cRNA probe on the sections , 80µl of anti-DIG antibody solution (dilution 1/2500 in blocking solution) were added to each section. The sections were then incubated for 1hour at room temperature. The sections were then rinsed in maleic acid buffer for 10min, and subsequently washed 2x30min in buffer B3 for 5min.
- Each section was then immersed into 1ml of staining solution (per 25ml: 112.5µl of NBT and 87.5µl of BCIP (Roche Molecular Biochemicals, Basel, CH) and completed with B3 buffer) for appropriate duration (2-48 hours) according to the intensity of the staining signal. Importantly, the slides had to be protected from light, as the staining solution is very sensitive to light. Once the desired staining intensity was reached, the sections were washed in PBS containing 1mM of EDTA (Sigma, Buchs, CH) for 10min to stop the staining.
- Individual section was then counterstained for 20s with Methylene Green (0.01 % in PBS) (Merck, Dietikon, CH). Each section was mounted with 60°C pre-warmed Kaisers glycerol gelatin (Sigma, Buchs, CH) under a coverslip. After having carefully removed all bubbles, the sections were allowed to dry at room temperature. All sections were analysed under a microscope and pictures of the sections were taken using a CCD camera mounted on top of the microscope (Nikon AG, Egg, CH).

## 2.2.6 Total RNA extraction and RT-PCR for non-microdissected tissues

### 2.2.6.1 isolation of Total RNA

- The extracted tissue was homogenized in 1ml of Trizol reagent per approx. 100mg tissue using a Polytron homogenizer for 20-30s. If the total RNA was isolated from cell cultures or from purified thymocytes or TECs (see section 2.2.13), 1ml of Trizol reagent was resuspended with  $10^4$ - $10^6$  cells. In case of less than  $10^4$  cells, the protocol for microdissected tissue was followed (see section 2.2.1.2). Hundred microliters of BCP (see 2.2.1.2) were added to the mixture, which was then vigorously shaken for 30s.
- Next, the mixture was incubated at room temperature for 5min, centrifuged at 12,000g for 15min at 4°C in a microcentrifuge. The aqueous phase was transferred into a new 1.5ml tube and 500µl of isopropanol (Sigma, Buchs, CH) was added. The mixture was then left for 15min at room temperature for the allowing the RNA to precipitate.
- The precipitated RNA was then centrifuged at 12,000g for 15min at 4°C. The supernatant was removed, the RNA pellet was then washed with 75% ethanol (Fluka, Buchs, CH) and centrifuged at 7,500g for 5min.
- The supernatant of the sample was removed and the pellet was allowed to dry for 5min under a hood. The RNA pellet was then resuspended in 20µl of milli-Q 18.2.
- The concentration of the total RNA in the sample was measured by optical density (OD) using the following formula:  
Concentration (µg/ml) =  $40 \times OD_{260} \times \text{dilution}$ . The  $OD_{260}/OD_{280}$  ratio of the samples were always found to be above 1.8.
- Five hundred microgramms of the total RNA was then analysed by gel electrophoresis (on a nondenaturing 1% agarose/ethidium bromide 0.5µg/ml) for verifying the quality of the RNA. All samples considered were found to have intact RNA. The samples were then store at -80°C until further processed.

### 2.2.6.2 Reverse transcription

As negative control, a test reaction has been included whereby the reverse transcriptase was omitted on purpose .

- For the preparation of the reverse transcription, 9µl of total RNA was added to a 0.5ml microtube containing the following master mix solution (per 9µl: 4µl of 5x First strand buffer (Invitrogen), 2µl DTT 0.1M (Invitrogen, Basel, CH), 1µl dNTP 10mM, 1µl DNase I 10U/µl (Roche, Basel, CH), SuperaseIn 20U/µl (Ambion, Huntingdon, UK). Importantly, the total RNA did never exceed 5µg of RNA to ensure a maximum of efficiency of synthesis. The mixture was then gently mixed and incubated in a thermal cycler for 30min at 37°C for digesting genomic DNA contaminants.
- One microliter of the oligo dT (500ng/µl) or alternatively 1µl of random hexamers N6 (500ng/µl) was added to the mixture. Importantly, in case of the analysis of microdissected tissue by qRT-PCR, 1µl of a pool (500ng/µl) of specific 18mers primers, which were located 3' downstream of the analysed PCR gene sequence to be examined was added instead to increase the efficiency of the reverse transcription.
- Next, the samples were incubated in a thermal cycler for 5 min at 70°C to allow the secondary structure of the RNA to denature and for inactivating the DNase I. The samples were then chilled on ice for 2 min for annealing the desired primer before the secondary structure was renatured.
- One microliter of Superscript II or III (200U/µl) (Invitrogen, Basel, CH) was added to each sample. After having pipetted up and down the mixture and briefly spined down the mixture, the samples were incubated in a thermal cycler for 1 hour at 42°C when using the Superscript II reverse transcriptase. Importantly, when using Superscript III enzyme, the reaction was incubated at 50°C. The reactions were then stored at -20°C until further processed.



### 2.2.6.3 Conventional PCR amplification

As positive control, a test reactions was included whereby the used cDNA originates from a tissue known to express the examined gene. As negative control, a test reaction containing the sample without the adjonction of reverse transcriptase was analysed.

- Each lyophilized oligonucleotide (Invitrogen, Basel, CH) to be stored was diluted with TE water for a final concentration of 100 $\mu$ M and aliquoted in samples of 10 $\mu$ M with milli-Q 18.2 water.
- Twenty microliters of a primer mixture (per 20 $\mu$ l: 1 $\mu$ l (2-10ng/ $\mu$ l) of cDNA template, 2 $\mu$ l of forward primer (10 $\mu$ M), 2 $\mu$ l of reverse primer (10 $\mu$ M) and 15 $\mu$ l of milli-Q 18.2 water) were pipetted into a 96 well PCR plate (Life Systems Design, Merenschwand, CH) or alternatively into a 0.2ml PCR microtube (Vaudaux-Eppendorf, Schonenbuch, CH).
- Thirty microliters of the PCR master mix solution (per 30 $\mu$ l: 5 $\mu$ l of 10x buffer (Sigma), 1 $\mu$ l of dNTP 10mM, 0.4 $\mu$ l of Jumpstart DNA polymerase (2.5U/ $\mu$ l) (Sigma, Buchs, CH), and 23.6 $\mu$ l of milli-Q 18.2 water) was added to mixture. The 96 well plate was then briefly spined at 700rpm in an adapted centrifuge (Vaudaux-Eppendorf, Schonenbuch, CH). In case of the use the of 0.2ml microtubes, the samples were briefly spined in a conventional microcentrifuge.
- The plate or the microtubes was then transferred to a thermocycler using the following PCR conditions: 2min at 94°C and subsequently for 30s at 94°C and 30s at 55°C, 1min at 72°C, respectively for the denaturation, the annealing and the elongation of the amplicons. These subsequent steps were repeated 39 times.

#### Analysis:

For the analysis of the amplicons, 10 $\mu$ l of each PCR reaction was examined by gel electrophoresis using a 2% agarose gel containing 0.25 $\mu$ g/ml of ethidium bromide (Sigma, Buchs, CH). The GelDoc2000 system (Biorad, Reinach, CH) was used for verifying the specificity of amplification and for taking pictures of the amplicons.

#### **2.2.6.4 Nested PCR (for microdissected tissue)**

Two different primer pairs have been designed for each tested gene as such as a primary PCR was done using primers (referred as outer primers) defining a DNA sepecific sequence of above 200bp in size. The amplicon of this PCR was subsequently amplified in a second PCR using primers (inner primers) whose sequence were designed as such to prime to the amplicon of the first PCR. The amplicon size of the second PCR was approx. 100bp. Positive and negative control were used as described above in section 2.2.6.3.

##### First PCR:

- Twenty two and a half microliters of a master mixture (per 22.5 $\mu$ l: 0.5 $\mu$ l of outer primers (5 $\mu$ M each), 2.5 $\mu$ l of 10x PCR buffer (Sigma, Buchs, CH), 0.5 $\mu$ l of dNTP 10mM, 0.1 $\mu$ l Jump start DNA polymerase (Sigma, Buchs, CH) and 18.9 $\mu$ l of milli-Q 18.2 water) were added for each reaction to a 96 well PCR plate (Life Systems Design, Merenschwand, CH).
- Two and a half microliters of cDNA were deducted from the reverse transcribed reaction (section 2.6.2) and then added to each reaction. Once all samples were loaded into the 96-well plate, the plate was sealed with an appropriate foil (Life Systems Design, Merenschwand, CH). The plate was then briefly spined at 700rpm for a few seconds in a centrifuge (Vaudaux-Eppendorf, Schonenbuch, CH).
- Next, the plate was transferred to a thermocycler (Vaudaux-Eppendorf, Schonenbuch, CH) using the following PCR conditions: 2min at 94°C and subsequently for 30s at 94°C and 40s at 55°C, 1min at 72°C, respectively for the denaturation, the annealing and the elongation of the amplicons. These subsequent steps were repeated 19 times before being incubated at 72°C for 10min. At the end of the PCR, the samples were kept at 4°C until further processed.

##### Second PCR (nested PCR):

- Twenty two and a half microliters of a qPCR master mixture (per 22.5 $\mu$ l: 0.75 $\mu$ l of inner primers (10 $\mu$ M each), 12.5 $\mu$ l of 2x SybrGreen master mix (Applied Biosystems, Rotkreuz, CH) and 9.25 $\mu$ l of milli-Q 18.2 water) were used per reaction.

- Two and a half microliters of the first PCR reaction were then deducted and added to each reaction. Once all samples were loaded into a qPCR 96-well plate (Applied Biosystems, Rotkreuz, CH), the plate was sealed with an appropriate foil (Applied Biosystems, Rotkreuz, CH). The plate was then briefly spined at 700rpm for a few seconds in a centrifuge (Vaudaux-Eppendorf, Schonenbuch, CH).
- Next, the plate was transferred to a qPCR 5700 instrument Applied Biosystems, Rotkreuz, CH) using the following PCR conditions: 2min at 94°C and subsequently for 30s at 94°C and 40s at 55°C, 1min at 72°C, respectively for the denaturation, the annealing and the elongation of the amplicons. These subsequent steps were repeated 19 times before being incubated at 72°C for 10min. At the end of the PCR, the samples were kept at 4°C until further processed.
- The analysis of the samples was examined as described in section 2.2.3 (quantitative PCR).

### **2.2.7 Transfection and purification of hWIF-IgG**

For the transfection, a plasmid containing a fused sequence of the hWIF1 and human Immunoglobulin (hIgG) (kindly provided by Dr.J.Hsieh (New York, USA)) was transfected into HEK293 cells. As a control, the same plasmid but containing only the hIgG sequence was taken along in parallel (kindky providen by Dr.J.Hsieh). The plasmid that served as template for the production of the fused protein hWIF-IgG was previously shown to generate a functional Wnt inhibitor factor 1 when transferred into HEK293 cells (Hsieh *et al.*, 1999). Therefore, all our transfection were established in HEK 293 cells. The purification of the hWIG-IgG conditioned media was either done by affinity or by size-filtration.

- The HEK293 cells were in a 175cm<sup>2</sup> flask grown to 1/3 of confluency in 40ml of IMDM media supplemented with 2% FCS as described in section 2.1.3 (see also section 2.1.4) and subsequently replaced with fresh FCS-supplemented media. Importantly, if the hWIF-IgG products were purified by affinity, the supplemented FCS was replaced with Immunoglobulin-depleted FSC. This FCS was depleted by affinity purification on G sepharose columns (Sigma, Buchs, CH).
- Approximately 1.7ml of a prepared transfection mixture (per 175cm<sup>2</sup> flask: 1650µl of serum free IMDM media, 66µl of Fugene reagent (Roche, Basel, CH) and 22µg of DNA plasmid

(ranging between 1-2 $\mu\text{g}/\mu\text{l}$ ) was added dropwise to the media of each flask . Each flask was then gently homogenized in a circular and horizontal fashion.

- All flasks were placed back in the incubator (37°C, 5% CO<sub>2</sub>). The flasks were left in the incubator for 48-66 hours according to the confluency of the cell layers. The media of each flask was collected in 50ml Falcons tubes (BD Biosciences, Allschwil, CH) and spined for 5min at 2000rpm in a centrifuge (Vaudaux-Eppendorf, Schonenbuch, CH). The media were subsequently filtered through an 0.2-0.4 $\mu\text{m}$  meshwork using a syringe.

#### Affinity purification of conditioned media:

- The collected media was loaded on G sepharose prepared columns (Sigma, Buchs, CH) for the affinity purification of hWIF-IgG containing media according to manufacturer's instructions. Importantly, the flow through were re-loaded twice on the columns before being extensively washed with PBS.
- For the elution of the affinity purified of hWIF-IgG, the columns was subsequently eluated with 10ml of 100mM glycine (Sigma, Buchs, CH) solution adjusted to pH 2.7. The eluates were subsequently collected in 1ml fraction directly from the column in 1.5ml microtubes.
- The eluate fractions were subsequently neutralized to pH 7.0 with appropriate volumes of 1M Tris HCl (Sigma, Buchs, CH) adjusted to pH 9.0. Importantly, this step was achieved within a minute in order to avoid an eventual irreversible denaturation of the purified protein. The column was extensively rinsed with PBS and the different fractions were stored at 4°C.
- Ten microliters of each fraction was measured by optical density (OD) at 280nm, in order to reveal with fractions were containing the high yields of affynity purified hWIF-IgG. The fractions that contained the two highest yields were pooled together in a new 1.5ml tube. The pooled volume was loaded onto vivaspin2 (cut off 50KDa) columns (Sartorius, Dietikon, CH) for concentrating the purified hWIF-IgG containing solution for approximately 20 times and for exchanging the neutralized eluate solution for a PBS buffer. This was achieved according the manufacturer's instructions.
- The concentrated solutions were stored at 4°C. One microliter was deducted of each samples and subsequently diluted in 249 $\mu\text{l}$  of PBS. Five microliters of the diluted solution was then analysed by SDS-page electrophoresis and by Western blot for the verification of the size of the produced and purified protein (see section 2.2.8).

- For the evaluation of the concentration of purified hWIF-IgG in the samples, the Bicinchoninic acid (BCA) protein assay kit (Pierce, Rockford, IL) was used according to the manufacturer's instructions. Importantly, to evaluate the concentration of the sample, a standard curve was generated using the following reference concentrations of BSA diluted in PBS: 250µg/ml, 125µg/ml, 50µg/ml, 25µg/ml, 5µg/ml and blank diluted in PBS.
- One microliter of the examined sample was diluted with 249µl of PBS for the evaluation of its concentration in purified hWIF-IgG, from which 25µl was deducted and loaded into 96 Elisa plate (BD Biosciences, Allschwil, CH), as well as 25µl per well for each of the different concentrations of BSA for generating a standard reference curve. Each well was completed with a mixture of the BCA reagent according to the manufacturer's instructions. The Elisa plate was closed with an adapted Elisa cover plate (BD Biosciences, Allschwil, CH) and was then incubated so that it floated in a 60°C waterbath for 30 min to allow the measurement of a concentration down to 5µg/µl. The Elisa plate was allowed to cool down at room temperature for 15 min.
- Next, the Elisa plate was placed in an Elisa reader (Bucher Biotec AG, Basel, CH) and set to 562nm for its reading. The software of the instrument automatically allowed to generate a graph of the standard linear curve from the different BSA concentrations. Hence, from a linear regression of the standard curve, the concentration of the sample containing the purified hWIF-IgG could be deduced.

Purification of conditioned media by size-filtration:

- The conditioned media (40ml) was loaded on two vivaspin20 (cut off 30kDa) columns (Sartorius, Dietikon, CH) and filtered according to the manufacturer's instructions. Importantly, the columns were rinsed at least twice with 20ml fresh PBS and then once with 20ml of fresh IMDM serum free media pinning at 3000g at 4°C for 30min. The retained IMDM solution (containing the hWIF-IgG) was collected in a 5ml tube and stored at 4°C until used for FTOC. The solutions were never stored more than 2 days at 4°C.
- Next, the conditioned media was diluted to a quarter or to an eight with fresh 10% FCS supplemented IMDM media.
- For verifying that the control hIgG conditioned media contained a comparable amount of protein as the hWIF-IgG conditioned media, the protein concentration of each respective

sample was determined using the BCP protein assay as described above. For this BCA assay, the respective samples were diluted 250 times in PBS (1µl in 250µl of PBS).

## 2.2.8 Western blot for hWIF1-IgG

### SDS-Page Gel:

- For preparing an SDS-PAGE Gel, a separating gel solution (per gel: 2.5 ml 1.5M Tris-HCl pH 8.8 (Sigma, Buchs, CH), 50µl of 20% sodium dodecyl sulfate (SDS) (Eurobio, Courtaboeuf, FR), 4.5ml of 30% Acrylamide/Bis solution, 29:1 (3.3% C, Biorad, Reinach, CH), 2.9ml of milli-Q water, 50µl of 10% ammonium persulfate (Sigma, Buchs, CH) and 10µl of TEMED (Eurobio, Courtaboeuf, FR) was prepared. Importantly, TEMED and APS were always added as last reagents to the solution as polymerization occurs few minutes after their adjonction. This solution was then loaded into an assembled mini-Protein 3 Electrophoresis glass plate system (Biorad, Reinach, CH). Next, 1ml of water was loaded onto the poored solution and the gel was left at room temperature to allow the separating gel to polymerizate.
- The stacking gel solution (per gel: 0.625ml 1M of Tris HCl pH 6.8, 25µl of 20% SDS, 0.650ml of 30% Acrylamide/Bis solution, 29:1 (3,3% C, Biorad, Reinach, CH), 3.675ml of milli-Q water, 25µl of 10% APS, 5µl of TEMED) was loaded onto the polymerized separating gel after having removed the overlayed water that was poored on top it, and subsequently an appropriated comb was inserted into the poored gel. The Gel was then incubated for 15min at room temperature to allow its polymerization.
- Once polymerized, the entire apparatus was mounted into an Electrophorsis support containing 1L of running buffer solution (per 1L of 10 times concentrated running buffer: 144g Glycine (BioRad, Reinach, CH), 30g Tris base (Sigma, Buchs, CH), 50ml of 20% SDS and completed with milli-Q water to 1L).
- The loaded samples were heated at 100°C for 5min in protein sample buffer (per 8ml of 2 times concentrated sample buffer: 1ml of 0.5M Tris HCl pH 6.8, 0.8ml of Glycerol (Sigma, Buchs, CH), 0.2ml of 1% Bromophenol blue (Sigma, Buchs, CH), 0.4ml of β-mercaptoethanol (Sigma, Buchs, CH) and 4.8ml of milli-Q water). In addition, 5µl of a

colored marker (Sigma, Buchs, CH) was loaded in one of the lanes and the gel electrophoresis was run at 150V for 1hour. Importantly, two identical gels were prepared to allow subsequently a western blot for hWIF and for hIgG, respectively.

#### Transfer:

- The separating gels were separated from the stacking gel using a razor blade and were washed twice with water.
- For the transfer, a nitrocellulose membrane of identical dimension as the separating gel was placed on top of each gel, as well as two blotting paper on each respective side of the gel in a "sandwich" manner and then inserted into a transfer plate apparatus and subsequently in a electrophoresis support (BioRad, Reinach, CH), according the manufacturer's instructions.
- One liter of transfer buffer solution (per 1L: 14.4g of Glycine, 3.03g of Tris base, 150ml of methanol (Fluka, Buchs, CH) and completed to 1L with milli-Q water) was poured into the apparatus and subsequently surrounded by ice. Importantly a stirrer was placed at the bottom of the apparatus to allow an constant homogenization during the transfer. The electrophoresis was run at 100V for 1hour.
- Once the transfer was finished, the nitrocellulose membranes were washed twice with TPBS (PBS with 0.1% Tween 20 (Sigma, Buchs, CH) for at least 5min onto a shaker.
- The remaining separating gels were considered for an Blue Coomassie staining (BioRad, Reinach, CH) according to the manufacturer's instructions for verifying the efficiency of the transfer.

#### Western Blot:

- The washed nitrocellulose membranes were then incubated into 10ml of blocking blotting solution (5% of fat less milk powder (Coop, Basel, CH) and 10ml of TPBS) for 1 hour at room temperature onto a shaker.
- The membranes were subsequently incubated overnight at 4°C with either 10ml of primary antibody solution (20µl of rabbit anti-hWIF1 aliquot, see section 2.1.5, or with goat anti-hIgG-HRP conjugated (Sigma, Buchs, CH), diluted with blotting solution).
- The membranes were washed 3 times with TPBS solution for 5min at room temperature.

- The membrane were incubated with anti-hWIF1 and subsequently incubated in 10ml of secondary antibody solution (goat anti-rabbit IgG at 0.15 $\mu$ g/ml, see section 2.1.5, diluted with fresh blotto solution). The membrane were then washed 3 times with TPBS for 5min.
- Next, the membranes were stained with AEC solution (see immunohistochemistry section 2.2.4 for its preparation) for 20min on a shaker at room temperature before being rinsed with PBS.

### **2.2.9 Fetal thymic organ culture (FTOC)**

- Thirteen and a half days of mouse gestation embryos were carefully extracted from euthanized timed pregnant mice and placed into a IMDM medium (Invitrogen Corporation, Basel, CH) in a 10 cm Petri dish (BD Biosciences, Allschwil, CH) on ice.
- The embryos were then opened in the upper part so that the hear and the lungs were exposed in order to be able to extract the developing thymic lobes with the help of fine microdissection forceps and a binocular instrument (Leica, Glattbrugg, CH). The thymic lobes were placed in a 3cm Petri dish filled (BD Biosciences, Allschwil, CH) with IMDM medium on ice.
- The "shiny" sides of Track-Etch membranes (Nucleopore #PC MB 13 mm, 0.8  $\mu$ m pores) (SPI supplies, West chester, USA) were placed into each well of an 24-well plate (BD Biosciences, CH) filled with 500 $\mu$ l of FTOC medium (IMDM medium supplemented with 10% FCS and ) including either 0, 10, 20 or 40 $\mu$ g of respectively affinity purified hWIF-IgG or hIgG (see section 2.2.7). Alternatively the FTOC medium was supplemented to one fourth or one eighth of its volume with concentrated conditioned IMDM media containing either hWIF-IgG or hIgG (see section 2.2.7). Importantly, the Track-Etch membranes were boiled in water for 30 min and kept sterile in dry Petri dish under a hood.
- Eight isolated thymic lobes were placed on top of each of those membranes by aspirating and expelling separately each lobe into a 200  $\mu$ l micropipette tip after having been rinsed once in IMDM fresh media. The 24-well plate was then covered with its respective plate-cover and incubated at 37°C in a 5% CO<sub>2</sub> adjusted cell culture incubator for 10 days. Importantly, the respective media of each well was replaced with fresh media every 2 days.



### **2.2.10 Staining Protocol for flow cytometry**

- The isolated cells were counted and resuspended at a concentration of  $10 \times 10^6$  cells/ml ( $1 \times 10^6$  cells/100 $\mu$ l). The cells were resuspended in PBS/BSA/Az solution (PBS containing 0.1% BSA and 0.02% Na<sub>2</sub>Azide (Sigma, Buchs, CH)). All stains were based on a cell concentration of  $1.0 \times 10^6$  cells per sample.
- The cells were distributed in 100 $\mu$ l aliquots of polystyrene 4ml tubes.
- The used antibodies were diluted prior to use in PBS/BSA/Az solution to the desired concentration. Twenty microliters of diluted antibody was resuspended with the  $1 \times 10^6$  cells (100 $\mu$ l). The mixture was then incubated on ice for 15min.
- Three milliliters of PBS/BSA/Az solution were added to the mixture and subsequently spined at 1200rpm for 5min in a centrifuge (Vaudaux-Eppendorf, Schonenbuch, CH). The supernatant was gently poured off. Next, the cells were resuspended in 100 $\mu$ l of PBS/BSA/Az solution.
- Twenty microliters of diluted 2<sup>nd</sup> antibody (appropriate concentration in PBS/BSA/Az solution) and added where necessary to the samples. The samples were then subsequently incubated on ice for 15min.
- The samples were analysed by Flow cytometry using a FACSCalibur instrument and its Cell Quest software (BD Biosciences, Allschwil, CH).

### **2.2.11 Immunofluorescent analysis using confocal microscopy**

- For the cryosectioning, 5 $\mu$ m sections were cut with a Leica cryotome (Leica, Glattbrugg, CH) and mounted on SuperFrost plus slides (Menzel-Gläser, Braunschweig, Germany). The slides were incubated for at least 2 hours at room temperature.
- The sections were fixed with ice cold mixture of acetone (-20°C) for 5min.
- The sections were blocked for unspecific protein binding by being incubated in PBS supplemented with 10% of FCS (Invitrogen, Basel, CH) for 1hour at room temperature.
- The sections were incubated at an appropriate dilution with the primary antibody in 10% FCS/PBS solution overnight at 4°C.

- The sections were subsequently washed 3 times with PBS for 5 min each and were incubated with appropriate dilution of the secondary antibody conjugated to a fluorochrome (see section 2.1.5).
- The sections were subsequently washed cells 3 times with PBS for 5 min each. The sections were then mounted in a drop of Moviol mounting media (Calbiochem, Luzern, CH) under coverslips (Menzel-Gläser, Braunschweig, Germany). The sections were then left at room temperature for at least 2 hours.
- The sections were analysed using confocal microscopy (Carl Zeiss AG, Feldbach, CH) according to the manufacturer's instructions.

## **2.2.12 Rapid amplification of cDNA ends (RACE)**

EST1 and EST2 DNA sequences have both been extended using smart 5' and 3' rapid amplification of cDNA ends (RACE) methods using the Smart RACE kit (Biosciences, Allschwil, CH). EST1 was further extended using the marathon RACE kit (Biosciences, Allschwil, CH). Both protocols will be here described.

### **2.2.12.1 Smart RACE**

The following primers or primer mixture were used in the smart RACE:

Smart II oligonucleotide (10 $\mu$ M): 5'-AAGCAGTGGTATCAACGCAGAGTACGCGGG-3'

10x Universal Primer mix (400 $\mu$ l):

(0.4 $\mu$ M): 5'-CTAATACGACTCACTATAGGGCAAGCAGTGGTATCAACGCAGAGT-3'

(2 $\mu$ M): 5'-CTAATACGACTCACTATAGGGC-3'

Nested Universal Primer (50 $\mu$ l):

(10 $\mu$ M): 5'-AAGCAGTGGTATCAACGCAGAGT-3'

T7 Primer (10 $\mu$ M): 5'-GTAATACGACTCACTATAGGG-3'

The above Smart II was used as an adapter for 5' RACE (Rapid Amplification of cDNA Ends), as well as the oligonucleotide dT-T7 oligonucleotide described in linear amplification section 2.2.2.

The "outer" and "inner" gene specific primers (see nested PCR section 2.2.6.3) were also used for generating the RACE products of respectively EST1 and EST2 genes. The used protocol was essentially adapted from the Ambion RACE protocol (Ambion, Huntingdon, CH).

#### Reverse transcription:

- For reverse transcribing the mRNA, 10µg of total RNA template (i.e Ad. Lymph nodes for EST1 and Ad. Brain for EST2) were pipetted into a RNase free 0.5ml tube (Vaudaux-Eppendorf, Schönenbuch, CH). Subsequently, 4µl of a dNTP 10mM mixture (Roche, Basel, CH) were added to the solution, as well as either 1µl of SmartII oligo (10µM) for 5' RACE reaction or 1µl of dT-T7 oligo (10µM) for the 3'RACE reaction.
- To each of the respective mixture, 1µl of reverse outer primer (10µM) for 5'RACE reaction or respectively 1µl of forward outer primer (10µM) for a 3' RACE reaction was added. Subsequently, 4µl of 5x First strand buffer, 2µl of DTT (0.1M) (Invitrogen Corporation, Basel, CH), 1µl of Superscript II (200U/µl) (Ambion, Huntingdon, UK) and 1µl of Superscript II (200U/µl) (Invitrogen Corporation, Basel, CH) were added to the mixture. The mixture was then filled to 20µl with milli-Q 18-2 water, gently mixed and briefly spined before being incubated at 42°C for 1 hour.
- The reaction products were stored at -20°C until further processed with the first PCR step.

#### First PCR:

- One microliter of the reverse transcription of each respective reaction was pipetted into a 0.2ml microtube. Subsequently, 5µl of 10x PCR buffer (Sigma, Buchs, CH), 4µl of dNTP 10mM (Roche, Basel, CH), as well as either 2µl of reverse outer primer (10µM) for 5'RACE or 2µl of forward outer primer (10µM) for 3'RACE reactions.
- Five microliters of the 10x Universal Primer Mix (BD Biosciences, Allschwil, CH) for 5'RACE or 2µl of T7 primer (10µM) for 3'RACE respectively. Then, 1.25U of Jumpstart DNA polymerase (Sigma, Buchs, CH) was added to each mixture and completed to 50µl with milli-Q-18.2 water.

- After having been briefly spined, the microtubes were transferred to a thermocycler using the following PCR conditions: 3min at 94°C and subsequently for 30s at 94°C, 30s at 60°C and 3min at 72°C for the denaturation, the annealing and the elongation of the amplicons, respectively. These subsequent steps were repeated 34 times and the reactions were incubated at 72°C for 7 min before being kept at 4°C until further processed.

#### Second PCR (nested PCR):

- For the subsequent PCR, 1µl of the first PCR reaction was added to a 0.2ml microtube, as well as 5µl of 10x PCR buffer (Sigma, Buchs, CH), 4µl of dNTP 10mM, 2µl of reverse inner primer (10µM) for 5'RACE or 2µl of forward inner primer (10µM) for the 3'RACE, respectively.
- The reactions were then completed with 2µl of Nested Universal Primer for 5'RACE or 2µl of T7 primer (10µM) for 3'RACE, as well as 1.25U Jumpstart DNA polymerase and adjusted to 50µl with milli-Q 18.2 water. The subsequent steps were done as in the first PCR.
- The amplicons were analysed by gel electrophoresis on a 1% agarose/ethidium bromide 0.25µg/ml gel. The PCR products that could clearly be distinguished within an eventual smear and more than 300bp were then isolated and cloned as described in section 2.2.11.

#### **2.2.12.2 Marathon RACE**

For this RACE, the Marathon clontech RACE kit (BD Biosciences, Allschwil, CH) was used according the manufacturer's instructions. As it was strongly recommended to use, mRNA was used as starting material instead of total RNA. The mRNA was isolated from total RNA (Ad. Lymph Node for EST1 and Ad. Brain for EST2) as these tissues were shown to express these genes at high levels respectively. For the marathon RACE, specific outer and inner primers using primerexpress 1.0 software (see section 2.2.6.3) were designed but the annealing temperature was set to 68°C instead of the default setting of 60°C.

#### Messenger RNA extraction:

For the isolation of mRNA or polyA RNA from total RNA, the oligotex mRNA Spin-Column kit (Qiagen, Hombrechtikon, CH) was used according to the manufacturer's instructions for an amount of less than 250µg of total RNA. The purified mRNA was then subsequently concentrated using YM-50 Microcon columns (Millipore AG, Volketswil, CH) according to the manufacturer's instructions and collected in 10µl of milli-Q 18.2 water and measured by optical density to determine its concentration as described in section 2.2.6.1. For verifying the quality of the purified and concentrated mRNA approx. 0.5µg of mRNA was analysed by gel electrophoresis using a 1% agarose/ethidium bromide (0.25µg/ml) gel. Proceed with first strand synthesis.

#### First strand synthesis:

- For the first strand synthesis, 1µg of mRNA (1-4µl) was pipetted into a 0.5ml RNase free tube (Vaudaux-Eppendorf, Schönenbuch, CH), as well as 1µl of cDNA synthesis Primer (10µM) and completed to a final volume of 5µl with milli-Q 18.2 water. The mixture was then incubated at 70°C for 2min in a thermocycler and was cooled on ice.
- The following reagents were subsequently added to the mixture: 2µl of 5x First strand buffer, 1µl of dNTP (10mM), 1µl of AMV Reverse transcriptase (20U/µl) and 1µl of milli-Q 18.2 water. The reaction was then incubated at 42°C for 1 hour in a thermal cycler.

#### Second strand synthesis:

- For the second strand synthesis, 48.4µl of milli-Q 18.2 water was added to the 10µl of First strand synthesis reaction. Subsequently, 16µl of 5x second strand buffer, 1.6µl of dNTP (10mM), 4µl of 20x Second strand enzyme cocktail were added and the mixture was gently homogenized by pipetting up and down. The mixture was then briefly spined and incubated at 16°C for 1.5 hour in a thermal cycler.
- For generating blunt ends of synthesis dsDNA, 2µl (10U) of T4 DNA polymerase were then added to the mixture and the reaction was incubated at 16°C for 45min. To stop the reaction, 4µl of the EDTA/Glycogen mix were added to the mixture.
- For the purification of the dsDNA, 100µl of phenol:chloroform:isoamyl alcohol (25:24:1, Sigma, Buchs, CH) was added to the reaction. The mixture was then homogenized thoroughly and transferred to a Phase Lock Gel Heavy, 0.5 ml tubes (Vaudaux-Eppendorf, Schönenbuch, CH) for a safe separation of the organic phase from the aqueous phase. The mixture was

spined for 10min at 14,000rpm for the phase separation. The aqueous layer was then loaded into a new 0.5ml tube and was subsequently completed with 0.5 volumes of 4M Ammonium Acetate and 2.5 volumes of 95% ethanol (Fluka, Buchs, CH). The mixture was thoroughly homogenized before being spined at 14,000rpm for 20min at RT. The supernatant was carefully removed and the dsDNA pellet was washed by being overlaid with 300µl of 80% of ethanol (Fluka, Buchs, CH). The pellet was then spined at 14,000 rpm for 10min at 4°C in microcentrifuge. After all supernatant was removed, the pellet was allowed to desiccate for 10min at room temperature under a hood. The pellet was then resuspended in 10µl of milli-Q water and stored at -20°C until it was further processed.

#### Adaptor Ligation:

- Five microliteres of the purified dsDNA were pipetted into a new 0.5ml tube and subsequently, 2µl of Marathon cDNA Adaptor (10µM), 2µl of 5x DNA ligation buffer (Clontech), 1µl T4 DNA Ligase (1U/µl) were added to the mixture. After the reaction was briefly mixed and spined, it was incubated at 16°C overnight.
- The reaction was then incubated at 70°C for 5min for inactivating the ligase. One microliter of the reaction was diluted with either 50 or 250µl of Tricine-EDTA buffer while the undiluted adaptor-ligated cDNA was stored at -20°C. The respective diluted dsDNA was incubated at 94°C for 2min for denaturation and subsequently placed on ice for 2min before being briefly spined.

#### First PCR:

- For the first PCR reaction, 5µl of the respective diluted adaptor-ligated dsDNA were deducted and transferred to a 0.2ml microtube and subsequently, 5µl of the 10x PCR reaction buffer (Sigma, Buchs, CH), 1µl of dNTP (10mM), 1µl of Advantage 2 polymerase (50x), 1µl of AP1 primer (10µM) as well as 1µl of reverse outer primer (10µM) for 5'RACE or 1µl of forward outer primer (10µM) for 3'RACE were added. The reaction was filled to 50µl with milli-Q 18.2 water. Importantly, as negative control, the reverse outer primer was omitted in a parrallel reaction.

- The microtubes were then transferred to a thermocycler using the following PCR conditions: 1min at 94°C and subsequently 30s at 94°C, 10min at 70°C, respectively for the denaturation, the annealing and the elongation of the amplicons. These subsequent steps were repeated 4 times. Next, the reactions were subsequently incubated for 20s at 94°C and 10min at 68°C. These latter subsequent steps were repeated 24 times and then incubated at 4°C until further processed for a second PCR.

#### Second PCR (nested PCR):

- For the second PCR, 5µl of the first PCR reaction diluted with 245µl of Tricine-EDTA buffer were transferred to a new 0.2ml microtube. Subsequently, 5µl of 10x cDNA PCR reaction buffer (Sigma, Buchs, CH), 1µl of dNTP (10mM), 1µl of Advantage 2 polymerase (50x), 1µl of AP2 nested primer (10µM), 1µl of the reverse inner primer (10µM) for the 5'RACE as well as 1µl of the forward inner primer (10µM) for the 3'RACE were added to the mixture. The reaction was filled to 50µl with milli-Q 18.2 water. Importantly, similarly as for First PCR, as negative control reaction, the reverse inner primer was omitted in a parallel reaction.
- The subsequent steps were done as in First PCR.
- For the analysis of the First and second PCR, 5µl of each reaction was examined by gel electrophoresis using in a 1.2% agarose/ethidium bromide (0.25µg/ml) gel. The distinguishable PCR products (possibly within a smear) that had a length of more than 300bp were then subsequently cloned and sequenced as described in section 2.2.13.

## **2.2.13 Cloning & Sequencing of EST RACE products**

### **2.2.13.1 Cloning**

#### PCR product extraction from agarose Gel:

- For an extraction of the desired PCR products from the gel, a piece of gel as small as possible containing the amplicons was cut as out of the gel using a sterile razor blade under UV light (set at minimal energy). The piece of the gel was then placed into a 1.5ml tube that has been weighted before in order to be able to measure the amount of gel extracted.

- The subsequent purification of the amplicons from the piece of gel was done using the GelElute Purification kit (Sigma, Buchs, CH) according to the manufacturer's instructions. The purified amplicons were eluted in 30µl of TE buffer (see 2.1.6).

#### Ligation of PCR products into pGEM plasmids:

- For the ligation of the PCR product into a plasmid, 3µl of the purified amplicons were subsequently mixed with 1µl of linearized pGEM-T Easy vector ready for ligation mix (50ng/µl), 5µl of Rapid ligation buffer and 1µl of T4 DNA Ligase (3U/µl). All reagents are coming from a pGEM-easy vector system kit (Catalys AG, Wallisellen, CH). The sample was then incubated at 16°C overnight.

#### Generation of competent bacteria:

- For the preparation of competent bacteria, an inoculation of a single colony of DH5α bacteria in 100ml of LB medium (Sigma, Buchs, CH) was incubated at 37°C overnight in a shaker at 200rpm (Vaudaux-Eppendorf, Schönenbuch, CH). Five milliliters of the inoculation was mixed with 500ml of LB medium. The bacteria were subsequently grown at 37°C in a shaker at 200rpm until an approx optical density (OD<sub>600</sub>) was measured to be between 0.4 and 0.6. The bacteria culture was then chilled on ice for 30min and centrifuged at 3000rpm for 15min at 4°C. After the supernatant has been carefully removed, the bacteria pellet was resuspended in 100ml of ice-cold CaCl<sub>2</sub> sterilized solution (60mM CaCl<sub>2</sub>, 15% Glycerol, 10mM Pipes) adjusted to pH7.0) and subsequently centrifuged at 3000rpm for 15min at 4°C.
- The supernatant was removed and the pellet was resuspended in 10ml of CaCl<sub>2</sub> solution. Subsequently, 1ml aliquots of the suspension were frozen at -70°C.



### Transformation of competent bacteria:

- An aliquot of 1ml of the competent DH5 $\alpha$  bacteria was thawed on ice. Subsequently, 100 $\mu$ l of that aliquot were transferred to a new 1.5ml tube on ice and as well as 5 $\mu$ l of the ligation reaction were added to the mixture and the tube was briefly shaken by hands before left on ice for 30min.
- The mixture was then subsequently incubated for 1min at 42°C and been placed back on ice for 2min for the required Heat-shock. For allowing the bacteria to recover properly, 900 $\mu$ l of SOC medium (Sigma, Buchs, CH) was added to the mixture, which was then incubated at 37°C for 30min. In the mean time, 40 $\mu$ l X-Gal (10-20mg/ml) (Sigma, Buchs, CH) and 20 $\mu$ l of Isopropyl-Thio-B-D-Galactopyranoside IPTG (8-10mg/ml) (Sigma, Buchs, CH) was spread over and subsequently distributed on a 15cm agar plate (BD Biosciences, Allschwil, CH) containing ampicillin at 50-100 $\mu$ g/ml (Sigma, Buchs, CH) using a sterilized spatula.
- The plate was then incubated approx. 20min in the dark (as X-gal is sensitive to light) for allowing the added fluid to penetrate the agar. Subsequently, 200 $\mu$ l of bacteria from the SOC medium were spread over the plate and distributed with a sterilized spatula.
- For allowing the bacteria clones to grow, the plate was then incubated overnight at 37°C. The plate was stored at 4°C until subsequent clones were inoculated.

### Inoculation:

- For the inoculation, 10 individual clones of white colonies were respectively picked up using a sterile tip from the agar X-Gal and IPTG containing plate and transferred to a 5ml of LB buffer (Sigma, Buchs, CH) containing polypropylene tube (10ml) (BD Biosciences, Allschwil, CH). Importantly, the blues colonies were ignored as the likelihood of these colonies to contain a PCR product as insert is much smaller in comparison to a white colony. Namely, because of the fact that is more likely to pick up a blue colony of bacteria that contains an empty vector rather than a plasmid inserted with a PCR product which does not change the frameshift reading of the plasmid  $\beta$ -galactosidase.
- Five microliters of from an Ampicillin solution (100mg/ml) were then added to each tube. Each of the mixtures was shaken over night at 250rpm in an incubator at 37°C overnight. The

tubes were then centrifuged at 4000rpm for 10min at 4°C. The supernatant was discarded and the remaining pellet was further processed for a miniprep purification of the plasmid.

### Miniprep:

- For the Miniprep, a Kit (Macherey-Nagel, Oensingen, CH) was used to extract from each individual clone inoculation, the pGEM-T easy plasmid containing as an insert a PCR or RACE product. The purification was done according the manufacturer's instructions. Each of the purified plasmid was eluted in 50µl of the elution buffer.
- The concentration of the different purified plasmids was measured by optical density using the following formula: concentration (µg/ml) = 50 x OD<sub>260</sub> x dilution).
- For a verification of the size of the PCR or RACE plasmid insert, a appropriate digestion of the plasmid was done as following: 5µl of 10x EcoR1 buffer (Bioconcept, Allschwil, CH), 1µg of purified plasmid (pGEM with insert), 1µl of restriction enzyme EcoR1 (10U/µl). The reactions were filled to 50µl with milli-Q 18.2 water. Importantly, the pGEM-T easy vector is designed as such as to have two EcoR1 restriction sites at the 5' and at the 3' end of the insert. The reactions were then incubated at 37°C for 2 hours. Subsequently, 10µl of the digested plasmid was analysed by gel electrophoresis using a 1.2% agarose/Ethidium bromide 0.25µg/ml gel. Importantly, in case of unexpected bands due to extra restriction sites of EcoR1 within the insert, the subsequent sequencing step of the insert always confirmed these EcoR1 sites.

### **2.2.13.2 Sequencing of the pGEM insert**

- In order to be able to sequence the RACE insert of the pGEM plasmid, the following PCR reaction was prepared in a 0.2ml microtube: 4µl of Terminator Ready 3.0 Reaction Mix (Applied Biosystems, Rotkreuz, CH), 1µl of T7 primer (10µM) (see section 2.2.12.1 for its sequence) and 500ng of the purified plasmid. The reaction was completed to 10µl with milli-Q 18.2 water. For avoiding any evaporation, two drops of Chill-out 14 red wax (Genetic Research instrumentation, Braintree, UK) were added on top of the mixture.
- The microtubes were then transferred to a thermocycler using the following conditions: 2min at 96°C and subsequently for 15s at 96°C, 5s at 50°C and 4min at 60°C, respectively for the

denaturation, the annealing and the elongation of the transcribed products. These subsequent steps were repeated 24 times. The reaction was then stored at 4°C until purified.

- For the purification of the transcribed products, the reaction without the wax was pipetted into a new 0.5ml tube and completed to 20µl with milli-Q 18.2 water. The subsequent mixture was then loaded onto DyeEx 2.0 spin column (Qiagen, Hombrechtikon, CH) and purified according the manufacturer's instructions.
- For the sequencing, 5µl of the purified transcribed products were deducted and pipetted into a new 0.2ml microtube and 20µl of fresh Formamide (Sigma, Buchs, CH) was added to the mixture. The mixture was homogenized by pipetting up and down before being incubated at 96°C for 2min. The mixture was then placed on ice until sequenced using a ABI 310 instrument (Applied Biosystems, Rotkreuz, CH) according to the manufacturer's instructions.

The sequenced RACE products were analysed and aligned using the Seqman 5.0 software (DNASTAR, Madison, USA). All sequences were then blasted to the mouse genome at the NCBI database server (National center for biotechnology information) for a sequence verification. Importantly, only clones of EST1 and EST2 RACE products that were confirmed to belong to the same cluster or identical chromosomal location as of the affymetrix source sequence, which serves as a reference for the generation of the probe sets of these respective ESTs, were considered. Moreover, as the sequencing allows to sequence only approx. 700bp, the RACE products longer than 700bp were sequenced in more than one step by repeating the above steps but replacing the T7 primer with an appropriate specific primer.

### **2.2.14 LacZ staining**

- For the cryosection, the tissue was cut from an O.C.T block at -20°C as described in section 2.2.1, and mounted onto a Superfrost Plus slide (Menzel-Gläser, Braunschweig, Germany). The section was allowed to dessicate at room temperature for 1 hour.
- The sections were subsequently fixed 15 min at room temperature with 4% paraformaldehyde (Sigma, Buchs, CH) diluted in PBS (see section 2.1.6).
- The sections were then washed three times for 5 min with PBS and incubated in a Kopplin Jarr filled with LacZ buffer (Per1L: 1mM MgCl<sub>2</sub>, 0.1% Triton-100, 0.01% NP-40, 0.02%

deoxycholate (Sigma, Buchs, CH) for 10 min. Next, the sections were briefly rinsed with fresh LacZ solution.

- The sections were incubated in a LacZ solution containing 0.05% of X-gal (Sigma, Buchs, CH), as well as the  $K_4Fe(CN)_6$  and the  $K_3Fw(CN)_6$  reagents at a final concentration of 3mM. The sections were subsequently incubated at 37°C overnight on a shaker and protected from light.
- The stained sections were washed 3 times for 5min before being counterstained for 1min with nuclear fast red solution (Sigma, Buchs, CH). The sections were then extensively rinsed with PBS and were each mounted with Moviol mounting media (Calbiochem, Luzern, CH) under a coverslip (Menzel-Gläser, Braunschweig, Germany).
- The sections were then analysed under a microscope and pictures of the sections were taken with the help of an CCD camera mounted on top of the microscope (Nikon AG, Egg, CH).

## **2.2.15 Isolation of thymocytes and TECs**

### **2.2.15.1 Isolation of the entire pool of thymocytes from adult thymus**

The thymocytes were obtained from adult thymic tissue of 3-4 weeks old mice by disrupting the isolated thymic tissue between two frosted microscope slides (Menzel-Gläser, Braunschweig, Germany). The collected cells were transferred into a 15ml tube (BD Biosciences, Allschwil, CH) containing PBS supplemented with 0.5% FCS and the tube was left for 15min on ice to allow the cells to settle. The cell suspension was then centrifuged at 1200rpm for 5min. The supernatant was carefully discarded and the cell pellet was resuspended in a appropriate buffer according to its further processing, which was either a cell sorting (see section 2.2.15.2) or an total RNA extraction (see section 2.2.6).

### **2.2.15.2 Isolation of single positive mature thymocytes from adult thymus**

The procedure was essentially done as described by Balciunaite and colleagues (Balciunaite *et al.*, 2002). Cells were sorted from adult thymus for CD3 high and then respectively for CD4 and

CD8 molecules. The respective sorted cells ( $CD4^+CD8^-$  and  $CD4^-CD8^+$ ) were then pooled together for an total RNA extraction and RT-PCR see section 2.2.6.

### **2.2.15.3 Isolation of MTS24<sup>+</sup> and MTS24<sup>-</sup> thymic epithelial cells from adult thymus**

The procedure was essentially done as described by Gill and colleagues (Gill *et al.*, 2002). Cells were sorted from adult thymus for MHCII positive cells and subsequently for the MTS24 marker. MTS24<sup>+</sup> and MTS24<sup>-</sup> sorted cells were used for an total RNA extraction and RT-PCR (see section 2.2.6).

## 3.Results

### 3.1 Overview

The precise molecular control of early thymus development remains ill-defined. Thus, we intended to contribute to a better understanding of the events in thymus organogenesis by identifying the genetic programs that determine thymic epithelial cell fate commitment and differentiation. As endodermal contributions of the ventral aspects of the 3<sup>rd</sup> pharyngeal pouch (3<sup>rd</sup>pp) suffice to establish a normal cortical and medullary epithelial stroma, we investigated the gene expression profile of these cells (Gordon *et al.*, 2004; Le Douarin and Jotereau, 1975). To this end, we compared epithelial cells of the 3<sup>rd</sup>pp with cells of the 2<sup>nd</sup> and the 4<sup>th</sup>pp and we compared cells from the ventral aspect of the 3<sup>rd</sup>pp with cells from the dorsal circumference of the same pouch to identify genes that are associated with the commitment of epithelial cells to a thymus cell fate. With the help of laser capture microdissection (LCM), RNA from these distinct endodermal linings of the different pouches were isolated and faithfully amplified for microarray analysis.

To achieve an isolation of intact RNA, both the preparation of the tissue sections for LCM and the recovery of small RNA amounts were optimized starting with a protocol previously established in the laboratory for extracting RNA from tissue cryosections. The protocols for amplification of cDNA into cRNA were also adopted from methods for other purposes (e.g. microarray analysis) (Klur *et al.*, 2004). Following hybridization or gene microarrays and the analysis of the data, several candidate genes could be selected that fulfil the following criteria: (i) preferential or exclusive expression in the 3<sup>rd</sup>pp when compared to the 2<sup>nd</sup>pp, and (ii) an abundant expression of the candidate gene in the ventral aspect of the 3<sup>rd</sup>pp when compared to its dorsal part. The different candidate genes fulfilling these criteria have subsequently been examined first by quantitative PCRs (qRT-PCRs) using the cDNA which served as the template to generate the probes for the microarray analysis (direct confirmation of the microarray analysis). Next, a selection of verified candidate genes were analysed by qPCRs from tissue samples isolated independently. This step was taken to verify the correctness of the genes analysed by microarray as potential candidate genes. The candidate genes further considered were in particular CCL21, Klf16, Fgf12, CD44, WIF1, Nr3x1, Phlda2, Bmp4, Fst, c-Myc and Sp8. Gene products for which antibodies were available (i.e. CCL21, Meox2, CD44, Phlda2, WIF1, Fst), were further

investigated by immunohistochemistry (IHC) on tissue sections from E10.5, E11.5 and E12.5 to see whether the observed differential in gene transcription of the candidate genes would also hold true at the level of protein expression. For several of the candidate genes (Bmp4, Fst, WIF1, Nrnx1, Phlda2, c-Myc, Flrt3, Sp8) a thorough expression profile was done with RT-PCR analysis for several E16.5 tissues and organs taken from adult animals. Candidate genes for which the full sequence was not yet known, molecular methods were applied to identify the entire leading frame. To test the role of Wnt inhibitor factor 1 (WIF1) in thymus development, recombinant WIF1 protein was used in fetal thymic organ cultures (FTOC) and the development of their thymus was analysed in detail. Finally, for two of the candidate genes, Phlda2 and Sp8, knock-out mice made available for us were analysed for thymus development. The following section of this thesis will describe these results in detail.

## **3.2 Laser microscopy, RNA isolation and faithful amplification**

### **3.2.1 RNA isolation from embryonal sections prepared for LCM**

It is paramount that RNA isolated by LCM for microarray analysis is of the highest quality. Since nanograms of RNA could not be easily and directly measured at the onset of this PhD work, alternative approaches were taken to assess the RNA quality. To this end, two embryonal sagittal cryosections (10 $\mu$ m thick) from embryos at E16.5 were pooled and total RNA was extracted to be tested by gel electrophoresis. In contrast to previously published methods staining with Haematoxylin was replaced by Toluidine Blue so as to decrease the time for staining to only 10 seconds (s) and the following dehydration steps were shortened to 10s. These changes have been introduced to minimize the length of incubation during which the sections are in an aqueous phase, as this appears to degrade RNA integrity within minutes (Murakami et al., 2000). These preliminary experiments also tested whether the dehydration steps could also affect RNA integrity but the total RNA recovered from the sections revealed that dehydration did apparently not affect RNA quality (Fig.3.1A lane 1&2). The chosen methods were also safe for tissues taken at different developmental stages, e.g. E10.5 and E11.5 (Fig.3.1 A and B). Taken together, these results could reveal that intact RNA (Fig.3.11A) can be isolated from sections prepared for LCM.

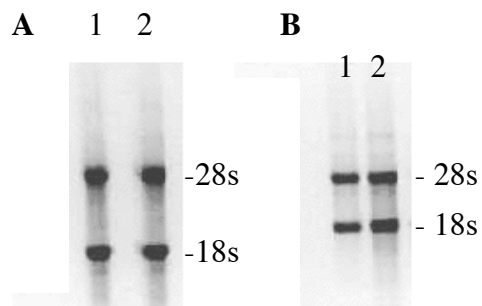


**Figure 3.1.** Intact RNA can be isolated from sections prepared for LCM. Total RNA isolated from sections (10 $\mu$ m) stained with Toluidine blue. Comparison of RNA isolated from dehydrated (lane1) and not dehydrated (lane2) tissue sections that had been isolated from embryos of E16.5 (left panel **A**) and E11.5 (right panel **B**).

### 3.2.2 FoxN1 expression in the third pharyngeal pouch

Using  $\beta$ -galactosidase as a knock-in into FoxN1 locus, expression of FoxN1 as detected by LacZ activity was established to occur at E11.25 while significant levels of *FoxN1* mRNA could only be detected by in situ hybridisation (ISH) as early as E11.5 (Gordon *et al.*, 2001; Manley *et al.*, 2004; Moore-Scott *et al.*, 2003; Moore-Scott and Manley, 2005). However, ISH is not a very sensitive method for the detection of gene transcription, therefore the presence of *FoxN1* in E10.5 embryos was evaluated using the more sensitive method of RT-PCR and tissue were taken from the 3<sup>rd</sup>pp. To determine whether the expression of *FoxN1* was restricted to the 3<sup>rd</sup>pp, cells microdissected by LCM from the endodermal lining of the 2<sup>nd</sup>pp and 4<sup>th</sup>pp from age-matched mice were also analysed. For these purposes, total RNA was extracted from approximately 1000 cells, reverse transcribed (see 2.2.6.2) and amplified using FoxN1 specific primers (see section 2.2.6.4). The results of this analysis (Fig.3.2) revealed that *FoxN1* specific mRNA could be detected as early as E10.5 and exclusively in the 3<sup>rd</sup>pp. Taken together, these experiments demonstrated that the methods employed allow for the detection of transcripts in a limited number of cells that have been isolated by LCM.



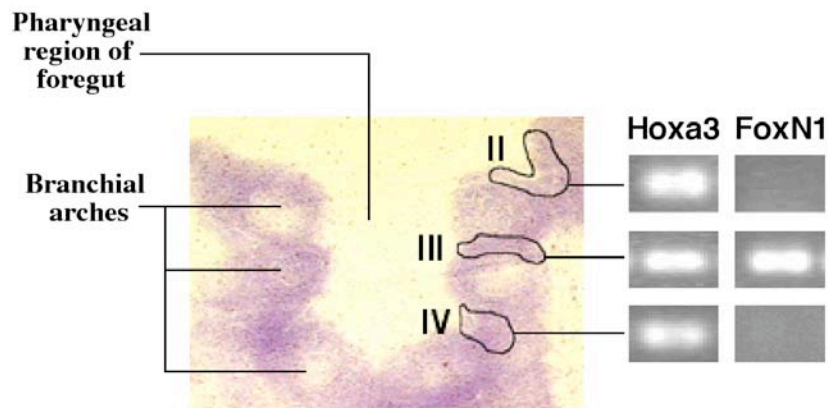


**Figure 3.2.** *FoxN1* is expressed as early as E10.5 in the 3<sup>rd</sup> pp. Part of this figure has previously been published in (Balciunaite *et al.*, 2002). II, III and IV indicate the 2<sup>nd</sup>, 3<sup>rd</sup> and 4<sup>th</sup> pharyngeal pouches, respectively. *Hoxa3* expression in the different pharyngeal pouches served as internal positive control for the RT-PCR analysis.

### 3.2.3 Amplification of RNA for microarray analysis

Presently, any analysis by microarrays requires substantial amounts of template (10 $\mu$ g cRNA) which cannot be recovered easily in the experimental systems we had chosen to study. Thus, a method had to be employed which allows for a representative amplification of small amounts of RNA as typically extracted from a few cells. A linear amplification protocol was therefore employed that consists of two cycles of cDNA synthesis each followed by in vitro transcription (Eberwine *et al.*, 1992). The first cycle concerns the initial amplification of the mRNA, resulting in unlabeled cRNA; while the second cycle achieves further amplification and incorporation of the biotinylated nucleotides needed for the labelling step for microarray hybridisation. To evaluate whether a modified amplification protocol (Baugh *et al.*, 2001), which has previously been shown to perform better than the original protocol established by Eberwine and colleagues (Eberwine *et al.*, 1992; Van Gelder *et al.*, 1990) provides a faithful amplification, this protocol from Baugh and al. was applied to two different sources but of comparable amount of total RNA (10ng). The first sample was extracted from an unseparated juvenile thymus (4-5 weeks old) while the second sample was taken by LCM from 1000 cells of the 3<sup>rd</sup>pp of E11.5 embryos. For each of the two samples, RT-PCR was then performed for *GAPDH*, *HPRT*, *CXCR4*, *Wnt4*, *FoxNI*, *Hoxa3*, *Pax1* and *Pax9* on 50ng of cRNA. With the exception of *CXCR4*, specific transcripts for each of these genes could be detected in these tissue samples. As an additional control to test the faithfulness of the method, 5000ng of non-amplified total RNA (isolated from an juvenile thymus of 4-5 weeks old) corresponding to the approximative equivalent of 50ng of cRNA. This molecular basis to this conversion considers the facts that (i) 5% of total RNA corresponds to mRNA, and (ii) the average size of the mRNA (approx. 2kb) has been shortened by about 5 times when converted into cRNA (approx. 400bp) due to a 3' end bias of the second round of linear amplification. Thus, similar levels of amplicon synthesis could be expected for the tested genes when comparing the different samples. However, this assumption only holds true under the following two conditions: (i) the reverse transcription reaction (RT) of the tested samples is of similar efficiency, and (ii) the PCR reaction has not yet reached the plateau level. In that regard, a semi quantitative RT-PCR analysis for the highest expressed gene *GAPDH* on a sample containing 5000ng of RNA extracted from an juvenile thymus revealed that after 26 cycles of PCR the plateau level of the reaction has not been reached yet. Therefore, it was decided to cycle 26 times in the PCR for all examined samples. Using the approach mentioned above, it was established that for some (*GAPDH*, *HPRT*, *CXCR4*, *Wnt4*, *FoxNI* and *Pax1*) but

not others (*Hoxa3*, *Pax9*) the amplification used was faithful with regards to the correct, i.e. linear amplification (Fig.3.3). In other words, the fidelity of linear amplification using the Baugh protocol was not uniformly given. Thus, we have decided us for an alternative protocol based on random PCR to amplify the RNA extracted by LCM. This protocol has been established by Roche diagnostics in the purpose to use it for microarray analysis and it was demonstrated in an evaluation study of Klur and al. with our contribution that it is more reproducible, requires smaller RNA input, and generates cRNA of higher quality than linear amplification (Klur *et al.*, 2004).

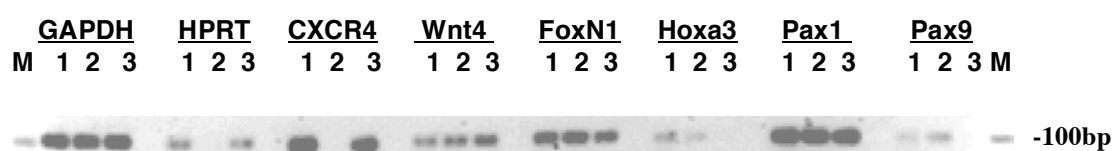


**Figure 3.3. Gene expression analysed by RT-PCR using non amplified and linear amplified RNA templates.** Lane 1: 5000ng of non amplified total RNA from adult thymus, lane 2: 50 ng of cRNA from E11.5 3<sup>rd</sup>pp isolated by LCM, lane 3: 50ng of cRNA isolated from Adult thymus. M: DNA marker, 100bp: 100 base pairs.

### 3.3 Identification of candidate genes for thymic epithelial cell fate commitment and function

#### 3.3.1 Differential expression analysis between the 2<sup>nd</sup> and 3<sup>rd</sup>pp

To identify genes that are involved in thymus development, a first microarray analysis was performed in which at E10.5 the gene expression profile of epithelial cells from the 2<sup>nd</sup> and 3<sup>rd</sup>pp was compared. Three independent samples were generated for this experiment, taken each from the 2<sup>nd</sup> and of the 3<sup>rd</sup>pp. The amplified cRNA was tested on the murine genome MGU74v2 genechip microarrays which allowed to monitor and quantify the expression of more than 36000 sequences taken from mouse genes and ESTs, respectively. The data obtained was then analysed using the Affymetrix microarray suite 5.0 software.

### 3.3.1.1 Comparing the expression of *FoxN1*, *Gcm2* and *Pax1* using either qPCR or microarrays

The qRT-PCR analysis for the expression of *FoxN1*, *Gcm2* and *Pax1* by qPCR was used to verify the data obtained by microarray analysis (Fig.3.5). It was generally observed that genes that are expressed at very low levels (and hence at as close to the limits of detection) will have their PM (perfect match) and MM (mismatch) values less reliably reflected (see 2.2.1.6). Consequently, an absent call (see 2.2.1.6 for explanation) does not necessarily indicate the real lack of expression but signifies that the examined gene might be not expressed highly enough to report a present call (see 2.2.1.6 for explanation). An instructive example to this point is the expression of *FoxN1*, which was scored absent when analysing microarrays (see Table 3.1, Fig.3.4 for PM/MM pattern) but which can reliably be detected by qRT-PCR in all samples generated for the microarray analysis (Fig.3.5). The intensity values obtained for *FoxN1* from the microarray data were found to be much higher in the 3<sup>rd</sup>pp when compared to the 2<sup>nd</sup>pp samples with a ratio of 4.19 (Table 3.1), a value that is generally indicative of differential gene expression. *Gcm2* was reported to be expressed at E9.5 in the 2<sup>nd</sup> and 3<sup>rd</sup>pp but its expression becomes restricted to the 3<sup>rd</sup>pp by E10.5 (Gordon *et al.*, 2001). Indeed analysis of cells taken at E10.5 from the 3<sup>rd</sup>pp confirmed the *Gcm2* expression (Fig.3.5). *Gcm2* expression was, however, also observed in one but not all samples in the 2<sup>nd</sup>pp (Fig.3.5). However, in the sample that detected some expression of *Gcm2*, the qRT-PCR data revealed an Ct value of above 36 and hence was close to the limit of detection. Furthermore, this data did indicate that *Gcm2* at E10.5 was expressed at least 5000 fold less ( $\Delta$ Ct of 12.3) in the 2<sup>nd</sup>pp when compared to the 3<sup>rd</sup>pp (Fig.3.5). *Gcm2* is represented on the U74Av2 microarray by two different probe sets. One probe set (ID 94709\_at) provides expression data that are in agreement with the qRT-PCR data presented in Table 3.1. In contrast the other probe set (ID 94710\_g\_at) failed to confirm the qRT-PCR data presented in Table 3.1 and Fig.3.5 in regard to the expression of *Gcm2* in the 2<sup>nd</sup>pp.

**Table 3.1**  
**Comparative analysis of *FoxN1*, *Gcm2* and *Pax1* expression using either qRT-PCR or microarrays**

Probe ID <sup>1</sup>	Gene name	Gene Symbol	2_1	2_2	3_1	3_2	Microarray Ratio <sup>4</sup>	QRT-PCR ratio <sup>5</sup>
92674_at	Forkhead box N1	FoxN1	A <sup>2</sup>	A	A	A	4.19	Ex.3 <sup>6</sup>
94709_at	Glial cells missing homolog 2	Gcm2	P <sup>3</sup>	A	P	P	3.89	5095.47
94710_g_at	Glial cells missing homolog 2	Gcm2	A	A	A	P	2,98	5095.47
96595_at	Paired box gene 1	Pax1	P	A	P	P	14.38	49.01

Explanations: (1) Probe ID refers to the Affymetrix reference number for a probe set specific for a given gene. (2) A= absent, (3) P=present. (4) Microarray ratio is calculated as average intensity 3<sup>rd</sup>pp/ average intensity 2<sup>nd</sup>pp and (5) qRT-PCR ratio is calculated as  $2^{(\text{average } \Delta\text{Ct } 2^{\text{nd}}\text{pp}) - (\text{average } \Delta\text{Ct } 3^{\text{rd}}\text{pp})}$  where the  $\Delta\text{Ct}$  is the difference in Ct values between the gene of interest and the housekeeping gene, *GAPDH*. Samples of the 2<sup>nd</sup>pp and 3<sup>rd</sup>pp are annotated as 2\_1, 2\_2, 3\_1 and 3\_2 respectively. (6) Ex.3 denotes *FoxN1* was exclusively found to be expressed in the 3<sup>rd</sup>pp when compared to the 2<sup>nd</sup>pp.

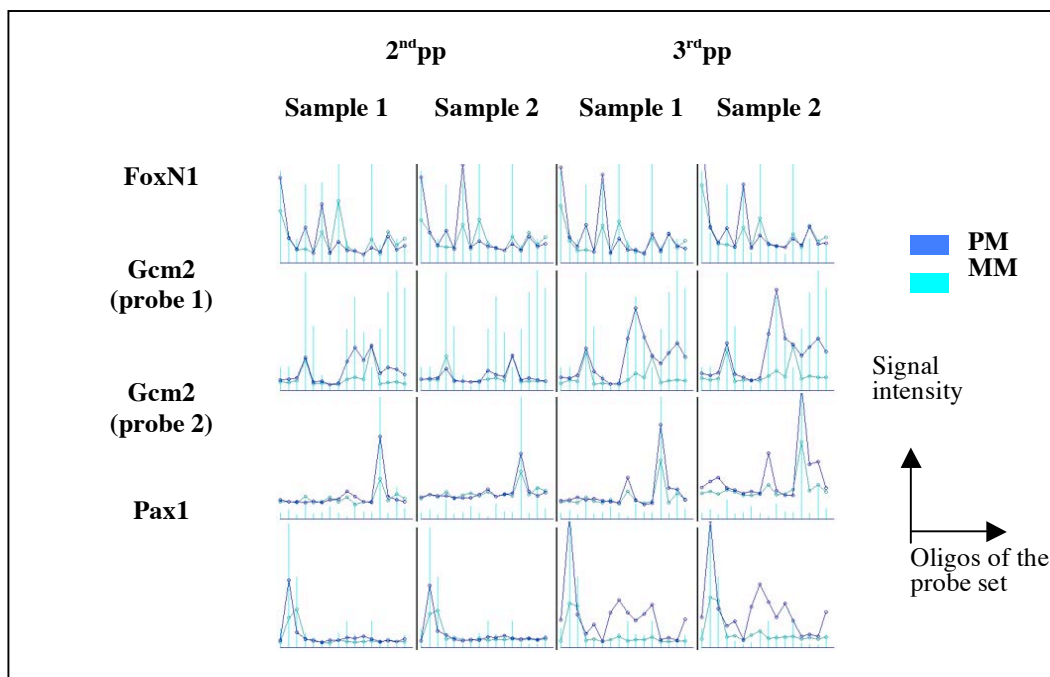


**Figure 3.4. Microarray analysis: Perfect match (PM) versus Mismatch (MM) pattern for *FoxN1*, *Gcm2* and *Pax1* expression in the 2<sup>nd</sup>pp and 3<sup>rd</sup>pp.** Probe 1 for *Gcm2* appears to hybridize better than its homolog Probe 2. The probe set of *FoxN1* appears to not hybridize optimally as the PM signal is not clearly above the MM signal in the 3<sup>rd</sup>pp for that gene. In contrast, *Pax1* and *Gcm2* PM signal are clearly above their MM signal in the 3<sup>rd</sup>pp.

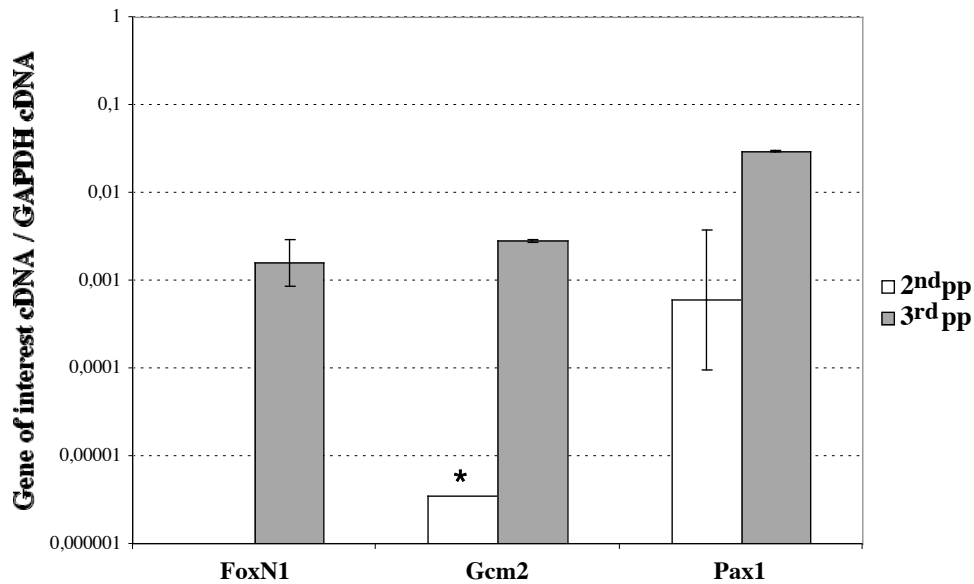


**Figure 3.5.** qRT-PCR analysis for the expression of *FoxN1*, *Gcm2* and *Pax1* from cDNA generated and amplified from tissue of the 2<sup>nd</sup>pp and 3<sup>rd</sup>pp, respectively. Data has been normalised to *GAPDH* expression. The ratio “gene of interest cDNA / *GAPDH* cDNA” corresponds to the calculated difference in signal intensity between the examined gene and *GAPDH*. The errors bars represent the difference in the calculated ratio between two samples generated independently.\* *Gcm2* was only found to be expressed in one of two samples of the 2<sup>nd</sup>pp.

Microarray analysis did also underestimate the fold difference in the level of expression when comparing different probe sets for the same gene (see Table 3.1). Taken together, the quality of the microarray data did depend on the hybridization efficiency of each individual probe set, as for *FoxN1*, *Gcm2* or *Pax1* (see Fig.3.4).

### 3.3.1.2 Comparison of differential gene expression

The semi-quantitative detection of gene expression (i.e. the P/M/A calls, see 2.2.1.6 for explanations) together with the intensity values of each of the gene represented on the MGU74v2 microarrays were compiled and differences in the intensities between the samples taken from the 2<sup>nd</sup> and of 3<sup>rd</sup>pp were calculated. To evaluate how many genes of the MGU74v2 set are predicted to be preferentially if not exclusively expressed in the 3<sup>rd</sup>pp, the following criteria were considered: (i) the intensity ratio 3<sup>rd</sup>pp/2<sup>nd</sup>pp should be more than 2, and (ii) at least one of the 3<sup>rd</sup>pp samples should have a marginal (M) call. Using these criteria 2533 probe sets fulfilled both limitations. Of these 2533 probe sets, 1478 had a present call for both 3<sup>rd</sup>pp samples, whereas the results for 857 probe sets were discordant with regards to their A/M/P calls when comparing the

two analysed samples (Fig.3.6). The same criteria for selection were used to investigate genes that are expressed at a higher concentration in the 2<sup>nd</sup>pp when compared to the 3<sup>rd</sup>pp. This second analysis identified 1359 probe sets to be preferentially if not exclusively expressed in the 2<sup>nd</sup>pp. Of these 1359 probe sets, 509 had a present call in both of the 2<sup>nd</sup>pp samples tested (Fig.3.7). In summary, our analysis revealed that of the 3607 gene probe sets (2533+1359) to be differentially expressed between the 2<sup>nd</sup> and 3<sup>rd</sup>pp, 1987 (1478+509) fulfilled the set selection criteria that is a difference in gene expression of 2 and more fold if not of an exclusive expression in either the 2<sup>nd</sup> or the 3<sup>rd</sup>pp when considering these two pouches.

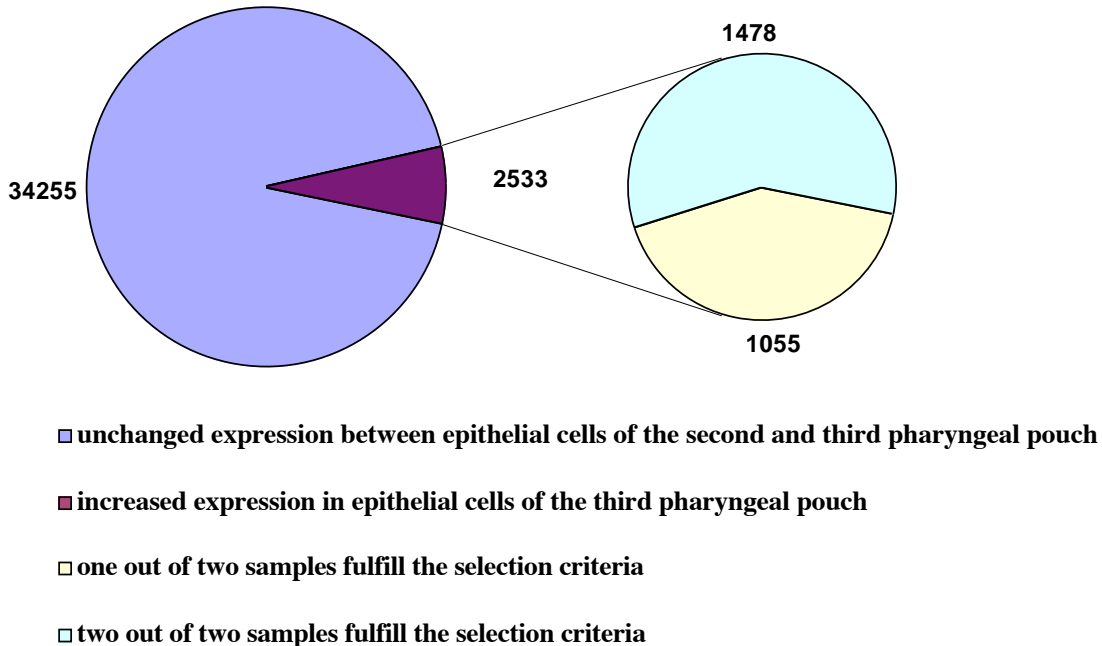


**Figure 3.6. Microarray based analysis of differential gene expression comparing epithelial cells of the 2<sup>nd</sup> and 3<sup>rd</sup> pharyngeal pouch.** The numbers represent the probe sets identified for each of the categories detailed.

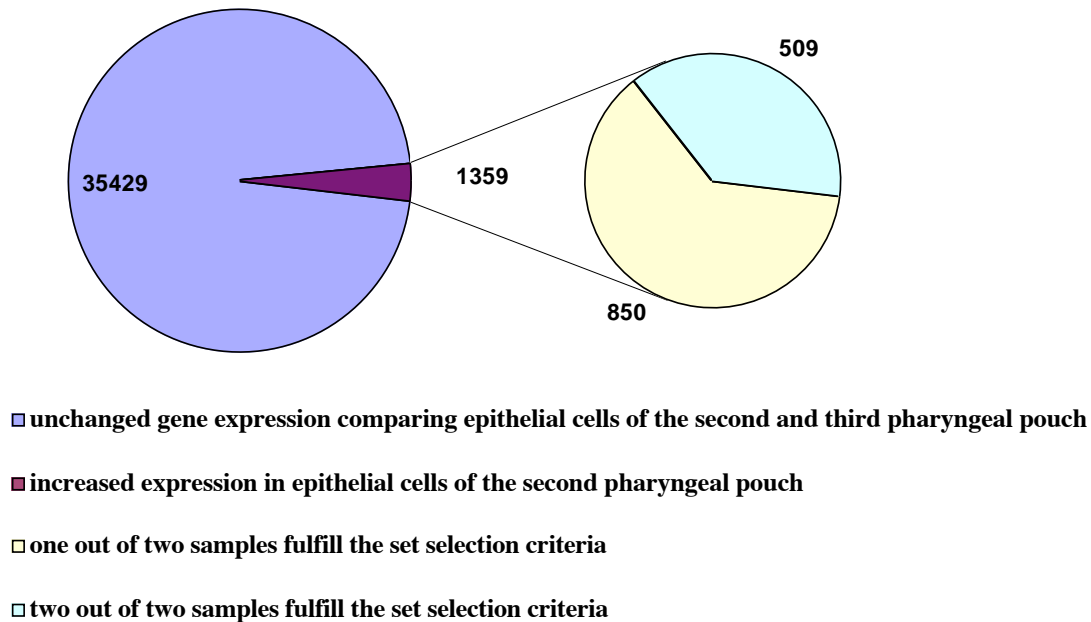
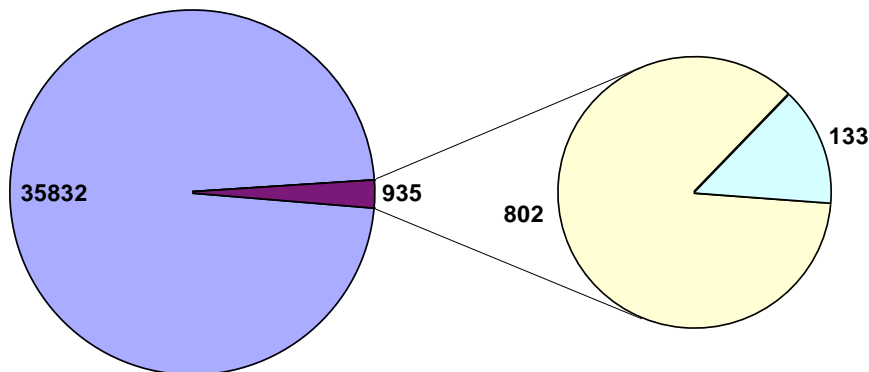


**Figure 3.7. Microarray based analysis of differential gene expression comparing epithelial cells of the 2<sup>nd</sup> and 3<sup>rd</sup> pharyngeal pouch.** The numbers represent the probe sets identified for each of the categories detailed.

### 3.3.1.3 Identification of genes that are upregulated in the third pharyngeal pouch

The next step in the analysis of differential gene expression between epithelia positioned in the 2<sup>nd</sup> and 3<sup>rd</sup>pp concerns the identification of these genes among the 2533 sequences demonstrated to be differently expressed between these two sites. To this end, an increased selection stringency was used in comparison to the previous microarray analysis so as to identify candidate genes that have a higher likelihood to be truly differentially expressed. For this second screen, the three following criteria were used for selection: (i) have at least a 6 fold difference in the expression level when comparing the 2<sup>nd</sup>pp with the 3<sup>rd</sup>pp, (ii) absent call in the microarray analysis for the 2<sup>nd</sup>pp, and (iii) a present call in both 3<sup>rd</sup>pp samples. As expected, this stringent re-analysis of the data resulted in a smaller pool of candidate genes, which now corresponded to 133 independent genes (Fig.3.8). Eight hundred and two genes fulfilled the first two criteria (i) and (ii) but did not score as present in both samples of the 3<sup>rd</sup>pp while only 21 genes met the first two criteria but did not score as present in both of the two 3<sup>rd</sup>pp samples (not shown).





- unchanged gene expression comparing epithelial cells of the second and third pharyngeal pouch
- increased expression in epithelial cells of the third pharyngeal pouch
- one out of two samples fulfill the set selection criteria
- two out of two samples fulfill the set selection criteria

**Figure 3.8. Microarray based analysis of differential gene expression comparing epithelial cells of the 2<sup>nd</sup> and 3<sup>rd</sup> pharyngeal pouch.** The numbers indicated represent the number of probe sets identified for each of the categories detailed.

From the 133 genes identified in the second screening, 19 candidates were chosen based on their function in transcriptional regulation. Their differential gene expression was then independently verified by qRT-PCR. Results of the comparison between the microarray and qRT-PCR are summarized in Table 3.2. In addition to these 19 genes, an additional 7 candidate sequences (*Map3k3*, *Pxk*, *Clock*, *Meox1* and 3 *ESTs*) were also further analysed by qRT-PCR. These sequences did not fulfil the three selection criteria but displayed a significant increase (more than three fold) in their expression in the 3<sup>rd</sup>pp when compared to the 2<sup>nd</sup>pp (Table 3.3).

**Table 3.2****Comparison of gene expression analysed by the microarray and qRT-PCR for 19 selected genes (see text).**

Probe ID <sup>1</sup>	Gene name	Gene Symbol	Gene function	2_1	2_2	3_1	3_2	Microarray Ratio (4)	qRT-PCR ratio (5)
115106_at	EST	EST	Unknown	A <sup>2</sup>	A	P <sup>3</sup>	P	74.75	8.49
103012_at	chemokine (C-C motif) ligand 21c	CCL21	Chemotaxis	A	A	P	P	62.90	1458.23
168542_f_at	EST	EST <sup>2</sup>	Unknown	A	A	P	P	42.37	59.30
92210_at	angiopoietin 2	Angpt2	Antagonist of Angpt1 signalling in vasculogenesis	A	A	P	P	40.28	5461.19
92727_at	amyloid beta (A4) precursor protein-binding A2	Apba2	Binds to amyloid protein precursor	A	A	P	P	32.05	31.23
114280_at	yippee-like 1 (Drosophila)	Ypel1	Induces an epithelial-like morphology in fibroblasts	A	A	P	P	28.88	2.23
99441_at	gephyrin	Gphn	Plays a role in signal transduction	A	A	P	P	26.88	2957.17
98059_s_at	lamin A	Lmna	Involved in nuclear mechanics	A	A	P	P	24.13	83.29
163492_at	EST	EST	Unknown	A	A	P	P	23.68	1.86
110833_at	protein kinase, AMP-activated, gamma 2 non-catalytic subunit	Prkg2	Responsible for Wolf-Parkinson-White syndrome	A	A	P	P	20.29	1.34
165740_at	Double sex and mab-3 related transcription factor 2	Dmrt2	Transcription factor	A	A	P	P	19.20	12944.04
99937_at	Mesenchyme homeobox 2	Meox2	Transcription factor	A	A	P	P	18.17	Ex.3 <sup>3</sup>
165776_i_at	Kruppel-like factor 16	Klf16 <sup>2</sup>	Transcription factor	A	A	P	P	15.96	Ex.3
98890_at	EST	EST	Unknown	A	A	P	P	13.36	25.37
109380_at	Spfh1 domain, family, member 1	Spfh1	Unknown	A	A	P	P	12.22	1.21
96841_at	proviral integration site 3	Pim3	Serine/Threonine kinase	A	A	P	P	10.61	3.45
100899_s_at	zinc finger protein 297	Zfp297	Transcription factor	A	A	P	P	8.09	3.41
138087_at	fibroblast growth factor 12	Fgf12	Growth factor	A	A	P	P	7.41	Ex.3
93635_at	kinesin family 3C	Kif3c	Unknown	A	A	P	P	6.62	24.34

Explanations: (1) Probe ID refers to the Affymetrix reference number for a probe set specific for a given gene. (2) A= absent, (3) P=present. (4) Microarray ratio is calculated as average intensity 3<sup>rd</sup>pp/ average intensity 2<sup>nd</sup>pp and (5) qRT-PCR ratio is calculated as  $2^{(\text{average } \Delta\text{Ct } 2^{\text{nd}}\text{pp}) - (\text{average } \Delta\text{Ct } 3^{\text{rd}}\text{pp})}$  where the  $\Delta\text{Ct}$  is the difference in Ct values between the gene of interest and the housekeeping gene, *GAPDH*. Samples of the 2<sup>nd</sup>pp and 3<sup>rd</sup>pp are annotated as 2\_1, 2\_2, 3\_1 and 3\_2 respectively. (6) Ex.3 denotes the gene was exclusively found to be expressed in the 3<sup>rd</sup>pp when compared to the 2<sup>nd</sup>pp.

**Table 3.3**  
**Comparison of gene expression as analyzed by microarray and qRT-PCR for 7 additional genes (see text).**

Probe ID <sup>1</sup>	Gene name	Gene Symbol	Gene function	2_1	2_2	3_1	3_2	Microarray Ratio (4)	qRT-PCR ratio (5)
94947_g_at	mitogen activated protein kinase kinase kinase 3	Map3k3	Regulates SAPK and ERK pathways	A <sup>2</sup>	A	A	P <sup>3</sup>	10.19	0.46
103405_at	EST	EST	Unknown	A	A	P	A	9.90	57.68
160815_at	EST	EST	Unknown	A	A	A	A	7.51	2.87
97325_at	PX domain containing serine/threonine kinase	Pxx	Phosphorylation in intracellular signalling	A	A	M	M	6.95	62.47
97355_at	EST	EST	Unknown	A	A	M	A	6.24	2.36
92257_at	Circadian locomoter output cycles kaput	Clock	Transcription factor	A	A	P	P	5.04	0,57
98419_at	mesenchyme homeobox 1	Meox1	Transcription factor	A	P	P	P	3.99	9541.50

Explanations: (1) Probe ID refers to the Affymetrix reference number for a probe set specific for a given gene. (2) A= absent, (3) P=present. (4) Microarray ratio is calculated as average intensity 3<sup>rd</sup>pp/ average intensity 2<sup>nd</sup>pp and (5) qRT-PCR ratio is calculated as  $2^{(\text{average } \Delta\text{Ct } 2^{\text{nd}}\text{pp}) - (\text{average } \Delta\text{Ct } 3^{\text{rd}}\text{pp})}$  where the  $\Delta\text{Ct}$  is the difference in Ct values between the gene of interest and the housekeeping gene, *GAPDH*. Samples of the 2<sup>nd</sup>pp and 3<sup>rd</sup>pp are annotated as 2\_1, 2\_2, 3\_1 and 3\_2 respectively. (6) Ex.3 denotes the gene was exclusively found to be expressed in the 3<sup>rd</sup>pp when compared to the 2<sup>nd</sup>pp.

Conformational analysis for the 26 genes examined by qRT-PCR using the cDNA previously employed for the microarray analysis revealed that 12 candidate genes (48%) remained differently expressed when comparing epithelia form the 3<sup>rd</sup>pp with cells taken from the 2<sup>nd</sup>pp. Among these 12 genes, three, *Fgf10*, *Meox2* and *Klf16*, were present exclusively in the 3<sup>rd</sup>pp and 9 genes, *CCL21*, *Angpt2*, *Gphn*, *Dmrt2*, *Zfp297*, *Meox1* and 3*ESTs* were observed with a preferential expression in the 3<sup>rd</sup>pp (Fig.3.9).

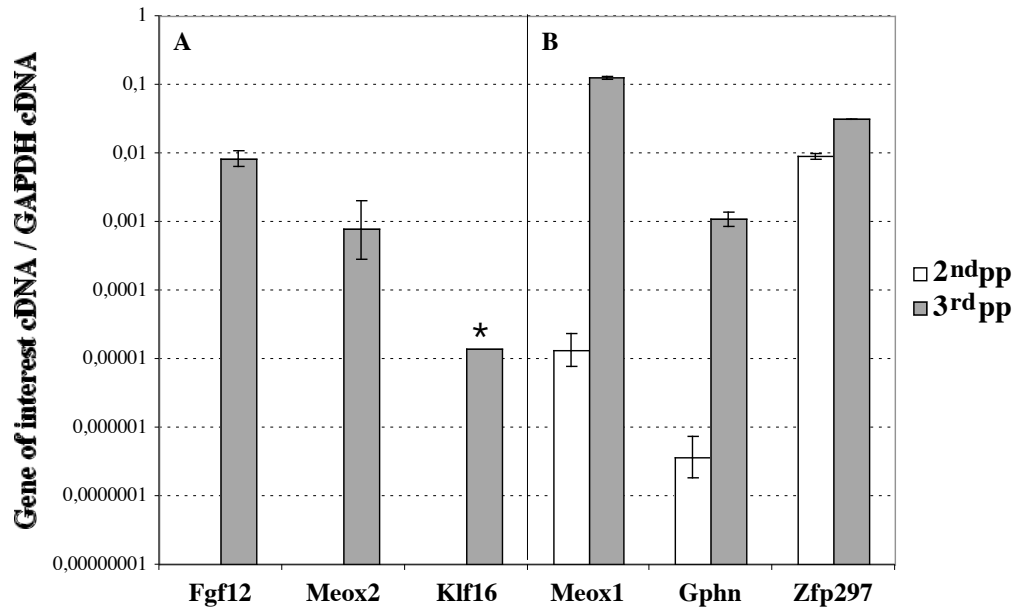
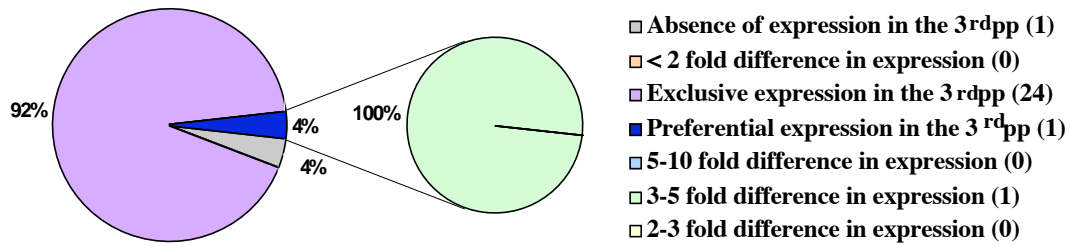


**Figure 3.9. qRT-PCR data for 6 genes found either exclusively (panel A) or preferentially (panel B) expressed in the 3<sup>rd</sup>pp.** Data has been normalised to *GAPDH* expression. The ratio “gene of interest cDNA / *GAPDH* cDNA” corresponds to the calculated difference in signal intensity between the examined gene and *GAPDH*. The errors bars represent the difference in the calculated ratio between two samples generated independently.\* *Klf16* was only found to be expressed in one of two samples of the 2<sup>nd</sup>pp.

Interestingly, when comparing the microarray with that of the qPCR data for the 26 genes target genes identified by microarray, only 3 out of the 24 genes classified by microarray analysis as being exclusively expressed in the 3<sup>rd</sup>pp epithelium could be confirmed by qPCR as such while 11 of those genes were noted to be preferentially expressed in the 3<sup>rd</sup>pp. Hence, qRT-PCR analysis appeared to be more sensitive when compared to the microarray analysis (Fig.3.10). This is not a surprise as a qRT-PCR reaction produces for a given gene much more copies of a target sequence than can be found in any sample loaded onto the microarrays for hybridization. As a consequence, the resulting signal intensity for a given gene, in particular for low-expresser, is much more likely to be detected by qRT-PCR than by microarrays.

### A Microarray



### B qRT-PCR

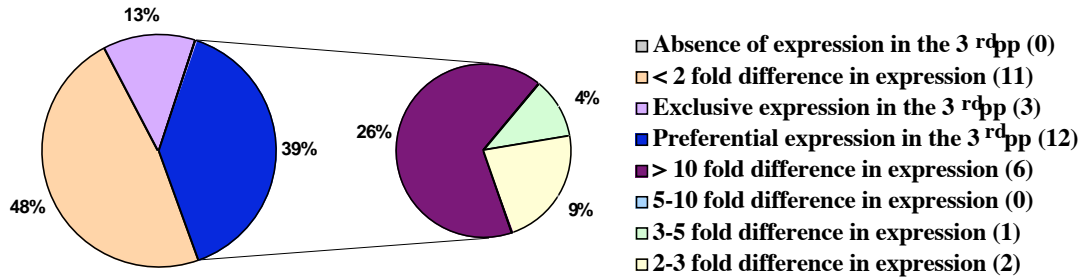


**Figure 3.10. Comparative analysis between microarray (A) and qPCR (B) for the 26 candidate genes, identified by microarray analysis to be upregulated if not exclusively expressed in the epithelium of the 3<sup>rd</sup>pp when compared to the 2<sup>nd</sup>pp. The number of genes in each category is represented in brackets.**

#### 3.3.1.4 Independent confirmation of candidate genes

To verify that *Fgf12*, *Klf16*, *Meox1&2*, *CCL21*, *Angpt2*, *Dmrt2* and *Gphn* are differentially expressed between 3<sup>rd</sup>pp and 2<sup>nd</sup>pp, epithelium was anew isolated from either the 2<sup>nd</sup>pp and the 3<sup>rd</sup>pp of E10.5 by use of LCM. An analysis by qRT-PCR confirmed that *FoxN1*, *Gcm2*, *Meox2* and *Klf16* are exclusively expressed and *Fgf12*, *CCL21*, *Angpt2*, *Dmrt2* are preferentially expressed in the epithelium lining the 3<sup>rd</sup>pp (Table 3.4 & Fig.3.11). However, *Meox1* and *Gphn* could not be verified by qRT-PCR analysis (Table 3.4 & Fig.3.11) to be differentially expressed. In summary, this independent qRT-PCR analysis verifies the differential expression on independent cDNA source 6 candidate genes initially picked up by the gene array analysis.

**Table 3.4**  
**Independent confirmation of expression of candidate genes**

Probe ID <sup>1</sup>	Gene name	Gene Symbol	qRT-PCR ratio <sup>2</sup>
99937_at	Mesenchyme homeobox 2	Meox2	515,6
165776_i_at	Kruppel-like factor 16	Klf16	8,2
138087_at	Fibroblast growth factor 12	Fgf12	1172,1
103012_at	Chemokine (C-C motif) ligand 21c	CCL21	6,4
98419_at	Mesenchyme homeobox 1	Meox1	0,9
92210_at	Angiopoietin 2	Angpt2	3,8
165740_at	Double sex and mab-3 related transcription factor 2	Dmrt2	6,7
99441_at	Gephyrin	Gphn	1,2

Explanations: (1) Probe ID refers to the Affymetrix reference number for a probe set specific for a given gene. Gene expression was analysed by qRT-PCR in two samples generated independently, which are each derived from either the 2<sup>nd</sup> or the 3<sup>rd</sup> pp. (2) The qRT-PCR ratio is defined as the average fold difference in signal intensity comparing the samples taken from the 3<sup>rd</sup> pp and the 2<sup>nd</sup> pp.

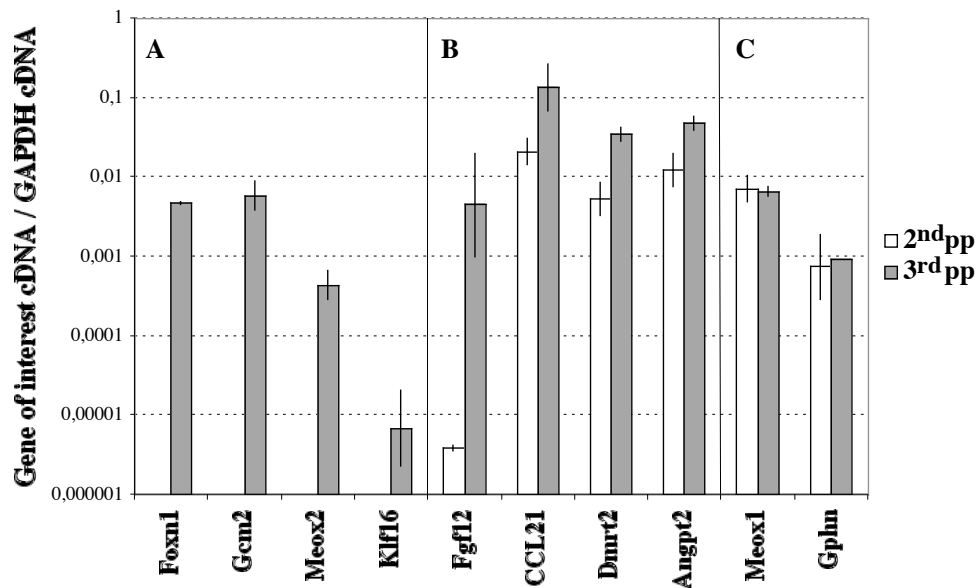


**Figure 3.11. Expression analysis by qPCR for 8 target genes identified by microarray to be differentially expressed comparing the 2<sup>nd</sup> pp and 3<sup>rd</sup> pp.** Exclusive (A), preferential (B) and unchanged (C) expression in the 3<sup>rd</sup> pp when compared to the 2<sup>nd</sup> pp. Data has been normalised to *GAPDH* expression. The ratio “gene of interest cDNA / *GAPDH* cDNA” corresponds to the calculated difference in signal intensity. The errors bars represent the difference in the calculated ratio between two samples independently generated.

### 3.3.1.5 Immunohistochemical analysis for CCL21 and Meox2 expression in the 3<sup>rd</sup> pharyngeal pouch

To verify the expression of CCL21 (Chemokine C-C motif ligand 21) and Meox2 (Mesenchyme homeobox 2) at the protein-level, immunohistochemistry (IHC) was carried out on tissues of E10.5 embryos. CCL21 is a chemokine that has been shown to be involved in the recruitment of T-cell precursors to the fetal thymus (Liu *et al.*, 2005). This findings have been demonstrated from CCL21-deficient *plt/plt* mice whose fetal thymus colonization was partially defective in these mice. Furthermore, fetal thymus colonization could be markedly diminished by neutralizing antibodies specific for CCL21 and CCL25 in FTOC experiments (Liu *et al.*, 2005). Hence, these findings indicate that CCL21 suggest that the combination of CCL21 and CCL25 plays a major role in fetal thymus colonization. The exclusive expression of the chemokine ligand CCL21 in the 3<sup>rd</sup>pp when compared to the other pouches was confirmed by IHC (Fig.3.12A). Moreover, this expression was confined to the anterior aspect of the 3<sup>rd</sup>pp (Fig.3.12A). At E11.5, the expression of CCL21 appeared to extend into the immediate mesenchymal surrounding but remained restricted to the anterior aspects of the 3<sup>rd</sup>pp (Fig.3.12B).

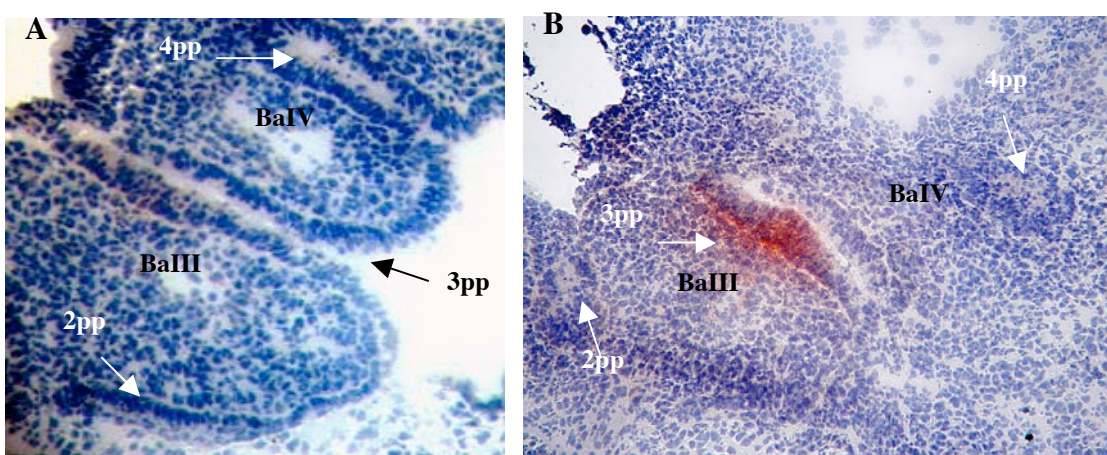


**Figure 3.12. Immunohistochemistry (IHC) for CCL21 on coronal sections of the pharyngeal region at E10.5 (A) and E11.5 (B).** BaIII and BaIV signify the third and fourth branchial arches. Anterior is at the bottom and Posterior is at the top of the images. The images have been taken with a magnification of 20x.

Meox2 is a transcription factor, which has revealed from knockout studies to have a crucial role in the differentiation and morphogenesis of the limb muscles (Mankoo *et al.*, 1999). Interestingly, Meox1 and Meox2, both revealed to be expressed in the 3<sup>rd</sup>pp (Fig.3.11), have demonstrated to function together and upstream of Pax genes in the development of somites (Mankoo *et al.*, 2003). However in contrast to CCL21, any role for Meox genes in the development of the thymus has been attributed so far. At E10.5, Meox2 could be weakly detected by IHC in the 1<sup>st</sup> and 2<sup>nd</sup>pp (Fig.3.13A&B). In contrast, Meox2 is strongly expressed in the ventral aspect of the 3<sup>rd</sup>pp and in the entire 4<sup>th</sup>pp. The expression of Meox2 in these sites was at E10.5 considerably stronger in the endodermal lining of the 3<sup>rd</sup>pp and 4<sup>th</sup>pp when compared to the surrounding mesenchyme. At E11.5, Meox2 expression was observed throughout the entire 3<sup>rd</sup>pp (Fig.3.13C&D).

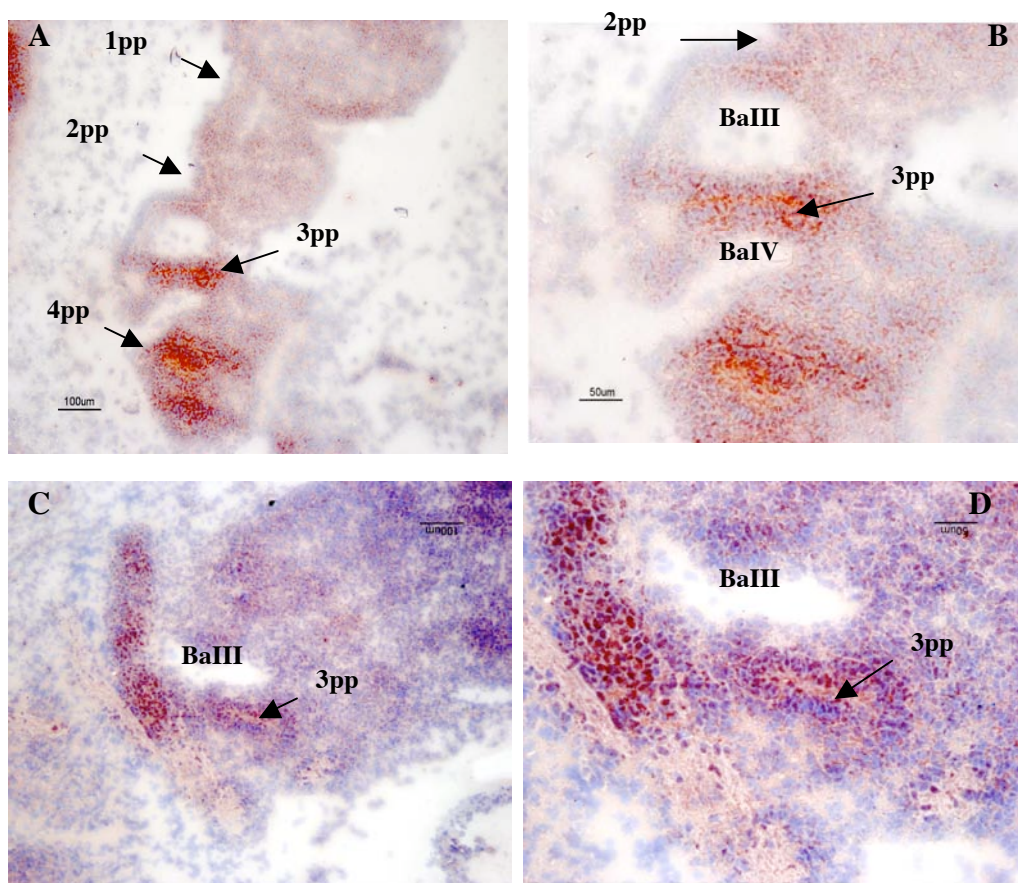


**Figure 3.13. Immunohistochemistry for Meox2 expression in sagittal sections of the pharyngeal region at E10.5 (A&B) and at E11.5 (C&D).** BaIII and BaIV denote the third and fourth branchial arches, respectively. Anterior is at the top and posterior is at the bottom of the image, ventral is positioned on the right and dorsal on the left. The images have been taken with a magnification of 10x (A&C) or 20x (B&D).



### 3.3.2 Differential expression analysis between the dorsal and ventral aspect of the 3<sup>rd</sup>pp

As outlined in the introduction, the ventral aspect of the 3<sup>rd</sup>pp gives rise to the thymic epithelium while the dorsal aspect constitutes the parathyroid anlage (Gordon *et al.*, 2001). Thus, comparing the gene expression in epithelial cells from the ventral with that of the dorsal circumference of the 3<sup>rd</sup>pp at E10.5, we sought to identify sequences that correlate with the commitment of endodermal cells to a thymic cell fate. For each of these restricted anatomical sites, two independent cDNA samples were generated by LCM (Fig.3.14). The material was then processed to generate cDNA, which was then faithfully amplified for the purpose of microarray analysis.

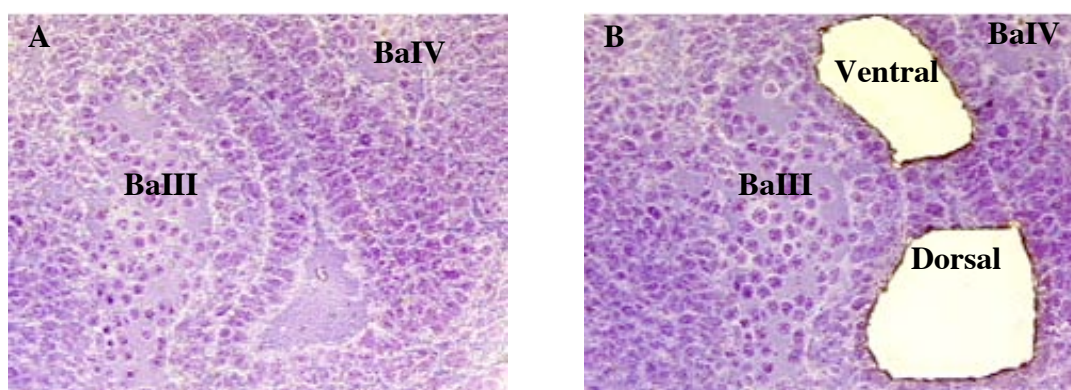


**Figure 3.14. Laser capture microdissection of the dorsal and ventral aspects of the 3<sup>rd</sup>pp at E10.5.** A The sagittal section of the pharyngeal region was stained with toluidine blue to reveal the third pharyngeal pouch. B The sagittal section of the pharyngeal region after the isolation of epithelial cells positioned at the dorsal and ventral poles of the 3<sup>rd</sup>pp. BaIII and BaIV indicate the third and fourth branchial arches, respectively.

#### 3.3.2.1 Comparing the expression of *FoxN1*, *Gcm2* and *Ehox* using either qRT-PCR or microarrays.

Since epithelial cells in separate parts of the 3<sup>rd</sup>pp give rise either to the thymus or the parathyroids, the expression of the tissue specific transcription factors *FoxN1* and *Gcm2* were used to monitor the origin of the tissue taken. The qRT-PCR analysis of the samples generated revealed that the expression of *FoxN1* was already restricted to the ventral aspect of the 3<sup>rd</sup>pp (Table 3.5 and Fig.3.15). In contrast, *Gcm2* was expressed in the dorsal aspects of the 3<sup>rd</sup>pp at a higher concentration but its transcripts could also be detected in limited amounts in the ventral aspect of the 3<sup>rd</sup>pp using qRT-PCR (Table 3.5 and Fig.3.17).

The gene expression microarray data for the samples of the ventral aspect of the 3<sup>rd</sup>pp suggested that *FoxN1* was absent in all of the examined samples (Table 3.5 & Fig.3.16). In fact, this result was in agreement with previous microarray analysis using cDNA from the entire 3<sup>rd</sup> pharyngeal pouch, as evidenced by Table 3.1 and Fig.3.4. On the other hand, one of two *Gcm2* probe sets revealed a preferential expression in the dorsal aspect of the 3<sup>rd</sup>pp when compared to its ventral counterpart as confirmed by qRT-PCR (Table 3.5, Fig.3.15 and Fig.3.16). In contrast, an other probe set reported very limited and strict expression of *Gcm2* in the dorsal circumference of the 3<sup>rd</sup>pp (Table5 & Fig.16). This discrepancy in the expression data for *Gcm2* is likely to be explained by differences in hybridization efficiencies between these probe sets (Fig.3.16) since verification by qRT-PCR clearly detailed the presence of *Gcm2* transcripts although preferentially in the dorsal circumference but in both aspects of the 3<sup>rd</sup>pp.

Moreover, an other transcription factor called *Ehox* (Embryonic homeobox) has been revealed by ISH analysis to become restricted by E10.5 in the pharyngeal region to the ventral end of the 2<sup>nd</sup> and 3<sup>rd</sup>pp (Jackson *et al.*, 2003). However, *Ehox* is not represented on the MGU74v2 microarray set. Therefore, to verify this finding and to further test whether the cDNA samples generated for the purpose of a comparative microarray analysis between the dorsal and ventral aspect of the 3<sup>rd</sup>pp are in agreement with published data, the expression of *Ehox* was examined by qRT-PCR in these samples. In contrast to the ISH finding, the qRT-PCR analysis revealed that *Ehox* was preferentially (9.09 fold) but not exclusively expressed in the ventral part when compared to its dorsal counterpart (Fig.3.15). This result could be confirmed on independently generated cDNA samples, although with a smaller difference in expression (7.07 fold) by an other member of the lab (Mr.K.Na, result not shown).

**Table 3.5****Comparative analysis of microarray and qPCR data for the expression of FoxN1 and Gcm2**

Probe ID <sup>1</sup>	Gene name	Gene Symbol	D_1	D_2	V_1	V_2	Microarray Ratio (3)	qRT-PCR ratio (4)
92674_at	Forkhead box N1	FoxN1	A <sup>2</sup>	A	A	A	3.35	Ex. V <sup>5</sup>
94709_at	Glial cells missing homolog 2	Gcm2	P <sup>2</sup>	P	P	P	0.36	0,1609
94710_g_at	Glial cells missing homolog 2	Gcm2	M <sup>2</sup>	A	A	A	0.42	0,1609

Explanations: (1) Probe ID refers to the Affymetrix reference number for a probe set specific for a given gene. (2) A; M and P denote absent, marginal and present calls, respectively. The ratio is defined as the average fold difference in signal intensity between two samples independently generated taken from the dorsal and the ventral epithelium of the 3<sup>rd</sup>pp, as measured by qRT-PCR (4) or microarray analysis (3). Samples 1 and 2 of the dorsal and ventral aspects of the 3<sup>rd</sup>pp are annotated as D\_1, D\_2, V\_1 and V\_2, respectively. (5) Ex.V denotes that the gene was exclusively found to be expressed by qRT-PCR in the ventral epithelium of the 3<sup>rd</sup>pp.

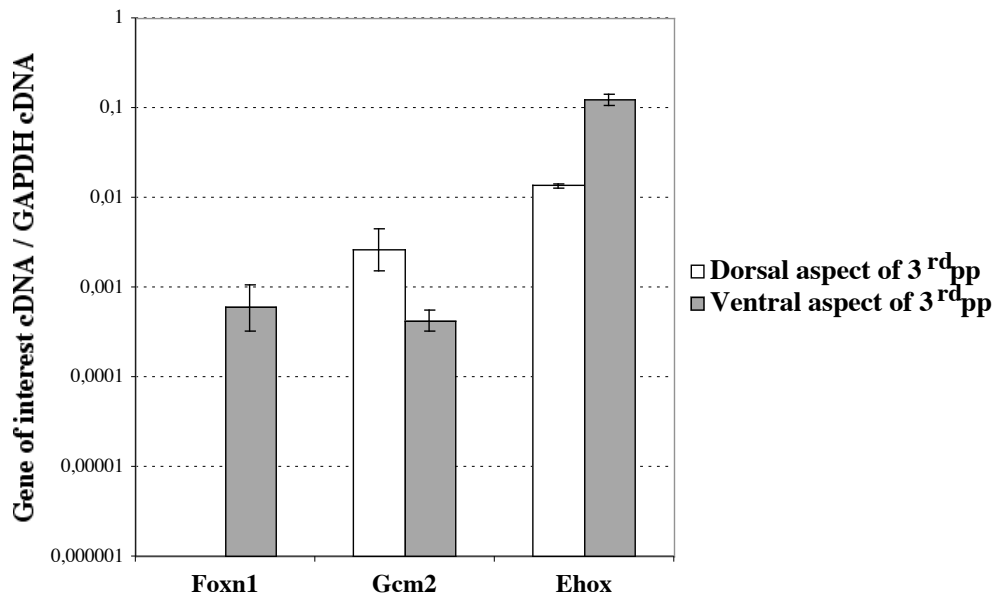


**Figure 3.15. Expression of FoxN1, Gcm2 and Ehox expression in the ventral and dorsal aspects of the 3<sup>rd</sup>pp as analysed by qRT-PCR.** qPCR was performed on amplified cDNA and the data are normalised to GAPDH expression. The ratio “gene of interest cDNA/ GAPDH cDNA” correspond to the calculated difference in signal intensity between the gene of interest and GAPDH. The errors bars represent the difference in the calculated ratio between two samples generated independently.

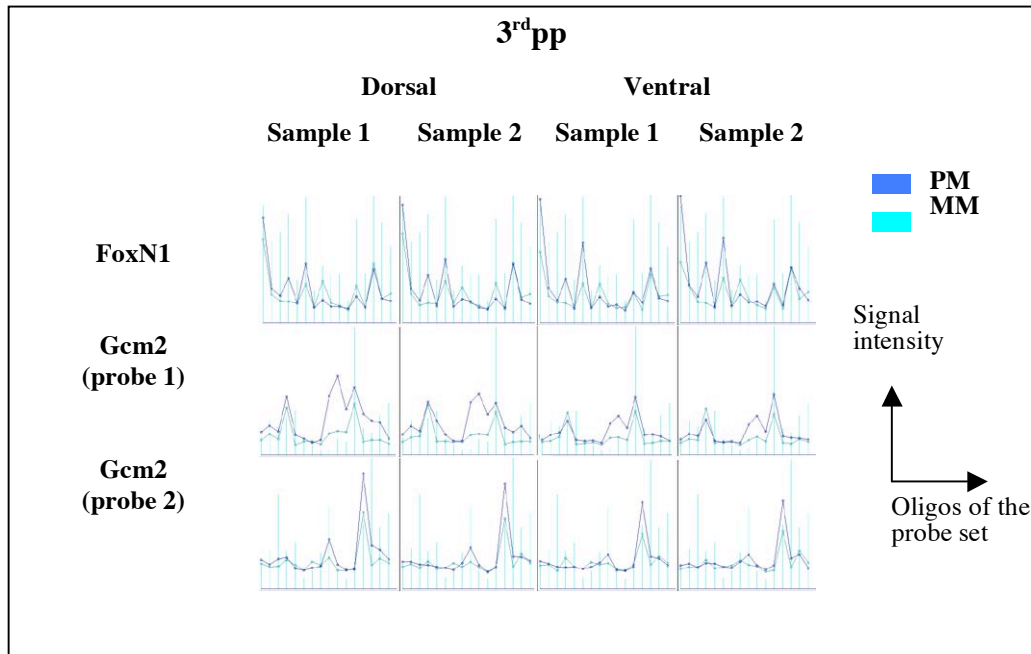
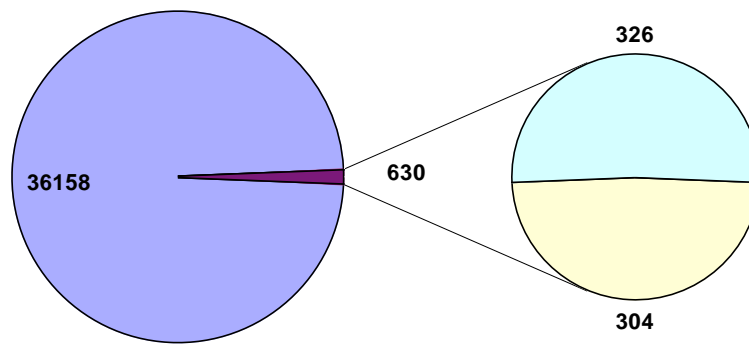


**Figure 3.16. Perfect match (PM) versus mismatch (MM) pattern for the expression of *FoxN1* and *Gcm2* in the dorsal and ventral aspect of the 3<sup>rd</sup>pp.** Probe set 1 for *Gcm2* clearly shows that the difference between PM and MM signal intensity in the dorsal aspect is higher than in its ventral counterpart while this difference in signal intensity is less obvious to notice for probe set 2 between the dorsal and the ventral aspect of the 3<sup>rd</sup>pp. Hence, probe set 1 for *Gcm2* hybridizes more efficiently in comparison to probe set 2. *FoxN1* probe set does not hybridize efficiently enough to notice a considerable difference between the PM and the MM signal in the ventral aspect of the 3<sup>rd</sup>pp and was therefore called absent by the microarray software. This finding results most likely from sensitivity issues since qRT-PCR analysis clearly detailed the presence of *FoxN1* transcripts in the ventral aspect of the 3<sup>rd</sup>pp.

### 3.3.2.2 Comparison of differential gene expression

Next, the number of genes that are represented by 36785 probe sets of the MGu74v2 microarrays was analysed that are preferentially or exclusively expressed in the ventral aspect of the 3<sup>rd</sup>pp. To this end, the following criteria were applied to filter the data: (i) the signal intensity ratio ventral vs. dorsal in the 3<sup>rd</sup>pp had to be more than 2, (ii) at least one of the ventral samples needed to give a present or a marginal call. Using these criteria, 630 of the 36788 probe sets scored positively (Fig.3.17). If these stringent criteria were chosen and that in addition both ventral 3<sup>rd</sup>pp samples had to be called present, than 326 probe sets were differentially expressed between the two circumferences with a higher concentration in the ventral aspect (Fig.3.17).



- unchanged expression comparing the ventral and dorsal aspects of the third pharyngeal pouch epithelium
- increased expression in epithelial cells of the ventral aspect of the third pharyngeal pouch
- one out of two samples fulfill the set selection criteria
- two out of two samples fulfill the set selection criteria

**Figure 3.17. Diagram detailing the number of genes preferentially or exclusively expressed in epithelium of the ventral aspect of the 3<sup>rd</sup>pp.** The numbers indicated reveal the number of probe sets fulfilling the different criteria (see text). Genes preferentially expressed in the ventral aspect of the 3<sup>rd</sup>pp will be distinguished in section 3.2.2.3 from genes exclusively expressed in this circumference.

The same selection criteria were also used to identify genes that are preferentially or exclusively expressed in the dorsal aspect of the 3<sup>rd</sup>pp (Fig.3.18). Here, 541 probe sets were more abundantly expressed in the dorsal aspect of the 3<sup>rd</sup>pp, with 223 of these detected in both samples under investigation. Taken together, 1171 probe sets (630 and 541) are differentially expressed between the ventral and dorsal aspect of the 3<sup>rd</sup>pp. In contrast, approximately three fold as many probe sets (3892 probe sets) were identified to be differentially expressed when comparing the gene expression profile between the second and the third pharyngeal pouch endoderm (see 3.3.1.2).

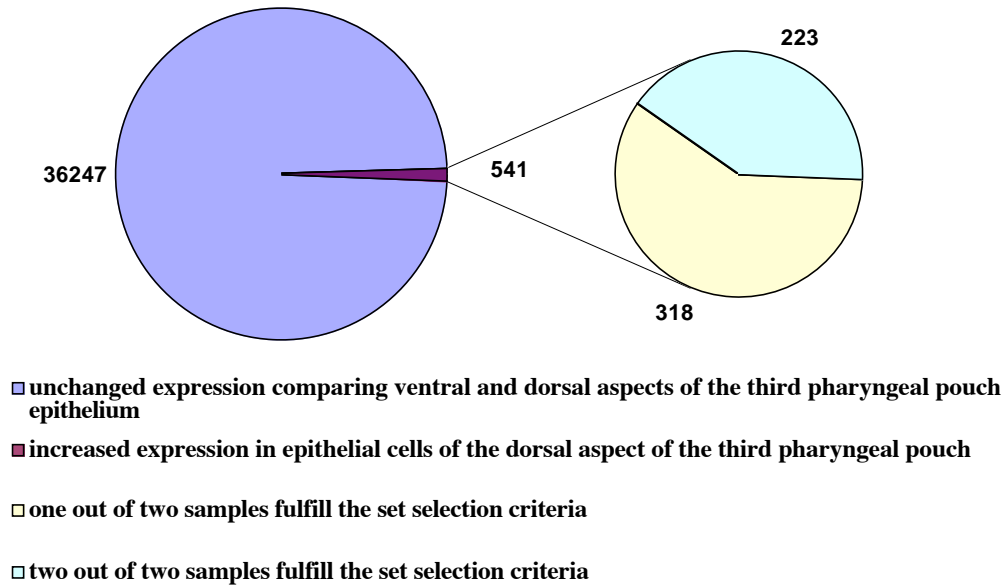


**Figure 3.18. Diagram detailing the number of genes preferentially or exclusively expressed in epithelium of the dorsal aspect of the 3<sup>rd</sup>pp.** The numbers indicated reveal the number of probe sets fulfilling the different criteria (see text).

### 3.3.2.3 Identification of genes specifically upregulated among ventral epithelial cells of the third pharyngeal pouch

The 630 probe sets (Fig.3.17) identified as being expressed in ventral epithelial cells of the 3<sup>rd</sup>pp were next subjected to an additional filter in that only probe sets were further considered that displayed an absence (A call) of expression in both samples of the dorsal epithelium. This third criterium thus excluded probe sets that were not exclusively expressed in the ventral aspects of the third pharyngeal pouch. Using this additional third criterium, 391 probe sets fulfilled now all three conditions and approximately a fifth of the probe sets concerned genes (85 genes) involved in transcription and were therefore verified by qRT-PCR (Fig.3.19A).

To allow the detection of genes, which may be marginally expressed in epithelial cells of the ventral part of the 3<sup>rd</sup>pp but were reported as absent (A call) in expression by the microarray analysis and hence did not fulfil the second criterium (see Table 3.6), I applied three additional criteria (iv), (v) and (vi) (see Table 3.6) to the samples that fulfilled the criteria (i) and (iii) stated

above and reminded in Table 3.6. Using this extended list of criteria, 468 probe sets were identified (Fig.3.19A). Thirty-three genes from this list were subsequently verified by qRT-PCR.

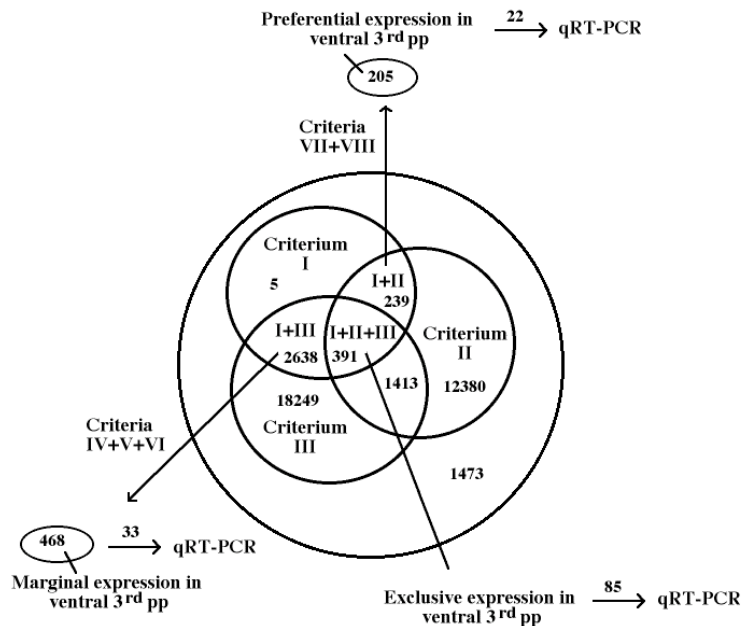
To identify additional target genes expressed preferentially but not exclusively in the ventral epithelium of the 3<sup>rd</sup>pp, two other criteria (vii) and (viii) (see Table 3.6) were applied to the list of probe sets that had a signal intensity ratio “ventral/dorsal 3<sup>rd</sup>pp” of more than 2 (criterion i). Using the criteria (i), (vii) and (viii), the analysis identified a list of 205 probe sets (Fig.3.19A). From this list, 22 genes possibly involved in transcription were selected and verified by qRT-PCR.

Finally, the microarray data set was also analysed by an additional software, dchip 1.3 (see Fig.3.19B). Using the default criterium (ix) of this software which relies on the model-based expression index (MBEI) for two or more independent samples (Li and Wong, 2001), 541 probe sets were identified to be expressed either preferentially or exclusively expressed in the ventral aspect of the 3<sup>rd</sup>pp (Fig19B). Among these probe sets, 7 genes were analysed by qRT-PCR. These genes are involved in transcriptional regulation and had not been identified using the Affymetrix microarray suite 5.0 software with the criteria (i) to (vi) or, alternatively, (vii) and (viii).

**Table 3.6**  
**Criteria used as filters for the analysis of the microarray data.**

(i)	signal intensity ratio ventral/dorsal 3 <sup>rd</sup> pp more than 2
(ii)	at least one of the samples of the ventral aspect of the 3 <sup>rd</sup> pp display a M or P call
(iii)	A call for both samples of the dorsal aspect of the 3 <sup>rd</sup> pp
(iv)	A call for both samples of the ventral aspect of the 3 <sup>rd</sup> pp
(v)	signal intensity ratio ventral/dorsal 3 <sup>rd</sup> pp more than 3
(vi)	signal intensity of more than 5 for both samples of the ventral aspect of the 3 <sup>rd</sup> pp
(vii)	present call for both samples of the ventral aspect of the 3 <sup>rd</sup> pp
(viii)	at least one of the samples of the dorsal aspect of the 3 <sup>rd</sup> pp display a M or P call
(ix)	lowest value of the 90% confidence interval of the signal intensity ratio ventral/dorsal 3 <sup>rd</sup> pp more than 1.2

## A Affymetrix



## B dchip

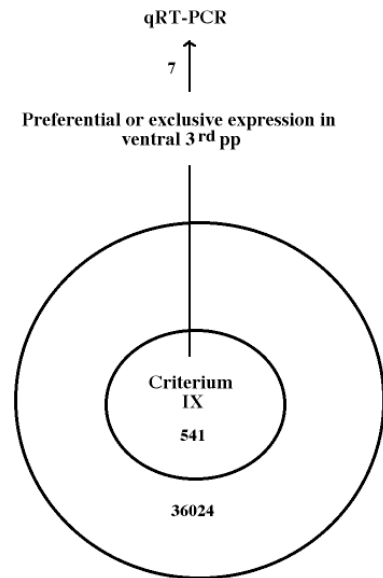
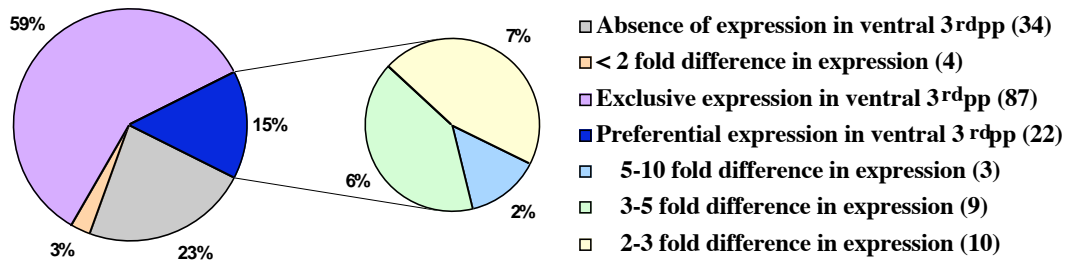


**Figure 3.19. Microarray based analysis of differential gene expression among epithelial cells of the ventral and dorsal aspects of the 3<sup>rd</sup>pp using either the Affymetrix 5.0 (A) or the dchip 1.3 (B) software.** The description of the different criteria which have been used to filter and to identify genes being either preferentially, exclusively or marginally expressed in the ventral circumference of the 3<sup>rd</sup>pp are described here above in Table 6. The numbers represented in each pool mention the numbers of probe sets identified when using the indicated criteria (combined or alone) whereas the numbers above the arrows represent the number of candidate genes taken subsequently for a verification by qRT-PCR. Indeed, many candidate genes (39 out of 140 genes) identified when using the Affymetrix software and the criteria I to VI or, alternatively, VII and VIII were also observed in the list of genes filtered with criterium IX of the dchip software. Nevertheless, 7 genes were only identified with the help of the criterium IX and were therefore added to the list of candidate genes retained for a verification by qRT-PCR of their differential expression.



### A Microarray



### B qRT-PCR

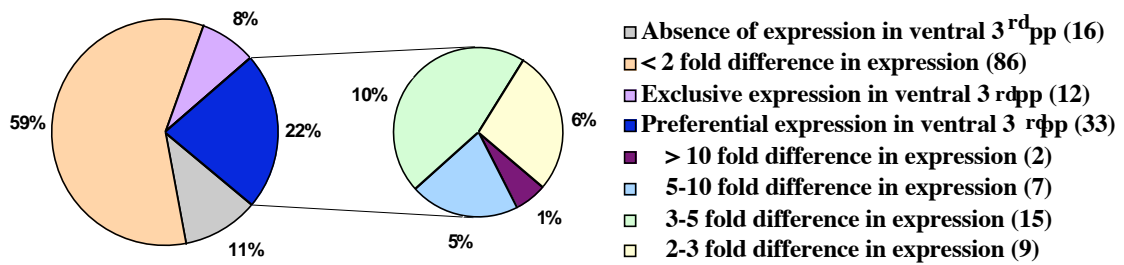


**Figure 3.20. Comparative between microarray (A) and the qRT-PCR (B) data analysing 147 candidate genes.** Exclusive expression denotes genes that were found to be only expressed in the ventral but not in the dorsal epithelium of the 3<sup>rd</sup>pp. Absence of expression denotes the lack of expression as analysed by either microarray or qPCR in one or both of the tested samples from the dorsal and ventral epithelium, respectively. The number of genes in each category is represented in brackets.

Taken together, 147 candidate genes (Annex 1) were identified by the different filters (see Table 3.6) applied to the microarray data set. Eighty-seven of these candidate genes were predicted by the microarray analysis to be exclusively expressed in the ventral aspect of the 3<sup>rd</sup>pp when compared to the dorsal circumference and 34 genes displayed an absence (A) of expression call in the dorsal and the ventral epithelium of the 3<sup>rd</sup>pp (see Fig.3.20A and Annex1). Twenty-two of the 147 candidate genes identified by the set of filters were predicted by the microarray analysis to have an increase in expression in the ventral epithelium when compared to its dorsal counterpart. This increase of expression corresponded for 3 (*Bmp4*, *Tmem16A* and an *EST*) of these 22 genes to an 5 to 10 fold and to an 3 to 5 fold for 9 others (*Galnt3*, *Flrt3*, *Asah2*, *Bambi*, *Six1*, *Gata3*, *c-Myc* and 2 two *ESTs*), see Fig.3.20A and Annex1 for details. The remaining ten genes (*Lef1*, *Khdrbs3*, *Sema6d*, *Capn6*, *Hs2st1*, *Sh3glb1*, *Pcp4* and three *ESTs*) of these list of 22 genes displayed an increase of 2 to 3 fold in their expression. Finally, 4 genes (*Tnfrsf19*, *Tbx3*, *Gpm6b* and *Meox2*), which were revealed by the differential analysis using the dchip1.3 software, had an increase lower than 2 when comparing ventral with dorsal epithelium(see Fig.3.20A and Annex1).

The expression of these 147 candidate genes was next verified by qRT-PCR. This analysis confirmed 45 candidate genes (30%) to be truly differentially expressed with 12 of these present only in the ventral aspect of the 3<sup>rd</sup>pp (Fig.3.20B and Fig.3.21A). Two genes (*Lmcd1* and *Bmp4*) in this list were at least 10 fold more abundant in the ventral aspect of the 3<sup>rd</sup>pp (see Fig.3.20B and Fig.3.21B), while transcripts for 7 genes (*Fst*, *c-Myc*, *Tmem16A*, *Khdrbs3*, *Flrt3* and 2 *ESTs*) were expressed 5 to 10 fold more frequently in the ventral epithelium of the 3<sup>rd</sup>pp when compared to the dorsal aspects (see Fig.3.20B and Fig.3.21C). A 3 to 5 fold increase in the ventral epithelia was observed for 15 candidate genes (*Bambi*, *Tnfrsf19*, *Galnt3*, *Tec*, *Msx2*, *Hs2st1*, *Tmem37* and 5 *ESTs*) and an increase of 2 to 3 fold was noted for an other 9 candidate genes (*Magel2*, *Sh3glb1*, *Srpk2*, *Tbx3*, *Meox2*, *Slc19a1*, *Sytl4*, *Csnk1d* and an *EST*) as shown in Fig.3.20B and Fig.3.21D+E.

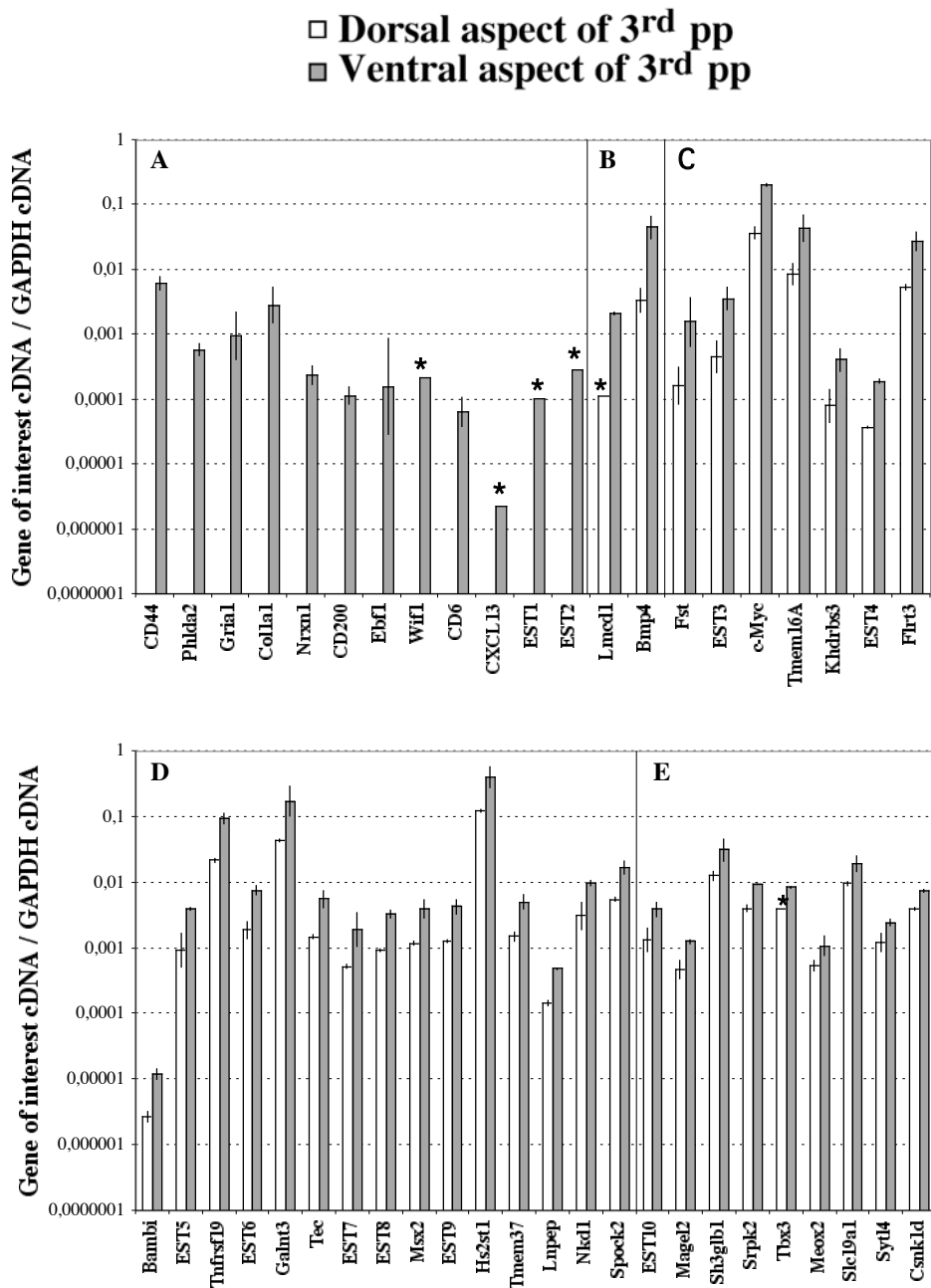


**Figure 3.21. qRT-PCR analysis for 45 candidate genes identified to be specifically upregulated in ventral epithelia of the 3<sup>rd</sup>pp.** A. Genes exclusively expressed in the ventral circumference. B-E Genes expressed preferentially in ventral epithelia with more than a 10 fold (B); with a 5-10 (C); with a 3-5 fold (D); and a 2-3 fold difference (E). Data are normalised to *GAPDH* expression. The ratio “gene of interest cDNA/ *GAPDH* cDNA” is the calculated difference in signal intensity between the gene of interest and *GAPDH*. The errors bars represent the difference in the calculated ratio between two samples generated independently. \* indicates that the examined gene was only found to be expressed in one of two samples of the ventral aspect of the 3<sup>rd</sup>pp or the dorsal circumference of the 3<sup>rd</sup>pp for *Lmcd1*.

Table 3.7 lists the 47 genes confined by qRT-PCR to be differentially expressed and provides details as to their function as well as to their microarray and qRT-PCR data. It was noticed that among 34 genes predicted by the microarray analysis to have an absence of specific expression in neither the ventral or the dorsal epithelia of the 3<sup>rd</sup>pp, 4 candidate genes (*Ebfl*, *CD6*, *CXCL13* and *EST1*) were only identified by qRT-PCR to be exclusively expressed in the ventral circumference of the 3<sup>rd</sup>pp. From the 87 candidate genes identified to be exclusively expressed in ventral epithelia by microarrays only 8 could be confirmed by qRT-PCR (Table 3.7). Nevertheless, 19 of those 87 candidate genes were revealed by qRT-PCR to have a preferential expression in the ventral circumference of the 3<sup>rd</sup>pp (Table 3.7). Taken together, qRT-PCR is more sensitive to identify differential gene expression among epithelia of the ventral vs. the dorsal aspect of the 3<sup>rd</sup>pp than microarrays.

**Table 3.7**

**Candidate genes differentially expressed in epithelia of the ventral aspect of the 3<sup>rd</sup>pp when compared to epithelia of the dorsal aspect of the 3<sup>rd</sup>pp as revealed by microarray and qRT-PCR analysis.**

Probe ID <sup>1</sup>	Gene name	Gene Symbol	Biological function	D1	D3	V1	V3	Microarray ratio (3)	qRT-PCR ratio (4)
109403_at	CD44 antigen	CD44	Cell adhesion	A <sup>2</sup>	A	P <sup>2</sup>	P	7,76	Ex.V <sup>5</sup>
104548_at	Pleckstrin homology-like domain, family A, member 2	Phlda2	Inhibitor of placental growth	A	A	P	A	2,09	Ex.V
92943_at	Glutamate receptor, ionotropic, AMPA1 (alpha 1)	Gria1	Glutamate transporter	A	A	P	M <sup>2</sup>	13,78	Ex.V
94305_at	Procollagen, type I, alpha 1	Col1a1	Cell adhesion	A	A	M	A	9,96	Ex.V
114766_at	Neurexin I	Nrxn1	Calcium regulator	A	A	P	P	2,37	Ex.V
101851_at	CD200 antigen	CD200	myeloid cell regulator	A	A	P	P	1,73	Ex.V
92535_at	Early B-cell factor 1	Ebfl	B-cell regulator	A	A	A	A	3,61	Ex.V
163423_at	Wnt inhibitory factor 1	Wif1	Wnt signalling inhibitor	A	A	M	A	3,65	Ex.V
92203_s_at	CD6 antigen	CD6	T cell activator	A	A	A	A	8,93	Ex.V
102025_at	Chemokine (C-X-C motif) ligand 13	CXCL13	Chemotaxis	A	A	A	A	2,50	Ex.V
137059_at	EST	EST1	Unknown	A	A	A	A	8,44	Ex.V
101154_at	EST	EST2	Unknown	A	A	P	P	2,92	Ex.V
117331_at	LIM and cysteine-rich domains 1	Lmcd1	Inhibitor of Gata6 activation	A	A	A	P	4,97	18,51
93455_s_at	Bone morphogenetic protein 4	Bmp4	Tgfb2 signalling	P	P	P	P	7,82	13,50
98817_at	Follistatin	Fst	Tgfb2 signalling inhibitor	A	A	P	P	10,40	9,71
130608_at	EST	EST3	Unknown	A	A	P	A	2,42	8,00
104712_at	Myelocytomatosis oncogene	c-Myc	Transcription factor	P	P	P	P	3,01	5,60
107112_at	Transmembrane protein 16A	Tmem16A	Unknown	A	P	P	P	5,18	5,21
164237_at	KH domain containing, RNA binding, signal transduction associated 3	Khdrbs3	Posttranscriptional regulation	A	A	M	M	2,21	5,13
104066_at	EST	EST4	Unknown	A	A	P	M	2,51	5,10
167905_f_at	Fibronectin leucine rich transmembrane protein 3	Flrt3	Modulator of Fgf-Mapk signalling	P	P	P	P	3,81	4,98
162531_at	Bmp and activin membrane-bound inhibitor, homolog ( <i>Xenopus laevis</i> )	Bambi	Inhibitor of Tgfb2 signalling	P	A	P	P	3,17	4,39
135615_at	EST	EST5	Unknown	A	A	P	P	4,60	4,32
160670_at	Tumor necrosis factor receptor superfamily, member 19	Tnfrsf19	Induces JNK pathway and NFkB signalling	A	P	P	P	1,95	4,32
134352_at	EST	EST6	Unknown	A	A	P	P	10,76	4,01
99011_at	UDP-N-acetyl-alpha-D-galactosamine:polypeptide N-	Galnt3	Involved in posttranslational	P	P	P	P	4,57	3,94

	acetylgalactosaminyltransferase 3		modification						
103539_at	Cytoplasmic tyrosine kinase, Dscr28C related (Drosophila)	Tec	Intracellular signalling	A	A	P	P	3,48	3,76
168351_at	EST	EST7	Unknown	A	A	P	P	2,34	3,68
116782_at	EST	EST8	Unknown	P	A	P	P	7,28	3,58
102956_at	Homeo box, msh-like 2	Msx2	Transcription factor	A	A	P	P	2,91	3,36
117279_at	EST	EST9	Unknown	A	A	P	P	4,95	3,32
102306_at	Heparan sulfate 2-O-sulfotransferase 1	Hs2st1	Sulfotransferase activity	P	P	P	P	2,60	3,31
95465_s_at	Transmembrane protein 37	Tmem37	Calcium transporter	A	A	P	P	4,74	3,27
133727_at	Leucyl/cystinyl aminopeptidase	Lnpep	Protein metabolism	A	A	P	P	4,31	3,27
110311_at	Naked cuticle 1 homolog (Drosophila)	Nkd1	Inhibitor of Wnt signalling	A	A	A	A	5,81	3,14
104375_at	Sparc/osteonectin, cwcv and kazal-like domains proteoglycan 2	Spock2	Extracellular matrix	A	A	P	P	3,19	3,10
136661_at	EST	EST10	Unknown	A	A	A	P	3,92	2,92
92681_at	Melanoma antigen, family L, 2	Magel2	Regulation of transcription	A	A	P	P	1,77	2,64
103569_at	SH3-domain GRB2-like B1 (endophilin)	Sh3glb1	Inducer of apoptosis	P	P	P	P	2,52	2,45
163582_at	Serine/arginine-rich protein specific kinase 2	Srpk2	Activator of apoptosis	A	A	P	P	2,11	2,33
103538_at	T-box 3	Tbx3	Transcription factor	M	A	P	P	1,73	2,08
99937_at	Mesenchyme homeobox 2	Meox2	Transcription factor	P	P	P	P	1,24	2,03
94419_at	Solute carrier family 19 (sodium/hydrogen exchanger), member 1	Slc19a1	Folate carrier	A	A	P	P	2,70	2,01
161026_s_at	Synaptotagmin-like 4	Sytl4	Inhibitor of exocytosis	A	A	P	P	2,22	1,99
97264_r_at	Casein kinase 1, delta	Csnk1d	Modulator of the mammalian clock	A	A	A	A	4,64	1,87

Explanations: (1) Probe ID refers to the Affymetrix reference number for a probe set specific for a given gene. (2) A; M and P denote absent, marginal and present calls, respectively. The ratio is defined as the average fold difference in signal intensity between two samples independently generated taken from the dorsal and the ventral epithelium of the 3<sup>rd</sup>pp, as measured by qRT-PCR (4) or microarray analysis (3). Samples 1 and 2 of the dorsal and ventral aspects of the 3<sup>rd</sup>pp are annotated as D\_1, D\_2, V\_1 and V\_2, respectively. (5) Ex.V denotes that the gene was exclusively found to be expressed by qRT-PCR in the ventral epithelium of the 3<sup>rd</sup>pp.

When re-screening the three different pools of genes differentially expressed i.e. marginal, preferential and exclusive expression in the ventral aspect of the 3<sup>rd</sup>pp (see Fig.3.19A), three genes involved in gene transcription, delta like 1 (*Dlk1*), transforming growth factor 2 and the forkhead protein G1 (*FoxG1*) and transforming growth factor beta 2 (*Tgfβ2*) were noticed. These 3 genes, which demonstrated a clear increase of expression in the ventral circumference of the 3<sup>rd</sup>pp (Fig.3.22) when compared to their dorsal counterpart, were indeed not in the list of the 47 candidate genes verified by qRT-PCR but their differential expression was confirmed in an independent microarray analysis of the ventral and the dorsal aspect of the 3<sup>rd</sup>pp.

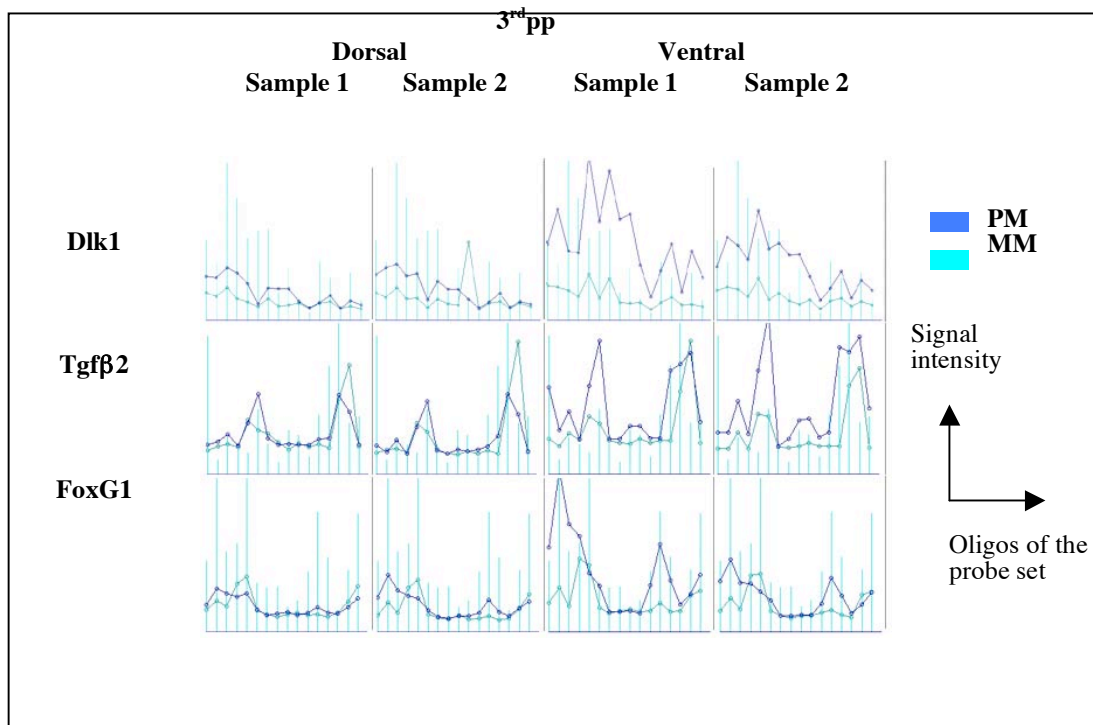


**Figure 3.22. Perfect match (PM) versus Mismatch (MM) pattern for Dlk1, Tgfβ2 and FoxG1 in the dorsal and ventral aspect of the 3<sup>rd</sup>pp.** These three genes reveal a considerable increase in the ventral aspect of the 3<sup>rd</sup>pp when compared to the dorsal counterpart.

Finally, the gene for trans-acting transcription factor 8 (*Sp8*) appears to be up regulated in the ventral aspects of the 3<sup>rd</sup>pp as confirmed by qRT-PCR (Fig.3.23). Since more than 8000 mRNA sequences (including *Sp8*) are not represented in the MGU74v2 microarrays in comparison to the newly generated set of microarrays, consideration of *Sp8* to play a possible role in early thymus development was based on the following data: (i) *Sp8* is upstream of *Fgf8* and downstream of *Fgf10* during the development of the limb (Kawakami *et al.*, 2004), and (ii) *Fgf8* and *Fgf10* are required for normal thymus development (Abu-Issa *et al.*, 2002; Frank *et al.*, 2002b; Revest *et al.*, 2001b). Analysis by qRT-PCR for the expression of *Sp8* but not *Fgf8* and *Fgf10* revealed respectively more abundant transcripts in the ventral aspect of the 3<sup>rd</sup>pp when compared to its dorsal counterpart (Fig.3.23).

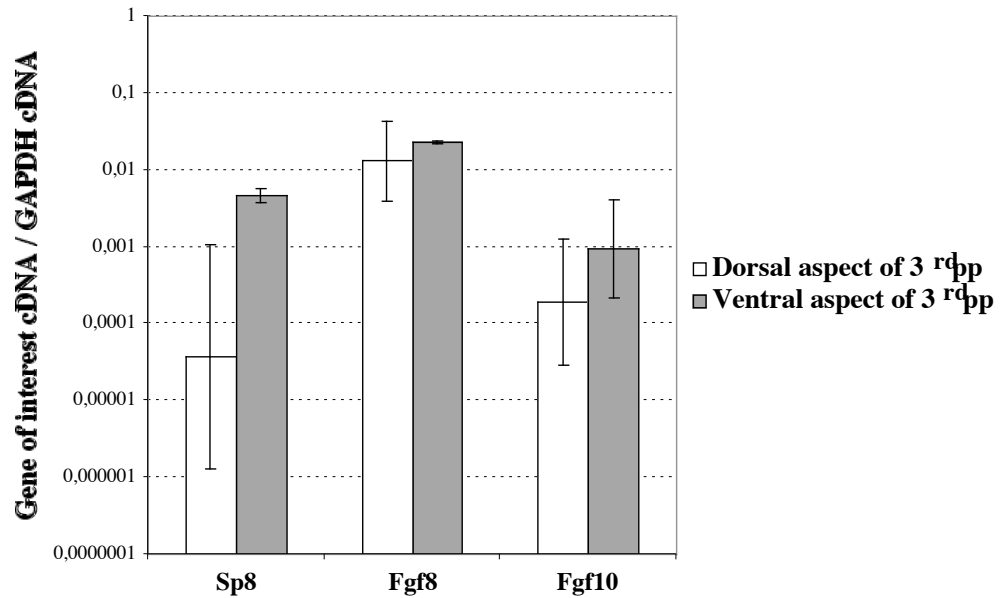


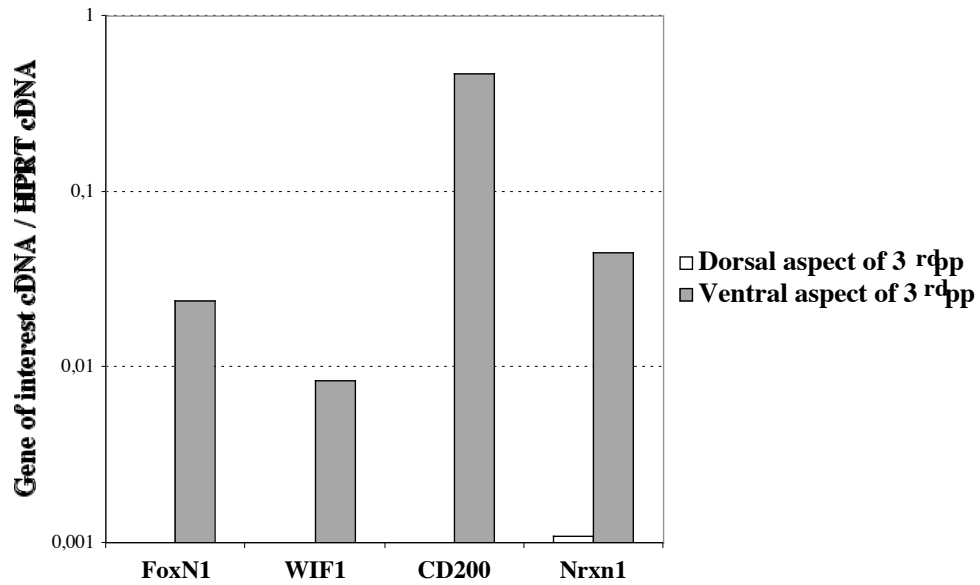
**Figure 3.23. Expression analysis by qRT-PCR for *Sp8*, *Fgf8* and *Fgf10* in the dorsal and ventral aspect of the 3<sup>rd</sup> pp.** Data are normalised to *GAPDH* expression. The ratio “gene of interest cDNA/ *GAPDH* cDNA” is the calculated difference in signal intensity between the gene of interest and *GAPDH*. The errors bars represent the difference in the calculated ratio between two independent samples generated independently.

#### 3.3.2.4 Independent verification by qRT-PCR of some candidate genes

Next, candidate genes were verified by qRT-PCR using samples taken from both the ventral and the dorsal aspects of the 3<sup>rd</sup>pp (newly generated). This analysis (Fig.3.24) confirmed the exclusive expression of *FoxN1*, *WIF1* (antagonist of Wnt signalling), *CD44* (Fig.3.24B) and *CD200* (delivers an inhibitory signal for the macrophage lineage) (Fig.3.24A) in the ventral aspect of the 3<sup>rd</sup>pp. In contrast to previous analysis (Fig.3.21), *Nrxn1* (Neurexin1, involved in cell-cell interaction) transcripts could also be detected in the dorsal aspect of the 3<sup>rd</sup>pp, albeit at very low concentrations (Fig.3.24A). This discrepancy was brought about by the low concentration of cDNA initially used as repeat experiments with a 15-fold higher concentration resulted in the marginal detection of *Nrxn1* transcripts (data not shown). Differential expression was also noticed for *Gcm2* (an internal control of the analysis), *Ehox* (embryonic homeobox gene), *Lmcd1* (Lim and cysteine-rich domains 1) and *Fst* (Follistatin, a regulator of Bmp signalling) and *c-Myc* (an oncogene). In contrast, neither *CD6* (involved in T-cell activation), *Grial* (Glutamate receptor) nor the two ESTs could be confirmed to be differentially expressed between the ventral and the dorsal aspects of the 3<sup>rd</sup>pp (data not shown). The absence of detection of these genes (*CD6*, *Grial* and the two *ESTs*) in the ventral aspect of the 3<sup>rd</sup>pp is most likely due to sensitivity issues since lower amounts of enriched or amplified cDNA was used for this qRT-PCR analysis than in the previous analysis. In fact, a gel electrophoresis analysis used systematically in the purpose to verify the quality of the enriched cDNA by random PCR revealed that after 21 cycles of PCR for samples of this qRT-PCR (Batch3), the amount of amplified cDNA was considerable lower in comparison to samples of previous analysis (Batch1 & 2) for an identical PCR cycling number (see 2.2.1.3 and Fig.2.1). In regard to *Bmp4* expression, this analysis in contrast to previous examinations (Fig.3.21) did not detect any *Bmp4* transcripts in the dorsal aspect of the 3<sup>rd</sup>pp (Fig.3.24B). This may also be due to the fact that less intake of cDNA has been used for this analysis than previously. Notably, this analysis revealed considerable much lower levels of expression for *CD44* and *Fst* (Fig.3.24B) than observed in previous analysis (Fig.3.21). Taken together, these data show that most of the differential expression between the ventral and the dorsal aspect of the 3<sup>rd</sup>pp of the candidate genes examined can be verified independently, although the fold difference in level of expression can differ or the absence of detection can be noticed if lower amounts of enriched cDNA is used as template for PCR.



A



B

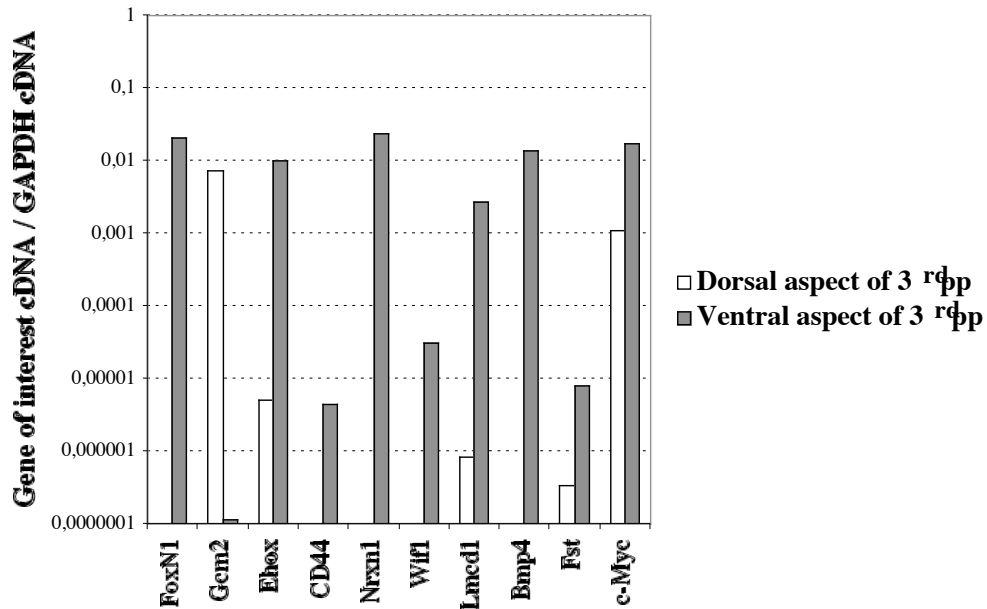


**Figure 3.24. Expression analysis of candidate genes by qRT-PCR for a verification of their differential expression between the dorsal and ventral aspects of the 3<sup>rd</sup>pp.** The cDNA used as template for the qPCR step has been previously enriched in particular for the genes examined by PCR using specific primers of these genes (A) or unspecifically by using random primers (decamers) (B), see material and method. Data are normalized to *HPRT* (A) and to *GAPDH* (B) expression. The ratio “gene of interest cDNA / *GAPDH* or *HPRT* cDNA” is the calculated difference in signal intensity. *HPRT* was used for the nested qPCR (A) instead of *GAPDH* because *HPRT* levels of expression are much lower than *GAPDH*. Hence for PCR cycling reasons the former one is more suited for the enrichment of the cDNA when using specific primers.

### 3.3.2.5 Expression of candidate genes in the 2<sup>nd</sup>, 3<sup>rd</sup> and 4<sup>th</sup>pp

Next, the expression of the candidate genes *CD44*, *WIF1*, *Phlda2*, *Nrxn1*, *Sp8*, *Bmp4*, *Fst*, *c-Myc* and *Flrt3* was examined for the 2<sup>nd</sup>, 3<sup>rd</sup> and 4<sup>th</sup>pp by qRT-PCR (see Fig.3.25). Of these candidates, only *WIF1* was exclusively detected in the 3<sup>rd</sup>pp while the others displayed variable expression levels also in 2<sup>nd</sup>pp and 4<sup>th</sup>pp. For example, *CD44* was more abundantly expressed in the 2<sup>nd</sup>pp when compared to the 3<sup>rd</sup>pp and could be detected in the 4<sup>th</sup>pp. The expression of *Bmp4*, an agonistic ligand for the *Tgfb2* signaling appears to progressively increase in its expression from the 2<sup>nd</sup>pp caudally to the 4<sup>th</sup>pp, whereas *Fst*, an inhibitor of *Tgfb2* signalling, displayed a gradient in this area, which was highest at the 2<sup>th</sup>pp. The concentration of *Sp8* and *Flrt3* specific transcripts were not much different in all 3 pharyngeal pouches examined.

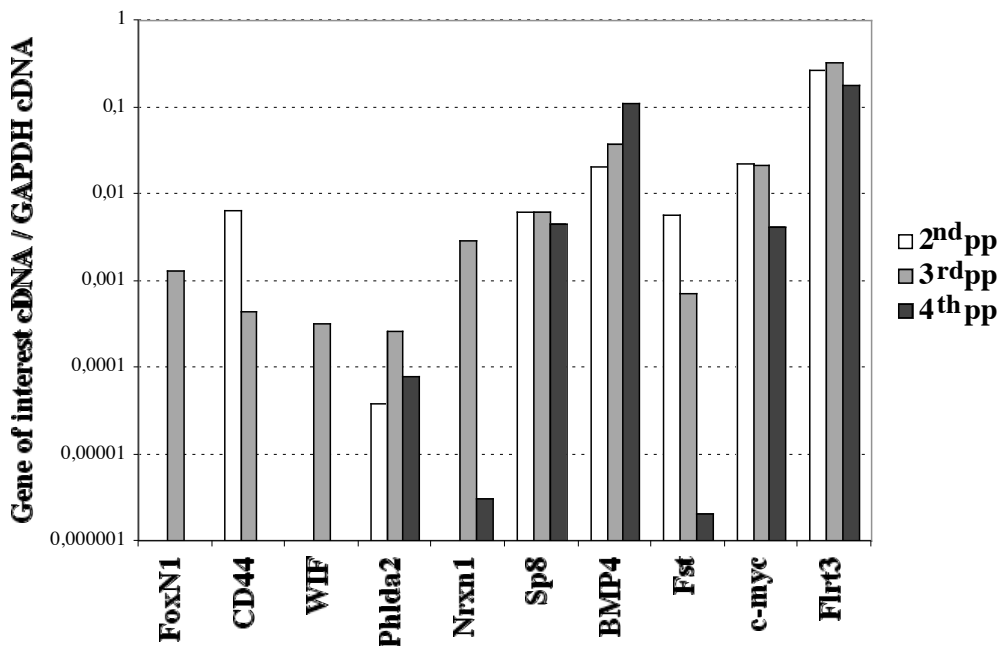


**Figure 3.25.** qRT-PCR analysis for the expression at E10.5 in the 2<sup>nd</sup>, 3<sup>rd</sup> and 4<sup>th</sup>pp for several candidate genes identified by microarray as being differentially expressed between the dorsal and ventral domains of the 3<sup>rd</sup>pp. Approximately 1000 cells were isolated by LCM from coronal sections for an RNA extraction of the 2<sup>nd</sup>, 3<sup>rd</sup> and 4<sup>th</sup>pp. Data have been normalized to *GAPDH*. The ratio “gene of interest cDNA / *GAPDH* cDNA is the calculated difference in signal intensity between the examined gene and *GAPDH*.

### **3.3.2.6 Verification by Immunohistochemistry (IHC) the upregulation of some confirmed candidate genes**

The differential expression of the candidate genes CD44, WIF1, Phlda2, Fst was next assessed at the protein level by histochemistry (IHC).

#### CD44:

The IHC analysis confirmed at the protein level the expression pattern of CD44 to be restricted to the 3<sup>rd</sup>pp and the 2<sup>nd</sup>pp. Moreover, CD44 could only be detected in the ventral aspects of the 3<sup>rd</sup>pp (Fig.3.26 A&B). Since CD44 expression occurs in different splice forms, we next investigated whether the CD44 variants typically expressed in keratinocytes and thymic epithelial cells i.e CD44v.6 and CD44v10 were detected at E10.5 within the area of the 3<sup>rd</sup>pp (Fig.3.26 C&D), which gives already rise to the thymus (Ponta *et al.*, 2003). In fact, CD44v10 demonstrated a role in the emigration of mature thymocytes in the thymus (Esser *et al.*, 2004). IHC revealed that both splice variants of CD44 could be easily detected in the ventral aspects of the 3<sup>rd</sup>pp but absent from the 2<sup>nd</sup>pp (Fig.3.26 C&D and data not shown).

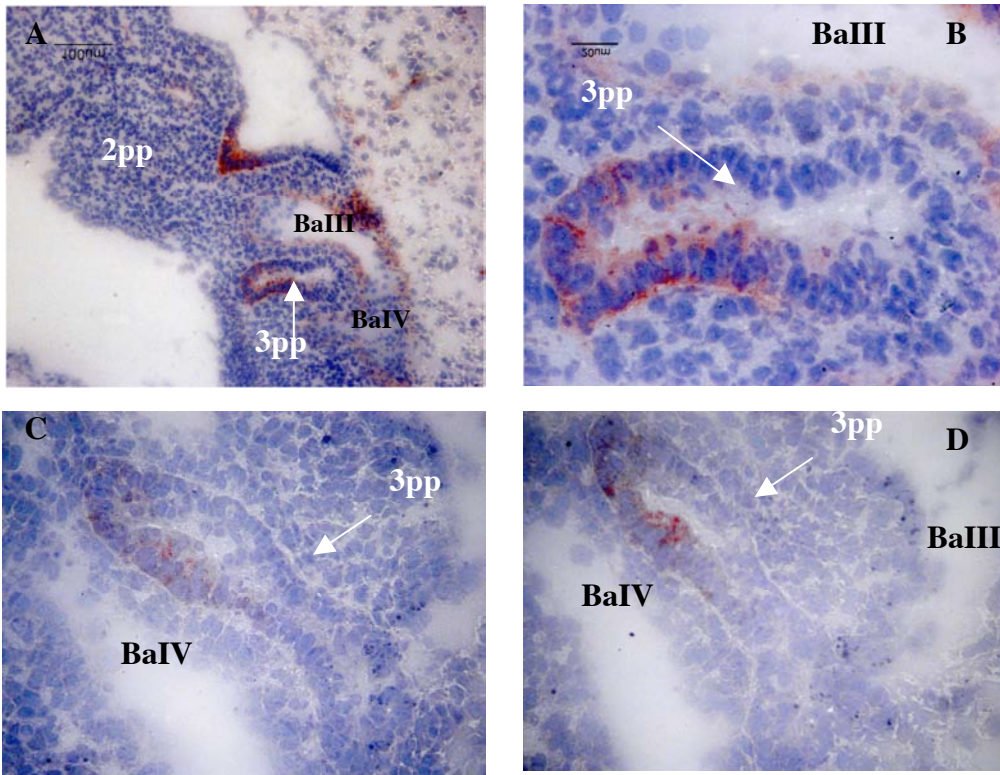


**Figure 3.26. Pharyngeal expression of CD44 and the splice variants CD44v6 and CD44v10 at E10.5.** Common CD44 expression (**A**: 10x magnification, **B**: 40x magnification). Expression of CD44v6 (**C**) and CD44v10 (**D**). Ventral is left and dorsal is at the right, anterior is up and posterior is down in each figure. BaIII & BaIV indicate the branchial arches III & IV, respectively. The arrows point respectively to the respective 2<sup>nd</sup>pp (2pp) and 3<sup>rd</sup>pp (3pp).

### WIF1(Wnt inhibitor factor 1):

The IHC analysis for WIF1 on E10.5s confirmed the upregulation of WIF1 expression in the ventral aspect of the 3<sup>rd</sup>pp (Fig.3.27). Moreover, WIF1 was preferentially expressed there in the posterior aspect of the ventral aspect. In contrast to the qRT-PCR analysis (Fig.3.25), WIF1 expression was also detected by IHC in the 2<sup>nd</sup>pp and 4<sup>th</sup>pp as well as the surrounding mesodermal cells. The pattern of WIF1 also changed between E10.5 and E12.5. At E11.5, WIF1 was expressed in the entire 3<sup>rd</sup>pp, and at E12.5 WIF1 protein was only detected in some of the thymic epithelial cells of the thymus primordium (Fig.3.27).

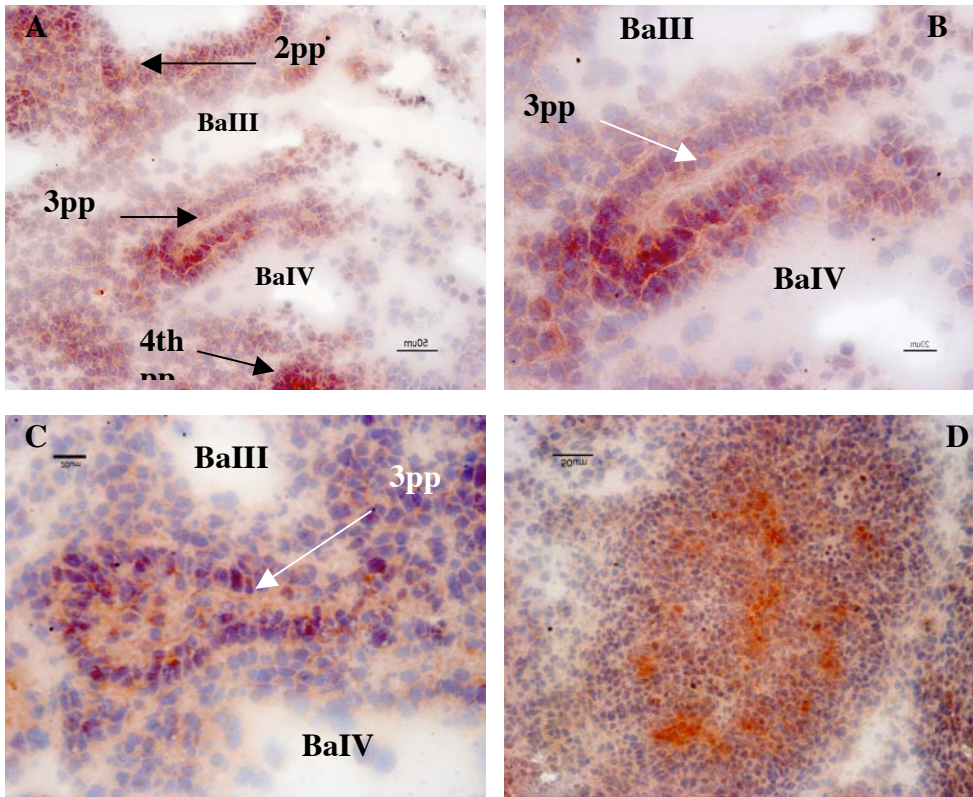


**Figure 3.27. Pharyngeal WIF1 expression during early thymus development.** WIF1 expression at E10.5 (**A**: magnification 20x, **B**: magnification 40x) and at E11.5 (**C**: magnification 40x). WIF1 expression at E12.5 on sagittal sections of the thymus (**D**). Ventral is on the left and dorsal on the right, anterior is up and posterior is down of the respective images. BaIII & BaIV indicate the branchial arches III & IV, respectively. The arrows point respectively to the respective 2<sup>nd</sup>pp (2pp), 3<sup>rd</sup>pp (3pp) and 4<sup>th</sup>pp (4pp).

### Phlda2:

Phlda2 (Pleckstrin homology-like domain, family A, member 2) also known as Imprinted, placenta and liver gene, IPL; or Tumor suppressor cDNA3, Tssc3 was expressed at E10.5 in the endodermal lining of the 2<sup>nd</sup>pp, 3<sup>rd</sup>pp and 4<sup>th</sup>pp but not in the adjacent mesoderm and branchial clefts as predicted by the qRT-PCR analysis (Fig.3.25). However, an exclusive expression of Phlda2 in the ventral aspect of the 3<sup>rd</sup>pp, as suggested from the qRT-PCR analysis could not be confirmed by IHC as revealed by Fig.3.28. Again, a preferential expression for Phlda2 in the posterior part of the ventral aspect of the 3<sup>rd</sup>pp was observed (see Fig.3.28).

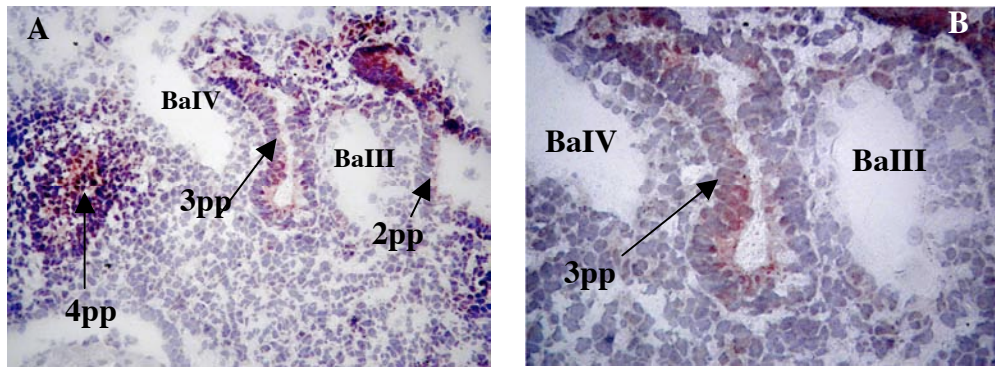


**Figure 3.28. Pharyngeal Phlda2 expression during early thymus development.** Phlda2 expression at E10.5 (**A**: magnification 20x, **B**: magnification 40x). Ventral is on the bottom and dorsal is up, posterior is on the left and anterior is on the right of the respective images. BaIII & BaIV indicate the branchial arches III & IV, respectively. The arrows point respectively to the respective 2<sup>nd</sup>pp (2pp), 3<sup>rd</sup>pp (3pp) and 4<sup>th</sup>pp (4pp).

### **Fst (Follistatin):**

The investigation of Fst expression on E10.5s (Fig.3.29), revealed that Fst was expressed throughout the entire pharyngeal region albeit at a lesser degree in the mesenchyme. A particular emphasis in expression was noticed for the entire 3<sup>rd</sup>pp but a differential pattern between the dorsal and ventral aspects could not be appreciated. Although in contrast to the qRT-PCR data (Fig.3.21), analysis of Fst protein concentrations by IHC may just not be sensitive enough to uncover a difference of 5-fold. This explanation also holds true for the lack of a Fst gradient between the 2<sup>nd</sup>pp and 4<sup>th</sup>pp. An expression pattern similar to that at E10.5 was also noted for Fst at E11.5 (Fig.3.29).

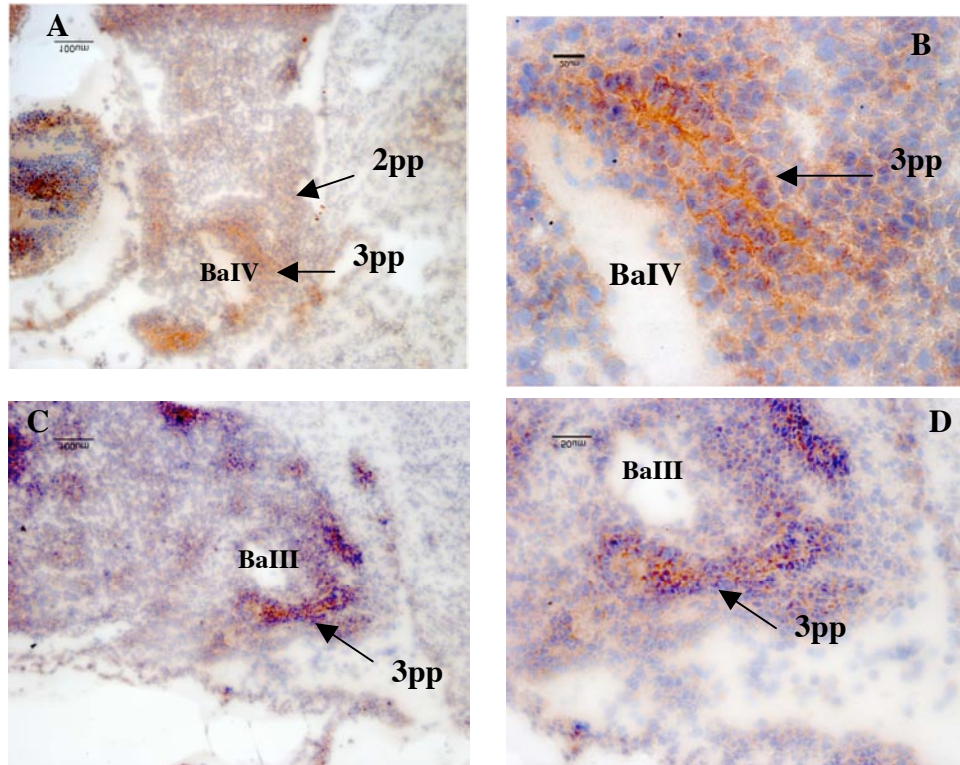


**Figure 3.29. Pharyngeal Fst expression during early thymus development.** Fst expression at E10.5 (**A**: magnification 20x, **B**: magnification 40x) and at E11.5 (**C**: magnification 20x, **D**: magnification 40x). Ventral is on the left and dorsal on the right, anterior is up and posterior is down of the respective images. BaIII & BaIV indicate the branchial arches III & IV, respectively. The arrows point respectively to the respective 2<sup>nd</sup>pp (2pp) and 3<sup>rd</sup>pp (3pp).

### Sp8 (trans-acting transcription factor 8):

The expression pattern for Sp8 was inspected in detail by taking advantage of mice where LacZ ( $\beta$ -galactosidase) was knocked-in to its locus (Treichel *et al.*, 2003). As antibodies specific for Sp8 are not available, an lacZ staining as well as an IHC for LacZ on E10.5 tissue sections from such homozygous mice (kindly provided by Dr. Mansouri) could not detect any signals in the pharyngeal region (Fig.3.30). The strong staining of LacZ in the posterior region of the brain and in the somites (Fig.3.30) are in agreement with previous reports (Treichel *et al.*, 2003).

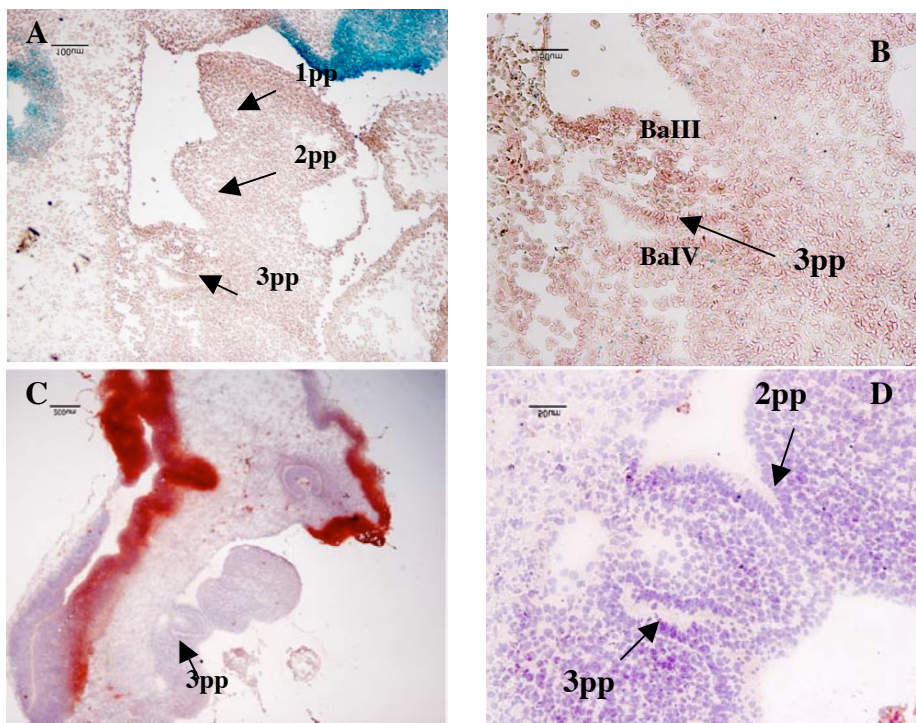


**Figure 3.30. Pharyngeal Sp8 expression during early thymus development.** Sp8 expression at E10.5 in homozygous mice deficient for Sp8 by lacZ staining (A: magnification 10x, B: magnification 20x) and by IHC for  $\beta$ -galactosidase (C: magnification 10x, D: magnification 20x). Ventral is on the left and dorsal on the right, anterior is up and posterior is down of the respective images. BaIII & BaIV indicate the branchial arches III & IV, respectively. The arrows point respectively to the respective 2<sup>nd</sup>pp (2pp) and 3<sup>rd</sup>pp (3pp).



### 3.3.2.7 *Nrxn1* expression in the common thymus-parathyroid primordium at E10.5 and in E12.5 thymus

The spatial expression *Nrxn1* was detailed by in situ hybridization (ISH) as specific antibodies are not available for this gene product. As demonstrated in Fig.3.31A, *Nrxn1*-specific transcripts could be detected throughout the 3<sup>rd</sup>pp providing an expression profile different from that expected from the qRT-PCR data (compare to Fig.3.24). The reason for this discrepancy remains unknown. At E12.5, *Nrxn1* expression was robustly expressed throughout the thymus (Fig.3.31B). As this *Nrxn1* expression appears to be common to all cells of the thymus at that stage, this finding would suggest that *Nrxn1* is also expressed in immature thymocytes. In agreement with this data is the observation that *Nrxn1* was also found to be expressed by qRT-PCR in adult thymocytes (see section 3.2.2.12).

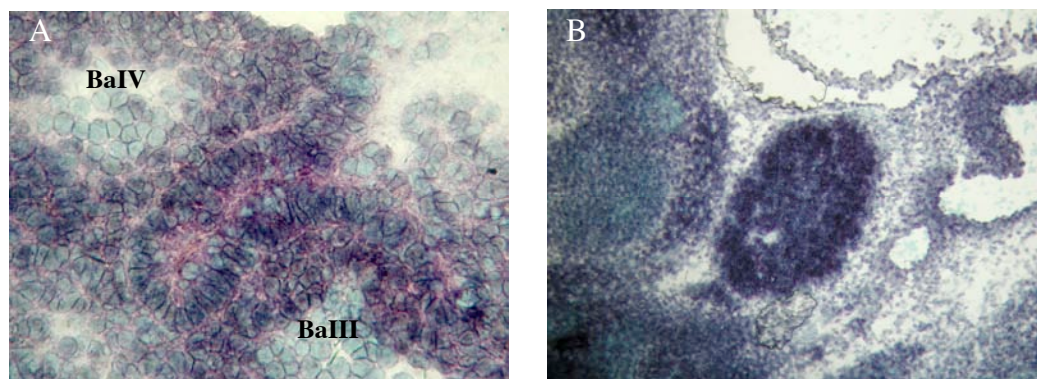


**Figure 3.31. ISH analysis for *Nrxn1* in the common thymus-parathyroid primordium.** A) Expression of *Nrxn1* in the 3<sup>rd</sup>pp at E10.5, magnification (40x). B) expression of *Nrxn1* in the thymus at E12.5 magnification (10x). BaIII and BaIV stand respectively for third and fourth branchial arches. Anterior is at the bottom, posterior at the top, dorsal is left and ventral is right.

### 3.3.2.8 Expression of *Nrxn1* isoforms in the ventral aspect of the 3<sup>rd</sup>pp

In humans, the *Nrxn1* gene generates two separate transcripts,  $\alpha$ -*Nrxn1* (~9kb) and  $\beta$ -*Nrxn1* (~5.3kb) from two different promoters as described (Rowen *et al.*, 2002). Sequence comparisons at the genomic and at the RNA level in silico for mouse *Nrxn1* revealed that it contains 24 exons. Twenty-three of those (exons 1-17 and 19-24) are used for the  $\alpha$ -*Nrxn1* transcript and 7 (exon 18-24) for the  $\beta$ -transcript. Thus, exon 18 is specific for  $\beta$ -transcripts whereas the first 17 exons are specific for  $\alpha$ -*Nrxn1*. To detail a differential expression, specific primers for  $\alpha$ -*Nrxn1* (exon16)

and for  $\beta$ -*Nrxn1* (exon 18) transcripts, were chosen for a qRT-PCR analysis. This analysis revealed that  $\beta$ -*Nrxn1* but not  $\alpha$ -*Nrxn1* transcripts are expressed in the ventral aspect of the 3<sup>rd</sup>pp (Fig.3.32). In contrast,  $\alpha$ -*Nrxn1* but not  $\beta$ -*Nrxn1* could be detected in adult thymic tissue (Fig.3.32).

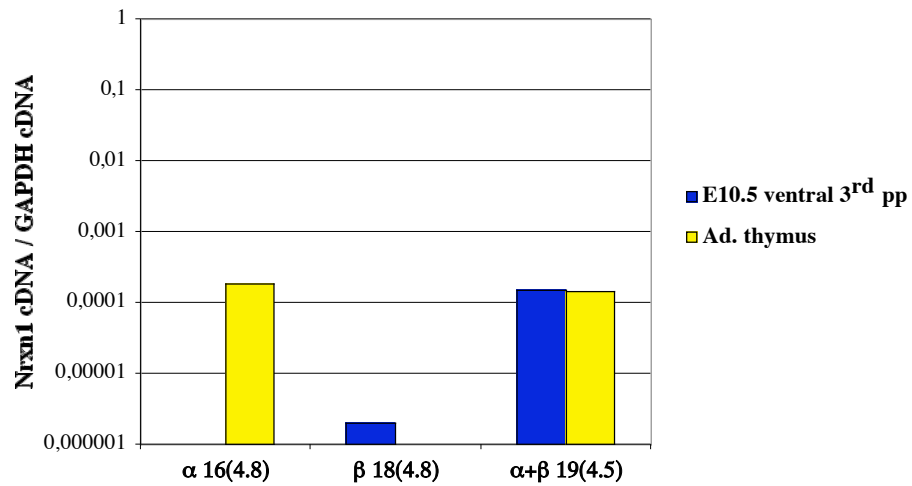


**Figure 3.32. Differential expression of *Nrxn1* isoforms.** The qRT-PCR each was designed for single exon specific amplification to identify  $\alpha$ -*Nrxn1* (exon16),  $\beta$ -*Nrxn1* (exon18) and both isoforms (exon19). Number in brackets indicate approximately the number of kilo base pairs separating the PCR amplicon from the polyA tail of *Nrxn1*.

### 3.3.2.9 Expression of candidate genes during thymus development

The thymic expression of *Nrxn1*, *WIF1*, *Bmp4*, *Fst*, *c-myc*, *Phlda2*, *Sp8* and *Flrt3* was next examined by qRT-PCR at E10.5, E12.5, E16.5, E18.5 and in adult mice and compared to the level of *FoxN1* expression (Fig.3.33). At E10.5, *Nrxn1* and *FoxN1* expression were comparable while at E12.5 and beyond the expression level of *FoxN1* was always considerably higher than of *Nrxn1*, although in contrast to *FoxN1*, *Nrxn1* transcripts have also been detected in thymocytes (Fig.3.34). The thymic expression of *WIF1* which has not been detected in adult thymocytes but in primary TECs (Fig.3.34) was always detected at lower levels than *FoxN1* and declined progressively between E12.5 and E18.5 at much higher rates than *FoxN1*. In contrast, the thymic expression of *Flrt3*, also not found to be expressed in adult thymocytes but in primary TECs, (Fig.3.34) was noticed at higher levels than *FoxN1* between E10.5 and E16.5, while at comparable levels than *FoxN1* beyond E18.5.

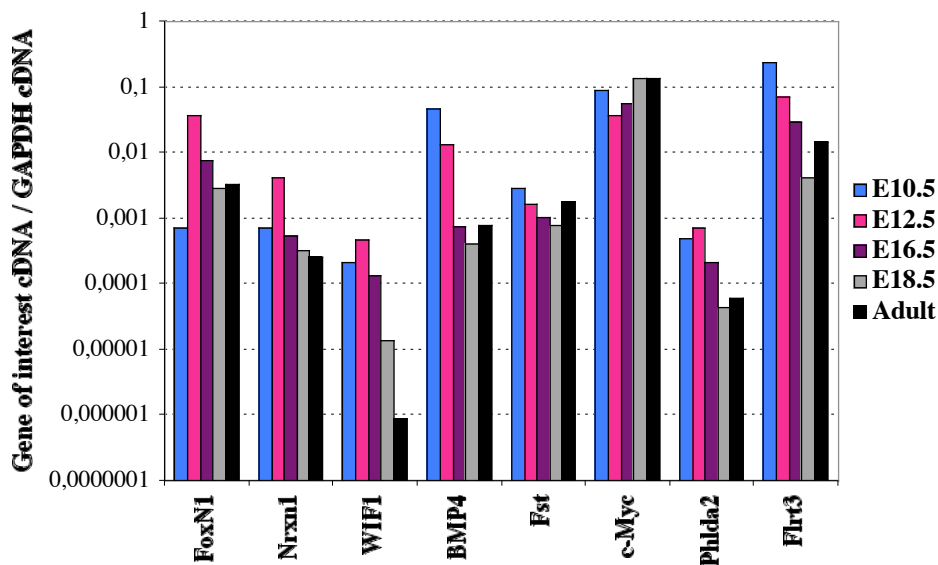


**Figure 3.33. Thymic expression analysis by qRT-PCR for some candidate genes at different embryonal stages of development and in adult mice.** The extracted tissue at E10.5 (ventral aspect of the 3<sup>rd</sup>pp) and at E12.5 has been extracted by LCM while at other stages of development unseparated thymus have been removed with the help of forceps. Data are normalized to *GAPDH*. The ratio “gene of interest cDNA/ *GAPDH* cDNA is the calculated difference in signal intensity.

In regard to the thymic expression of *Bmp4* and *Phlda2*, although the transcripts of these genes were detected in thymocytes (Fig.3.34), their thymic expression was detected at considerable higher levels at early stages of development (E10.5 to E12.5) than at E18.5 or in adult mice. In

contrast, the thymic expression of *Fst* and *c-Myc* also detected in thymocytes (Fig.3.34) was found to be at comparable levels of expression during development.

### 3.3.2.10 Expression of candidate genes in adult thymic epithelial cells and thymocytes

To assess the expression of *Nrxn1*, *WIF1*, *Bmp4*, *Fst*, *c-myc*, *Phlda2* and *Flrt3* adult thymic tissue, we next analysed by qRT-PCR MTS24<sup>+</sup> and MTS24<sup>-</sup> primary adult TECs, unseparated thymocytes and single positive thymocytes (Fig.3.34). *WIF1* was expressed in adult primary sorted TECs but only in those devoided of MTS24 expression. *Fst* was more abundantly expressed in MTS24<sup>+</sup> TECs when compared to MTS24<sup>-</sup> TECs. In contrast, transcripts for *Nrxn1*, *Phlda2* and *Flrt3* were more numerous in MTS24<sup>-</sup> TECs (Fig.3.34).

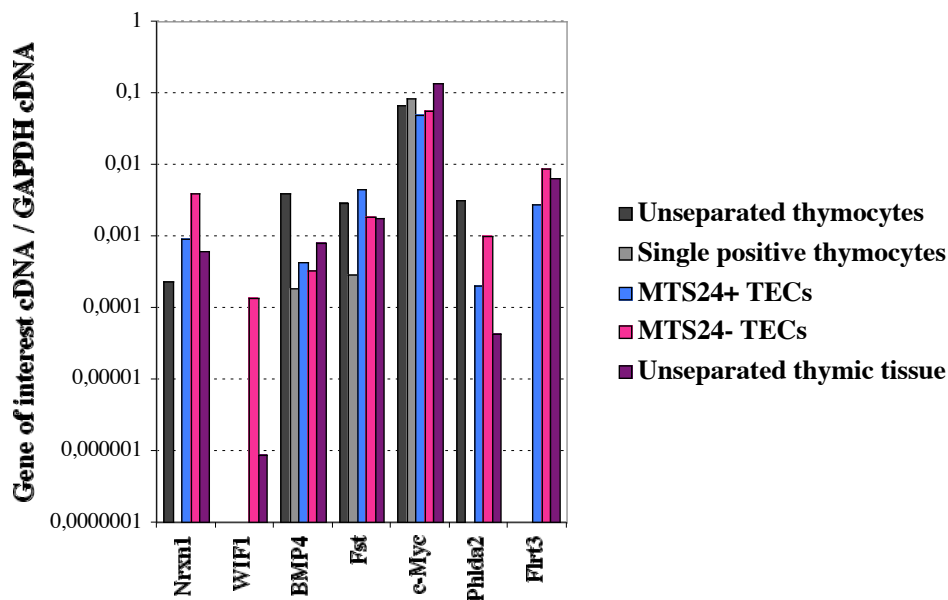


**Figure 3.34. Expression of candidate genes by qRT-PCR in different cellular compartments of the adult thymus.** Data are normalized to *GAPDH*. The ratio “gene of interest cDNA / *GAPDH* cDNA is the calculated difference in signal intensity.

Among unseparated adult thymocytes, *WIF1* and *Flrt3* could not be detected. *Nrxn1* and *Phlda2* were typically expressed in immature thymocytes only, while *Bmp4*, *Fst* and *c-Myc* transcripts were found in both mature and immature thymocytes. Attempting to quantify the expression of the different candidate genes in separate cell types, *Nrxn1* appeared to be more abundantly expressed in TECs than in thymocytes, while *Bmp4* and *Phlda2* levels were higher in thymocytes. In contrast, *Fst* and *c-Myc* appeared to be at comparable levels of expression.

### 3.3.2.11 Expression of candidate genes in thymic epithelial cell lines

The expression of *Nrxn1*, *WIF1*, *Bmp4*, *Fst*, *c-myc*, *Phlda2* and *Flrt3* candidate genes was also examined in established cortical (c) and medullary (m) TEC cell lines (Fig.3.35). While *Fst*, *c-myc*, *Phlda2* and *Flrt3* could be detected in all cell lines tested, *Nrxn1*, *WIF1* and *Bmp4* were differentially expressed among these cells lines. *Nrxn1* and *WIF1* were found to be present only in cTECs with the latter not detected in some of the cortical TECs.

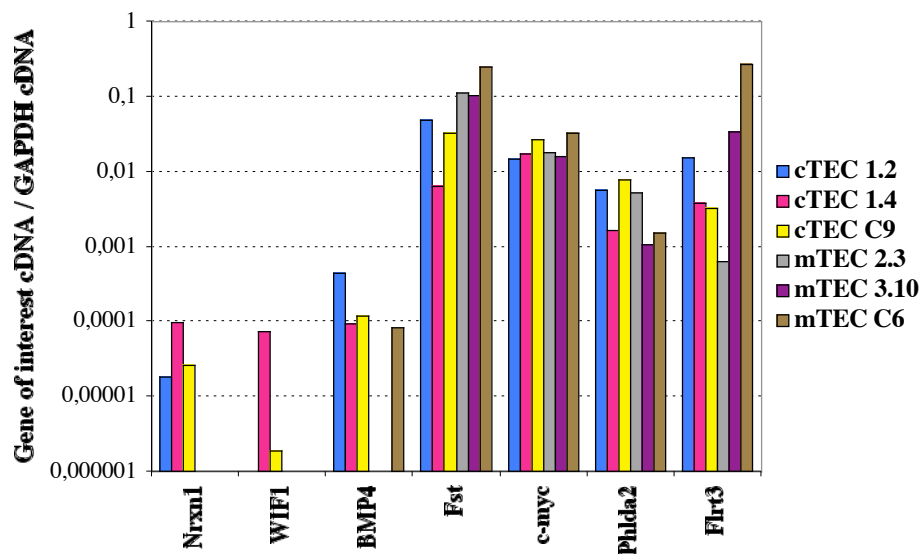


**Figure 3.35. Expression of some candidate genes in different established TEC cell lines.** Data have been normalized to *GAPDH*. The ratio gene of interest / *GAPDH* cDNA is the calculated difference in signal intensity between the examined gene and *GAPDH*.

### 3.3.2.12 Expression of candidate genes in embryonal and adult tissues

The expression of *Nrxn1*, *WIF1*, *Bmp4*, *Fst*, *Phlda2*, *Sp8* as well as the two candidate ESTs (Affymetrix ID: 137059\_at and 101154\_at) were next analysed by conventional RT-PCR in different organs of embryonic E16.5 (Fig.3.36) and in adult mice (Fig.3.37). *Nrxn1*, *Bmp4* and *Fst* could be detected almost in all tissues examined at E16.5 and in adult mice, albeit at different concentrations (Fig.3.36 and Fig.3.37). In contrast, *WIF1*, *Phlda2*, *Sp8* and the two *ESTs* were found to have a more restricted pattern of expression at E16.5 and in adult mice with the notable expression of *EST1* which has not been detected in any of the tissues analysed at E16.5. In regard to *WIF1* and *Sp8*, the thymic expression of these genes was not detected at E16.5 and in adult mice by this RT-PCR for sensitive issues since their thymic expression could be detected by qRT-PCR, although at very low levels in E16.5s as well as in adult mice (Fig.3.33 and results not shown).

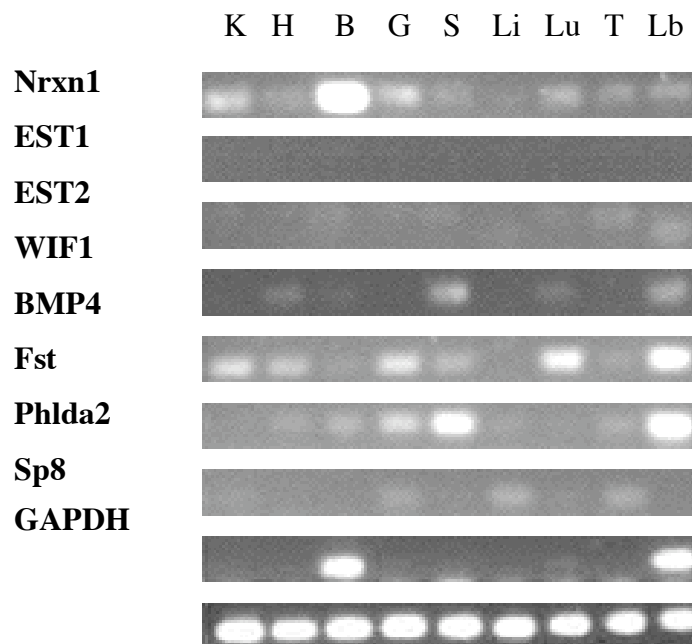


**Figure 3.36. Expression of candidates genes in E16.5 mouse tissues..** RT-PCR analysis of RNA from kidney (K), heart (H), brain (B), gut (G), skin (S), liver (Li), lung (Lu), thymus (T) and Limb (Lb).

Importantly, it may appear that certain PCR products were revealed to have migrated longer during the electrophoresis than others for given genes (e.g *WIF1* and *EST2* in Fig.37). Hence, these short PCR products (lowest in the electrophoresis gel) are most likely primer-dimers and indeed in such a case, the specific PCR products are than the clear upper ones in the gel.

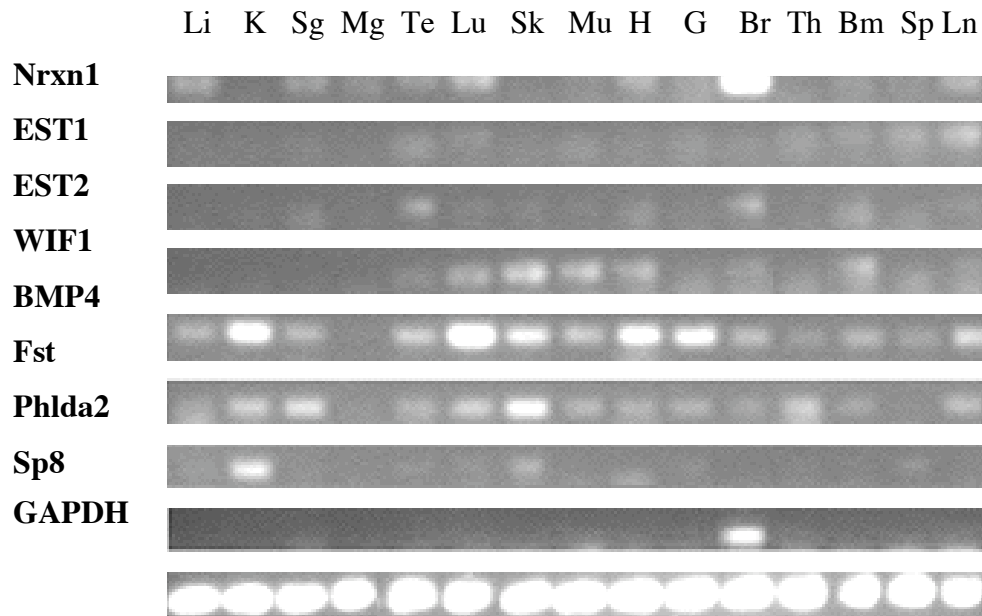


**Figure 3.37. Expression of candidates genes in adult mouse tissues.** RT-PCR analysis of RNA from liver (Li), kidney (K), salivary glands (Sg), mammary glands (Mg), testis (Te), lung (Lu), skin (Sk), muscle (Mu), heart (H), small and large gut (G), brain (Br), thymus (Th), bone marrow (Bm), spleen (Sp) and lymph node (Ln).

### 3.3.2.13 Extension of EST mRNA sequences

To detail the two candidate *ESTs* (*EST1* and *EST2*) further, full length cloning and sequencing was carried out using 5' and 3' rapid amplification of cDNA ends (RACE) methods. This provided for *EST1* a sequence of 1444 bp, which, however does not yet represent the full length message. The poly-A tail of that sequence is placed right at its 3'end (Fig.3.38). The sequence

obtained for *EST2* using 3' and 5' RACE spanned 1065 bp including the polyA signal (Fig.3.39). Sequence and alignment analysis for *EST1* indicated that this gene belongs to the gene cluster of the ATP-binding cassette MHC1 transporter (*TAP1*) situated on the mouse chromosome 17. In fact, *EST1* 5' and 3' extended sequence encodes for the full peptide sequence of the ATP-binding cassette of the *TAP1* transporter. In addition, this analysis revealed that the very 5' end of *EST1* mRNA sequence matches to the beginning of exon 7 of *TAP1* (*TAP1* encodes 11 exons). In contrast to *TAP1* which has its polyA tail at the 3' end of exon11, *EST1* has its polyA tail downstream of exon 10 (597 bp) in intron10 of *TAP1*, which is indeed located 5' of exon 11 of *TAP1*. Ten different clones of *EST1* have confirmed these findings which show that *EST1* in contrast to *TAP1* does not take usage of exon11 and splices differentially its exon10. The sequence analysis demonstrated that *EST2* is located on chromosome 3 but appears to represent a novel, yet not already defined gene transcript. An open reading frame analysis for the so far established sequences for *EST1* and *EST2* predicts a 88 and a 42 amino acid sequence length, respectively, suggesting further that parts of the complete sequence are still missing.

```

1  GGCCTCCAGG GGCTGACGTT CACCCTGCAT CCTGGAACGG TGACAGCGTT GGTGGGACCC
61  AATGGATCAG GGAAGAGCAC CGTGGCTGCC CTGCTGCAGA ACCTGTACCA GCCCACCAGG
121 GGCCAGCTGC TGCTGGATGG CCAAGTGCCTG GTCCAGTATG ATCACCATTA CCTGCACACT
181 CAGGTGGCCG CAGTGGGACA AGAGCCGCTG CTATTTGGAA GARGCTTTCG AGAAAATATT
241 GCGTATGGCC TGAACCGGAC TCCACCCATG GAGGAATCA CAGCTGTGGC CGTGGAGTCT
301 GGAGCCCACG ATTTTCATCTC TGGGTTCCCT CAGGGCTATG ACACAGAGGT AGGTGAGACT
361 GGGAACCCAGC TGTCAGGAGG TCAGCGACAG GCAGTGGCCT TGGCCCAGC CTTGATCCGG
421 AAGCCACTCC TGCTTATCTT GGATGATGCC ACCAGTGCCC TGGATGCTGG CAACCAGCTA
481 CGGGTAAAGT TCTGGCTCTC ACCCTTGTG TTTTGGAGCC ATCTTGCTAT GTGATCTTGG
541 CTGGCCTGGA CCTCACTTTG AAGACAATGC TGGTCTCAGA CCCTTGGTAG TCTTCCTGCT
601 GCTACCTCTG GAGGGCTGGG TCACCCTGCT GTGTCATCTC CCTGAAGTCT CATTCCCATG
661 GGAGCTTTGC TTCTGCCACT CCTCCTGTGT TAGTTATACC AACACAGAA CTGTTCAAAC
721 CTGTCCTTGG AACTCTTGGT CCCATTAGCT TTTCTCCCAG ACACGGGAC CAGTGAGCAG
781 GGCTACTGTC CTAACATCT GTATGGGCTA AGCTTGCTTT GTGTCGTAGA CGTTCATCC
841 CACCCTTTGT ACTAATTTGT CCATCAGAGT CTTTTGCTGT GCTTATTCTG TAGATGACAA
901 AATAGAGGCT AGGAGAGGTT GATTACCTT CTAAAAGTCA CACAGCTTTT GAGCAGTGGA
961 GCCTGGGTCC AGACACAAT CATCCAAACA CTCGTGCTCT TTGTTACTCT TACTCTTTTT
1021 TTTTTTAAT TAAGATTAAT TTATTTTATG TGTATGAGTG TTTAGCCTGA ATGTATGTAT
1081 GTGCCCAGTG TCTCTGAAG TCAGAGAGAG GTGTGGATCC CCTGGAACTG CCGTTATGGA
1141 TGGTTGTGAA CCACTATGTG GGTACTGGAA GTCAGGCCCT GGTCTGCTGG AAGAGCAGCC
1201 AGTGCTCTTA ACTGCTGAGC TGACTCTCCA GCCCCTGCAT TACATTTCTT TAGATTGACT
1261 ATAAAAAATT CTCATTTTAG GGGCTGAGGG GTGGCTCAGC AGTTAATAGC ATTAGTTTAA
1321 AGAGCATTAG CTGCTCTTCC AGAGGACCTG GGTTCATTC TCAGCACCCA CATGGCAGCT
1381 CACAACCATC TGCAGCTCCA GCTCCAGGGT TTCTGACACC TGCACACAAG CAAAACGTCA
1441 ATGA

```

**Figure 3.38. Part of the mRNA sequence for *EST1*.** The polyA tail of *EST1* is beginning at position1444. The Affymetrix Genechip source sequence (public database ID: AA267973) of *EST1* is outlined in pink whereas the rest of the sequence has been revealed by 5' and 3' RACE methods.



```

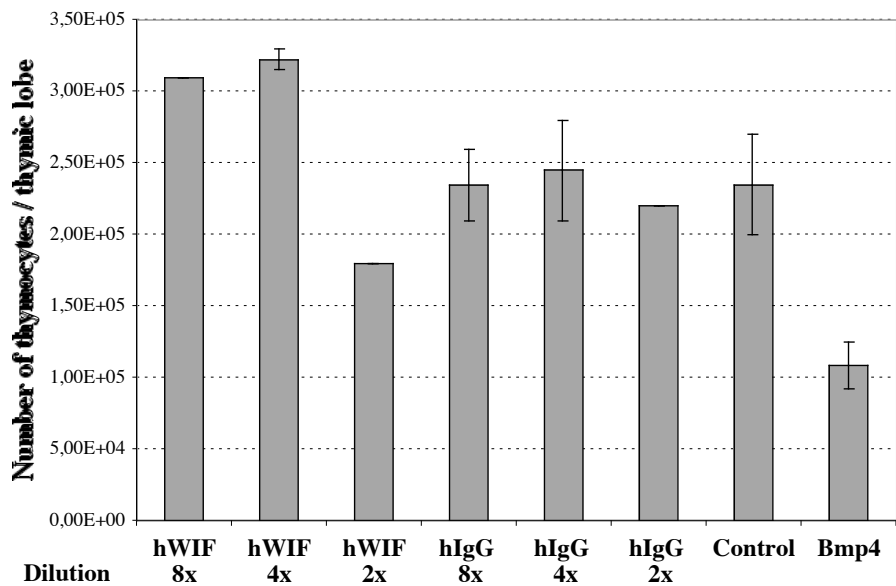
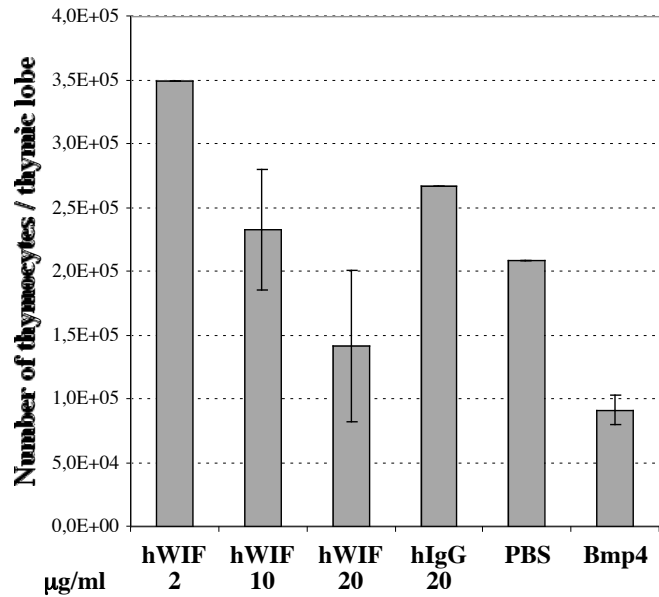
1  ACTGGGGTGG  TARTGCTGAA  TGGAAAGGAG  AACAGGTTGA  TAGAACTAT  TCAGCCTGGC
61  AACACACAGG  AACACAAAGA  TTTCAATTAG  AACATTCTC  AGTGGTCAGT  GTTATACTG
121  GACTAGAGTC  AGAAGAAAC  AAACCACGGT  GCAGAAAGT  GGAAATAT  TGCCCTTAA
181  TTTCAATTT  CATTAAAGTA  ATTTACTTT  ATATGTGAG  AATGTAATA  CAAGAATAC
241  TAGTGAATT  GTAGAGTATT  CTTAAATCA  AACACGAAG  GAACATAAT  ATTATGGCTG
301  GAAGAAAAA  CATTATTTAG  AAGCAGTGG  AAGCTGAGG  GAGGAGGCC  GAGACAGTG
361  AACTCATCG  AATGCATAA  AGAATCCCT  TAACTTCAG  TCTTATCCT  AAAATAATAT
421  TCATTTTGA  GATGAAGAG  AGAGTTTCA  TTTAAAGCT  ATTGGAATG  GAGAGCAGG
481  TCTGCACCT  AGAATCTTA  AGAAAAAAT  TCAATGAGA  AATATATAT  ATGAATCCA
541  ACTTTGATG  ATACAGAGC  AGAAGATTA  GTGGATGTG  TAGCAATTT  CATATTAATC
601  TATTGTCTG  ACATTTTGG  CAGTCATGT  AAGGGATCA  AACCTATGAT  TGAGTGCCAA
661  ACACCCTACA  TATAACAGA  AATGGATTG  ATCAGACTTA  AATAAAGAC  CACATTTAG
721  CAGCAACAC  ATTGAGGGT  GTTGTGAG  TTTGCTTGT  GCTTAGTGA  TGTGGGAGC
781  CGAGGAGGA  GGATGGAT  TTGGAGAC  GTTAGGAA  CTTGTACT  GTAGAATAG
841  CCTTTGAGAT  CTAGTTCAG  GGTACATAG  ATTTACTGT  TGGAAACAG  ATAAACCAC
901  ACCAGGACCA  AATGTTTAC  AAGATATAT  TTTGAGAAT  GCTTATCTT  CTAATAAAA
961  AAAAAGGAA  CAAAAGCCA  TAATATTTA  ATGTATGCG  CATAGAAAT  ATTTGTGTAT
1021  AAGTTAATAT  AATGAATTT  CAGGATAATA  AAAATTAATA  GTTTA

```

**Figure 3.39. Part of the mRNA sequence for *EST2*.** The polyA tail of *EST2* is beginning at position 1444. The Affymetrix Genechip source sequence (public database ID: AA517023) of *EST2* is outlined in turquoise. pink whereas the rest of the sequence has been revealed by the 5' RACE method.

### 3.3.2.14 Effect of WIF1 on thymopoiesis in fetal thymic organ culture

Next, a potential role of WIF1 in thymopoiesis was assessed using E13.5 FTOC. Thymic lobes were treated in vitro for 10 days with affinity purified human WIF1-IgG (2, 10 and 20 mg/ml), a fusion protein composed of the human IgG heavy-chain and the hWIF1 full length. In fact, hWIF1 displays at the cDNA level 93% homology to its mouse orthologue. This fusion protein has been demonstrated to be biologically active as it could inhibit Wingless signaling in vitro (Hsieh *et al.*, 1999). Control FTOCs were incubated with affinity purified human IgG at the concentration of 20mg/ml. Moreover, FTOCs were also cultured either in FTOC media (IMDM media with 10% FCS) without any supplementation, or in the presence of Bmp4 at the concentration of 100ng/ml to expand immature thymocytes (Hager-Theodorides *et al.*, 2002). After 10 days in culture, thymocytes were harvested, measured for their cellularity, stained for the surface expression of CD44/CD25 and CD4/CD8, and analysed by flow cytometry. The thymocyte cellularity of these FTOCs has revealed that in the presence of the lowest concentration of WIF1 (2µg/ml), FTOCs was at considerable higher values ( $3.5 \times 10^5$  cells) than control FTOC ( $2.5 \times 10^5$  cells). In contrast, the cellularity of thymocytes (approx  $2.5 \times 10^5$  cells) in the presence of 10µg/ml of hWIF-IgG was comparable to control FTOC (hIgG), while in the presence of 20µg/ml of hWIF-IgG, this cellularity was considerable lower ( $1.5 \times 10^5$  cells) than control FTOCs (hIgG) (see Fig.3.40A). To purify hWIF-IgG, a pH of 2.9 was required for elution from the column, which may have altered the biological activity of the fusion protein. FTOCs were therefore grown alternatively in freshly conditioned media from hWIF1-IgG transfected HEK293 cells. As controls, FTOCs were cultured in media supplemented with either conditioned media for hIgG transfected HEK293 cells, with Bmp4 (100ng/ml), or no further additions. In fact, FTOCs were incubated in different dilutions of the conditioned media (dilution factor of 2, 4 or 8 with FTOC media) for hWIF-IgG or for hIgG (Fig.3.40B).

**R**

**Figure 3.40. FTOC cellularity following culture with WIF1. A** FTOCs were incubated in the presence of affinity purified human WIF1-IgG (hWIF 2,10 or 20µg/ml). Control FTOCs were incubated in the presence of affinity purified human IgG (hIgG 20µg/ml), of PBS (10µl, volume of affinity purified hWIF1-IgG or hIgG), or of Bmp4 (100ng/ml). **B** FTOCs were incubated in conditioned media for hWIF1-IgG (hWIF: diluted with FTOC media with a dilution factor of 2, 4, or 8). Control FTOCs were incubated in conditioned media for human IgG (hIgG: diluted 2,4 or 8 times with FTOC media). For (A) and (B), 6 thymic lobes were pooled for each analysis. If error bars are displayed than samples have been made in duplicates and error bars show the difference between these samples.

Similarly, as FTOCs treated with hWIF-IgG (2 $\mu$ g/ml), the thymocyte cellularity was higher than control FTOC (3 $\times 10^5$  cells) if the conditioned media was diluted with FTOC media for a dilution factor of more than 2 (above 3 $\times 10^5$  cells) (see Fig.3.40B). In contrast, as previously observed in FTOCs treated with too high concentrations of affinity purified hWIF-IgG (Fig.3.40A), the thymocyte cellularity of these FTOCs in the presence of conditioned media for hWIF1-IgG (dilution factor equal to 2) was lower (1.5 $\times 10^5$  cells) than the control FTOC (approx 2.5 $\times 10^5$  cells). These observations could be due to toxic effects on FTOC by WIF1 at too high concentrations. Nevertheless, since FTOCs in the presence of affinity purified hWIF1-IgG or of conditioned media for hWIF1-IgG reveal similar data, the affinity purification at pH 2.9 of hWIF1-IgG does not seem to have altered the biological activity of WIF1. Taken together, these FTOC data (Fig.3.40 A&B) reveal that WIF1 may stimulate the expansion of immature thymocytes. However, the analysis for CD44/CD25 and CD4/CD8 surface expression of FTOCs treated with affinity purified of hWIF-IgG (Fig.3.41) or with conditioned media for hWIF-IgG (Fig.3.42) does not seem to have altered the normal development of thymocytes, as SP thymocytes (CD4<sup>+</sup>CD8<sup>-</sup>) and (CD4<sup>-</sup>CD8<sup>+</sup>) were generated in proportions comparable to control FTOC (hIgG). Nevertheless, the analysis for CD44/CD25 surface expression revealed that FTOCs in the presence of increasing amounts of affinity purified hWIF-IgG (Fig.3.41A) seem to have the tendency to accumulate the subpopulation of DN1 (CD44<sup>+</sup>CD25<sup>-</sup>) thymocytes (36.6%, 42.9% and 46.5%) and seem to have a concurrent decrease of DN4 (CD44<sup>-</sup>CD25<sup>-</sup>) thymocytes (23.9%, 15.8% and 12.7%). These observations could not be noticed in FTOCs incubated in conditioned media for hWIF-IgG (Fig.3.42A). Anyway, these observations do not seem to be biologically significant as DN2, DN3 as well as DN (CD4<sup>-</sup>CD8<sup>-</sup>), DP (CD4<sup>+</sup>CD8<sup>+</sup>) and SP (CD4<sup>+</sup>CD8<sup>-</sup> or CD4<sup>-</sup>CD8<sup>+</sup>) thymocytes were noticed at comparable proportions than in the control FTOC (hIgG) (see Fig.3.41). In summary, these data suggest that overexpressing WIF1 does not affect the differentiation of thymocytes, however, loss of function analysis using neutralizing antibodies for WIF1 in FTOC may in contrast to these FTOCs eventually reveal more defined roles for WIF1 in the development of thymocytes.

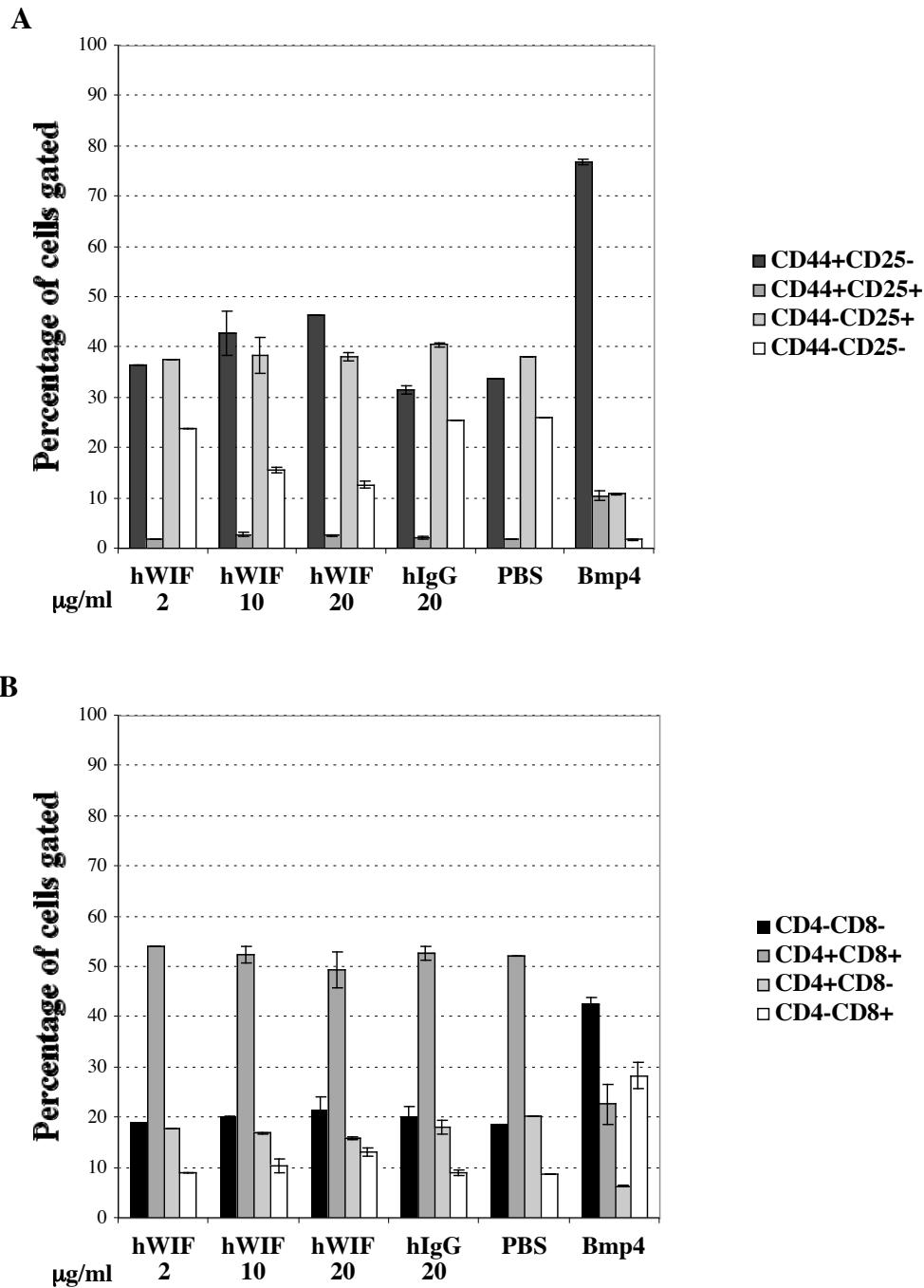
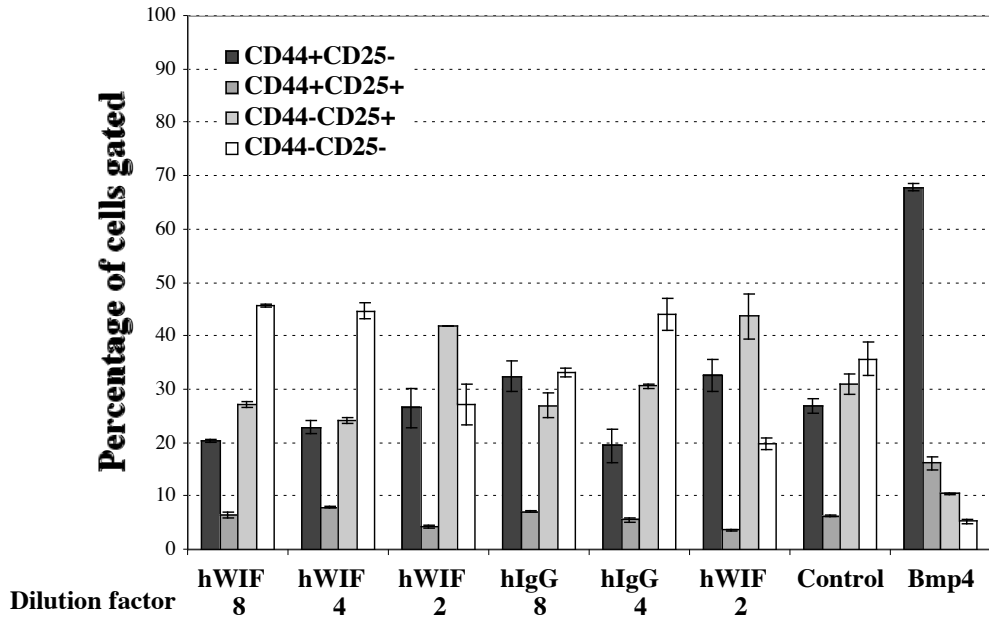


**Figure 3.41. Thymopoiesis in FTOCs in the presence of affinity purified hWIF1-IgG.** Flow cytometry analysis for the cell surface expression of CD44/CD25 among TN thymocytes (**A**) and CD4/CD8 among all thymocytes (**B**). FTOCs were incubated in the presence of human WIF1-IgG (hWIF: 2, 10 or 20 mg/ml). Control FTOCs were incubated in the presence of human IgG (20 mg/ml), of PBS (10 ml, volume of affinity purified hWIF1-IgG) or of Bmp4 (100 ng/ml). 6 thymic lobes were pooled for each analysis. If error bars are displayed then samples have been made in duplicates (generated independently) and error bars show the difference between these samples.

A



B

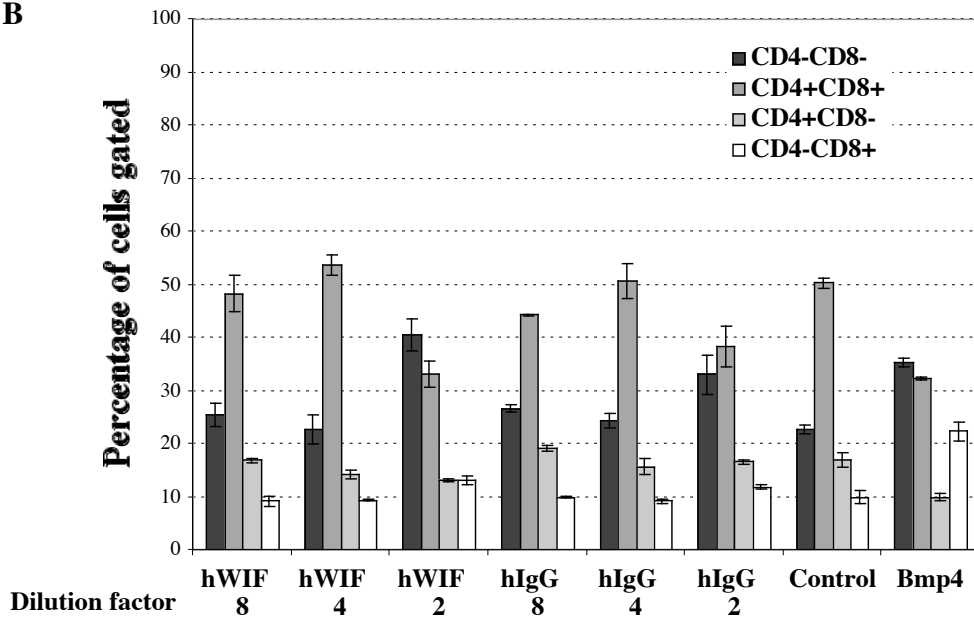


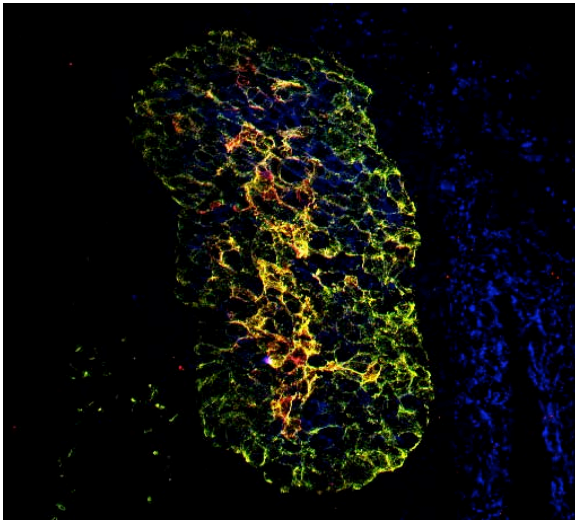
**Figure 3.42. Thymopoiesis in FTOCs in the presence of conditioned media for hWIF1-IgG.** Flow cytometric analysis for the cell surface expression of CD44/CD25 among TN thymocytes (A) and CD4/CD8 among all thymocytes (B). FTOCs were incubated in conditioned media for human WIF1-IgG (diluted with FTOC media at a dilution factor of 2, 4 or 8). Control FTOCs were incubated in conditioned media for human IgG (diluted with FTOC media at a dilution factor of 2,4 or 8), in FTOC media (IMDM with 10% FCS), or in FTOC media with a supplementation of Bmp4 (100ng/ml). 6 thymic lobes were pooled for each analysis. If error bars are displayed than samples have been made in duplicates (generated independently) and error bars show the difference between these samples.

In contrast, FTOC cultures in presence of Bmp4 (100ng/ml) demonstrated an accumulation of DN1 (CD44<sup>+</sup>CD25<sup>-</sup>) thymocytes and a concurrent decrease of DN3 and DN4 thymocytes indicating an initial block in early thymocyte differentiation. Notably, overexpressing Bmp4 (see Fig.3.41 and Fig.3.42) appears to favour differentiation of DP thymocytes (CD4<sup>+</sup>CD8<sup>+</sup>) into CD8<sup>+</sup> SP cells (proportion above 20%) rather than into CD4<sup>+</sup> SP cells (proportion below 10%). This is in contrast to control FTOC, which favoured a differentiation into CD4<sup>+</sup> SP cells corresponding to approximately 10% for CD8<sup>+</sup> SP cells and to 15-20% for CD4<sup>+</sup> SP cells). Hence, these data could suggest that Bmp4 signalling may have also have a role in the differentiation of DP (CD4<sup>+</sup>CD8<sup>+</sup>) into CD8<sup>+</sup> SP thymocytes. However, these observations are most likely not biologically significant, as the FTOC treated with Bmp4 affected drastically the cellularity of thymocytes (1x10<sup>5</sup> cells) in comparison to the control FTOC (2.5x10<sup>5</sup> cells). Nevertheless, these data confirm previous reports on the effect of overexpressing Bmp4 in FTOCs in regard to the initial block in early thymocyte differentiation (Hager-Theodorides *et al.*, 2002; Tsai *et al.*, 2003).

### 3.3.2.15 Confocal analysis of E13 thymus of Phlda2 deficient mice

To reveal an eventual role for the Phlda2 candidate gene in early thymic organogenesis by IHC, the thymic expression of the TEC markers K5 and K8 and the expression of CD45 was investigated in E13.5 embryos deficient for Phlda2. However, the confocal analysis (see Fig.3.43) did not reveal any differences in the expression of these three markers (K5, K8 and CD45) when comparing thymic tissue from Phlda2 deficient and wild type mice. The thymus from Phlda2 deficient embryos appeared to be about twice in size in comparison to that of wild type. These data suggest that Phlda2 does not seem to have a non-redundant role in the early differentiation of thymic epithelial cells. However, Phlda2 may modulate the expansion of the thymic epithelium, as E13.5 embryos deficient for Phlda2 appeared to have a bigger thymus than that of wild type in this analysis.

**A**



**B**

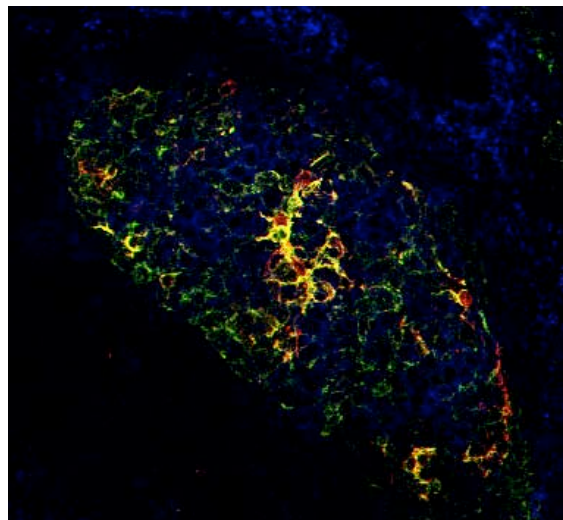


**Figure 3.43. IHC analysis of the thymus in a Phlda2 deficient E13.5.** The expression of K5 (red), K8 (green) and CD45 (blue) was analysed on thymic sections from E13.5 wild type (A) and Phlda2 deficient (B) littermates.



### 3.3.2.16 Genes confirmed to be preferentially expressed in the dorsal aspect of the 3<sup>rd</sup>pp

The absence in the expression of a specific gene may also contribute to the cellular fate of a specific tissue. I therefore investigated which genes by microarray analysis are either preferentially or exclusively expressed in the dorsal aspects of the 3<sup>rd</sup>pp when compared to the ventral circumference and I next verified their differential expression by qRT-PCR. This analysis revealed that FoxA1, FoxA2, Sfrp2 and CXCL12 are in addition to Gcm2 upregulated more than 4-fold in the dorsal part of the 3<sup>rd</sup>pp when analysed by qRT-PCR (Table 3.8 and Fig.3.44). In addition, Tbx1 (which is not represented on MGU74v2 microarrays) was also upregulated at this anatomical site.

**Table 3.8**

**Genes preferentially expressed in the dorsal aspect of the 3<sup>rd</sup>pp as analysed by microarrays and qRT-PCR.**

Probe ID <sup>1</sup>	Gene name	Gene Symbol	Biological function	D_1	D_2	V_1	V_2	Microarray Ratio (4)	qRT-PCR ratio (5)
	T-box 1	Tbx1	Transcription factor						4.8
92697_at	Forkhead box A1	FoxA1	Transcription factor	P <sup>3</sup>	P	P	P	3.98	8.4
93950_at	Forkhead box A2	FoxA2	Transcription factor	A <sup>2</sup>	A	A	A	7,17	4.0
93503_at	Soluble frizzled related protein 2	Sfrp2	Inhibitor of Wnt signalling	P	P	P	P	9.14	15.5
162234_f_at	Chemokine (C-X-C motif) ligand 12	CXCL12	Chemotaxis	P	P	P	P	3.83	5.5

Explanations: (1) Probe ID refers to the Affymetrix reference number for a probe set specific for a given gene. (2) A= absent, (3) P=present. (4) Microarray ratio is calculated as average intensity 3<sup>rd</sup>pp/ average intensity 2<sup>nd</sup>pp and (5) qRT-PCR ratio is calculated as  $2^{(\text{average } \Delta\text{Ct } 2^{\text{nd}}\text{pp}) - (\text{average } \Delta\text{Ct } 3^{\text{rd}}\text{pp})}$  where the  $\Delta\text{Ct}$  is the difference in Ct values between the gene of interest and the housekeeping gene, *GAPDH*. Samples of the 2<sup>nd</sup>pp and 3<sup>rd</sup>pp are annotated as 2\_1, 2\_2, 3\_1 and 3\_2, respectively.

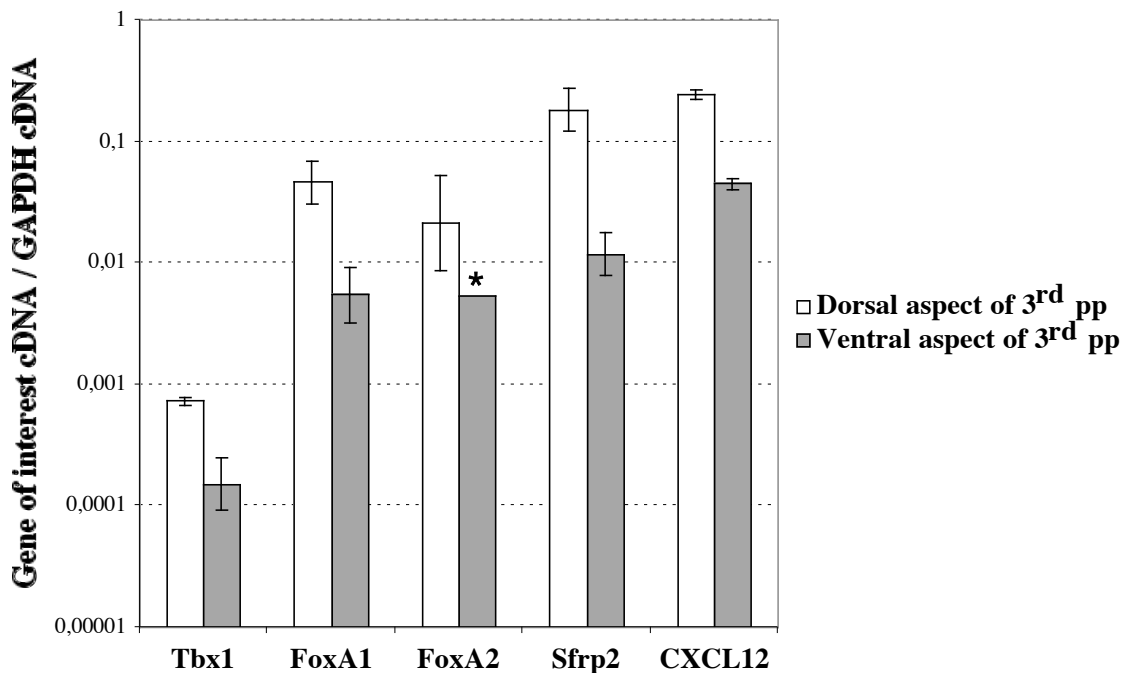


**Figure 3.44. Preferential expression of *Tbx1*, *FoxA1*, *FoxA2*, *Sfrp2* and *CXCL12* in the dorsal aspect of the 3<sup>rd</sup>pp in comparison to its expression in its ventral counterpart as measured by qRT-PCR.** Data has been normalised to *GAPDH* expression. The ratio “gene of interest cDNA / *GAPDH* cDNA” corresponds to the calculated difference in signal intensity between the examined gene and *GAPDH*. The errors bars represent the difference in the calculated ratio between two samples generated independently.\* *FoxA2* was only found to be expressed in one of two samples of the ventral aspect of the 3<sup>rd</sup>pp.

### 3.3.2.17 Expression of candidate genes in the 4<sup>th</sup>pp

Numerous important genes involved in thymus and parathyroid development such as (*Pax1*, *Pax9*, *Hoxa3* and *Shh*) were also found to be expressed in the 2<sup>nd</sup> and 4<sup>th</sup>pp but rarely found to be exclusively expressed in the 3<sup>rd</sup>pp as *FoxN1* or *Gcm2*. I therefore investigated by microarray analysis whether candidate genes revealed to be upregulated or exclusively expressed in either the ventral aspect of the 3<sup>rd</sup>pp when compared to the dorsal circumference, or upregulated in the entire 3<sup>rd</sup>pp when compared to the 2<sup>nd</sup>pp, are also expressed in the 4<sup>th</sup>pp. This analysis revealed that 22 of the candidate genes were also found to be expressed in the 2<sup>nd</sup>pp and/or the 4<sup>th</sup>pp, while 15 candidate genes (*CCL21*, *Meox2*, *Msx2*, *Phlda2*, *Gria1*, *Cd6*, *CD44*, *WIF1*, *c-Myc*, *Fst*, *Lmcd1*, *Tnfrsf19*, *Colla1* and the two ESTs) were revealed to be only expressed in the 3<sup>rd</sup>pp of the pharyngeal pouch when compared to the 2<sup>nd</sup>pp and 4<sup>rd</sup>pp (see Table 3.9). However, *Phlda2*, *Fst* could be detected in the 4<sup>th</sup>pp by qRT-PCR (Fig.3.25) although at very low levels, possibly explaining the absence of detection of these two genes by microarray analysis.

**Table 3.9**

**Microarray expression data in the 4<sup>th</sup>pp for 37 genes confirmed by qRT-PCR to be differentially expressed between either the 2<sup>nd</sup> and the 3<sup>rd</sup>pp or within the 3<sup>rd</sup>pp.**

Probe ID <sup>1</sup>	Gene Symbol	D_1	D_2	V_1	V_2	3_1	3_2	2_1	2_2	4_1	4_2	4_3	Microarray V/D Ratio (3)	Microarray 3/2 ratio (4)
103012_at	CCL21	A <sup>2</sup>	M <sup>2</sup>	M	P <sup>2</sup>	P	P	A	A	A	A	A	1,13	62,90
162234_f_at	CXCL12	P	P	P	P	A	P	P	A	P	P	P	0,26	0,50
102025_at	CXCL13	A	A	A	A	A	A	A	A	A	A	A	2,50	1,21
114280_at	Ypel1	P	P	P	P	P	P	A	A	P	P	P	1,37	12,22
165740_at	Dmrt2	P	P	P	P	P	P	A	A	M	P	P	1,09	19,20
100899_s_at	Znf297	P	P	P	P	P	P	A	A	A	A	P	1,09	8,09
99937_at	Meox2	P	P	P	P	P	P	A	A	A	A	A	1,24	18,17
165776_i_at	Klf16	P	A	P	M	P	P	A	A	A	A	P	2,35	15,96
102956_at	Msx2	A	A	P	P	A	A	A	A	A	A	A	2,91	1,50
92535_at	Ebf1	A	A	A	A	P	A	A	A	A	P	A	3,61	12,08
104548_at	Phlda2	A	A	P	A	A	P	A	A	A	A	A	2,09	2,58
92943_at	Gria1	A	A	P	M	A	A	A	A	A	A	A	13,78	1,08
92203_s_at	CD6	A	A	A	A	A	A	A	A	A	A	A	8,93	3,27
109403_at	CD44	A	A	P	P	P	A	P	A	A	A	A	7,76	1,38
101851_at	CD200	A	A	P	P	P	A	P	A	A	A	M	1,73	0,95
138087_at	Fgf12	P	A	P	A	P	P	A	A	A	A	A	1,22	7,41
110370_at	Flrt3	P	P	P	P	P	A	P	P	P	P	P	6,28	4,56
163423_at	WIF1	A	A	M	A	A	A	A	A	A	A	A	3,65	0,21
93455_s_at	Bmp4	P	P	P	P	P	P	P	P	P	P	P	7,82	1,92
98817_at	Fst	A	A	P	P	A	A	A	A	A	A	A	10,40	5,55
162531_at	Bambi	P	A	P	P	A	P	A	A	P	P	P	3,17	1,64
93300_at	Tgfb $\beta$ 2	A	A	P	P	P	P	P	A	A	P	P	3,76	0,42
104712_at	c-Myc	P	P	P	P	P	P	A	A	A	A	A	3,01	3,84
117331_at	Lmcd1	A	A	A	P	A	A	A	A	A	A	A	4,97	18,62
92210_at	Angpt2	P	P	P	P	P	P	A	A	P	P	P	1,07	40,28
160670_at	Tnfrsf19	A	P	P	P	P	A	A	A	A	A	A	1,95	1,37
101975_at	Dlk1	P	P	P	P	P	P	P	P	P	P	P	3,39	2,35
94305_at	Colla1	A	A	M	A	A	A	A	A	A	A	A	9,96	6,56
104375_at	Spock2	A	A	P	P	P	P	P	A	A	A	A	3,19	0,70
99011_at	Galnt3	P	P	P	P	P	P	P	A	P	P	P	4,57	5,26
102306_at	Hst2nst1	P	P	P	P	P	P	P	P	P	P	P	2,60	0,45
114766_at	Nrxn1	A	A	P	P	A	A	A	A	P	A	A	2,37	1,99
137059_at	EST1	A	A	A	A	A	A	A	A	A	A	A	8,44	7,63
101154_at	EST2	A	A	P	P	A	A	A	A	A	A	A	2,92	0,58
92697_at	FoxA1	P	P	P	P	P	P	P	P	P	P	P	0,25	0,25
93950_at	FoxA2	A	A	A	A	A	A	A	P	A	A	A	0,14	0,36
93503_at	Sfrp2	P	P	P	P	P	P	P	P	P	P	P	0,11	0,20

Explanations. (1) Probe ID refers to the Affymetrix reference number for a probe set specific for a given gene. (2) P, M, A denotes for Present, Absent and Marginal calls, respectively. Microarray ratio (3&4) is the average signal intensity difference between (3) the ventral vs. dorsal (V/D) epithelium of the 3<sup>rd</sup>pp and (4) between the 3<sup>rd</sup>pp vs. 2<sup>nd</sup>pp (3/2) (4). The examined samples are annotated D\_1, D\_2 for dorsal, V\_1, V\_2 for ventral, 2\_1, 2\_2 for 2<sup>nd</sup>pp, 3\_1, 3\_2 for 3<sup>rd</sup>pp and 4\_1, 4\_2 and 4\_3 for 4<sup>th</sup>pp.

## 4. Discussion

This thesis reports on the transcriptome of epithelial cells at E10.5 of the 2<sup>nd</sup>, 3<sup>rd</sup> and 4<sup>th</sup>pp of mouse embryos. This multiple microarray analysis were carried out to identify genes (referred to as candidate genes) that may play a role in the development of the thymus. Numerous genes have been identified to be differentially expressed between these different anatomical sites that display also a different fate in organ formation. Thus, data from microarray analysis should serve as a valuable resource to identify genes involved in the commitment of endodermal cells of the ventral aspects of the 3<sup>rd</sup>pp to a thymic epithelial cell fate.

First, I will start to comment the discrepancies and the confirmation rate between qRT-PCR and microarray analysis of the genes identified by microarrays to be differentially expressed within the 3<sup>rd</sup>pp. Next, candidate genes revealed to have a differential in expression between the ventral and the dorsal aspects of the 3<sup>rd</sup>pp or between the entire 3<sup>rd</sup>pp and 2<sup>nd</sup>pp will be discussed concerning their potential function if not known in thymus organogenesis. The genes will be discussed in separate sections according their category or biological function and will be based on findings, which have been previously been reported as well as on data, which have been revealed in the result section. Hence, I will begin to discuss the roles of the candidate genes (i.e. CCL21, CXCL12 and CXCL13), which are known to be involved in the chemotaxis and I will follow with an analysis of those which are known to be transcription factors (i.e. Dmrt2, Znf297, Meox2, Klf16, FoxG1, Ebf1, Msx2, Tbx3, FoxA1, FoxA2 and Sp8). Then, I will proceed with the examination of candidates genes known to be cell surface antigens (i.e. CD44, CD200 and CD6) and comments will be given for those involved in the signal transduction of growth factor (Fgf12, Phlda2 and Flrt3), Wnt (WIF1, Nkd1 and Sfrp2) or Tgf $\beta$  (Bmp4, Fst, Bambi and Tgf $\beta$ 2) signalling. This part will also include in separate sections the discussion of c-Myc (regulated by Wnt and Tgf $\beta$  signalling), Tnfrsf19 (involved in NF $\kappa$ B signalling) and Dlk1 (regulates Hes1, which is a target of Notch signalling) genes and comments on their eventual roles in the development of the thymus will be made. The discussion will provide further details and findings on  $\alpha$ -*Nrxn1* and  $\beta$ -*Nrxn1* transcripts, and about its transcriptional regulation and function. Finally, this part will comment on candidate genes which are involved in the extracellular matrix

(*Colla1*, *Spock2*, *galnt3* and *Hs2st1*) to finish with a discussion of the two expressed sequence targets (*EST1* and *EST2*) found to be upregulated in the ventral aspect of the 3<sup>rd</sup>pp when compared to the dorsal aspect of the 3<sup>rd</sup>pp.

#### **4.1 Comparative analysis between data sets from microarrays and qRT-PCR**

When comparing the microarray and the qRT-PCR data of the candidate genes, a confirmation rate of nearly 33% of the genes identified by microarrays to be differentially expressed and verified by qRT-PCR was revealed. In fact, microarray analysis is more susceptible to display false positives than qRT-PCR in regard to the information of whether a gene is expressed or not. For example, two probe sets of *Gcm2* displayed differences in their A, M or P calls between either the two samples of the ventral or the dorsal aspects of the 3<sup>rd</sup>pp (Table 3.5). In addition, the difference in signal intensity between two probe sets for a given gene can differ to a considerable degree. For example, the expression of *Follistatin* (*Fst*) was increased for one probe set by 10.40 fold in the ventral aspect of the 3<sup>rd</sup>pp when compared to the dorsal localisation of the same pouch. However, a second probe set for *Fst* revealed only an expression difference of 0.96 fold. In fact, the latter probe set displayed an absence of specific expression (A call) for *Fst* in both samples of the ventral aspect of the 3<sup>rd</sup>pp while the first one could report a specific expression for *Fst* (P call) in both samples of the ventral epithelium of the 3<sup>rd</sup>pp. These disparate results between two different probe sets for a given gene indicate that the reliability of the microarray analysis also depends on the individual performance of the different probe sets. Since the great majority of the genes are only represented by a single probe set in the microarrays, the difference in hybridization performance between individual probe sets can explain, at least partially, why only approximately a third of the differential expression of the candidate genes identified by microarrays could be verified by qRT-PCR. Finally, the fold difference in expression level measured as measured by qRT-PCR was not always consistent with that of the microarray analysis. For example, *Bmp4* showed an 8 fold increase in the ventral aspect of the 3<sup>rd</sup>pp by microarray and a 14 fold by qRT-PCR when examined on identical source of cDNA (Table 3.7). This is most likely due to sensitivity issues. In fact, such differences have been observed in other studies of microarray analysis (Buttitta *et al.*, 2003). Thus, microarray analysis is very useful for identifying genes differentially expressed between two tissues but a verification of this

differential expression by a more sensitive and more reliable method such as qRT-PCR is strongly recommended.

In the next sections, the candidate genes whose differential expression was verified by qRT-PCR will now be more deeply commented about their eventual function in the thymus within the context of their categorical biological activity or signalling pathway.

## **4.2 Genes that are involved in the chemotaxis and that are upregulated in the 3<sup>rd</sup>pp**

The chemokine *CCL21* (a T-cell chemoattractant) is the only chemokine that has been noticed to be upregulated in the 3<sup>rd</sup>pp when compared to the 2<sup>nd</sup>pp (Table 3.9) but was not found to be differentially expressed between the dorsal and the ventral aspect of the 3<sup>rd</sup>pp (result not shown). An IHC analysis for *CCL21* at E10.5 and at E11.5 revealed that its expression in the 3<sup>rd</sup>pp was confined to the anterior domain of the pouch (Fig.3.12), a domain where *FoxN1* expression was also observed to be restricted to (result not shown). Taken together, these expression data for *CCL21* are highly indicative for a role of *CCL21* in the recruitment of T cells precursors to the fetal thymus. This finding is in keeping with a recent report that demonstrates that *CCL21* is involved in the recruitment of the T-cell precursors to the fetal thymus (Liu *et al.*, 2005). Two other chemokines, *CXCL12* (Table 3.8) and *CXCL13* (Table 3.7) were the only chemokines noticed to be differentially expressed between the dorsal and the ventral aspect of the 3<sup>rd</sup>pp. *CXCL12* was found to be strongly upregulated in the dorsal aspect of the 3<sup>rd</sup>pp (Table 3.8 & Fig.3.44) whereas *CXCL13* was found to be exclusively expressed in the ventral aspect of the 3<sup>rd</sup>pp (Table 3.7 & Fig.3.21). Interestingly, *CXCL12* is a T-cell chemoattractant that was found to be one of the rare chemokines to attract T-cell precursors (DN1 population) with *CCL21* and *CCL25* (Liu *et al.*, 2005). In contrast to *CXCL12*, *CXCL13* was shown to be unable to attract T-cells (Legler *et al.*, 1998). The colonization of the fetal thymus was not affected by use of anti-*CXCL12* antibodies in FTOC whereas neutralizing antibodies for *CCL21* and *CCL25* affected DN1 entry to fetal thymic lobes (Liu *et al.*, 2005). Hence, as suggested by Liu and colleagues, *CCL21* and *CCL25* chemokines in contrast to *CXCL12* have a role in the recruitment of T-cell precursors to the fetal thymus. Nevertheless, *CXCR4* (the receptor for *CXCL12*) has been shown

to be critical for T-cell progenitor localization within the cortex of the thymus as thymus-specific deletion of CXCR4 *in vivo* results in failed cortical localization of immature thymocytes (Plotkin *et al.*, 2003). Furthermore, the expansion of T-cell precursors at the DN3, DN4 and at the DP stage has been shown to be affected during embryogenesis in mice deficient for CXCL12 or CXCR4 (Ara *et al.*, 2003). Thus, the notification that *CXCL12* was found to have an increase in expression in the dorsal aspect of the 3<sup>rd</sup>pp was especially surprising as this anatomical site will give rise to the parathyroids, an organ devoided of T cells. Also astonishing is the expression of CXCL13 in the ventral circumference of the 3<sup>rd</sup>pp as CXCL13 was shown to be unable to attract T lymphocytes but rather acts as a B-cell chemoattractant (Legler *et al.*, 1998). Collectively, these findings suggest that CXCL12, CXCL13 and CCL21 may have a different role in organogenesis beside their chemokine function. However, neither CXCL12 nor CXCL13 are crucial for thymus development as mice deficient for either of these genes display normal thymus organogenesis (Ansel *et al.*, 2000; Ma *et al.*, 1998).

### **4.3 Differential expression of transcriptional regulators within the 3<sup>rd</sup>pp**

Regular thymus patterning is dependent on several transcription factors including FoxN1, Pax1, Pax9, Hoxa3, Six1 and Eya1 (see Introduction). All these genes are encoding for factors whose transcripts were detected by microarrays within the 3<sup>rd</sup>pp (Annex 2). But among these transcripts, only those of FoxN1 and Pax1 have previously been reported to be differentially expressed between the 3<sup>rd</sup>pp, the 2<sup>nd</sup> and the 4<sup>th</sup>pp (Gordon *et al.*, 2001; Wallin *et al.*, 1996). *Ehox* is an other transcriptional regulator that can be added to this list of genes previously reported to be differentially expressed but its function for the thymus needs still to be defined (Jackson *et al.*, 2003). Notably, *Six1* was observed to have a considerable increase of expression in the ventral aspect of the 3<sup>rd</sup>pp when compared to the dorsal circumference of the 3<sup>rd</sup>pp by microarray analysis (Annex 2) but this differential expression could not be confirmed in a qRT-PCR analysis (result not shown). In contrast, the transcription factors Ypel1, Dmrt2, Znf297, Meox2 and Klf16 could be identified to be differentially expressed between the 2<sup>nd</sup> and the 3<sup>rd</sup>pp (Table 3.2). *Meox2* and *Klf16* expression were confined to the 3<sup>rd</sup>pp with only the former demonstrating a 2 fold increase in expression in the ventral epithelium when compared to the dorsal circumference (Fig.3.21). Taken together, these data reveal that among the transcription factors identified to be differentially expressed between the 3<sup>rd</sup>pp, the 2<sup>nd</sup> and the 4<sup>th</sup>pp only two genes, *FoxN1* and

*Meox2* as well as *Gcm2* demonstrated a clear differential expression within the 3<sup>rd</sup>pp. Interestingly, *Meox2* has been demonstrated to physically interact with *Pax3*, which is required for the correct development of the thymus and to regulate *Pax3* expression in the limb (Conway *et al.*, 1997; Franz, 1989; Mankoo *et al.*, 1999). Similarly, *Meox1*, an other transcription factor which was revealed to be expressed in the 3<sup>rd</sup>pp (Fig.3.9), has been shown to physically interact with *Pax1* to act in concert with *Meox2* upstream of *Pax1* and *Pax3* during limb development (Mankoo *et al.*, 2003; Stamatakis *et al.*, 2001). Taken together, these findings evolve the possibility that *Pax1* and *Pax3* thymic expression might be regulated by *Meox1* and *Meox2* but this has yet to be demonstrated. In addition, *Meox2* may also associate with *Msx2*, one of the transcription factors which was shown to be preferentially expressed within the 3<sup>rd</sup>pp in the ventral aspect (Table 3.7 and Fig.3.21) and which has been demonstrated to operate downstream of *Bmp4* and upstream of *FoxN1* in the skin (Andl *et al.*, 2004; Ma *et al.*, 2003). *Msx2* and *Meox2* are genes that are expressed in the epithelium of the 3<sup>rd</sup>pp but as well in the mesenchymal cells in proximity of that pharyngeal pouch (Fig.3.13)(Bleul and Boehm, 2005). Similarly, *Meox2* and *Msx2* were both found to be expressed in epithelial and mesenchymal cells of the human placenta where both of them have been suggested to regulate the mesenchymal-epithelial interaction (Quinn *et al.*, 2000). Since *Bmp4* and *FoxN1* are both upregulated in the ventral circumference of the 3<sup>rd</sup>pp and that thymic *Msx2* expression is affected in mice transgenic for *noggin* under *FoxN1* promoter, these findings may predict that *Meox2* and *Msx2* may act in concert to regulate thymic mesenchymal-epithelial interaction (Quinn *et al.*, 2000).

A role for *Klf16* and *Dmrt2* in the thymus development is less clear as *Klf16* (a.k.a. DRPP, Dopamine-receptor regulating transcription factor) has been demonstrated to regulate dopamine receptors, whereas *Dmrt2* is a sex-determining gene (Hwang *et al.*, 2001; Muroya *et al.*, 2000). In contrast, the transcription factor *Ypel1* may despite a very small increase (2,23 fold, Table 3.2) in expression in the 3<sup>rd</sup>pp when compared to the 2<sup>nd</sup>pp play an important role in the commitment of endodermal cells of the ventral aspect of the 3<sup>rd</sup>pp to an epithelial cell fate, as transfection of mouse fibroblasts with *Ypel1* induces an epithelial-like morphology (Farlie *et al.*, 2001). However, as the cells of the 2<sup>nd</sup>pp are also epithelial cells, other factors are most likely required that may act in concert with *Ypel1* to specify the commitment of endodermal cells of the ventral aspect of the 3<sup>rd</sup>pp to adopt a thymic epithelial cells fate.



When comparing the expression of the genes between the ventral and the dorsal aspect of the 3<sup>rd</sup>pp by microarrays, the transcription factors *Ebf1*, *Msx2*, *FoxG1* and *Tbx3* were identified to be upregulated if not exclusively expressed in the ventral circumference of the 3<sup>rd</sup>pp (Table 3.7, Fig.3.21 and Fig.3.22). *FoxG1* has been demonstrated to be positioned downstream of *Tbx1* as *FoxG1* expression is downregulated at E9.5 in the entire pharyngeal region of *Tbx1* deficient mice (Ivins *et al.*, 2005). *Tbx3* was shown to specify the identity of the posterior digits through *Shh* and *Bmp* signalling (Suzuki *et al.*, 2004). Since *Shh* and *Bmp* are two genes that have been shown to play a role in the patterning of the thymus to the ventral aspect of the 3<sup>rd</sup>pp (see Introduction), it is therefore conceivable that *Tbx3* might be involved in the dorsal-ventral patterning. *Ebf1* is an early B-cell factor whose expression was even found within the 3<sup>rd</sup>pp to be restricted to the ventral aspect (Fig.3.21). However, mice deficient for *Ebf1* have a normal thymus (Lin and Grosschedl, 1995). In regard to *Msx2*, this gene may be involved in the thymus in a *Bmp4*/*FoxN1* pathway that was suggested to operate in the epithelial skin development (Ma *et al.*, 2003) since both of these genes are expressed in the ventral aspect of the 3<sup>rd</sup>pp. However, a study from Bleul and colleagues showed that blocking thymic *Bmp* signalling in transgenic mice for *noggin* does not influence *FoxN1* expression, although a hypoplastic thymus was found to be ectopically located with an altered expression of *Msx1* and *Bmp4* in these mice (Bleul and Boehm, 2005). In that regard, a recent study of *Msx1* and *Msx2* double deficient mice reported an abnormal location of the thymus (Ishii *et al.*, 2005). Furthermore, *Msx1* was found to be expressed in the 3<sup>rd</sup>pp (see Annex 2). Taken together, these findings suggest that *Msx2* in concert with *Msx1* play a role in the migration of the thymus/parathyroid primordium from the pharyngeal region to the mediastinum.

Expression profiling of the dorsal side of the 3<sup>rd</sup>pp revealed that *FoxA1*, *FoxA2* and *Tbx1* transcription factors are expressed at least 3 times more when compared to the 3<sup>rd</sup>pp epithelia of the ventral circumference (Table 3.8 & Fig.3.44). *FoxA2* was identified as being upstream of *Tbx1* by binding to a Fox box regulatory element of *Tbx1* promoter under *Shh* signalling in the pharyngeal endoderm at E9.5 (Yamagishi *et al.*, 2003). Therefore, *FoxA2* and *Tbx1* upregulation in the dorsal aspect of the 3<sup>rd</sup>pp are consistent with these findings. In contrast, *Shh* expression was not observed by microarray and by IHC analysis to be differentially expressed between the dorsal and the ventral aspect of the 3<sup>rd</sup>pp (data not shown). Considering this together with the fact that *Tbx1* deficiency was shown to be responsible for the DiGeorge syndrome, it is nevertheless

conceivable that FoxA2 may be required for normal levels of Tbx1 expression in the ventral aspect of the 3<sup>rd</sup>pp and hence be required for the normal development of the thymus (Jerome and Papaioannou, 2001; Lindsay *et al.*, 2001; Merscher *et al.*, 2001).

The last transcription factor that was revealed to be differentially expressed between the dorsal and the ventral aspect of the 3<sup>rd</sup>pp is Sp8 (Fig.3.25). Sp8 was initially identified as being a potential candidate gene involved in thymus organogenesis when a study in the limb revealed that Sp8 lies upstream of Fgf8, a gene when mutated in mice can phenocopy the complete array of anomalies of the DiGeorge syndrome (Frank *et al.*, 2002b; Kawakami *et al.*, 2004). In addition, Sp8 was revealed to be downstream of Fgf10 and further expression analysis of that study presented evidence that during early limb development it is required for maintaining but not for initiating Wnt/beta-catenin-dependent FGF, Shh, and BMP-mediated signalling (Bell *et al.*, 2003; Treichel *et al.*, 2003). However, embryos deficient for Sp8 revealed that at E10.5 the 3<sup>rd</sup>pp appeared to be normal (Fig.3.30) and that at E18.5 the size and location of the thymic lobes were undistinguishable from wild type mice (not shown). In regard to the absence of detection of  $\beta$ -galactosidase in the pharyngeal region by lacZ and IHC stainings of Sp8 deficient E10.5 (Fig.3.35), this result was unexpected as *Sp8* is expressed according a qRT-PCR analysis in the 3<sup>rd</sup>pp at levels about 10 times higher than for example *Phlda2* (Fig.3.25), whose protein product was clearly detected by IHC (Fig.3.28). An explanation for this unexpected finding is that the feedback mechanism that has been proposed to occur for Sp8 in the development of the AER (apical ectodermal ridge) might operate as well in the pharyngeal region in order to express normal levels of Sp8 (Bell *et al.*, 2003).

#### **4.4 Differential expression of cell surface antigens in the ventral aspect of the 3<sup>rd</sup>pp**

The differential expression analysis between the dorsal and the ventral aspect of the 3<sup>rd</sup>pp identified three cell surface antigens CD6, CD44 and CD200 to be exclusively expressed in the ventral circumference of the 3<sup>rd</sup>pp (Table 3.7, Fig.3.21). CD6 is an accessory molecule that is primarily expressed on thymocytes where it is believed to be involved in T-cell activation and/or differentiation and this immunological function of CD6 may contribute to thymocyte survival and

selection (Gimferrer *et al.*, 2003; Singer *et al.*, 2002). CD6 expression in the ventral aspect of the 3<sup>rd</sup>pp at E10.5 was unexpected as ligands for CD6 (CD166) were shown to be expressed in the thymic epithelium as well (Singer *et al.*, 2002). CD44 expression within the pharyngeal region was essentially restricted to the 2<sup>nd</sup>pp and the ventral aspect of the 3<sup>rd</sup>pp (Fig.3.25 and Fig.3.26) but the expression of some CD44 splice variants (i.e. CD44v6 and CD44v10) were exclusively found to be expressed in the ventral circumference of the 3<sup>rd</sup>pp (Fig.3.26). These findings for CD44v6 and CD44v10 splice variants are indicative for a role of these isoforms in the thymus. In that regard, functional studies demonstrated that only cells expressing CD44 isoforms (CD44v) from fetal liver and adult bone marrow could efficiently populate fetal thymic stroma and develop into mature T cells (Schwarzler *et al.*, 2001). Furthermore, in fetal thymic organ cultures, anti-CD44v antibodies specifically blocked thymocyte development and presented evidence that CD44v are required for the initial interaction of haematopoietic progenitor cells with the thymic stroma (Schwarzler *et al.*, 2001). Other fetal thymic organ cultures (FTOCs) revealed a role for CD44 molecules in the emigration of thymocytes as the adjunction of anti-CD44 antibodies to these FTOCs decreased the emigration of mature thymocytes (Esser *et al.*, 2004). However, CD44 deficient mice have been reported to have a normal and functional development of the thymus (Protin *et al.*, 1999). The presence of regular thymus development and function, despite the lack of CD44 in these mice, may reflect the redundant role of CD44, which could eventually be compensated by Rhamm, as this latter gene is a product acting as an alternative hyaluronan receptor. Rhamm is indeed highly expressed in the 3<sup>rd</sup>pp at E10.5 (data not shown) and could compensate in situ for the loss of CD44 function, which has recently been observed in murine models of inflammation (Nedvetzki *et al.*, 2004). Interestingly, the intracellular domain of CD44 was also recently demonstrated to physically interact with Smad1 (member of the Tgf $\beta$ -signaling pathway) upon Bmp7 stimulation (Peterson *et al.*, 2004). Smad1 and Bmp7 were both found to be highly expressed in the 3<sup>rd</sup>pp at E10.5 (Annex 2). These findings may predict CD44 as a modulator of the Tgf $\beta$  signalling pathway, in particular when knowing that the Tgf $\beta$ -signaling pathway has been demonstrated to be involved in thymus organogenesis (Bleul and Boehm, 2005; Ohnemus *et al.*, 2002).

CD200 has been shown to deliver an inhibitory signal to cells of the macrophage lineage as these cells in mice, which are deficient for CD200, were more numerous. However, the thymus as well as the development of its thymocytes in these mutant mice is normal (Hoek *et al.*, 2000).

## 4.5 Differential expression of genes involved in growth factor signalling in the 3<sup>rd</sup>pp

A qRT-PCR analysis for the expression of *Fgf8* and *Fgf10* and their respective receptors, *Fgfr2IIIb* and *Fgfr1*, has revealed that these genes were expressed in the 3<sup>rd</sup>pp at levels comparable between the dorsal and the ventral circumference of that pouch and are at comparable levels of expression in the 2<sup>nd</sup>pp and 4<sup>th</sup>pp (Fig.3.23, Annex 2 and result not shown). In contrast, *Fgf12* was clearly differentially expressed between the 3<sup>rd</sup>pp and the 2<sup>nd</sup>pp (Fig.3.9, Fig.3.11 and Table 3.4). Expressed in the developing brain, the connective tissue of the limb and the heart, the function of *Fgf12* still remains unknown (Hartung *et al.*, 1997; Smallwood *et al.*, 1996).

Among the candidate genes that were revealed to be differentially expressed within the 3<sup>rd</sup>pp and that have a potential role to be involved in growth factor signalling of the thymus are the two following genes: *Phlda2* and *Flrt3* (Fig.3.21 and Table 7.3). The *Phlda2* (a.k.a. IPL and Tssc3) gene lies in an extended imprinted region of distal mouse chromosome 7, which also encodes for the insulin-like growth factor 2 (*Igf2*) gene. Expression of *Phlda2* is highest in placenta and the yolk sac, where its mRNA is derived almost entirely from the maternal allele (Frank *et al.*, 2002a). *Phlda2* encodes a small cytoplasmic protein with a pleckstrin-homology (PH) domain. Mice rendered deficient for *Phlda2* do not have a phenotype with the notable exception of an enlarged placenta (Frank *et al.*, 2002a). A defect, which could be corrected by an additional lack of *Igf2* (Frank *et al.*, 2002a). Thus, these findings indicate that *Phlda2* can act, at least in part, independently of insulin-like growth factor-2 signalling. *Igf2* was found by microarray analysis to be expressed in the 3<sup>rd</sup>pp at E10.5 (Annex 2). Mice overexpressing *Igf2*, revealed the abnormal appearance of large clusters of TECs immunoreactive to the monoclonal antibody KL1, which specifically recognizes highly differentiated TECs (Savino *et al.*, 2005). Taken together, these findings suggest that *Phlda2* might be a modulator of *Igf2* signalling in the thymic epithelium. On the other hand, *Phlda2* could be upregulated by *Tbx1* as *Phlda2* was found to be downregulated in the pharyngeal region of *Tbx1* deficient E9.5s (Ivins *et al.*, 2005). In fact, the *Phlda2* protein product was observed within the pharyngeal region to be essentially restricted to the pharyngeal endoderm lining of the 2<sup>nd</sup>, 3<sup>rd</sup> and 4<sup>th</sup>pp and not in the surrounding mesoderm (Fig.3.28). *Phlda2*

transcripts were also found to be expressed in immature but not SP thymocytes as well as in TECs (Fig.3.34). Despite this pattern of expression mice deficient for *Phlda2* had a regular thymic architecture at E13.5 as assessed by the K5 and K8 markers (Fig.3.43). Based on these data and on the fact that *Tbx1* deficient mice display thymic hypoplasia suggest that *Phlda2* might be involved in the expansion process of the thymic epithelium but if such is the case than the function of *Phlda2* in thymus appears to be redundant (Jerome and Papaioannou, 2001; Merscher *et al.*, 2001).

*Flrt3* is a gene coexpressed with *Fgf8*, a gene that was revealed from studies of mice mutant for *Fgf8* to be involved in the development of the thymus as these mutant mice displayed hypoplasia and aplasia of the thymus [Frank, 2002 #57 4](Abu-Issa *et al.*, 2002). Interestingly, *Fgf8* expression is abolished in the pharyngeal endoderm of mice deficient for *Tbx1* (Vitelli *et al.*, 2002). *Flrt3* expression can be induced and downregulated by respectively injections of *Fgf8* and dominant-negative *Fgfr1* (a receptor for *Fgf8*) in xenopus embryos (Bottcher *et al.*, 2004). In that regard, *Fgfr1* was shown to physically interact with *Flrt3* in co-immunoprecipitation analysis (Bottcher *et al.*, 2004) and an analysis of the expression of *Flrt3* in the thymus revealed that it was found to be expressed in adult TECs (Fig.3.34) as well as in TEC cell lines (Fig.3.35), but not in thymocytes (Fig.3.34). Taken together, these findings may predict a model where *Flrt3* is involved in the *Fgf8* signalling of thymic epithelial cells and where *Fgf8* is downstream of *Tbx1*.

#### **4.6 Genes involved in Wnt-mediated signalling are differentially expressed in the 3<sup>rd</sup>pp**

Wnt signal molecules (including *Wnt4* and *Wnt5b*) are present in the 3<sup>rd</sup>pp without displaying a pattern of differential expression between the dorsal and ventral aspect of the pouch at E10.5 (Balciunaite *et al.*, 2002). In contrast, three inhibitors of the Wnt signalling pathway (*WIF1*, *Nkd1* and *Sfrp2*) were found to be differentially expressed within the 3<sup>rd</sup>pp at E10.5 by microarray analysis (Table 3.7, Fig.3.21 and Fig.3.44). *WIF1* and *Sfrp2* antagonizes Wnt signalling, whereas *Nkd1* effect its function via inhibiting dishevelled signal transduction (Hsieh *et al.*, 1999; Hunter *et al.*, 2004; Lee *et al.*, 2000; Wharton *et al.*, 2001; Zeng *et al.*, 2000). In fact, *WIF1* has been demonstrated to physically interact with *Wnt4* whereas *Sfrp2* competes with membrane-bound

frizzled receptors for the binding of Wnts (i.e. Wnt1, Wnt4) (Hunter *et al.*, 2004; Lee *et al.*, 2000). Since Wnt4 interacts with WIF1 and that Wnt4 has been shown to upregulate the expression of FoxN1 in the cTEC1.2 cell line, the upregulation of WIF1 protein levels in the ventral aspect of the 3<sup>rd</sup>pp (Fig.3.29) may predict a role for WIF1 in modulating Wnt4/ $\beta$ -catenin/FoxN1 signaling in thymic epithelium (Balciunaite *et al.*, 2002). This antagonizing role of WIF1 in Wnt4 signalling could be possibility supported by the contribution of Nkd1 as both were observed to be upregulated if not exclusively expressed in the ventral aspect of the 3<sup>rd</sup>pp. In fact, both molecules were reported to be co-upregulated in a murine granulosa cell tumor (Boerboom *et al.*, 2006).

An examination of WIF1 protein level of expression by IHC in the pharyngeal region of E10.5s revealed that WIF1, in addition to its expression in the 3<sup>rd</sup>pp, was also detected in the 2<sup>nd</sup> and 4<sup>th</sup>pp (Fig.3.27A&B). However, these results contrast with qRT-PCR data that revealed that WIF1 was expressed in the 3<sup>rd</sup>pp but not in the 2<sup>nd</sup> or the 4<sup>th</sup>pp (Fig.3.24). This conflicting set of results may be explained by the fact that the anti-WIF1 antibody used in IHC may recognize an epitope within the well conserved and large WIF (Wnt inhibitory factor) domain of WIF1, which is known to be shared with other proteins (e.g. RYK, receptor-like tyrosine kinase) (Cheyette, 2004; Patthy, 2000). This explanation is not unlikely because RYK is a coreceptor of the canonical Wnt signaling pathway that was revealed by microarray analysis to be clearly expressed at E10.5 in the 2<sup>nd</sup>, 3<sup>rd</sup> and 4<sup>th</sup>pp (Annex 2) and since about half of the peptide sequence of the mouse recombinant WIF1 used for immunisation corresponds to the WIF domain (Cheyette, 2004; Keeble *et al.*, 2006; Lu *et al.*, 2004). Hence, if this is the case, part of the staining in the IHCs for WIF1 might have been contributed by the binding of anti-WIF1 antibody to other proteins sharing a WIF domain such as Ryk. By E12.5, the expression of WIF1 was most likely restricted to some clusters of thymic epithelial cells (Fig.3.27D) as WIF1 was not found in adult mice to be expressed by thymocytes but in TECs (Fig.3.34). WIF1 thymic epithelial cell expression was noticed to be more prominently expressed in comparison to FoxN1 before E16.5 (Fig.3.33) suggesting that the WIF1 antagonizing function in Wnt signaling seems to play a role in the early stages of thymus organogenesis. When trying to reveal the importance of this role in FTOCs of E13.5 thymi in presence of an increasing amount of affinity purified hWIF-IgG in the thymus, it was noticed that overexpressing WIF1 at not too high levels in these FTOCs enhanced the overall cellularity of thymocytes (Fig.3.40) but did not appear to affect the normal

development of thymocytes (Fig.3.41 and Fig.3.42). Nevertheless, the Wnt-signalling cascade is known to be required for several crucial steps during early embryogenesis and its activity is modulated by various agonists and antagonists to provide spatiotemporal-specific signalling (Creyghton *et al.*, 2006). Thus, the restricted pattern of WIF1 thymic epithelial expression observed at E12.5 may suggest together with the finding that WIF1 can influence the expansion of immature thymocytes that Wnt signalling operates in the cross-talk between TECs and thymocytes and that this regulation could be tightly modulated spatiotemporally by WIF1. In addition, this antagonizing activity of WIF1 could be synergized or sustained by other antagonist of the Wnt signalling such as *Nkd1*, *Sfrp2* and *Dkk3* (Dickkopf 3) all noticed to be expressed in the ventral aspect of the 3<sup>rd</sup>pp (Fig.3.21, Fig.3.44 and results not shown). The pattern of expression of these antagonists do not necessarily have to overlap but could alternatively be differentially expressed within the thymus, as it is the case for *Sfrp1* and *Sfrp2* during the metanephric development (Yoshino *et al.*, 2001). In that regard, WIF1 and *Dkk3* could be coexpressed in the thymus as a study of Wnt antagonists in gastrointestinal tissues revealed that WIF1 and *Dkk3* were both upregulated and coexpressed in the deep gastric glands and colonic crypt bases, a region where stem cells reside (Byun *et al.*, 2005). Based on these findings, the authors of that study have suggested that WIF1 and *Dkk3* could contribute to the maintenance of the gastric stem cell pool. In that regard, *WIF1* adult thymic expression was noticed by qRT-PCR analysis to be close to the limit of detection (Fig.3.33) in contrast to *FoxN1*, while thymic WIF1 protein product could not even be detected by IHC in adult mice (result not shown). Thus, these results might predict that WIF1 adult thymic expression is much more restricted than *FoxN1* within the epithelium of the thymus. Hence, as proposed for the stomach, WIF1 may eventually be expressed in close proximity of rare populations of thymic epithelial such as TEC progenitors and may serve to maintain for instance this latter population of cells undifferentiated. If such is the case, then WIF1 is predicted to act in a paracrine way on thymic epithelial progenitor cells since *WIF1* thymic expression was observed in *MTS24<sup>-</sup>* TECs but not in *MTS24<sup>+</sup>* TECs (Fig.3.34). Taken together, the notification of the differential expression of several Wnt antagonist (i.e *WIF1*, *Nkd1* and *Sfrp2*) within the 3<sup>rd</sup>pp suggests that Wnt signaling is spatiotemporally regulated between the dorsal and the ventral aspects of the 3<sup>rd</sup>pp and is most likely regulated this way as well within the developing thymus. This spatiotemporally regulation of these factors might be essential for a proper patterning and/or differentiation of the thymic

epithelium. To reveal such an eventual role for WIF1 in thymus organogenesis, mice rendered deficient for WIF1 are now being generated in our lab.

#### **4.7 Differential expression within the 3<sup>rd</sup>pp of genes involved in the Tgf $\beta$ signalling**

Four genes (Bmp4, Fst, Bambi and Tgf $\beta$ 2), all involved in the Tgf $\beta$  signalling pathway were identified to be upregulated in the ventral aspect of the 3<sup>rd</sup>pp when compared to the dorsal circumference (Table 3.7 & Fig.3.21). Bmp4 and Tgf $\beta$ 2 are activators whereas Fst and Bambi are inhibitors of the Tgf $\beta$  signalling pathway. The expression of these ligands correlates well with the presence of several receptors belonging to this family of signalling molecules such as Bmpr1 (Bmp receptor 1) and Acvr2 (activin receptor 2). In fact, the Tgf $\beta$  signalling pathway has been previously demonstrated to be implicated in thymus organogenesis (Bleul and Boehm, 2005; Ohnemus *et al.*, 2002). These studies were based on the analysis of the thymus from mice transgenic for noggin under the control of a genomic fragment of either the Hoxa2 or of the FoxN1 promoter. Both of these transgenic mice were reported to have a hypoplastic thymic tissue, which was ectopically located when found but functional in thymopoiesis (Bleul and Boehm, 2005; Ohnemus *et al.*, 2002). These observations also relate to the present finding that Noggin, an antagonist of Bmp4, is expressed in the dorsal but not in the ventral aspect of the 3<sup>rd</sup>pp (Patel *et al.*, 2006) and Annex2. Interestingly, Shh deficient mice do have an absence of Gcm2 and an expansion of Bmp4 and FoxN1 expression throughout the 3<sup>rd</sup>pp, which results in an subsequent absence of development of the parathyroid glands (Moore-Scott and Manley, 2005). In other studies, Shh and Bmp4 proteins were shown to negatively regulate each others transcription and resulting in a strict complementarity between these two gene patterns on each side of the Hensen's node in chick embryos (Monsoro-Burq and Le Douarin, 2001). Taken together, these findings suggest that Shh signalling and Noggin limits Bmp4 signalling throughout the entire 3<sup>rd</sup>pp and are required to pattern the thymus anlage to the ventral aspect and the parathyroids to the dorsal circumference of the 3<sup>rd</sup>pp (Moore-Scott and Manley, 2005; Patel *et al.*, 2006). These observations also strongly suggest a direct role for Bmp4 in the thymic development. Using overexpressing studies of Bmp4 in thymic organ cultures, it was concluded that Bmp4 modulates thymic stroma, alters FoxN1 transcription and regulates thymocyte DN1



differentiation via a molecule mechanism engaging Fgf signalling (Hager-Theodorides *et al.*, 2002; Tsai *et al.*, 2003). However, a role for Bmp4 appears to be redundant since the inhibition of Bmp4 signalling by overexpression of Noggin did not affect the normal thymocyte differentiation in vivo (Bleul and Boehm, 2005). In keeping with this in vivo observation, FTOCs exposed to Noggin display an accelerated rate of thymopoiesis (Hager-Theodorides *et al.*, 2002). To elucidate precisely the role of Bmp4 in early thymus organogenesis, mice rendered deficient for Bmp4 expression in the thymic epithelium shall be generated as conventional knockout mice die between E6.5 and E9.5 (Winnier *et al.*, 1995).

Fst (Follistatin) and Bambi are two inhibitors of the Tgf $\beta$  signalling pathway that were identified to be expressed in the ventral aspect of the 3<sup>rd</sup>pp (Grotewold *et al.*, 2001; Nakamura *et al.*, 1991; You and Kruse, 2002). The spatiotemporal expression pattern of Bambi closely matches that of Bmp4 during mouse embryonic development and this inhibitor is part of a feed-back mechanism that is upregulated in response to activation of the Tgf $\beta$  signalling pathway (as well as Wnt signalling) (Sekiya *et al.*, 2004a) (Grotewold *et al.*, 2001; Sekiya *et al.*, 2004b). Follistatin is a secreted and activin-binding protein and as well as an activin (member of the Tgf $\beta$  signalling pathway) antagonist in vitro that can bind to heparan sulphate proteoglycans and that may function in vivo to present activins to their receptors. In that regard, activin (a.k.a. as inhba) was revealed by microarrays to be strictly confined to the ventral aspect of the 3<sup>rd</sup>pp when compared to its dorsal counterpart (Annex 2). In the mouse, Follistatin messenger RNA is first detected in the deciduum (on embryonic day 5.5), and later in the developing thymus, gut, hindbrain, somites, vibrissae, teeth, epidermis, muscle (Matzuk *et al.*, 1995) and Fig.3.36. At E11.5, Fst is strongly expressed in the epithelium of the 3<sup>rd</sup>pp when compared to its surrounding mesoderm (Fig.3.29). Interestingly, the progressive decrease of *Fst* expression from the 2<sup>nd</sup>pp to the 4<sup>th</sup>pp observed by qRT-PCR (Fig.3.25) contrasts with changing gradient of *Bmp4* expression from the 2<sup>nd</sup>pp to the 4<sup>th</sup>pp in the opposite direction (Fig.3.25). Moreover, when analysing Fst expression by IHC at E10.5 and E11.5, Fst proteins were noticed to be also detected at considerable levels in the extracellular matrix (ECM) between the anterior and posterior endodermal cells of the 3<sup>rd</sup>pp (Fig.3.29). In that regard, Nakamura and colleagues have suggested that Fst binds to heparan sulfate side chains of proteoglycans of the ECM to regulate the various actions of activin (Nakamura *et al.*, 1991).

Other studies on *Fst* have revealed that *Fst* is induced by activin signalling in dental epithelium and that *Fst* inhibits the ameloblast-inducing activity of *Bmp4* in which the ameloblasts are derived from dental epithelium (Wang *et al.*, 2004). In fact, overexpressing *Fst* in the murine dental epithelium resulted in an inhibition of ameloblast differentiation while *Fst* deficient mice display ameloblasts that differentiate ectopically (Wang *et al.*, 2004). These findings may predict a role for *Fst* in the patterning and/or differentiation of the thymus primordium since *Fst* and *Bmp4* were both found to be upregulated in the ventral aspect of the 3<sup>rd</sup>pp when compared to the dorsal circumference. In regard to thymic *Fst* expression, *Fst* could operate downstream of *Tbx1*, as *Fst* was shown to be downregulated in the pharyngeal region of *Tbx1* deficient E9.5s (Ivins *et al.*, 2005). But *Fst* could also be a downstream target of activin signalling (as in dental epithelium) or of *Wnt4* signalling (as in mammalian ovary) or of both signalling pathways since *Wnt4* and *Activin* were both found to be expressed in the ventral aspect of the 3<sup>rd</sup>pp (Wang *et al.*, 2004; Yao *et al.*, 2004).

*Fst* is also expressed in the adult thymus by primary epithelial cells and thymocytes at comparable levels (Fig.3.34) as well as in all examined TEC cell lines (Fig.3.35). Among primary epithelial cells, *Fst* was considerably more abundant in MTS24<sup>+</sup> when compared to MTS24<sup>-</sup> TECs (Fig.3.34) and was maintained throughout fetal and post-natal development. These findings are compatible with the notion that *Fst* (together with other inhibitors of Tgf $\beta$ -signaling, such as *Bambi*) might be controlled by activin/*Bmp4*/Tgf $\beta$ 2 and/or *Wnt4* mediated signalling. In that regard, *Fst* may modulate in the developing thymus the actions of several members of the transforming growth factor-beta family that were found to be expressed in the ventral aspect of the 3<sup>rd</sup>pp (i.e. Tgf $\beta$ 2, *Bmp4*, *activin*) as defects in mice deficient for *Fst* are more widespread than those seen in *activin*-deficient mutant mice (Matzuk *et al.*, 1995). However, a function for *Fst* in the thymus has not been reported so far as studies on *Fst* deficient mice have not been reported to have a thymus defect (Matzuk *et al.*, 1995).

#### **4.8 Increased expression of c-Myc, a target gene of Wnt and Tg $\beta$ signalling in the ventral aspect of the 3<sup>rd</sup>pp**

The *c-Myc* gene is an oncogene that in conjunction with other gene products promotes cell growth and transformation and is essential for vasculogenesis and angiogenesis during tumor development and progression (Baudino *et al.*, 2002). *c-Myc* is upregulated in the ventral aspect of the 3<sup>rd</sup>pp (Table 3.7, Fig.3.21). *c-Myc* was also demonstrated to play a role in neural crest specification as well as the finding that the transcriptional regulation of *c-Myc* acts in response to the activation of the Wnt and of the Tg $\beta$  signalling pathways (Barembaum and Bronner-Fraser, 2005; Hu and Rosenblum, 2005; Paez-Pereda *et al.*, 2003). *c-Myc* is expressed in the pharyngeal region at levels comparable between the 2<sup>nd</sup>pp, 3<sup>rd</sup>pp and 4<sup>th</sup>pp (Fig.3.25). The thymic expression of *c-Myc* remained unchanged over time when analysing unseparated tissue at different embryonic stages and in the adult animal Fig.3.33). In the latter, *c-Myc* is expressed at comparable levels by thymocytes and by primary thymic epithelial cells (Fig.3.34). Mice deficient for *c-Myc* die by E10.5 displaying a growth deficiency as well as cardiac and neural developmental defects (Baudino *et al.*, 2002). These defects are associated in part with a requirement of *c-Myc* for the expression of the vascular endothelial growth factor (VEGF) (Baudino *et al.*, 2002). VEGF on the other hand has been shown to upregulate *Tbx1* expression in the pharyngeal region. A target deletion of VEGF in TECs revealed an hypovascularized thymus (Muller *et al.*, 2005; Stalmans *et al.*, 2003). Moreover, mice deficient for either *Tbx1* or for an isoform of VEGF (VEGF<sup>164</sup>) have both defects including the thymus similar than those observed in the DiGeorge syndrome (Stalmans *et al.*, 2003). *c-Myc* has also been shown to be required for the expression of Angiopoietin 2 (*Agpt2*) in embryonal stem and yolk sac cells (Baudino *et al.*, 2002). *Agpt2* is a gene that was found to be upregulated in both the ventral and dorsal epithelial cells of the 3<sup>rd</sup>pp when compared to those of the 2<sup>nd</sup>pp (Table 3.2 & 3.6, Fig.3.13). *Agpt2* is involved in the angiogenesis of the parathyroids and is transcriptionally upregulated by PTH (Parathyroid hormone), which in fact also upregulates *VEGF* expression (Carter and Ward, 2001). It is therefore not a surprise that *Agpt2* is expressed in the common thymic-parathyroid primordium at E10.5 (Fig.3.13). All these findings suggest that under the control of Wnt and/or Tg $\beta$  signalling, *c-Myc* may possibly be involved in a regulation model of the thymus in which it is upstream of *Agpt2* and VEGF while the latter one upregulates *Tbx1* expression for a proper

development of the thymus epithelium and/or blood vessel architecture. To elucidate precisely the role of c-Myc in thymus organogenesis mice rendered deficient for c-Myc expression in the thymus epithelium need to be generated as conventional mice die by E10.5 (Baudino *et al.*, 2002).

#### **4.9 Increased expression of Tnfrsf19 in the ventral aspect of the 3<sup>rd</sup>pp**

Tnfrsf19 (a.k.a. Toxicity and JNK inducer Taj or alternatively designated Troy) is a member of the tumor necrosis factor receptor superfamily (TNFR) that was revealed to be upregulated (4.32 fold) in the ventral aspect when compared to the dorsal circumference of the 3<sup>rd</sup>pp (Fig.3.21). Tnfrsf19 is involved in signalling via the nuclear factor kappaB (NFκB) through interaction with Traf6, which controls the maturation of a subpopulation of medullary TECs (mTECs) and was also expressed in the 3<sup>rd</sup>pp (see Annex 2) but without a considerable difference between the ventral and dorsal side (Akiyama *et al.*, 2005; Kojima *et al.*, 2000; Ohazama *et al.*, 2004). Tnfrsf19 was shown to be a target of Wnt signalling (Buttitta *et al.*, 2003). Taken together, these findings may predict that Tnfrsf19 is targeted by Wnt signalling to induce or upregulate signal transduction via Traf6 and NFκB and hence promote the differentiation of thymic epithelial progenitors into a mTEC cell fate.

#### **4.10 Increased expression of Delta-like homolog 1 in the ventral aspect of the 3<sup>rd</sup>pp**

Delta-like homolog 1 (Dlk1 a.k.a. preadipocyte factor Pref1), which displays as indicated by its name a homology to Delta-like 1 (Dll1). Dlk1 is a member of the epidermal growth factor-like family and has been shown to be a regulator of adipocyte differentiation (Moon *et al.*, 2002). Dlk1 is expressed in the 2<sup>nd</sup>, 3<sup>rd</sup>pp and 4<sup>th</sup>pp (Annex 2) and can be detected at higher levels in the ventral aspect of the 3<sup>rd</sup>pp when compared to the dorsal side (Fig.3.22). Dlk1 is expressed in thymic epithelial cells where it influences thymocyte cellularity (Kaneta *et al.*, 2000). In fact, when a dimeric form of Dlk1 is added to a FTOC it increases the overall number of lymphoid cells, whereas when a monomeric form of Dlk1 or the presence of anti-Dlk1 antibodies are added to a FTOC, the cellularity of lymphoid cells is reduced (Kaneta *et al.*, 2000). Signalling via Dlk1

does not apparently influence the developmental choice among the thymocyte lineages in these FTOCs (Kaneta *et al.*, 2000). Interestingly, the expression of the hairy and enhancer of split1 (*Hes1*) in thymocytes was increased in these FTOCs in presence of dimeric Dlk1, while FTOCs from mice deficient for *Hes1* were hypocellular and unresponsive to the Dlk1 dimer (Kaneta *et al.*, 2000). *Hes1* was also found to be expressed in the 3<sup>rd</sup>pp (Annex 2). Hence, these findings reveal that *Hes1* is not only expressed by thymocytes and may therefore predict that *Dlk1* also regulates *Hes1* expression in TECs. Although *Hes1* is a target of notch signalling, which has been demonstrated to be essential in T cell lineage commitment. Several delta-like ligands (i.e. Dll1, 3 and 4), which are members of the notch signalling pathway were not detected in the 3<sup>rd</sup>pp at E10.5 (Annex 2) (Kim and Siu, 1998; Radtke *et al.*, 2004; Radtke *et al.*, 1999; Wilson *et al.*, 2001). Nevertheless, *Dll1* and *Dll4* are expressed in thymic epithelial cells at E12.5 and were shown to be a downstream target of FoxN1 (Tsukamoto *et al.*, 2005). Taken together, these findings suggest that notch signalling is not operating at E10.5 in the ventral aspect of the 3<sup>rd</sup>pp and that *Dlk1* as well as *Hes1* thymic epithelial expression are most likely not dependent on Notch signalling. In that regard, *Dlk1* expression is upregulated in some tissues by FoxA2, which appears to be positioned upstream of *Tbx1* and of *Shh* signalling (Wolfrum *et al.*, 2003; Yamagishi *et al.*, 2003). However, *Tbx1* and *FoxA2* were both preferentially expressed in the dorsal epithelium within the 3<sup>rd</sup>pp (Table 3.8 & Fig.3.46).

#### **4.11 Increased expression of Neurexin 1 in the ventral aspect of the 3<sup>rd</sup>pp, a gene involved in cell-cell interaction**

Neurexin 1 (*Nrxn1*) consists of two related proteins generated by alternative use of promoters. The protein of *Nrxn1* consists of a single transmembrane region and extracellular domain with repeated sequences similar to that of laminin A. The gene for *Nrxn1* has two independent promoters so that a longer mRNA encoding for  $\alpha$ -*Nrxn1* and a shorter mRNA encoding for  $\beta$ -*Nrxn1* are generated (Rowen *et al.*, 2002). The genomic organisation consists of a total of 24 exons whereby 23 are used in the  $\alpha$ -*Nrxn1* transcript and 7 in the *Nrxn1*  $\beta$ -transcript (Rowen *et al.*, 2002). As *Nrxn1* transcripts are also extensively spliced at five sites with the sites 1, 2, and 3 unique for the  $\alpha$ -*Nrxn1* transcripts and the sites 4 and 5 common to both,  $\alpha$ -*Nrxn1* and  $\beta$ -*Nrxn1*, transcripts (Rowen *et al.*, 2002). As many as 288 different variants can be generated for  $\alpha$ -*Nrxn1*

and 4 for  $\beta$ -*Nrxn1* (Rowen *et al.*, 2002).  $\alpha$ -*Nrxn1* is a receptor for alpha-latrotoxin and neurexophilins, whereas  $\beta$ -*Nrxn1* is a receptor for neuroligins (Ichtchenko *et al.*, 1995; Missler *et al.*, 1998; Ushkaryov *et al.*, 1992). Mice deficient for  $\alpha$ -*Nrxn1* are viable and display no obvious structural phenotype but have defective release of calcium-triggered neurotransmitters (Geppert *et al.*, 1998; Kattenstroth *et al.*, 2004; Missler *et al.*, 2003). *Nrxn1* is also expressed outside of the neuronal system (Fig.3.36 and Fig.3.37). Its role may thus also relate to the formation and function of other organs.  $\beta$ -*Nrxn1* but not  $\alpha$ -*Nrxn1* transcripts were detected in the ventral aspect of the 3<sup>rd</sup>pp (Fig.3.32).  $\beta$ -*Nrxn1* binds CASK (Calcium/Calmodulin-dependent serine protein kinase), which effects the signal transduction (Zhang *et al.*, 2001). Transcripts for *Nrxn1* are ubiquitously expressed in epithelial cells lining the 2<sup>nd</sup>, 3<sup>rd</sup> and 4<sup>th</sup>pp (Annex 2). *Nrxn1* ( $\alpha + \beta$ ) expression is maintained throughout thymic development in both thymic epithelia and thymocyte with the notable exception of single positive mature thymocytes (Fig.3.33 & Fig.3.34). There is circumstantial evidence that would suggest that  $\beta$ -*Nrxn1* is a target of Bmp4, as overexpressing Bmp4 in vitro can initiate *Nrxn1* expression ectopically in the brain and it is therefore conceivable but by no means proven that this molecule plays a role in early thymus organogenesis. Support for this contention is furthermore provided by the concomitant expression of CASK in the ventral aspect of the 3<sup>rd</sup>pp and by the fact that mice deficient for *Tbx1* have downregulated the expression of *Nrxn1* as early as E9.5 (Ivins *et al.*, 2005).

#### **4.12 Genes upregulated in the ventral aspect of the 3<sup>rd</sup>pp involved in extracellular matrix interactions**

In vitro studies have demonstrated the roles of Heparan sulfate proteoglycans (HSPGs) in many cellular events. Recently, in vivo studies have begun to clarify their essential functions in organogenesis (Lin, 2004). In particular, HSPGs play crucial roles in regulating key developmental signalling pathways such as the Wnt, Hedgehog, transforming growth factor-beta and fibroblast growth factor pathways (Lin, 2004). HSPGs are part of macromolecules complexes of the cell-surface and extracellular matrix (ECM) and are composed of a core protein decorated with covalently linked glycosaminoglycan (GAG) chains (Lin, 2004). *Col1a1* (Procollagen, type1 alpha 1), *Spock2* (Sparc/osteonectin and kazal-like domains proteoglycan 2), *Galnt3* (N-acetylgalactosaminyl transferase 3) and *Hs2st1* (Heparan sulfate 2-O-sulfotransferase 1) form part

of the ECM or contribute to its assembling and have an increase of their mRNA transcripts in the ventral aspect of the 3<sup>rd</sup>pp by at least 3 fold if not exclusively expressed when compared to the dorsal side (Fig.3.21). *Spock2* (a.k.a. testican-2), which encodes a member of a novel Ca(2+)-binding proteoglycan family was suggested to play a role in the development of the central nervous system while *Galnt3* encodes a glycosyltransferase responsible for initiating mucin-type O-glycosylation on glycoproteins (Schnepp *et al.*, 2005; Topaz *et al.*, 2004; Vannahme *et al.*, 1999). *Colla1* transcripts were restricted to the ventral part of the 3<sup>rd</sup>pp (Fig.3.21). Although the expression of *Colla1* has been shown to be regulated by Tgf $\beta$ 1 in fetal fibroblasts nothing is known regarding the transcriptional control in thymic epithelial cells (Gallivan *et al.*, 1997). Nevertheless, transcripts for *Tgf $\beta$ 2* (Fig.3.29) but not of *Tgf $\beta$ 1* (Annex 2) are also present in the ventral circumference of the 3<sup>rd</sup>pp and even more there when compared to the dorsal part. *Colla1* may hence be eventually upregulated by Tgf $\beta$ 2 and/or an other member of the Tgf $\beta$  signalling family. *Hs2st1* encodes for a heparan sulphate 2-O-sulphotransferase, which acts at an intermediate stage in the biosynthesis of heparan sulphate (HS). A cortical prerequisite for HS to bind to different ligands including Fst (Follistatin)/activin-binding protein, which was identified as being differentially expressed within the 3<sup>rd</sup>pp (Fig.3.21) (Nakamura *et al.*, 1991). It is presently thought that different sulfation patterns created by distinct sulfotransferases such as *Hs2st1* of HSPGs result in differences in the capacity to bind cell growth factors and thus in diverse signalling outcomes (Nogami *et al.*, 2004). Mice deficient for *Hs2st1* die in the neonatal period and exhibit bilateral renal agenesis and defects of the eye and the skeleton, a phenotype that has been suggested to be a consequence of compromised interactions between growth factors and their signal-transducing receptors (Bullock *et al.*, 1998; Wilson *et al.*, 2002). Data of these mutant mice have provided evidence that the regulated synthesis of differentially glycosylated proteoglycans can affect morphogenesis during murine development (Bullock *et al.*, 1998). Taken together, these results may predict that *Hs2st1* generates different sulfation patterns of HSPGs between the dorsal and ventral aspect of the 3<sup>rd</sup>pp to provide an appropriate and spatio-temporal extracellular environment for morphogenetic signal transduction such as the Bmp and/or Tgf $\beta$  signalling. *Hs2st2* may also play a role in the modulation of these signals so that the ventral aspect of the 3<sup>rd</sup>pp can adopt a thymic epithelial cell fate since Fst, an antagonist of the Tgf $\beta$  signalling, is known to bind to HSPGs. However, mice deficient for *Hs2st1* have not been reported to have thymic anomalies.

### 4.13 Expressed sequence target genes upregulated in the 3<sup>rd</sup>pp

Among the genes specifically present in the ventral aspect of the 3<sup>rd</sup>pp when compared to the dorsal part, two expressed sequence target genes (*EST1* and *EST2*) were identified (Fig.3.21). The expression of *EST1* in adult mice is detected in lymph tissues (i.e. thymus, bone marrow, spleen, lymph nodes) (Fig.3.37). *EST1* was also detected in MTS24<sup>+</sup> and MTS24<sup>-</sup> adult primary TECs as well as in several TEC cell lines (i.e. cTEC1.2, mTEC C6 and mTEC 3.10) but not in thymocytes (data not shown). As stated earlier, *EST1* was found to belong to the *TAP1* gene cluster. Hence, the fact that *EST1* expression is essentially restricted to lymph tissues (Fig.3.37) in contrast to *TAP1*, which is almost expressed in all cell types, predicts that *EST1* and *TAP1* may have a different function. This is consistent with the observation that the polyA tail of *EST1* is located at 5' upstream of *TAP1* and that *EST1* does not encode for exon11 of *TAP1*. Nevertheless, both transcripts, *EST1* and *TAP1*, encode for the ATP-binding cassette. Taken together, these data suggest that *EST1* is an alternative splice variant of *TAP1* that may have a particular function for the immune system.

In contrast to *EST1*, *EST2* expression was not detected in any lymphoid tissues (including the thymus) examined by conventional RT-PCR but in the brain and testis (Fig.3.37). In regard to *EST2* thymic expression, *EST2* has been detected in the cTEC1.2 cell line but otherwise its expression could not be detected in adult primary TECs, in adult thymocytes or other TEC cell lines (cTEC 1.4, cTEC C9, mTEC 2.3, mTEC 3.10, and mTEC C6) examined (data not shown). *EST2* transcripts were also found to be expressed in an entire E6.5 mouse cDNA library. This early expression in development as well as its expression in the ventral aspect of the 3<sup>rd</sup>pp and other tissues (e.g. Brain, testis) predicts a potential role in organogenesis. However, neither for *EST1* nor for *EST2* sufficient and substantial data are known so far to predict a function of these genes in the thymus.



## 5. Conclusions

The work described in this thesis leads to the following facts:

- The establishment of a protocol for the microdissection and recovery of tissue for RNA extraction. This method combined with gene expression profiling by microarrays allows the identification of genes differentially expressed between two tiny anatomical sites, i.e. the ventral and the dorsal aspects of the 3<sup>rd</sup>pp in mouse embryos at E10.5.
- The identification of genes differentially expressed in the 3<sup>rd</sup>pp and thus potentially associated with early thymus development. Based on the limited number of experiments carried out, neither CD44, Phlda2 or Sp8 when not expressed in mice result in a disturbed commitment of endodermal cells to the thymic epithelial cell fate.
- Most of the genes identified by this method were expressed in the thymus during development and post-natal life. Some of the gene products, could be detected both in thymic epithelial cells and thymocytes (e.g. Bmp4, Fst, c-Myc, Sp8, Phlda2 and Nrnx1), whereas others, e.g. WIF1 and Flrt3, were restricted in their expression to thymic epithelial cells.
- Several of the genes identified to be differentially expressed in the 3<sup>rd</sup>pp are involved in the Tgf $\beta$  signalling (e.g. Bmp4, Fst, Tgf $\beta$ 2 and Bambi) or the Wnt signalling (e.g. WIF1, Nkd1 and Sfrp2) while others are targets of either or of both of these signalling pathways (e.g. c-Myc and Nrnx1).
- *Fst*, *Phlda2* and *Nrxn1* transcripts, which were identified to be upregulated in the ventral aspect of the 3<sup>rd</sup>pp at E10.5, were noticed to be downregulated in the pharyngeal region of mouse embryos deficient for Tbx1 at E9.5 and are thus revealing that these genes might be targeted by Tbx1 (Ivins *et al.*, 2005).

## 6. Perspectives and Outlook

Several candidate genes shown to be differentially upregulated or even exclusively expressed within the 3<sup>rd</sup>pp are involved in transcriptional regulation. For example, *Fst* and *Nrxn1* genes were both found to be downregulated in the pharyngeal region of *Tbx1* deficient embryos at E9.5 (Ivins *et al.*, 2005). Since the *Tbx1* gene is essential for the normal development of the thymus, I would first start to analyse the thymic expression of K5 and K8 TEC markers between 13.5 and 15.5 days of mouse gestation by immunohistochemistry in embryos deficient for *Fst* and *Nrxn1* genes, respectively. This in order to reveal whether or not the early development of the thymus proceeds normally in mice mutant for these candidate genes. In case, an abnormal thymus phenotype is revealed in the deficient mice, I would accordingly analyse the mutant thymus at earlier stages and at later stages than examined, always in comparison to wild type littermates to determine precisely at which stage of development, the candidate gene appears to be required.

In case, embryos deficient for a given candidate gene is not available or die before they reach the E12.5 stage of development, I would try to generate a conditional knock-out mice for the given candidate gene. In more detail, these mutants would be generated as such as that the expression of the candidate gene is abolished in thymic epithelial cells (using a Cre/loxP system) as early as at E10.5. For example, by generating a knock-in mice, in which loxP sites have been inserted into the locus of the gene of interest as such as these mutants have only an expression deficiency when crossed to mice transgenic for the Cre gene under the control of a promoter from a gene whose expression is well expressed at E10.5 in the ventral aspect of the 3<sup>rd</sup>pp and whose expression is relatively restricted to the pharyngeal area (e.g. *Hoxa3*). To further reveal a role of the candidate genes, I would also analyse in fetal thymic organ cultures (FTOCs) the effect of overexpressing the candidate gene or of neutralizing antibodies for the examined candidate gene on the development of thymocytes as well as their effects on the growth of thymic epithelial cells (using a BrdU staining protocol). In that regard, I would start to examine the effect of neutralizing antibodies for WIF1 in FTOCs on the development of thymocytes as well as its effect on the expansion of thymic epithelial cells since this has not been tested yet. In addition, a functional analysis could also be done by testing the effect of overexpressing the candidate gene in a TEC cell line (i.e. cTEC1.2) and determine whether its affects the expression of several

important genes for thymus development (e.g. FoxN1, Pax1, Pax9, Hoxa3, Six1, Eya1). In fact, this expression analysis of essential genes in thymus development could also be examined in the different FTOCs after their incubation in presence of either excessive amount or of neutralizing antibodies for that candidate gene to reveal whether the thymic expression of these genes are affected.

## 7. Appendix

### 7.1 Annexes

#### Annex 1

Genes differentially expressed within the 3<sup>rd</sup>pp as identified by microarray analysis.

Probe ID <sup>1</sup>	Gene name	Gene Symbol	D1	D3	V1	V3	Microarray ratio (3)
92943_at	glutamate receptor, ionotropic, AMPA1 (alpha 1)	Gria1	A <sup>2</sup>	A	P <sup>2</sup>	M <sup>2</sup>	13,78
92346_at	neurofilament 3, medium	Nef3	A	A	P	P	13,07
98817_at	folliculin	Fst	A	A	P	P	10,40
94305_at	procollagen, type I, alpha 1	Col1a1	A	A	M	A	9,96
92203_s_at	CD6 antigen	CD6	A	A	A	A	8,93
102204_at	v-maf musculoaponeurotic fibrosarcoma oncogene family, protein B	Mafb	A	A	P	A	8,76
160172_at	GTL2, imprinted maternally expressed untranslated mRNA	Gtl2	A	A	A	A	8,37
161346_f_at	protease, serine, 19 (neuropsin)	Prss19	A	A	P	A	8,03
99916_at	protein kinase C, eta	Prkch	A	A	P	A	7,96
93455_s_at	bone morphogenetic protein 4	Bmp4	P	P	P	P	7,82
100548_at	phosphoprotein enriched in astrocytes 15	Pea15	A	A	A	A	7,49
101538_i_at	carboxylesterase 3	Ces3	A	A	P	P	6,79
103378_at	prolactin-like protein A	Prlpa	A	A	A	A	6,71
92293_at	RIKEN cDNA C130076O07 gene	EST	A	A	A	A	6,27
94379_at	kinesin family member 1B	Kif1b	A	A	A	P	5,97
94515_at	sulfide quinone reductase-like (yeast)	Sqrdl	A	A	A	P	5,74
100746_at	EST	EST	A	A	A	A	5,41
162162_f_at	EST	EST	A	A	A	A	4,98
162319_i_at	EST	EST	A	A	A	A	4,86
95465_s_at	Transmembrane protein 37	Tmem37	A	A	P	P	4,74
93642_at	growth differentiation factor 1	Gdf1	A	A	P	A	4,74
97264_r_at	casein kinase 1, delta	Csnk1d	A	A	A	A	4,64
96486_at	Syntrophin, basic 1	Sntb1	A	A	P	P	4,45
104021_at	homeo box A11	Hoxa11	A	A	A	A	3,67
92535_at	early B-cell factor 1	Ebf1	A	A	A	A	3,61
95940_f_at	EST	EST	A	A	A	A	3,50
103539_at	cytoplasmic tyrosine kinase, Dscr28C related (Drosophila)	Tec	A	A	P	P	3,48
103794_i_at	T-cell immunoglobulin and mucin domain containing 2	Timd2	A	A	A	A	3,39
96789_i_at	galactose mutarotase	Galm	A	A	P	A	3,30
160860_at	growth differentiation factor 10	Gdf10	A	A	A	A	3,17
99876_at	src-like adaptor	Sla	A	A	A	A	3,16
96600_at	EST	EST	A	A	P	P	3,11
104712_at	myelocytomatosis oncogene	Myc	P	P	P	P	3,01
101154_at	EST	EST	A	A	P	P	2,92
102956_at	homeo box, msh-like 2	Msx2	A	A	P	P	2,91
103629_g_at	lymphoid enhancer binding factor 1	Lef1	P	A	P	P	2,90
92990_at	zinc finger protein 93	Zfp93	A	A	P	P	2,78
103569_at	SH3-domain GRB2-like B1 (endophilin)	Sh3glb1	P	P	P	P	2,52
104066_at	EST	EST	A	A	P	M	2,51
102025_at	chemokine (C-X-C motif) ligand 13	Cxcl13	A	A	A	A	2,50
100884_at	aldo-keto reductase family 1, member B8	Akr1b8	A	A	P	P	2,21
103570_at	C1q and tumor necrosis factor related protein 3	C1qtnf3	A	A	P	P	2,15
92681_at	melanoma antigen, family L, 2	Magel2	A	A	P	P	1,77
101851_at	Cd200 antigen	CD200	A	A	P	P	1,73
99937_at	mesenchyme homeobox 2	Meox2	P	P	P	P	1,24
114697_at	CD44 antigen	CD44	A	A	P	P	23,63
113088_at	zinc finger, DHHC domain containing 21	Zdhhc21	A	A	P	P	8,87
114048_at	DEAD (Asp-Glu-Ala-Asp) box polypeptide 3, Y-linked	Ddx3y	A	A	P	P	8,22
116782_at	EST	EST	P	A	P	P	7,28
163730_i_at	EST	EST	A	A	A	A	6,32
107112_at	Transmembrane protein 16A	Tmem16A	A	P	P	P	5,18

117331_at	LIM and cysteine-rich domains 1	Lmcd1	A	A	A	P	4,97
117279_at	EST	EST	A	A	P	P	4,95
115683_at	EST	EST	A	A	P	P	4,78
163423_at	Wnt inhibitory factor 1	Wif1	A	A	M	A	3,65
116747_at	blood vessel epicardial substance	Bves	A	A	P	P	3,42
106971_at	RIKEN cDNA A630031M04 gene	Vps13d	A	A	A	A	3,34
162531_at	BMP and activin membrane-bound inhibitor, homolog (Xenopus laevis)	Bambi	P	A	P	P	3,17
114148_at	EST	EST	A	A	P	P	3,16
162739_at	inositol polyphosphate-5-phosphatase F	Inpp5f	A	A	P	M	3,10
107952_i_at	whn-dependent transcript 2	Wdt2	A	A	M	P	3,04
163934_at	sema domain, transmembrane domain (TM), and cytoplasmic domain, (semaphorin) 6D	Sema6d	A	P	P	P	2,77
108760_at	EST	EST	A	A	P	P	2,42
114766_at	neurexin I	Nrxn1	A	A	P	P	2,37
163829_r_at	chemokine (C-C motif) receptor 9	Ccr9	A	A	P	P	2,33
164237_at	KH domain containing, RNA binding, signal transduction associated 3	Khdrbs3	A	A	M	M	2,21
114338_at	v-maf musculoaponeurotic fibrosarcoma oncogene family, protein B	Mafb	A	A	P	P	2,16
163582_at	serine/arginine-rich protein specific kinase 2	Srpk2	A	A	P	P	2,11
108001_at	EST	EST	A	A	P	P	2,08
106290_at	EST	EST	A	A	P	P	2,01
167347_i_at	EST	EST	A	A	A	A	10,90
134352_at	EST	EST	A	A	P	P	10,76
137059_at	EST	EST	A	A	A	A	8,44
166199_at	gene model 1752, (NCBI)	Gm1752	A	A	P	P	6,12
141032_at	EST	EST	A	A	M	A	5,42
166264_at	FYN binding protein	Fyb	A	A	A	A	5,11
137321_at	EST	EST	A	A	A	A	4,61
135615_at	EST	EST	A	A	P	P	4,60
133727_at	leucyl/cystinyl aminopeptidase	Lnpep	A	A	P	P	4,31
134357_at	EST	EST	A	A	P	A	4,31
165813_at	EST	EST	A	A	A	A	4,17
166569_f_at	SH3-domain binding protein 1	Sh3bp1	A	A	P	A	4,12
136661_at	EST	EST	A	A	A	P	3,92
167905_f_at	fibronectin leucine rich transmembrane protein 3	Flrt3	P	P	P	P	3,81
169259_f_at	EST	EST	P	P	P	P	3,75
139234_at	CAP, adenylate cyclase-associated protein, 2 (yeast)	Cap2	A	A	M	A	3,66
138501_r_at	EST	EST	A	A	P	A	3,48
128821_at	EST	EST	A	A	M	M	3,32
135184_at	EST	EST	A	A	P	P	3,11
135317_at	EST	EST	A	A	P	P	3,07
169068_i_at	EST	EST	A	A	P	A	3,03
137713_at	EST	EST	A	A	M	P	2,88
166600_at	KH domain containing, RNA binding, signal transduction associated 3	Khdrbs3	P	P	P	P	2,81
134774_at	EST	EST	A	A	P	A	2,77
166521_f_at	Gene model 106 (NCBI)	Gm106	A	A	A	P	2,62
169997_i_at	p21 (CDKN1A)-activated kinase 3	Pak3	A	A	P	A	2,62
133203_at	EST	EST	A	A	P	A	2,58
129286_at	EST	EST	A	A	P	A	2,50
130608_at	EST	EST	A	A	P	A	2,42
130957_f_at	EST	EST	P	P	P	P	2,37
168351_at	EST	EST	A	A	P	P	2,34
137595_at	EST	EST	A	A	P	P	2,27
135649_at	EST	EST	A	A	P	P	2,23
166675_at	EST	EST	A	A	P	A	2,16
94101_at	zinc finger protein 98	Zfp98	A	A	A	A	5,78
98818_at	nuclear receptor subfamily 3, group C, member 1	Nr3c1	A	A	A	A	4,72
102653_at	ryanodine receptor 2, cardiac	Ryr2	A	A	A	A	4,22
102280_at	protocadherin 7	Pcdh7	A	A	P	P	3,97
162439_at	POU domain, class 2, associating factor 1	Pou2af1	A	A	A	A	3,81
102299_at	protein kinase C, alpha	Prkca	A	A	P	A	3,49
93711_at	EST	EST	A	A	A	P	3,44
104375_at	sparc/osteonectin, cwcv and kazal-like domains proteoglycan 2	Spock2	A	A	P	P	3,19
101178_at	sema domain, immunoglobulin domain (Ig), short basic domain, secreted, (semaphorin) 3C	Sema3c	A	A	P	P	2,97
95625_at	solute carrier family 6 (neurotransmitter transporter, creatine), member	Slc6a8	A	A	P	P	2,83

	8						
94419_at	solute carrier family 19 (sodium/hydrogen exchanger), member 1	Slc19a1	A	A	P	P	2,70
100943_at	solute carrier family 1 (glutamate/neutral amino acid transporter), member 4	Slc1a4	A	A	P	P	2,66
161882_f_at	retinol dehydrogenase 13 (all-trans and 9-cis)	Rdh13	A	A	A	M	2,54
101879_s_at	complement receptor related protein	Crry	A	A	P	P	2,32
103090_at	EST	EST	A	A	P	P	2,26
161026_s_at	synaptotagmin-like 4	Sytl4	A	A	P	P	2,22
104548_at	pleckstrin homology-like domain, family A, member 2	Phlda2	A	A	P	A	2,09
110311_at	naked cuticle 1 homolog (Drosophila)	Nkd1	A	A	A	A	5,81
106100_at	histamine receptor H 1	Hrh1	A	A	A	A	3,80
106861_at	adaptor-related protein complex 3, sigma 2 subunit	Ap3s2	A	A	A	M	3,40
114507_at	GTP binding protein 2	Gtpbp2	A	A	A	A	3,35
107779_at	NIMA (never in mitosis gene a)-related expressed kinase 4	Nek4	A	A	A	A	3,05
164972_r_at	nerve growth factor receptor (TNFRSF16) associated protein 1	Ngfrap1	A	A	P	A	2,96
106017_at	adaptor-related protein complex 1, sigma 2 subunit	Ap1s2	A	A	A	P	2,39
109301_i_at	calpastatin	Cast	A	A	A	P	2,25
169398_i_at	EST	EST	A	A	A	A	7,45
166402_i_at	solute carrier family 35 (UDP-N-acetylglucosamine (UDP-GlcNAc) transporter), member 3	Slc35a3	A	A	P	A	4,77
170678_i_at	EST	EST	A	A	A	A	3,51
169016_at	EST	EST	A	A	A	A	3,38
167747_f_at	EST	EST	A	A	M	A	2,06
99011_at	UDP-N-acetyl-alpha-D-galactosamine:polypeptide N-acetylgalactosaminyltransferase 3	Galnt3	P	P	P	P	4,57
92722_f_at	Sine oculis-related homeobox 1 homolog (Drosophila)	Six1	P	P	P	P	3,12
100924_at	GATA binding protein 3	Gata3	P	P	P	P	3,04
97942_g_at	calpain 6	Capn6	P	P	P	P	2,65
102306_at	heparan sulfate 2-O-sulfotransferase 1	Hs2st1	P	P	P	P	2,60
93568_i_at	EST	EST	P	P	P	P	2,57
160899_at	Purkinje cell protein 4	Pcp4	P	P	P	P	2,15
160670_at	tumor necrosis factor receptor superfamily, member 19	Tnfrsf19	A	P	P	P	1,95
103538_at	T-box 3	Tbx3	M	A	P	P	1,73
99178_at	glycoprotein m6b	Gpm6b	P	P	P	P	1,58
110654_at	N-acylsphingosine amidohydrolase 2	Asah2	P	P	P	P	3,57
164044_r_at	EST	EST	P	P	P	P	3,15
111896_at	EST	EST	P	P	P	P	2,30

Explanations: (1) Probe ID refers to the affymetrix reference number for a probe set specific for a given gene. (2) A; M and P denote absent, marginal and present calls, respectively. The ratio is defined as the average fold difference in signal intensity between two samples independently generated taken from the dorsal and the ventral epithelium of the 3<sup>rd</sup>pp, as measured by microarray analysis (3). Samples 1 and 2 of the dorsal and ventral aspects of the 3<sup>rd</sup>pp are annotated as D\_1, D\_2, V\_1 and V\_2, respectively.

## Annex 2

### Microarray data for genes potentially involved if not known to be important for thymus development.

Probe ID	Gene Symbol	D_1	D_2	V_1	V_2	3_1	3_2	2_1	2_2	4_1	4_2	4_3	Microarray V/D ratio	Microarray 3/2 ratio
92674_at	FoxN1	A	A	A	A	A	A	A	A	A	A	A	3,35	4,19
115295_at	FoxN1	A	A	A	M	A	A	A	A	A	A	A	2,80	6,02
161049_at	FoxG1	A	P	P	P	P	A	A	A	A	A	A	2,21	0,68
94709_at	Gcm2	P	P	P	P	P	A	P	P	P	P	P	0,36	3,89
96595_at	Pax1	P	P	P	P	P	A	P	P	A	M	M	1,32	14,38
100697_at	Pax3	A	A	A	A	A	A	A	A	A	A	A	0,39	0,97
98838_at	Pax9	P	P	P	P	P	A	P	P	A	P	A	0,68	2,00
163890_at	Hoxa3	P	P	P	P	P	A	P	P	P	P	P	1,13	3,88
169259_f_at	Six1	P	P	P	P	P	A	P	P	A	A	M	3,75	11,37
94706_s_at	Eya1	P	P	P	P	P	P	P	P	P	P	P	1,52	1,29
98419_at	Meox1	P	P	P	P	A	P	P	P	P	P	P	0,66	3,99
109325_at	Bmp7	P	P	P	P	P	P	P	P	P	M	P	0,88	0,51
101526_at	Msx1	A	P	P	P	P	P	A	P	A	A	A	1,98	1,34
102984_g_at	Smad1	P	P	P	P	A	P	P	P	P	P	P	1,08	0,86
97509_f_at	Fgfr1	P	P	P	P	P	A	P	A	A	A	A	2,10	0,75
162171_f_at	Fgfr2	P	P	P	P	P	A	P	P	P	M	P	0,90	0,47
100277_at	Inhba	A	A	P	P	P	A	P	A	M	A	A	1,63	0,13
101918_at	Tgfb1	A	A	A	A	A	A	A	A	A	A	A	0,36	1,12
108468_at	Bmpr1a	P	P	P	P	P	P	P	P	P	P	P	1,54	1,27
98841_at	Acvr2	P	P	P	P	P	P	P	P	P	P	P	0,97	0,89
97727_at	Nog	A	P	A	A	M	A	P	A	A	A	A	0,58	1,29
141073_at	VEGF	A	A	A	A	A	A	A	A	A	A	A	0,42	0,61
160887_at	Hes1	P	P	P	P	P	P	A	P	M	M	A	0,69	1,41
98623_g_at	Igf2	P	P	P	P	P	P	P	P	P	P	P	1,50	1,36
160453_at	Ryk	P	M	P	P	P	M	P	P	A	A	P	1,19	2,18
94134_at	Wnt1	A	A	A	A	A	A	A	A	P	A	A	0,78	0,97
101975_at	Dlk1	P	P	P	P	P	P	P	P	P	P	P	3,39	2,35
92931_at	Dll1	A	A	A	A	A	A	A	A	A	A	A	0,97	1,17
102746_at	Dll3	A	A	A	A	A	A	A	A	A	A	A	1,01	1,15
163429_at	Dll4	A	A	A	A	A	A	A	A	A	A	A	2,47	0,84
102248_f_at	CASK	P	P	P	P	P	P	P	P	P	P	P	1,20	0,99
104189_at	Traf6	P	P	P	P	P	A	P	P	P	P	P	1,31	3,21

Explanations. A, M, P denote an absent, a marginal and a present call, respectively. The ratio is defined as the average fold difference in signal intensity between two samples (generated independently) of the dorsal and the ventral epithelium of the 3<sup>rd</sup>pp (V/D) and the 2<sup>nd</sup> and 3<sup>rd</sup>pp (3/2), respectively, as measured by microarray analysis. Duplicate samples of the dorsal and the ventral 3<sup>rd</sup>pp epithelium of the 3<sup>rd</sup>pp and 2<sup>nd</sup>pp and 3<sup>rd</sup>pp are respectively annotated as D\_1, D\_2 and V\_1, V\_2, and 2\_1, 2\_2 and 3\_1, 3\_2.

## 8. References

Abu-Issa, R., Smyth, G., Smoak, I., Yamamura, K., and Meyers, E. N. (2002). Fgf8 is required for pharyngeal arch and cardiovascular development in the mouse. *Development* **129**, 4613-25.

Akashi, K., Traver, D., Miyamoto, T., and Weissman, I. L. (2000). A clonogenic common myeloid progenitor that gives rise to all myeloid lineages. *Nature* **404**, 193-7.

Akiyama, T., Maeda, S., Yamane, S., Ogino, K., Kasai, M., Kajiura, F., Matsumoto, M., and Inoue, J. I. (2005). Dependence of Self-Tolerance on TRAF6-Directed Development of Thymic Stroma. *Science* .

Allman, D., Punt, J. A., Izon, D. J., Aster, J. C., and Pear, W. S. (2002). An invitation to T and more: notch signaling in lymphopoiesis. *Cell* **109 Suppl**, S1-11.

Ammann, A. J., Wara, D. W., Cowan, M. J., Barrett, D. J., and Stiehm, E. R. (1982). The DiGeorge syndrome and the fetal alcohol syndrome. *Am J Dis Child* **136**, 906-8.

Anderson, G., Anderson, K. L., Tchilian, E. Z., Owen, J. J., and Jenkinson, E. J. (1997). Fibroblast dependency during early thymocyte development maps to the CD25+ CD44+ stage and involves interactions with fibroblast matrix molecules. *Eur J Immunol* **27**, 1200-6.

Anderson, G., Hare, K. J., and Jenkinson, E. J. (1999). Positive selection of thymocytes: the long and winding road. *Immunol Today* **20**, 463-8.

Anderson, G., and Jenkinson, E. (1997). Piecing together the thymic puzzle. *Immunol Today* **18**, 363-4.

Anderson, G., and Jenkinson, E. J. (2001). Lymphostromal interactions in thymic development and function. *Nature Rev Immunol* **1**, 31-40.



Anderson, G., Jenkinson, E. J., Moore, N. C., and Owen, J. J. (1993). MHC class II-positive epithelium and mesenchyme cells are both required for T-cell development in the thymus. *Nature* **362**, 70-3.

Anderson, G., Moore, N. C., Owen, J. J., and Jenkinson, E. J. (1996). Cellular interactions in thymocyte development. *Annu Rev Immunol* **14**, 73-99.

Anderson, M. S., Venanzi, E. S., Klein, L., Chen, Z., Berzins, S., Turley, S. J., Von Boehmer, H., Bronson, R., Dierich, A., Benoist, C., and Mathis, D. (2002). Projection of an Immunological Self-Shadow Within the Thymus by the Aire Protein. *Science* **10**, 10.

Andl, T., Ahn, K., Kairo, A., Chu, E. Y., Wine-Lee, L., Reddy, S. T., Croft, N. J., Cebra-Thomas, J. A., Metzger, D., Chambon, P., Lyons, K. M., Mishina, Y., Seykora, J. T., Crenshaw, E. B., 3rd, and Millar, S. E. (2004). Epithelial *Bmpr1a* regulates differentiation and proliferation in postnatal hair follicles and is essential for tooth development. *Development* **131**, 2257-68.

Ansel, K. M., Ngo, V. N., Hyman, P. L., Luther, S. A., Forster, R., Sedgwick, J. D., Browning, J. L., Lipp, M., and Cyster, J. G. (2000). A chemokine-driven positive feedback loop organizes lymphoid follicles. *Nature* **406**, 309-14.

Ara, T., Itoi, M., Kawabata, K., Egawa, T., Tokoyoda, K., Sugiyama, T., Fujii, N., Amagai, T., and Nagasawa, T. (2003). A role of CXC chemokine ligand 12/stromal cell-derived factor-1/pre-B cell growth stimulating factor and its receptor CXCR4 in fetal and adult T cell development in vivo. *J Immunol* **170**, 4649-55.

Ardavin, C., Wu, L., Li, C. L., and Shortman, K. (1993). Thymic dendritic cells and T cells develop simultaneously in the thymus from a common precursor population. *Nature* **362**, 761-3.

Bachiller, D., Klingensmith, J., Shneyder, N., Tran, U., Anderson, R., Rossant, J., and De Robertis, E. M. (2003). The role of chordin/Bmp signals in mammalian pharyngeal development and DiGeorge syndrome. *Development* **130**, 3567-78.

Balciunaite, G., Keller, M. P., Balciunaite, E., Piali, L., Zuklys, S., Mathieu, Y. D., Gill, J., Boyd, R., Sussman, D. J., and Hollander, G. A. (2002). Wnt glycoproteins regulate the expression of FoxN1, the gene defective in nude mice. *Nat Immunol* **15**, 15.

Baldwin, K. K., Trenchak, B. P., Altman, J. D., and Davis, M. M. (1999). Negative selection of T cells occurs throughout thymic development. *J Immunol* **163**, 689-98.

Banwell, C. M., Partington, K. M., Jenkinson, E. J., and Anderson, G. (2000). Studies on the role of IL-7 presentation by mesenchymal fibroblasts during early thymocyte development. *Eur J Immunol* **30**, 2125-2129.

Barembaum, M., and Bronner-Fraser, M. (2005). Early steps in neural crest specification. *Semin Cell Dev Biol* .

Baudino, T. A., McKay, C., Pendeville-Samain, H., Nilsson, J. A., Maclean, K. H., White, E. L., Davis, A. C., Ihle, J. N., and Cleveland, J. L. (2002). c-Myc is essential for vasculogenesis and angiogenesis during development and tumor progression. *Genes Dev* **16**, 2530-43.

Baugh, L. R., Hill, A. A., Brown, E. L., and Hunter, C. P. (2001). Quantitative analysis of mRNA amplification by in vitro transcription. *Nucleic Acids Res* **29**, E29.

Bell, S. M., Schreiner, C. M., Waclaw, R. R., Campbell, K., Potter, S. S., and Scott, W. J. (2003). Sp8 is crucial for limb outgrowth and neuropore closure. *Proc Natl Acad Sci U S A* **100**, 12195-200.

Bennett, A. R., Farley, A., Blair, N. F., Gordon, J., Sharp, L., and Blackburn, C. C. (2002). Identification and characterization of thymic epithelial progenitor cells. *Immunity* **16**, 803-14.

Bevan, M. J. (1997). In thymic selection, peptide diversity gives and takes away. *Immunity* **7**, 175-8.

Bhalla, D. K., and Karnovsky, M. J. (1978). Surface morphology of mouse and rat thymic lymphocytes: an in situ scanning electron microscopic study. *Anat Rec* **191**, 203-20.

Bix, M., and Raulet, D. (1992). Inefficient positive selection of T cells directed by haematopoietic cells. *Nature* **359**, 330-3.

Blackburn, C. C., Augustine, C. L., Li, R., Harvey, R. P., Malin, M. A., Boyd, R. L., Miller, J. F., and Morahan, G. (1996). The nu gene acts cell-autonomously and is required for differentiation of thymic epithelial progenitors. *Proc Natl Acad Sci U S A* **93**, 5742-6.

Blackburn, C. C., and Manley, N. R. (2004). Developing a new paradigm for thymus organogenesis. *Nat Rev Immunol* **4**, 278-89.

Bleul, C. C., and Boehm, T. (2005). BMP signaling is required for normal thymus development. *J Immunol* **175**, 5213-21.

Bockman, D. E. (1997). Development of the thymus. *Microsc Res Tech* **38**, 209-15.

Bockman, D. E., and Kirby, M. L. (1984). Dependence of thymus development on derivatives of the neural crest. *Science* **223**, 498-500.

Bockman, D. E., and Kirby, M. L. (1989). Neural crest function in thymus development. *Immunol Ser* **45**, 451-67.

Boehm, T., Scheu, S., Pfeffer, K., and Bleul, C. C. (2003). Thymic Medullary Epithelial Cell Differentiation, Thymocyte Emigration, and the Control of Autoimmunity Require Lympho-Epithelial Cross Talk via LT $\beta$ R. *J Exp Med* **198**, 757-769.

Boerboom, D., White, L. D., Dalle, S., Courty, J., and Richards, J. S. (2006). Dominant-stable beta-catenin expression causes cell fate alterations and Wnt signaling antagonist expression in a murine granulosa cell tumor model. *Cancer Res* **66**, 1964-73.

Bogden, A. E., Haskell, P. M., LePage, D. J., Kelton, D. E., Cobb, W. R., and Esber, H. J. (1979). Growth of human tumor xenografts implanted under the renal capsule of normal immunocompetent mice. *Exp Cell Biol* **47**, 281-93.

Bottcher, R. T., Pollet, N., Delius, H., and Niehrs, C. (2004). The transmembrane protein XFLRT3 forms a complex with FGF receptors and promotes FGF signalling. *Nat Cell Biol* **6**, 38-44.

Boursalian, T. E., and Bottomly, K. (1999). Survival of naive CD4 T cells: roles of restricting versus selecting MHC class II and cytokine milieu. *J Immunol* **162**, 3795-801.

Brown, C. B., Wenning, J. M., Lu, M. M., Epstein, D. J., Meyers, E. N., and Epstein, J. A. (2004). Cre-mediated excision of Fgf8 in the Tbx1 expression domain reveals a critical role for Fgf8 in cardiovascular development in the mouse. *Dev Biol* **267**, 190-202.

Bullock, S. L., Fletcher, J. M., Beddington, R. S., and Wilson, V. A. (1998). Renal agenesis in mice homozygous for a gene trap mutation in the gene encoding heparan sulfate 2-sulfotransferase. *Genes Dev* **12**, 1894-906.

Burkly, L., Hession, C., Ogata, L., Reilly, C., Marconi, L. A., Olson, D., Tizard, R., Cate, R., and Lo, D. (1995). Expression of relB is required for the development of thymic medulla and dendritic cells. *Nature* **373**, 531-6.

Buttitta, L., Tanaka, T. S., Chen, A. E., Ko, M. S., and Fan, C. M. (2003). Microarray analysis of somitogenesis reveals novel targets of different WNT signaling pathways in the somitic mesoderm. *Dev Biol* **258**, 91-104.

Byun, T., Karimi, M., Marsh, J. L., Milovanovic, T., Lin, F., and Holcombe, R. F. (2005). Expression of secreted Wnt antagonists in gastrointestinal tissues: potential role in stem cell homeostasis. *J Clin Pathol* **58**, 515-9.

Capone, M., Romagnoli, P., Beermann, F., MacDonald, H. R., and van Meerwijk, J. P. (2001). Dissociation of thymic positive and negative selection in transgenic mice expressing major histocompatibility complex class I molecules exclusively on thymic cortical epithelial cells. *Blood* **97**, 1336-42.

Carlyle, J. R., Michie, A. M., Furlonger, C., Nakano, T., Lenardo, M. J., Paige, C. J., and Zuniga-Pflucker, J. C. (1997). Identification of a novel developmental stage marking lineage commitment of progenitor thymocytes. *J Exp Med* **186**, 173-82.

Carlyle, J. R., and Zuniga-Pflucker, J. C. (1998). Requirement for the thymus in alphabeta T lymphocyte lineage commitment. *Immunity* **9**, 187-97.

Carter, W. B., and Ward, M. D. (2001). Parathyroid-produced angiopoietin-2 modulates angiogenic response. *Surgery* **130**, 1019-27.

Cheyette, B. N. (2004). Ryk: another heretical Wnt receptor defies the canon. *Sci STKE* **2004**, pe54.

Chidgey, A. P., and Boyd, R. L. (2001). Thymic stromal cells and positive selection. *Apmis* **109**, 481-92.

Chisaka, O., and Capecchi, M. R. (1991). Regionally restricted developmental defects resulting from targeted disruption of the mouse homeobox gene *hox-1.5*. *Nature* **350**, 473-9.

Colucci, F., Soudais, C., Rosmaraki, E., Vanes, L., Tybulewicz, V. L., and Di Santo, J. P. (1999). Dissecting NK cell development using a novel alymphoid mouse model: investigating the role of the *c-abl* proto-oncogene in murine NK cell differentiation. *J Immunol* **162**, 2761-5.

Conway, S. J., Henderson, D. J., and Copp, A. J. (1997). Pax3 is required for cardiac neural crest migration in the mouse: evidence from the *spotch* (*Sp2H*) mutant. *Development* **124**, 505-14.

Cordier, A. C., and Haumont, S. M. (1980). Development of thymus, parathyroids, and ultimobranchial bodies in NMRI and nude mice. *Am J Anat* **157**, 227-63.

Cordier, A. C., and Heremans, J. F. (1975). Nude mouse embryo: ectodermal nature of the primordial thymic defect. *Scand J Immunol* **4**, 193-6.

Cosgrove, D., Chan, S. H., Waltzinger, C., Benoist, C., and Mathis, D. (1992). The thymic compartment responsible for positive selection of CD4+ T cells. *Int Immunol* **4**, 707-10.

Couly, G., Lagrue, A., and Griscelli, C. (1983). [Di George syndrome, exemplary rhomboencephalic neurocristopathy]. *Rev Stomatol Chir Maxillofac* **84**, 103-8.

Creyghton, M. P., Roel, G., Eichhorn, P. J., Vredevelde, L. C., Destree, O., and Bernardts, R. (2006). PR130 is a modulator of the Wnt-signaling cascade that counters repression of the antagonist Naked cuticle. *Proc Natl Acad Sci U S A* **103**, 5397-402.

Derbinski, J., Schulte, A., Kyewski, B., and Klein, L. (2001). Promiscuous gene expression in medullary thymic epithelial cells mirrors the peripheral self. *Nat Immunol* **15**, 15.

Douagi, I., Andre, I., Ferraz, J. C., and Cumano, A. (2000). Characterization of T cell precursor activity in the murine fetal thymus: evidence for an input of T cell precursors between days 12 and 14 of gestation. *Eur J Immunol* **30**, 2201-10.

Dupe, V., Ghyselinck, N. B., Wendling, O., Chambon, P., and Mark, M. (1999). Key roles of retinoic acid receptors alpha and beta in the patterning of the caudal hindbrain, pharyngeal arches and otocyst in the mouse. *Development* **126**, 5051-9.

Eberwine, J., Yeh, H., Miyashiro, K., Cao, Y., Nair, S., Finnell, R., Zettel, M., and Coleman, P. (1992). Analysis of gene expression in single live neurons. *Proc Natl Acad Sci U S A* **89**, 3010-4.

Epstein, J. A., Li, J., Lang, D., Chen, F., Brown, C. B., Jin, F., Lu, M. M., Thomas, M., Liu, E., Wessels, A., and Lo, C. W. (2000). Migration of cardiac neural crest cells in Splotch embryos. *Development* **127**, 1869-78.

Erickson, M., Morkowski, S., Lehar, S., Gillard, G., Beers, C., Dooley, J., Rubin, J. S., Rudensky, A., and Farr, A. G. (2002). Regulation of thymic epithelium by keratinocyte growth factor. *Blood* **100**, 3269-78.

Esser, C., Temchura, V., Majora, M., Hundeiker, C., Schwarzler, C., and Gunthert, U. (2004). Signaling via the AHR leads to enhanced usage of CD44v10 by murine fetal thymic emigrants: possible role for CD44 in emigration. *Int Immunopharmacol* **4**, 805-18.

Farlie, P., Reid, C., Wilcox, S., Peeters, J., Reed, G., and Newgreen, D. (2001). Ypel1: a novel nuclear protein that induces an epithelial-like morphology in fibroblasts. *Genes Cells* **6**, 619-29.

Flanagan, S. P. (1966). 'Nude', a new hairless gene with pleiotropic effects in the mouse. *Genet Res* **8**, 295-309.

Frank, D., Fortino, W., Clark, L., Musalo, R., Wang, W., Saxena, A., Li, C. M., Reik, W., Ludwig, T., and Tycko, B. (2002a). Placental overgrowth in mice lacking the imprinted gene Ipl. *Proc Natl Acad Sci U S A* **99**, 7490-5.

Frank, D. U., Fotheringham, L. K., Brewer, J. A., Muglia, L. J., Tristani-Firouzi, M., Capecchi, M. R., and Moon, A. M. (2002b). An Fgf8 mouse mutant phenocopies human 22q11 deletion syndrome. *Development* **129**, 4591-603.

Franz, T. (1989). Persistent truncus arteriosus in the Splotch mutant mouse. *Anat Embryol (Berl)* **180**, 457-64.

Gabor, M. J., Godfrey, D. I., and Scollay, R. (1997). Recent thymic emigrants are distinct from most medullary thymocytes. *Eur J Immunol* **27**, 2010-5.

Gallivan, K., Alman, B. A., Moriarty, K. P., Pajerski, M. E., O'Donnell, C., and Crombleholme, T. M. (1997). Differential collagen I gene expression in fetal fibroblasts. *J Pediatr Surg* **32**, 1033-6.

Garg, V., Yamagishi, C., Hu, T., Kathiriya, I. S., Yamagishi, H., and Srivastava, D. (2001). Tbx1, a DiGeorge syndrome candidate gene, is regulated by sonic hedgehog during pharyngeal arch development. *Dev Biol* **235**, 62-73.

Gekas, C., Dieterlen-Lievre, F., Orkin, S. H., and Mikkola, H. K. (2005). The placenta is a niche for hematopoietic stem cells. *Dev Cell* **8**, 365-75.

Georgopoulos, K., Bigby, M., Wang, J. H., Molnar, A., Wu, P., Winandy, S., and Sharpe, A. (1994). The Ikaros gene is required for the development of all lymphoid lineages. *Cell* **79**, 143-56.

Geppert, M., Khvotchev, M., Krasnoperov, V., Goda, Y., Missler, M., Hammer, R. E., Ichtchenko, K., Petrenko, A. G., and Sudhof, T. C. (1998). Neurexin I alpha is a major alpha-latrotoxin receptor that cooperates in alpha-latrotoxin action. *J Biol Chem* **273**, 1705-10.

Gill, J., Malin, M., Hollander, G. A., and Boyd, R. (2002). Generation of a complete thymic microenvironment by MTS24(+) thymic epithelial cells. *Nat Immunol* **3**, 635-42.

Gill, J., Malin, M., Sutherland, J., Gray, D., Hollander, G., and Boyd, R. (2003). Thymic generation and regeneration. *Immunol Rev* **195**, 28-50.

Gimferrer, I., Farnos, M., Calvo, M., Mittelbrunn, M., Enrich, C., Sanchez-Madrid, F., Vives, J., and Lozano, F. (2003). The accessory molecules CD5 and CD6 associate on the membrane of lymphoid T cells. *J Biol Chem* **278**, 8564-71.

Godfrey, D. I., Izon, D. J., Tucek, C. L., Wilson, T. J., and Boyd, R. L. (1990). The phenotypic heterogeneity of mouse thymic stromal cells. *Immunology* **70**, 66-74.

Godfrey, D. I., Kennedy, J., Mombaerts, P., Tonegawa, S., and Zlotnik, A. (1994). Onset of TCR-beta gene rearrangement and role of TCR-beta expression during CD3-CD4-CD8-thymocyte differentiation. *J Immunol* **152**, 4783-92.

Godfrey, D. I., Kennedy, J., Suda, T., and Zlotnik, A. (1993). A developmental pathway involving four phenotypically and functionally distinct subsets of CD3-CD4-CD8- triple-negative adult mouse thymocytes defined by CD44 and CD25 expression. *J Immunol* **150**, 4244-52.



Godin, I., and Cumano, A. (2002). The hare and the tortoise: an embryonic haematopoietic race. *Nat Rev Immunol* **2**, 593-604.

Gordon, J., Bennett, A. R., Blackburn, C. C., and Manley, N. R. (2001). Gcm2 and Foxn1 mark early parathyroid- and thymus-specific domains in the developing third pharyngeal pouch. *Mech Dev* **103**, 141-3.

Gordon, J., Wilson, V. A., Blair, N. F., Sheridan, J., Farley, A., Wilson, L., Manley, N. R., and Blackburn, C. C. (2004). Functional evidence for a single endodermal origin for the thymic epithelium. *Nat Immunol* .

Grotewold, L., Plum, M., Dildrop, R., Peters, T., and Ruther, U. (2001). Bambi is coexpressed with Bmp-4 during mouse embryogenesis. *Mech Dev* **100**, 327-30.

Gunther, T., Chen, Z. F., Kim, J., Priemel, M., Rueger, J. M., Amling, M., Moseley, J. M., Martin, T. J., Anderson, D. J., and Karsenty, G. (2000). Genetic ablation of parathyroid glands reveals another source of parathyroid hormone. *Nature* **406**, 199-203.

Hager-Theodorides, A. L., Outram, S. V., Shah, D. K., Sacedon, R., Shrimpton, R. E., Vicente, A., Varas, A., and Crompton, T. (2002). Bone morphogenetic protein 2/4 signaling regulates early thymocyte differentiation. *J Immunol* **169**, 5496-504.

Han, W., Ye, Q., and Moore, M. A. (2000). A soluble form of human Delta-like-1 inhibits differentiation of hematopoietic progenitor cells. *Blood* **95**, 1616-25.

Hartung, H., Feldman, B., Lovec, H., Coulier, F., Birnbaum, D., and Goldfarb, M. (1997). Murine FGF-12 and FGF-13: expression in embryonic nervous system, connective tissue and heart. *Mech Dev* **64**, 31-9.

Heath, V. L., Moore, N. C., Parnell, S. M., and Mason, D. W. (1998). Intrathymic expression of genes involved in organ specific autoimmune disease. *J Autoimmun* **11**, 309-18.

Heino, M., Peterson, P., Sillanpaa, N., Guerin, S., Wu, L., Anderson, G., Scott, H. S., Antonarakis, S. E., Kudoh, J., Shimizu, N., Jenkinson, E. J., Naquet, P., and Krohn, K. J. (2000). RNA and protein expression of the murine autoimmune regulator gene (Aire) in normal, RelB-deficient and in NOD mouse. *Eur J Immunol* **30**, 1884-93.

Hetzer-Egger, C., Schorpp, M., Haas-Assenbaum, A., Balling, R., Peters, H., and Boehm, T. (2002). Thymopoiesis requires Pax9 function in thymic epithelial cells. *Eur J Immunol* **32**, 1175-81.

Hoek, R. M., Ruuls, S. R., Murphy, C. A., Wright, G. J., Goddard, R., Zurawski, S. M., Blom, B., Homola, M. E., Streit, W. J., Brown, M. H., Barclay, A. N., and Sedgwick, J. D. (2000). Down-regulation of the macrophage lineage through interaction with OX2 (CD200). *Science* **290**, 1768-71.

Hoffmann, M. W., Allison, J., and Miller, J. F. (1992). Tolerance induction by thymic medullary epithelium. *Proc Natl Acad Sci U S A* **89**, 2526-30.

Hoffmann, M. W., Heath, W. R., Ruschmeyer, D., and Miller, J. F. (1995). Deletion of high-avidity T cells by thymic epithelium. *Proc Natl Acad Sci U S A* **92**, 9851-5.

Hogan, B. L., and Yingling, J. M. (1998). Epithelial/mesenchymal interactions and branching morphogenesis of the lung. *Curr Opin Genet Dev* **8**, 481-6.

Hollander, G. A., Wang, B., Nichogiannopoulou, A., Platenburg, P. P., van Ewijk, W., Burakoff, S. J., Gutierrez-Ramos, J. C., and Terhorst, C. (1995). Developmental control point in induction of thymic cortex regulated by a subpopulation of prothymocytes. *Nature* **373**, 350-3.

Hsieh, J. C., Kodjabachian, L., Rebbert, M. L., Rattner, A., Smallwood, P. M., Samos, C. H., Nusse, R., Dawid, I. B., and Nathans, J. (1999). A new secreted protein that binds to Wnt proteins and inhibits their activities. *Nature* **398**, 431-6.

Hu, M. C., and Rosenblum, N. D. (2005). Smad1, beta-catenin and Tcf4 associate in a molecular complex with the Myc promoter in dysplastic renal tissue and cooperate to control Myc transcription. *Development* **132**, 215-25.

Hunter, D. D., Zhang, M., Ferguson, J. W., Koch, M., and Brunken, W. J. (2004). The extracellular matrix component WIF-1 is expressed during, and can modulate, retinal development. *Mol Cell Neurosci* **27**, 477-88.

Hwang, C. K., D'Souza, U. M., Eisch, A. J., Yajima, S., Lammers, C. H., Yang, Y., Lee, S. H., Kim, Y. M., Nestler, E. J., and Mouradian, M. M. (2001). Dopamine receptor regulating factor, DRRF: a zinc finger transcription factor. *Proc Natl Acad Sci U S A* **98**, 7558-63.

Ichtchenko, K., Hata, Y., Nguyen, T., Ullrich, B., Missler, M., Moomaw, C., and Sudhof, T. C. (1995). Neuroligin 1: a splice site-specific ligand for beta-neurexins. *Cell* **81**, 435-43.

Ishii, M., Han, J., Yen, H. Y., Sucov, H. M., Chai, Y., and Maxson, R. E., Jr. (2005). Combined deficiencies of Msx1 and Msx2 cause impaired patterning and survival of the cranial neural crest. *Development* **132**, 4937-50.

Ishikawa, H., Carrasco, D., Claudio, E., Ryseck, R. P., and Bravo, R. (1997). Gastric hyperplasia and increased proliferative responses of lymphocytes in mice lacking the COOH-terminal ankyrin domain of NF-kappaB2. *J Exp Med* **186**, 999-1014.

Itoi, M., Kawamoto, H., Katsura, Y., and Amagai, T. (2001). Two distinct steps of immigration of hematopoietic progenitors into the early thymus anlage. *Int Immunol* **13**, 1203-11.

Ivins, S., Lammerts van Beuren, K., Roberts, C., James, C., Lindsay, E., Baldini, A., Ataliotis, P., and Scambler, P. J. (2005). Microarray analysis detects differentially expressed genes in the pharyngeal region of mice lacking Tbx1. *Dev Biol* .

Jackson, M., Baird, J. W., Cambray, N., Ansell, J. D., Forrester, L. M., and Graham, G. J. (2002). Cloning and characterization of Ebox, a novel homeobox gene essential for embryonic stem cell differentiation. *J Biol Chem* **277**, 38683-92.

Jackson, M., Baird, J. W., Nichols, J., Wilkie, R., Ansell, J. D., Graham, G., and Forrester, L. M. (2003). Expression of a novel homeobox gene Ebox in trophoblast stem cells and pharyngeal pouch endoderm. *Dev Dyn* **228**, 740-4.

Jaleco, A. C., Neves, H., Hooijberg, E., Gameiro, P., Clode, N., Haury, M., Henrique, D., and Parreira, L. (2001). Differential effects of Notch ligands Delta-1 and Jagged-1 in human lymphoid differentiation. *J Exp Med* **194**, 991-1002.

Jameson, S. C., and Bevan, M. J. (1998). T-cell selection. *Curr Opin Immunol* **10**, 214-9.

Jenkinson, W. E., Jenkinson, E. J., and Anderson, G. (2003). Differential Requirement for Mesenchyme in the Proliferation and Maturation of Thymic Epithelial Progenitors. *J Exp Med* .

Jenkinson, W. E., Rossi, S. W., Jenkinson, E. J., and Anderson, G. (2005). Development of functional thymic epithelial cells occurs independently of lymphostromal interactions. *Mech Dev* .

Jerome, L. A., and Papaioannou, V. E. (2001). DiGeorge syndrome phenotype in mice mutant for the T-box gene, Tbx1. *Nat Genet* **27**, 286-91.

Jiang, X., Rowitch, D. H., Soriano, P., McMahon, A. P., and Sucov, H. M. (2000). Fate of the mammalian cardiac neural crest. *Development* **127**, 1607-16.

Kaneta, M., Osawa, M., Sudo, K., Nakauchi, H., Farr, A. G., and Takahama, Y. (2000). A role for pref-1 and HES-1 in thymocyte development. *J Immunol* **164**, 256-64.

Kanzler, B., Foreman, R. K., Labosky, P. A., and Mallo, M. (2000). BMP signaling is essential for development of skeletogenic and neurogenic cranial neural crest. *Development* **127**, 1095-104.

Kasai, M., Hirokawa, K., Kajino, K., Ogasawara, K., Tatsumi, M., Hermel, E., Monaco, J. J., and Mizuochi, T. (1996). Difference in antigen presentation pathways between cortical and medullary thymic epithelial cells. *Eur J Immunol* **26**, 2101-7.

Katsura, Y. (2002). Redefinition of lymphoid progenitors. *Nat Rev Immunol* **2**, 127-32.

Kattenstroth, G., Tantalaki, E., Sudhof, T. C., Gottmann, K., and Missler, M. (2004). Postsynaptic N-methyl-D-aspartate receptor function requires alpha-neurexins. *Proc Natl Acad Sci U S A* **101**, 2607-12.

Kawakami, N., Nishizawa, F., Sakane, N., Iwao, M., Tsujikawa, K., Ikawa, M., Okabe, M., and Yamamoto, H. (1999). Roles of integrins and CD44 on the adhesion and migration of fetal liver cells to the fetal thymus. *J Immunol* **163**, 3211-6.

Kawakami, Y., Esteban, C. R., Matsui, T., Rodriguez-Leon, J., Kato, S., and Belmonte, J. C. (2004). Sp8 and Sp9, two closely related buttonhead-like transcription factors, regulate Fgf8 expression and limb outgrowth in vertebrate embryos. *Development* **131**, 4763-74.

Kawamoto, H., Ohmura, K., Fujimoto, S., and Katsura, Y. (1999). Emergence of T cell progenitors without B cell or myeloid differentiation potential at the earliest stage of hematopoiesis in the murine fetal liver. *J Immunol* **162**, 2725-31.

Kawamoto, H., Ohmura, K., and Katsura, Y. (1998). Presence of progenitors restricted to T, B, or myeloid lineage, but absence of multipotent stem cells, in the murine fetal thymus. *J Immunol* **161**, 3799-802.

Kaye, J., Hsu, M. L., Sauron, M. E., Jameson, S. C., Gascoigne, N. R., and Hedrick, S. M. (1989). Selective development of CD4+ T cells in transgenic mice expressing a class II MHC-restricted antigen receptor. *Nature* **341**, 746-9.

Keeble, T. R., Halford, M. M., Seaman, C., Kee, N., Macheda, M., Anderson, R. B., Stacker, S. A., and Cooper, H. M. (2006). The Wnt receptor Ryk is required for Wnt5a-mediated axon guidance on the contralateral side of the corpus callosum. *J Neurosci* **26**, 5840-8.

Kim, H. K., and Siu, G. (1998). The notch pathway intermediate HES-1 silences CD4 gene expression. *Mol Cell Biol* **18**, 7166-75.

Kim, J., Jones, B. W., Zock, C., Chen, Z., Wang, H., Goodman, C. S., and Anderson, D. J. (1998). Isolation and characterization of mammalian homologs of the Drosophila gene glial cells missing. *Proc Natl Acad Sci U S A* **95**, 12364-9.

Kingston, R., Jenkinson, E. J., and Owen, J. J. (1984). Characterization of stromal cell populations in the developing thymus of normal and nude mice. *Eur J Immunol* **14**, 1052-6.

Kirby, M. L., and Bockman, D. E. (1984). Neural crest and normal development: a new perspective. *Anat Rec* **209**, 1-6.

Klein, L., Klein, T., Ruther, U., and Kyewski, B. (1998). CD4 T cell tolerance to human C-reactive protein, an inducible serum protein, is mediated by medullary thymic epithelium. *J Exp Med* **188**, 5-16.

Klein, L., Klugmann, M., Nave, K. A., Tuohy, V. K., and Kyewski, B. (2000). Shaping of the autoreactive T-cell repertoire by a splice variant of self protein expressed in thymic epithelial cells. *Nat Med* **6**, 56-61.

Klein, L., and Kyewski, B. (2000). Self-antigen presentation by thymic stromal cells: a subtle division of labor. *Curr Opin Immunol* **12**, 179-86.

Klug, D. B., Carter, C., Crouch, E., Roop, D., Conti, C. J., and Richie, E. R. (1998). Interdependence of cortical thymic epithelial cell differentiation and T-lineage commitment. *Proc Natl Acad Sci U S A* **95**, 11822-7.

Klug, D. B., Carter, C., Gimenez-Conti, I. B., and Richie, E. R. (2002). Cutting edge: thymocyte-independent and thymocyte-dependent phases of epithelial patterning in the fetal thymus. *J Immunol* **169**, 2842-5.

- Klur, S., Toy, K., Williams, M. P., and Certa, U. (2004). Evaluation of procedures for amplification of small-size samples for hybridization on microarrays. *Genomics* **83**, 508-17.
- Kojima, T., Morikawa, Y., Copeland, N. G., Gilbert, D. J., Jenkins, N. A., Senba, E., and Kitamura, T. (2000). TROY, a newly identified member of the tumor necrosis factor receptor superfamily, exhibits a homology with Edar and is expressed in embryonic skin and hair follicles. *J Biol Chem* **275**, 20742-7.
- Krumlauf, R. (1994). Hox genes in vertebrate development. *Cell* **78**, 191-201.
- Kuratani, S., and Bockman, D. E. (1990a). Impaired development of the thymic primordium after neural crest ablation. *Anat Rec* **228**, 185-90.
- Kuratani, S., and Bockman, D. E. (1990b). The participation of neural crest derived mesenchymal cells in development of the epithelial primordium of the thymus. *Arch Histol Cytol* **53**, 267-73.
- Kuratani, S., and Bockman, D. E. (1991). Capacity of neural crest cells from various axial levels to participate in thymic development. *Cell Tissue Res* **263**, 99-105.
- Kurobe, H., Liu, C., Ueno, T., Saito, F., Ohigashi, I., Seach, N., Arakaki, R., Hayashi, Y., Kitagawa, T., Lipp, M., Boyd, R. L., and Takahama, Y. (2006). CCR7-dependent cortex-to-medulla migration of positively selected thymocytes is essential for establishing central tolerance. *Immunity* **24**, 165-77.
- Laclef, C., Souil, E., Demignon, J., and Maire, P. (2003). Thymus, kidney and craniofacial abnormalities in Six1 deficient mice. *Mech Dev* **120**, 669-79.
- Lammer, E. J., Chen, D. T., Hoar, R. M., Agnish, N. D., Benke, P. J., Braun, J. T., Curry, C. J., Fernhoff, P. M., Grix, A. W., Jr., Lott, I. T., and et al. (1985). Retinoic acid embryopathy. *N Engl J Med* **313**, 837-41.
- Laufer, T. M., DeKoning, J., Markowitz, J. S., Lo, D., and Glimcher, L. H. (1996). Unopposed positive selection and autoreactivity in mice expressing class II MHC only on thymic cortex. *Nature* **383**, 81-5.

Le Douarin, N. M., and Jotereau, F. V. (1975). Tracing of cells of the avian thymus through embryonic life in interspecific chimeras. *J Exp Med* **142**, 17-40.

Lee, C. S., Buttitta, L. A., May, N. R., Kispert, A., and Fan, C. M. (2000). SHH-N upregulates *Sfrp2* to mediate its competitive interaction with WNT1 and WNT4 in the somitic mesoderm. *Development* **127**, 109-18.

Lee, D., Prowse, D. M., and Brissette, J. L. (1999). Association between mouse nude gene expression and the initiation of epithelial terminal differentiation. *Dev Biol* **208**, 362-74.

Legler, D. F., Loetscher, M., Roos, R. S., Clark-Lewis, I., Baggiolini, M., and Moser, B. (1998). B cell-attracting chemokine 1, a human CXC chemokine expressed in lymphoid tissues, selectively attracts B lymphocytes via BLR1/CXCR5. *J Exp Med* **187**, 655-60.

Li, C., and Wong, W. H. (2001). Model-based analysis of oligonucleotide arrays: expression index computation and outlier detection. *Proc Natl Acad Sci U S A* **98**, 31-6.

Lin, H., and Grosschedl, R. (1995). Failure of B-cell differentiation in mice lacking the transcription factor EBF. *Nature* **376**, 263-7.

Lin, X. (2004). Functions of heparan sulfate proteoglycans in cell signaling during development. *Development* **131**, 6009-21.

Lind, E. F., Prockop, S. E., Porritt, H. E., and Petrie, H. T. (2001). Mapping precursor movement through the postnatal thymus reveals specific microenvironments supporting defined stages of early lymphoid development. *J Exp Med* **194**, 127-34.

Lindsay, E. A., Botta, A., Jurecic, V., Carattini-Rivera, S., Cheah, Y. C., Rosenblatt, H. M., Bradley, A., and Baldini, A. (1999). Congenital heart disease in mice deficient for the DiGeorge syndrome region. *Nature* **401**, 379-83.



Lindsay, E. A., Vitelli, F., Su, H., Morishima, M., Huynh, T., Pramparo, T., Jurecic, V., Ogunrinu, G., Sutherland, H. F., Scambler, P. J., Bradley, A., and Baldini, A. (2001). Tbx1 haploinsufficiency in the DiGeorge syndrome region causes aortic arch defects in mice. *Nature* **410**, 97-101.

Liston, A., Gray, D. H., Lesage, S., Fletcher, A. L., Wilson, J., Webster, K. E., Scott, H. S., Boyd, R. L., Peltonen, L., and Goodnow, C. C. (2004). Gene dosage--limiting role of Aire in thymic expression, clonal deletion, and organ-specific autoimmunity. *J Exp Med* **200**, 1015-26.

Liston, A., Lesage, S., Wilson, J., Peltonen, L., and Goodnow, C. C. (2003). Aire regulates negative selection of organ-specific T cells. *Nat Immunol* **4**, 350-4.

Liu, C., Ueno, T., Kuse, S., Saito, F., Nitta, T., Piali, L., Nakano, H., Kakiuchi, T., Lipp, M., Hollander, G. A., and Takahama, Y. (2005). The role of CCL21 in recruitment of T-precursor cells to fetal thymus. *Blood* **105**, 31-9.

Lo, D., and Sprent, J. (1986). Identity of cells that imprint H-2-restricted T-cell specificity in the thymus. *Nature* **319**, 672-5.

Lu, W., Yamamoto, V., Ortega, B., and Baltimore, D. (2004). Mammalian Ryk is a Wnt coreceptor required for stimulation of neurite outgrowth. *Cell* **119**, 97-108.

Ma, L., Liu, J., Wu, T., Plikus, M., Jiang, T. X., Bi, Q., Liu, Y. H., Muller-Rover, S., Peters, H., Sundberg, J. P., Maxson, R., Maas, R. L., and Chuong, C. M. (2003). 'Cyclic alopecia' in Msx2 mutants: defects in hair cycling and hair shaft differentiation. *Development* **130**, 379-89.

Ma, Q., Jones, D., Borghesani, P. R., Segal, R. A., Nagasawa, T., Kishimoto, T., Bronson, R. T., and Springer, T. A. (1998). Impaired B-lymphopoiesis, myeloopoiesis, and derailed cerebellar neuron migration in CXCR4- and SDF-1-deficient mice. *Proc Natl Acad Sci U S A* **95**, 9448-53.

Mankoo, B. S., Collins, N. S., Ashby, P., Grigorieva, E., Pevny, L. H., Candia, A., Wright, C. V., Rigby, P. W., and Pachnis, V. (1999). Mox2 is a component of the genetic hierarchy controlling limb muscle development. *Nature* **400**, 69-73.

Mankoo, B. S., Skuntz, S., Harrigan, I., Grigorieva, E., Candia, A., Wright, C. V., Arnheiter, H., and Pachnis, V. (2003). The concerted action of Meox homeobox genes is required upstream of genetic pathways essential for the formation, patterning and differentiation of somites. *Development* **130**, 4655-64.

Manley, N. R., and Capecchi, M. R. (1995). The role of Hoxa-3 in mouse thymus and thyroid development. *Development* **121**, 1989-2003.

Manley, N. R., and Capecchi, M. R. (1998). Hox group 3 paralogs regulate the development and migration of the thymus, thyroid, and parathyroid glands. *Dev Biol* **195**, 1-15.

Manley, N. R., Selleri, L., Brendolan, A., Gordon, J., and Cleary, M. L. (2004). Abnormalities of caudal pharyngeal pouch development in Pbx1 knockout mice mimic loss of Hox3 paralogs. *Dev Biol* **276**, 301-12.

Mark, M., Ghyselinck, N. B., and Chambon, P. (2004). Retinoic acid signalling in the development of branchial arches. *Curr Opin Genet Dev* **14**, 591-8.

Markowitz, J. S., Auchincloss, H., Jr., Grusby, M. J., and Glimcher, L. H. (1993). Class II-positive hematopoietic cells cannot mediate positive selection of CD4+ T lymphocytes in class II-deficient mice. *Proc Natl Acad Sci U S A* **90**, 2779-83.

Marrack, P., McCormack, J., and Kappler, J. (1989). Presentation of antigen, foreign major histocompatibility complex proteins and self by thymus cortical epithelium. *Nature* **338**, 503-5.

Martin, G. R. (1998). The roles of FGFs in the early development of vertebrate limbs. *Genes Dev* **12**, 1571-86.

Matzuk, M. M., Lu, N., Vogel, H., Sellheyer, K., Roop, D. R., and Bradley, A. (1995). Multiple defects and perinatal death in mice deficient in follistatin. *Nature* **374**, 360-3.

Merkenschlager, M., Graf, D., Lovatt, M., Bommhardt, U., Zamoyska, R., and Fisher, A. G. (1997). How many thymocytes audition for selection? *J Exp Med* **186**, 1149-58.

Merscher, S., Funke, B., Epstein, J. A., Heyer, J., Puech, A., Lu, M. M., Xavier, R. J., Demay, M. B., Russell, R. G., Factor, S., Tokooya, K., Jore, B. S., Lopez, M., Pandita, R. K., Lia, M., Carrion, D., Xu, H., Schorle, H., Kobler, J. B., Scambler, P., Wynshaw-Boris, A., Skoultschi, A. I., Morrow, B. E., and Kucherlapati, R. (2001). TBX1 is responsible for cardiovascular defects in velo-cardio- facial/DiGeorge syndrome. *Cell* **104**, 619-29.

Meyers, E. N., Lewandoski, M., and Martin, G. R. (1998). An Fgf8 mutant allelic series generated by Cre- and Flp-mediated recombination. *Nat Genet* **18**, 136-41.

Missler, M., Hammer, R. E., and Sudhof, T. C. (1998). Neurexophilin binding to alpha-neurexins. A single LNS domain functions as an independently folding ligand-binding unit. *J Biol Chem* **273**, 34716-23.

Missler, M., Zhang, W., Rohlmann, A., Kattenstroth, G., Hammer, R. E., Gottmann, K., and Sudhof, T. C. (2003). Alpha-neurexins couple Ca<sup>2+</sup> channels to synaptic vesicle exocytosis. *Nature* **423**, 939-48.

Miyasaka, M., Pabst, R., Dudler, L., Cooper, M., and Yamaguchi, K. (1990). Characterization of lymphatic and venous emigrants from the thymus. *Thymus* **16**, 29-43.

Miyawaki, S., Nakamura, Y., Suzuka, H., Koba, M., Yasumizu, R., Ikehara, S., and Shibata, Y. (1994). A new mutation, aly, that induces a generalized lack of lymph nodes accompanied by immunodeficiency in mice. *Eur J Immunol* **24**, 429-34.

Monsoro-Burq, A., and Le Douarin, N. M. (2001). BMP4 plays a key role in left-right patterning in chick embryos by maintaining Sonic Hedgehog asymmetry. *Mol Cell* **7**, 789-99.

Moon, Y. S., Smas, C. M., Lee, K., Villena, J. A., Kim, K. H., Yun, E. J., and Sul, H. S. (2002). Mice lacking paternally expressed Pref-1/Dlk1 display growth retardation and accelerated adiposity. *Mol Cell Biol* **22**, 5585-92.

Moore-Scott, B. A., Gordon, J., Blackburn, C. C., Condie, B. G., and Manley, N. R. (2003). New serum-free in vitro culture technique for midgestation mouse embryos. *Genesis* **35**, 164-8.

Moore-Scott, B. A., and Manley, N. R. (2005). Differential expression of Sonic hedgehog along the anterior-posterior axis regulates patterning of pharyngeal pouch endoderm and pharyngeal endoderm-derived organs. *Dev Biol* **278**, 323-335.

Morrison-Graham, K., Schatteman, G. C., Bork, T., Bowen-Pope, D. F., and Weston, J. A. (1992). A PDGF receptor mutation in the mouse (Patch) perturbs the development of a non-neuronal subset of neural crest-derived cells. *Development* **115**, 133-42.

Muller, S. M., Terszowski, G., Blum, C., Haller, C., Anquez, V., Kuschert, S., Carmeliet, P., Augustin, H. G., and Rodewald, H. R. (2005). Gene targeting of VEGF-A in thymus epithelium disrupts thymus blood vessel architecture. *Proc Natl Acad Sci U S A* **102**, 10587-92.

Mulroy, T., McMahon, J. A., Burakoff, S. J., McMahon, A. P., and Sen, J. (2002). Wnt-1 and Wnt-4 regulate thymic cellularity. *Eur J Immunol* **32**, 967-71.

Mulroy, T., Xu, Y., and Sen, J. M. (2003). beta-Catenin expression enhances generation of mature thymocytes. *Int Immunol* **15**, 1485-94.

Muroya, K., Okuyama, T., Goishi, K., Ogiso, Y., Fukuda, S., Kameyama, J., Sato, H., Suzuki, Y., Terasaki, H., Gomyo, H., Wakui, K., Fukushima, Y., and Ogata, T. (2000). Sex-determining gene(s) on distal 9p: clinical and molecular studies in six cases. *J Clin Endocrinol Metab* **85**, 3094-100.

Murphy, K. M., Heimberger, A. B., and Loh, D. Y. (1990). Induction by antigen of intrathymic apoptosis of CD4+CD8+TCRlo thymocytes in vivo. *Science* **250**, 1720-3.

Nakamura, T., Sugino, K., Titani, K., and Sugino, H. (1991). Follistatin, an activin-binding protein, associates with heparan sulfate chains of proteoglycans on follicular granulosa cells. *J Biol Chem* **266**, 19432-7.

Naspetti, M., Aurrand-Lions, M., DeKoning, J., Malissen, M., Galland, F., Lo, D., and Naquet, P. (1997). Thymocytes and RelB-dependent medullary epithelial cells provide growth-promoting and organization signals, respectively, to thymic medullary stromal cells. *Eur J Immunol* **27**, 1392-7.

Nedvetzki, S., Gonen, E., Assayag, N., Reich, R., Williams, R. O., Thurmond, R. L., Huang, J. F., Neudecker, B. A., Wang, F. S., Turley, E. A., and Naor, D. (2004). RHAMM, a receptor for hyaluronan-mediated motility, compensates for CD44 in inflamed CD44-knockout mice: A different interpretation of redundancy. *Proc Natl Acad Sci U S A* **101**, 18081-6.

Nehls, M., Kyewski, B., Messerle, M., Waldschutz, R., Schuddekopf, K., Smith, A. J., and Boehm, T. (1996). Two genetically separable steps in the differentiation of thymic epithelium. *Science* **272**, 886-9.

Nehls, M., Pfeifer, D., Schorpp, M., Hedrich, H., and Boehm, T. (1994). New member of the winged-helix protein family disrupted in mouse and rat nude mutations. *Nature* **372**, 103-7.

Niederreither, K., Subbarayan, V., Dolle, P., and Chambon, P. (1999). Embryonic retinoic acid synthesis is essential for early mouse post-implantation development. *Nat Genet* **21**, 444-8.

Niederreither, K., Vermot, J., Le Roux, I., Schuhbaur, B., Chambon, P., and Dolle, P. (2003). The regional pattern of retinoic acid synthesis by RALDH2 is essential for the development of posterior pharyngeal arches and the enteric nervous system. *Development* **130**, 2525-34.

Nogami, K., Suzuki, H., Habuchi, H., Ishiguro, N., Iwata, H., and Kimata, K. (2004). Distinctive expression patterns of heparan sulfate O-sulfotransferases and regional differences in heparan sulfate structure in chick limb buds. *J Biol Chem* **279**, 8219-29.

Nossal, G. J. (1994). Negative selection of lymphocytes. *Cell* **76**, 229-39.

Ohazama, A., Courtney, J. M., Tucker, A. S., Naito, A., Tanaka, S., Inoue, J., and Sharpe, P. T. (2004). Traf6 is essential for murine tooth cusp morphogenesis. *Dev Dyn* **229**, 131-5.

Ohnemus, S., Kanzler, B., Jerome-Majewska, L. A., Papaioannou, V. E., Boehm, T., and Mallo, M. (2002). Aortic arch and pharyngeal phenotype in the absence of BMP-dependent neural crest in the mouse. *Mech Dev* **119**, 127-135.

Ohuchi, H., Hori, Y., Yamasaki, M., Harada, H., Sekine, K., Kato, S., and Itoh, N. (2000). FGF10 acts as a major ligand for FGF receptor 2 IIIb in mouse multi-organ development. *Biochem Biophys Res Commun* **277**, 643-9.

Owen, J. J., and Jenkinson, E. J. (1984). Early events in T lymphocyte genesis in the fetal thymus. *Am J Anat* **170**, 301-10.

Owen, J. J., McLoughlin, D. E., Suniara, R. K., and Jenkinson, E. J. (2000). The role of mesenchyme in thymus development [In Process Citation]. *Curr Top Microbiol Immunol* **251**, 133-7.

Paez-Pereda, M., Giacomini, D., Refojo, D., Nagashima, A. C., Hopfner, U., Grubler, Y., Chervin, A., Goldberg, V., Goya, R., Hentges, S. T., Low, M. J., Holsboer, F., Stalla, G. K., and Arzt, E. (2003). Involvement of bone morphogenetic protein 4 (BMP-4) in pituitary prolactinoma pathogenesis through a Smad/estrogen receptor crosstalk. *Proc Natl Acad Sci U S A* **100**, 1034-9.

Palmer, D. B., Viney, J. L., Ritter, M. A., Hayday, A. C., and Owen, M. J. (1993). Expression of the alpha beta T-cell receptor is necessary for the generation of the thymic medulla. *Dev Immunol* **3**, 175-9.

Palmer, E. (2003). Negative selection--clearing out the bad apples from the T-cell repertoire. *Nat Rev Immunol* **3**, 383-91.

Pantelouris, E. M. (1968). Absence of thymus in a mouse mutant. *Nature* **217**, 370-1.

Patel, S. R., Gordon, J., Mahbub, F., Blackburn, C. C., and Manley, N. R. (2006). Bmp4 and Noggin expression during early thymus and parathyroid organogenesis. *Gene Expr Patterns* .

Paterson, D. J., and Williams, A. F. (1987). An intermediate cell in thymocyte differentiation that expresses CD8 but not CD4 antigen. *J Exp Med* **166**, 1603-8.

Patthy, L. (2000). The WIF module. *Trends Biochem Sci* **25**, 12-3.

Peters, H., Neubuser, A., Kratochwil, K., and Balling, R. (1998). Pax9-deficient mice lack pharyngeal pouch derivatives and teeth and exhibit craniofacial and limb abnormalities. *Genes Dev* **12**, 2735-47.

Peterson, R. S., Andhare, R. A., Rousche, K. T., Knudson, W., Wang, W., Grossfield, J. B., Thomas, R. O., Hollingsworth, R. E., and Knudson, C. B. (2004). CD44 modulates Smad1 activation in the BMP-7 signaling pathway. *J Cell Biol* **166**, 1081-91.

Pignoni, F., Hu, B., Zavitz, K. H., Xiao, J., Garrity, P. A., and Zipursky, S. L. (1997). The eye-specification proteins So and Eya form a complex and regulate multiple steps in Drosophila eye development. *Cell* **91**, 881-91.

Pinson, K. I., Brennan, J., Monkley, S., Avery, B. J., and Skarnes, W. C. (2000). An LDL-receptor-related protein mediates Wnt signalling in mice. *Nature* **407**, 535-8.

Plotkin, J., Prockop, S. E., Lepique, A., and Petrie, H. T. (2003). Critical role for CXCR4 signaling in progenitor localization and T cell differentiation in the postnatal thymus. *J Immunol* **171**, 4521-7.

Pongracz, J., Hare, K., Harman, B., Anderson, G., and Jenkinson, E. J. (2003). Thymic epithelial cells provide WNT signals to developing thymocytes. *Eur J Immunol* **33**, 1949-56.

Ponta, H., Sherman, L., and Herrlich, P. A. (2003). CD44: from adhesion molecules to signalling regulators. *Nat Rev Mol Cell Biol* **4**, 33-45.

Protin, U., Schweighoffer, T., Jochum, W., and Hilberg, F. (1999). CD44-deficient mice develop normally with changes in subpopulations and recirculation of lymphocyte subsets. *J Immunol* **163**, 4917-23.

Pui, J. C., Allman, D., Xu, L., DeRocco, S., Karnell, F. G., Bakkour, S., Lee, J. Y., Kadesch, T., Hardy, R. R., Aster, J. C., and Pear, W. S. (1999). Notch1 expression in early lymphopoiesis influences B versus T lineage determination. *Immunity* **11**, 299-308.

Quinn, L. M., Latham, S. E., and Kalionis, B. (2000). The homeobox genes MSX2 and MOX2 are candidates for regulating epithelial-mesenchymal cell interactions in the human placenta. *Placenta* **21 Suppl A**, S50-4.

Radtke, F., Wilson, A., Mancini, S. J., and MacDonald, H. R. (2004). Notch regulation of lymphocyte development and function. *Nat Immunol* **5**, 247-53.

Radtke, F., Wilson, A., Stark, G., Bauer, M., van Meerwijk, J., MacDonald, H. R., and Aguet, M. (1999). Deficient T cell fate specification in mice with an induced inactivation of Notch1. *Immunity* **10**, 547-58.

Raff, M. C. (1992). Social controls on cell survival and cell death. *Nature* **356**, 397-400.

Rahemtulla, A., Fung-Leung, W. P., Schilham, M. W., Kundig, T. M., Sambhara, S. R., Narendran, A., Arabian, A., Wakeham, A., Paige, C. J., Zinkernagel, R. M., and et al. (1991). Normal development and function of CD8+ cells but markedly decreased helper cell activity in mice lacking CD4. *Nature* **353**, 180-4.

Revest, J. M., Spencer-Dene, B., Kerr, K., De Moerlooze, L., Rosewell, I., and Dickson, C. (2001a). Fibroblast growth factor receptor 2-IIIb acts upstream of Shh and Fgf4 and is required for limb bud maintenance but not for the induction of Fgf8, Fgf10, Msx1, or Bmp4. *Dev Biol* **231**, 47-62.



Revest, J. M., Suniara, R. K., Kerr, K., Owen, J. J., and Dickson, C. (2001b). Development of the thymus requires signaling through the fibroblast growth factor receptor  $\alpha 2$ -iib. *J Immunol* **167**, 1954-61.

Ritter, M. A., and Boyd, R. L. (1993). Development in the thymus: it takes two to tango [see comments]. *Immunol Today* **14**, 462-9.

Roberts, C., Ivins, S. M., James, C. T., and Scambler, P. J. (2005). Retinoic acid down-regulates Tbx1 expression in vivo and in vitro. *Dev Dyn* **232**, 928-38.

Rodewald, H. R., Kretzschmar, K., Takeda, S., Hohl, C., and Dessing, M. (1994). Identification of pro-thymocytes in murine fetal blood: T lineage commitment can precede thymus colonization. *Embo J* **13**, 4229-40.

Rodewald, H. R., Paul, S., Haller, C., Bluethmann, H., and Blum, C. (2001). Thymus medulla consisting of epithelial islets each derived from a single progenitor. *Nature* **414**, 763-768.

Ropke, C., Van Soest, P., Platenburg, P. P., and Van Ewijk, W. (1995). A common stem cell for murine cortical and medullary thymic epithelial cells? *Dev Immunol* **4**, 149-56.

Rowen, L., Young, J., Birditt, B., Kaur, A., Madan, A., Philipps, D. L., Qin, S., Minx, P., Wilson, R. K., Hood, L., and Graveley, B. R. (2002). Analysis of the human neurexin genes: alternative splicing and the generation of protein diversity. *Genomics* **79**, 587-97.

Sainte-Marie, G., and Leblond, C. P. (1965). Elaboration of a model for the formation of lymphocytes in the thymic cortex of young adult rats. *Blood* **26**, 765-83.

Savino, W., Cotta-de-Almeida, V., van Buul-Offers, S. C., Koster, J. G., and Dardenne, M. (2005). Abnormal thymic microenvironment in insulin-like growth factor-II transgenic mice. *Neuroimmunomodulation* **12**, 100-12.

Schaeren-Wiemers, N., and Gerfin-Moser, A. (1993). A single protocol to detect transcripts of various types and expression levels in neural tissue and cultured cells: in situ hybridization using digoxigenin-labelled cRNA probes. *Histochemistry* **100**, 431-40.

Schluep, M., Willcox, N., Ritter, M. A., Newsom-Davis, J., Larche, M., and Brown, A. N. (1988). Myasthenia gravis thymus: clinical, histological and culture correlations. *J Autoimmun* **1**, 445-67.

Schnepp, A., Komp Lindgren, P., Hulsmann, H., Kroger, S., Paulsson, M., and Hartmann, U. (2005). Mouse testican-2. Expression, glycosylation, and effects on neurite outgrowth. *J Biol Chem* **280**, 11274-80.

Schwarzler, C., Oliferenko, S., and Gunthert, U. (2001). Variant isoforms of CD44 are required in early thymocyte development. *Eur J Immunol* **31**, 2997-3005.

Sebzda, E., Mariathasan, S., Ohteki, T., Jones, R., Bachmann, M. F., and Ohashi, P. S. (1999). Selection of the T cell repertoire. *Annu Rev Immunol* **17**, 829-74.

Sekiya, T., Adachi, S., Kohu, K., Yamada, T., Higuchi, O., Furukawa, Y., Nakamura, Y., Nakamura, T., Tashiro, K., Kuhara, S., Ohwada, S., and Akiyama, T. (2004a). Identification of BMP and activin membrane-bound inhibitor (BAMBI), an inhibitor of transforming growth factor-beta signaling, as a target of the beta-catenin pathway in colorectal tumor cells. *J Biol Chem* **279**, 6840-6.

Sekiya, T., Oda, T., Matsuura, K., and Akiyama, T. (2004b). Transcriptional regulation of the TGF-beta pseudoreceptor BAMBI by TGF-beta signaling. *Biochem Biophys Res Commun* **320**, 680-4.

Shah, D. K., Hager-Theodorides, A. L., Outram, S. V., Ross, S. E., Varas, A., and Crompton, T. (2004). Reduced thymocyte development in sonic hedgehog knockout embryos. *J Immunol* **172**, 2296-306.

Shinkura, R., Kitada, K., Matsuda, F., Tashiro, K., Ikuta, K., Suzuki, M., Kogishi, K., Serikawa, T., and Honjo, T. (1999). A lymphoplasia is caused by a point mutation in the mouse gene encoding Nf-kappa b-inducing kinase. *Nat Genet* **22**, 74-7.

Shores, E. W., Van Ewijk, W., and Singer, A. (1991). Disorganization and restoration of thymic medullary epithelial cells in T cell receptor-negative scid mice: evidence that receptor-bearing lymphocytes influence maturation of the thymic microenvironment. *Eur J Immunol* **21**, 1657-61.

Shores, E. W., Van Ewijk, W., and Singer, A. (1994). Maturation of medullary thymic epithelium requires thymocytes expressing fully assembled CD3-TCR complexes. *Int Immunol* **6**, 1393-402.

Singer, N. G., Fox, D. A., Haqqi, T. M., Beretta, L., Endres, J. S., Prohaska, S., Parnes, J. R., Bromberg, J., and Sramkoski, R. M. (2002). CD6: expression during development, apoptosis and selection of human and mouse thymocytes. *Int Immunol* **14**, 585-97.

Smallwood, P. M., Munoz-Sanjuan, I., Tong, P., Macke, J. P., Hendry, S. H., Gilbert, D. J., Copeland, N. G., Jenkins, N. A., and Nathans, J. (1996). Fibroblast growth factor (FGF) homologous factors: new members of the FGF family implicated in nervous system development. *Proc Natl Acad Sci U S A* **93**, 9850-7.

Smith, C. (1965). Studies on the Thymus of the Mammal. Xiv. Histology and Histochemistry of Embryonic and Early Postnatal Thymuses of C57bl-6 and Akr Strain Mice. *Am J Anat* **116**, 611-29.

Smith, H., Chen, I. M., Kubo, R., and Tung, K. S. (1989). Neonatal thymectomy results in a repertoire enriched in T cells deleted in adult thymus. *Science* **245**, 749-52.

Soriano, P. (1997). The PDGF alpha receptor is required for neural crest cell development and for normal patterning of the somites. *Development* **124**, 2691-700.

Sprent, J., and Kishimoto, H. (2001). The thymus and central tolerance. *Philos Trans R Soc Lond B Biol Sci* **356**, 609-16.

Sprent, J., and Kishimoto, H. (2002). The thymus and negative selection. *Immunol Rev* **185**, 126-35.

Staal, F. J., Meeldijk, J., Moerer, P., Jay, P., van de Weerd, B. C., Vainio, S., Nolan, G. P., and Clevers, H. (2001). Wnt signaling is required for thymocyte development and activates Tcf-1 mediated transcription. *Eur J Immunol* **31**, 285-93.

Staal, F. J., Weerkamp, F., Baert, M. R., van den Burg, C. M., van Noort, M., de Haas, E. F., and van Dongen, J. J. (2004). Wnt target genes identified by DNA microarrays in immature CD34+ thymocytes regulate proliferation and cell adhesion. *J Immunol* **172**, 1099-108.

Stalmans, I., Lambrechts, D., De Smet, F., Jansen, S., Wang, J., Maity, S., Kneer, P., Von Der Ohe, M., Swillen, A., Maes, C., Gewillig, M., Molin, D. G., Hellings, P., Boetel, T., Haardt, M., Compennolle, V., Dewerchin, M., Plaisance, S., Vlietinck, R., Emanuel, B., Gittenberger-De Groot, A. C., Scambler, P., Morrow, B., Driscoll, D. A., Moons, L., Esguerra, C. V., Carmeliet, G., Behn-Krappa, A., Devriendt, K., Collen, D., Conway, S. J., and Carmeliet, P. (2003). VEGF: A modifier of the del22q11 (DiGeorge) syndrome? *Nat Med* .

Stamatakis, D., Kastriaki, M., Mankoo, B. S., Pachnis, V., and Karagogeos, D. (2001). Homeodomain proteins Mox1 and Mox2 associate with Pax1 and Pax3 transcription factors. *FEBS Lett* **499**, 274-8.

Starr, T. K., Jameson, S. C., and Hogquist, K. A. (2003). Positive and negative selection of T cells. *Annu Rev Immunol* **21**, 139-76.

Su, D., Ellis, S., Napier, A., Lee, K., and Manley, N. R. (2001). Hoxa3 and pax1 regulate epithelial cell death and proliferation during thymus and parathyroid organogenesis. *Dev Biol* **236**, 316-29.

Su, D. M., Navarre, S., Oh, W. J., Condie, B. G., and Manley, N. R. (2003). A domain of Foxn1 required for crosstalk-dependent thymic epithelial cell differentiation. *Nat Immunol* .

Suniara, R. K., Jenkinson, E. J., and Owen, J. J. (2000). An essential role for thymic mesenchyme in early T cell development. *J Exp Med* **191**, 1051-6.

Surh, C. D., and Sprent, J. (1994). T-cell apoptosis detected in situ during positive and negative selection in the thymus. *Nature* **372**, 100-3.

Suzuki, T., Takeuchi, J., Koshiba-Takeuchi, K., and Ogura, T. (2004). Tbx Genes Specify Posterior Digit Identity through Shh and BMP Signaling. *Dev Cell* **6**, 43-53.

Teh, H. S., Kisielow, P., Scott, B., Kishi, H., Uematsu, Y., Bluthmann, H., and von Boehmer, H. (1988). Thymic major histocompatibility complex antigens and the alpha beta T-cell receptor determine the CD4/CD8 phenotype of T cells. *Nature* **335**, 229-33.

Throsby, M., Herbelin, A., Pleau, J. M., and Dardenne, M. (2000). CD11c<sup>+</sup> eosinophils in the murine thymus: developmental regulation and recruitment upon MHC class I-restricted thymocyte deletion. *J Immunol* **165**, 1965-75.

Tokoro, Y., Sugawara, T., Yaginuma, H., Nakauchi, H., Terhorst, C., Wang, B., and Takahama, Y. (1998). A mouse carrying genetic defect in the choice between T and B lymphocytes. *J Immunol* **161**, 4591-8.

Topaz, O., Shurman, D. L., Bergman, R., Indelman, M., Ratajczak, P., Mizrachi, M., Khamaysi, Z., Behar, D., Petronius, D., Friedman, V., Zelikovic, I., Raimer, S., Metzker, A., Richard, G., and Sprecher, E. (2004). Mutations in GALNT3, encoding a protein involved in O-linked glycosylation, cause familial tumoral calcinosis. *Nat Genet* **36**, 579-81.

Toro, I., and Olah, I. (1967). Penetration of thymocytes into the blood circulation. *J Ultrastruct Res* **17**, 439-51.

Traver, D., Miyamoto, T., Christensen, J., Iwasaki-Arai, J., Akashi, K., and Weissman, I. L. (2001). Fetal liver myelopoiesis occurs through distinct, prospectively isolatable progenitor subsets. *Blood* **98**, 627-35.

Treichel, D., Schock, F., Jackle, H., Gruss, P., and Mansouri, A. (2003). mBtd is required to maintain signaling during murine limb development. *Genes Dev* **17**, 2630-5.

Tsai, P. T., Lee, R. A., and Wu, H. (2003). BMP4 acts upstream of FGF in modulating thymic stroma and regulating thymopoiesis. *Blood* **102**, 3947-53.

Tsukamoto, N., Itoi, M., Nishikawa, M., and Amagai, T. (2005). Lack of Delta like 1 and 4 expressions in nude thymus anlagen. *Cell Immunol* .

Ushkaryov, Y. A., Petrenko, A. G., Geppert, M., and Sudhof, T. C. (1992). Neurexins: synaptic cell surface proteins related to the alpha-latrotoxin receptor and laminin. *Science* **257**, 50-6.

van Ewijk, W., Hollander, G., Terhorst, C., and Wang, B. (2000a). Stepwise development of thymic microenvironments in vivo is regulated by thymocyte subsets. *Development* **127**, 1583-91.

van Ewijk, W., Kawamoto, H., Germeraad, W. T., and Katsura, Y. (2000b). Developing thymocytes organize thymic microenvironments [In Process Citation]. *Curr Top Microbiol Immunol* **251**, 125-32.

van Ewijk, W., Shores, E. W., and Singer, A. (1994). Crosstalk in the mouse thymus. *Immunol Today* **15**, 214-7.

van Ewijk, W., Wang, B., Hollander, G., Kawamoto, H., Spanopoulou, E., Itoi, M., Amagai, T., Jiang, Y. F., Germeraad, W. T., Chen, W. F., and Katsura, Y. (1999). Thymic microenvironments, 3-D versus 2-D? *Semin Immunol* **11**, 57-64.

Van Gelder, R. N., von Zastrow, M. E., Yool, A., Dement, W. C., Barchas, J. D., and Eberwine, J. H. (1990). Amplified RNA synthesized from limited quantities of heterogeneous cDNA. *Proc Natl Acad Sci U S A* **87**, 1663-7.

Van Vliet, E., Jenkinson, E. J., Kingston, R., Owen, J. J., and Van Ewijk, W. (1985). Stromal cell types in the developing thymus of the normal and nude mouse embryo. *Eur J Immunol* **15**, 675-81.

Vannahme, C., Schubel, S., Herud, M., Gosling, S., Hulsmann, H., Paulsson, M., Hartmann, U., and Maurer, P. (1999). Molecular cloning of testican-2: defining a novel calcium-binding proteoglycan family expressed in brain. *J Neurochem* **73**, 12-20.

Vermot, J., Niederreither, K., Garnier, J. M., Chambon, P., and Dolle, P. (2003). Decreased embryonic retinoic acid synthesis results in a DiGeorge syndrome phenotype in newborn mice. *Proc Natl Acad Sci U S A* .

Vitelli, F., Taddei, I., Morishima, M., Meyers, E. N., Lindsay, E. A., and Baldini, A. (2002). A genetic link between Tbx1 and fibroblast growth factor signaling. *Development* **129**, 4605-11.

von Boehmer, H. (1994). Positive selection of lymphocytes. *Cell* **76**, 219-28.

von Boehmer, H., and Fehling, H. J. (1997). Structure and function of the pre-T cell receptor. *Annu Rev Immunol* **15**, 433-52.

Von Gaudecker, B., Kendall, M. D., and Ritter, M. A. (1997). Immuno-electron microscopy of the thymic epithelial microenvironment. *Microsc Res Tech* **38**, 237-49.

Wallin, J., Eibel, H., Neubuser, A., Wilting, J., Koseki, H., and Balling, R. (1996). Pax1 is expressed during development of the thymus epithelium and is required for normal T-cell maturation. *Development* **122**, 23-30.

Wang, B., Biron, C., She, J., Higgins, K., Sunshine, M. J., Lacy, E., Lonberg, N., and Terhorst, C. (1994). A block in both early T lymphocyte and natural killer cell development in transgenic mice with high-copy numbers of the human CD3E gene. *Proc Natl Acad Sci U S A* **91**, 9402-6.

Wang, B., Levelt, C., Salio, M., Zheng, D., Sancho, J., Liu, C. P., She, J., Huang, M., Higgins, K., Sunshine, M. J., and et al. (1995). Over-expression of CD3 epsilon transgenes blocks T lymphocyte development. *Int Immunol* **7**, 435-48.

Wang, X. P., Suomalainen, M., Jorgez, C. J., Matzuk, M. M., Werner, S., and Thesleff, I. (2004). Follistatin regulates enamel patterning in mouse incisors by asymmetrically inhibiting BMP signaling and ameloblast differentiation. *Dev Cell* **7**, 719-30.

Weih, F., Carrasco, D., Durham, S. K., Barton, D. S., Rizzo, C. A., Ryseck, R. P., Lira, S. A., and Bravo, R. (1995). Multiorgan inflammation and hematopoietic abnormalities in mice with a targeted disruption of RelB, a member of the NF-kappa B/Rel family. *Cell* **80**, 331-40.

Wendling, O., Dennefeld, C., Chambon, P., and Mark, M. (2000). Retinoid signaling is essential for patterning the endoderm of the third and fourth pharyngeal arches. *Development* **127**, 1553-62.

Werdelin, O., Cordes, U., and Jensen, T. (1998). Aberrant expression of tissue-specific proteins in the thymus: a hypothesis for the development of central tolerance. *Scand J Immunol* **47**, 95-100.

Wharton, K. A., Jr., Zimmermann, G., Rousset, R., and Scott, M. P. (2001). Vertebrate proteins related to Drosophila Naked Cuticle bind Dishevelled and antagonize Wnt signaling. *Dev Biol* **234**, 93-106.

Wilson, A., MacDonald, H. R., and Radtke, F. (2001). Notch 1-deficient common lymphoid precursors adopt a B cell fate in the thymus. *J Exp Med* **194**, 1003-12.

Wilson, V. A., Gallagher, J. T., and Merry, C. L. (2002). Heparan sulfate 2-O-sulfotransferase (Hs2st) and mouse development. *Glycoconj J* **19**, 347-54.

Winnier, G., Blessing, M., Labosky, P. A., and Hogan, B. L. (1995). Bone morphogenetic protein-4 is required for mesoderm formation and patterning in the mouse. *Genes Dev* **9**, 2105-16.

Wolftrum, C., Shih, D. Q., Kuwajima, S., Norris, A. W., Kahn, C. R., and Stoffel, M. (2003). Role of Foxa-2 in adipocyte metabolism and differentiation. *J Clin Invest* **112**, 345-56.

Wu, L., Li, C. L., and Shortman, K. (1996). Thymic dendritic cell precursors: relationship to the T lymphocyte lineage and phenotype of the dendritic cell progeny. *J Exp Med* **184**, 903-11.



Wu, L., Scollay, R., Egerton, M., Pearse, M., Spangrude, G. J., and Shortman, K. (1991). CD4 expressed on earliest T-lineage precursor cells in the adult murine thymus. *Nature* **349**, 71-4.

Xu, P. X., Zheng, W., Laclef, C., Maire, P., Maas, R. L., Peters, H., and Xu, X. (2002). *Eya1* is required for the morphogenesis of mammalian thymus, parathyroid and thyroid. *Development* **129**, 3033-44.

Xu, X., Weinstein, M., Li, C., and Deng, C. (1999). Fibroblast growth factor receptors (FGFRs) and their roles in limb development. *Cell Tissue Res* **296**, 33-43.

Yagi, H., Furutani, Y., Hamada, H., Sasaki, T., Asakawa, S., Minoshima, S., Ichida, F., Joo, K., Kimura, M., Imamura, S., Kamatani, N., Momma, K., Takao, A., Nakazawa, M., Shimizu, N., and Matsuoka, R. (2003). Role of TBX1 in human del22q11.2 syndrome. *Lancet* **362**, 1366-73.

Yamagishi, H., Maeda, J., Hu, T., McAnally, J., Conway, S. J., Kume, T., Meyers, E. N., Yamagishi, C., and Srivastava, D. (2003). *Tbx1* is regulated by tissue-specific forkhead proteins through a common Sonic hedgehog-responsive enhancer. *Genes Dev* **17**, 269-81.

Yamazaki, H., Sakata, E., Yamane, T., Yanagisawa, A., Abe, K., Yamamura, K., Hayashi, S., and Kunisada, T. (2005). Presence and distribution of neural crest-derived cells in the murine developing thymus and their potential for differentiation. *Int Immunol* **17**, 549-58.

Yao, H. H., Matzuk, M. M., Jorgez, C. J., Menke, D. B., Page, D. C., Swain, A., and Capel, B. (2004). Follistatin operates downstream of *Wnt4* in mammalian ovary organogenesis. *Dev Dyn* **230**, 210-5.

Yoshino, K., Rubin, J. S., Higinbotham, K. G., Uren, A., Anest, V., Plisov, S. Y., and Perantoni, A. O. (2001). Secreted Frizzled-related proteins can regulate metanephric development. *Mech Dev* **102**, 45-55.

You, L., and Kruse, F. E. (2002). Differential effect of activin A and BMP-7 on myofibroblast differentiation and the role of the Smad signaling pathway. *Invest Ophthalmol Vis Sci* **43**, 72-81.

Yu, Q., Erman, B., Park, J. H., Feigenbaum, L., and Singer, A. (2004). IL-7 receptor signals inhibit expression of transcription factors TCF-1, LEF-1, and ROR $\gamma$ : impact on thymocyte development. *J Exp Med* **200**, 797-803.

Zeng, W., Wharton, K. A., Jr., Mack, J. A., Wang, K., Gadban, M., Suyama, K., Klein, P. S., and Scott, M. P. (2000). naked cuticle encodes an inducible antagonist of Wnt signalling. *Nature* **403**, 789-95.

Zerrahn, J., Volkmann, A., Coles, M. C., Held, W., Lemonnier, F. A., and Raulat, D. H. (1999). Class I MHC molecules on hematopoietic cells can support intrathymic positive selection of T cell receptor transgenic T cells. *Proc Natl Acad Sci U S A* **96**, 11470-5.

Zhang, Y., Luan, Z., Liu, A., and Hu, G. (2001). The scaffolding protein CASK mediates the interaction between rabphilin3a and beta-neurexins. *FEBS Lett* **497**, 99-102.

Zinkernagel, R. M., Althage, A., Waterfield, E., Kindred, B., Welsh, R. M., Callahan, G., and Pincetl, P. (1980). Restriction specificities, alloreactivity, and allotolerance expressed by T cells from nude mice reconstituted with H-2-compatible or -incompatible thymus grafts. *J Exp Med* **151**, 376-99.

Zuklys, S., Balciunaite, G., Agarwal, A., Fasler-Kan, E., Palmer, E., and Hollander, G. A. (2000). Normal thymic architecture and negative selection are associated with Aire expression, the gene defective in the autoimmune- polyendocrinopathy-candidiasis-ectodermal dystrophy (APECED). *J Immunol* **165**, 1976-83.

## 9. Curriculum Vitae

### Personal Details

Date of Birth: 13.10.73 Berkeley/California  
Nationality: Swiss / German / USA  
Marital Status: Single  
Home Address: 12, ch. du Miroir  
1090 La Croix s/Lutry  
Switzerland  
Tel. (021) 791'21'95

### Education and Qualifications

1980-85 Primary School, St-Sulpice and Lutry, Switzerland  
1990 Certificat secondaire scientifique, Lausanne, Switzerland  
Highschool Grant Park, Winnipeg/Canada  
1991-94 Gymnase du Bugnon, Lausanne (sect. Math-sci.)  
1994 Diplôme de culture générale scientifique, Lausanne  
Oct 1994 Study of Biology, University of Lausanne  
1998 Certificate in Molecular and Cellular Biology, University of Lausanne, Switzerland  
1998 Certificate in Pharmacology and Toxicology, University of Lausanne, Switzerland  
1999 Certificate in Cellular Biochemistry, University of Lausanne, Switzerland  
Certificate in Molecular Immunology, University of Lausanne, Switzerland  
March 2000 Diploma in Biology, Swiss Institute of Experim. Cancer Research (ISREC) and University of Lausanne, Epalinges, Switzerland  
Oct 2000 until now PhD student, Center of Biomedicine, University Basel, Basel, Switzerland

### Practical Experience

2000 Diploma Thesis: “Étude sur la régulation du gène de la sous-unité catalytique de la télomérase humaine (hTERT) à l’aide de la transcription inverse-PCR quantitative en temps réel” (Dr. M. Nabholz, Dr. J. Lingner)  
2000 Certificate at ISREC, Epalinges: “Quantitative reverse transcription-PCR assay of the catalytic subunit of human telomerase (hTERT) using SYBR Green detection system” (Dr. M. Nabholz)  
1999 Practical laboratory work on “General Immunology” (Prof. H. Acha Orbea)  
1999 Project at Inst. of Biochemistry, Medical School, Univ. of Lausanne: “General Biochemical Methods and Applications on Apoptosis ” (Prof. J. Tschopp)  
1999 Certificate at Inst. of Pharmacology and Toxicology/Medical School, Univ. of Lausanne: “Rôle du transporteur de glucose GLUT-2 dans l'induction

1998 par le glucose du gène de la L-pyruvate kinase dans des hépatocytes de souris en culture primaire” (Prof. B. Thorens)  
Project at Inst. of Animal Biology, Univ. of Lausanne, “Study of Peroxisome Proliferators Activated Receptors (PPARs)” (Prof. W. Wahli)

### Languages

French/German Mother languages  
English written and oral (good knowledge)

### Hobbies

Sports (skiing, bicycling,), astronomy

### References

Prof. Hans Acha-Orbea, Biochemistry, Univ. Lausanne, Epalinges

## 9.1 Publications

Ducrest, A. L., Amacker, M., **Mathieu, Y. D.**, Cuthbert, A. P., Trott, D. A., Newbold, R. F., Nabholz, M., and Lingner, J. (2001). Regulation of Human Telomerase Activity: Repression by Normal Chromosome 3 Abolishes Nuclear Telomerase Reverse Transcriptase Transcripts but Does Not Affect c-Myc Activity. *Cancer Res* **61**, 7594-602

Balciunaite, G., Keller, M. P., Balciunaite, E., Piali, L., Zuklys, S., **Mathieu, Y. D.**, Gill, J., Boyd, R., Sussman, D. J., and Hollander, G. A. (2002). Wnt glycoproteins regulate the expression of FoxN1, the gene defective in nude mice. *Nat Immunol* **15**, 15.

